



Flashback and Blowoff Characteristics of Gas Turbine Swirl Combustor

**A Thesis submitted to Cardiff University
for the Degree of Doctor of Philosophy
in Mechanical Engineering**

By

Mohammed Hamza Abdulsada AL-Hashimi

B.Sc. & M.Sc., Mechanical Power Engineering

**Institute of Energy
Cardiff School of Engineering
Cardiff University
Cardiff / UK
2011**

**Supervisors: Prof. Nicholas Syred
Prof. Philip Bowen**

ABSTRACT

Gas turbines are extensively used in combined cycle power systems. These form about 20% of global power generating capacity, normally being fired on natural gas, but this is expected in the future to move towards hydrogen enriched gaseous fuels to reduce CO₂ emissions. Gas turbine combined cycles can give electrical power generation efficiencies of up to 60%, with the aim of increasing this to 70% in the next 10 to 15 years, whilst at the same time substantially reducing emissions of contaminants such as NO_x.

The gas turbine combustor is an essential and critical component here. These are universally stabilized with swirl flows, which give very wide blowoff limits, and with appropriate modification can be adjusted to give very low NO_x and other emission. Lean premixed combustion is commonly used at pressures between 15 to 30 bar, these even out hot spots and minimise formation of thermal NO_x. Problems arise because improving materials technology/improved cooling techniques allow higher turbine inlet temperatures, hence higher efficiencies, but with the drawback of potentially higher emissions and stability problems.

This PhD study has widely investigated and analysed two different kinds of gas turbine swirl burners. The research has included experimental investigation and computational simulation. Mainly, the flashback and blowoff limits have been comprehensively analysed to investigate their effect upon swirl burner operation. The study was extended by using different gas mixtures, including either pure gas or a combination of more than one gas like natural gas, methane, hydrogen and carbon dioxide.

The first combustor is a 100 kW tangential swirl combustor made of stainless steel that has been experimentally and theoretically analysed to study and mitigate the effect of flashback phenomena. The use of a central fuel injector, cylindrical confinement and exhaust sleeve are shown to give large benefits in terms of flashback resistance and acts to reduce and sometimes eliminate any coherent structures which may be located along the axis of symmetry. The Critical Boundary Velocity Gradient is used for characterisation of flashback, both via the original Lewis and von Elbe formula and via new analysis using CFD and investigation of boundary layer conditions just in front of the flame front. Conclusions are drawn as to mitigation technologies. It is recognized how isothermal conditions produce strong Precessing Vortex Cores that are fundamental in producing the

final flow field, whilst the Central Recirculation Zones are dependent on pressure decay ratio inside the combustion chamber. Combustion conditions showed the high similarity between experiments and simulation. Flashback was demonstrated to be a factor highly related to the strength of the Central Recirculation Zone for those cases where a Combustion Induced Vortex Breakdown was allowed to enter the swirl chamber, whilst cases where a bluff body impeded its passage showed a considerable improvement to the resistance of the phenomenon. The use of nozzle constrictions also reduced flashback at high Reynolds number (Re). All these results were intended to contribute to better designs of future combustors.

The second piece of work of this PhD research included comprehensive experimental work using a generic swirl burner (with three different blade inserts to give different swirl numbers) and has been used to examine the phenomena of flashback and blowoff in the swirl burner in the context of lean premixed combustion. Cylindrical and conical confinements have been set up and assembled with the original design of the generic swirl combustor. In addition to that, multi-fuel blends used during the experimental work include pure methane, pure hydrogen, hydrogen / methane mixture, carbon dioxide/ methane mixture and coke oven gas.

The above investigational analysis has proved the flashback limits decrease when swirl numbers decrease for the fuel blends that contain 30% or less hydrogen. Confinements would improve the flashback limit as well.

Blowoff limits improve with a lower swirl number and it is easier to recognise the gradual extinction of the flame under blowoff conditions. The use of exhaust confinement has created a considerable improvement in blowoff. Hydrogen enriched fuels can improve the blowoff limit in terms of increasing heat release, which is higher than heat release with natural gas. However, the confinements complicate the flashback, especially when the fuel contains a high percentage of hydrogen. The flashback propensity of the hydrogen/methane blends becomes quite strong. The most important features in gas turbines is the possibility of using different kinds of fuel. This matter has been discussed extensively in this project. By matching flashback/blowoff limits, it has been found that for fuels containing up to 30% of hydrogen, the designer would be able to switch the same gas turbine combustor to multi-fuels whilst producing the same power output.

ACKNOWLEDGEMENTS

First of all, I would like to praise and thank **GOD** for helping me to complete this thesis.

I wish to express my gratefulness to my supervisors, **Prof. Nicholas Syred and Prof. Philip Bowen** for their continuous supervision, positive discussions and important ideas through this research work.

Also, very extraordinary deepest thanks to **Prof. Anthony Griffiths** for his special contribution and help in completing this work.

I would like also to thank the staff of School of Engineering, the staff of the Gas Turbine Research Centre (GTRC), the staff of the Mechanical Engineering Work Shop, and special thanks for whom I will never forget go to the following: (**Agustin Valera-Medina, Steve Morris, Peter Kays, Malcolm Seaborne, Terry Treherne, Paul Malpas, Chris Lee, Julie Cleaver, Julian Steer, Marytn Griffiths, Tony Giles, Andrew Hopkins, Gareth Hunt and Andrew Crayford**).

I would like to extend my thanks to the Iraqi Government for sponsoring my PhD study, and many thanks for the staff of the Iraqi cultural attaché in London for their help during my stay in the UK.

My deepest thanks, love and gratitude for all of my family, parents, brothers, sisters and extraordinary thanks for my wife and my lovely kids, Hassanien, Kawther and Ruqayyah.

This work would not have been completed without their love and continuous support.

PhD Thesis Research Achievements

Prizes and Awards

Second Best Poster Award

Event Title	Current Research in Combustion: A Forum For Research Students and Early Career Researchers
Organised by	IOP Combustion Physics Group
Title of poster	Flashback Avoidance Analysis using Geometrical Constrictions in a Tangential Swirl Burner
Place of conference	Loughborough University, Leicestershire, UK
Date of conference	Tue, 22 Sep 2009

Best Paper

Event Title	48th AIAA Aerospace Sciences Meeting Including the New Horizons Forum and Aerospace Exposition
Organised by	American Institute of Aeronautics and Astronautics
Title of paper	Studies of Large Coherent Structures and their Effects on Swirl Combustion
Place of conference	Orlando, Florida, USA
Date of conference	4 - 7 January 2010
Paper No.	AIAA 2010-1168

Best Paper and Presentation prize

Event Title	1 st Iraqi conference for Science and engineering for the PhD Iraqi students in The UK
Organised by	Iraqi Cultural Attaché
Title of poster	Effect of Swirl Number and Fuel Type upon the Combustion Limits in Gas Turbine Swirl Combustors
Place of conference	University of London UCL, London, UK
Date of conference	1 st – 2 nd October 2011

Conference and Journal papers:

- [1] A. Valera-Medina, M. Abdulsada, A. Griffiths & N. Syred, Flashback Avoidance Analysis using Geometrical Constrictions in a Tangential Swirl Burner 9 - 10 March 2009 British – French Flame Days 2009.
- [2] A. Valera-Medina, M. Abdulsada, N. Shelil, A. Griffiths & N. Syred, Flashback Analysis In Swirl Burners Using Passive Nozzle Constrictions And Different Fuels, 16th International IFRF Members' Conference 8th-10th Jun, 2009. Boston, USA.
- [3] Agustin Valera-Medina, Mohammed Abdulsada, Nicholas Syred and Anthony Griffiths, Studies of Large Coherent Structures and their Effects on Swirl

Combustion, 48th AIAA Aerospace Sciences Meeting Including the New Horizons Forum and Aerospace Exposition 4th -7th January 2010, Orlando, Florida, **AIAA 2010-1168**.*

- [4] Nicholas Syred, Mohammed Abdulsada, Anthony Griffiths, Tim O'Doherty, and Philip Bowen, The effect of hydrogen containing fuel blends upon flashback in swirl burners, PRO-TEM, TATA Conference Meeting, Newcastle, 3rd November, 2010.
- [5] Nicholas Syred, Mohammed Abdulsada, Anthony Griffiths, Tim O'Doherty, and Philip Bowen, The effect of hydrogen containing fuel blends upon flashback in swirl burners, Applied Energy, vol 89, p106-110, 2012.*
- [6] Mohammed Abdulsada, Nicholas Syred, Antony Griffiths, Phillip Bowen, Effect of Swirl Number and Fuel Type upon the Flashback in Swirl Combustors, 49th AIAA Aerospace Sciences Meeting Including the New Horizons Forum and Aerospace Exposition 4th -7th January 2010, Orlando, Florida, **AIAA 2011- 889442**.
- [7] Mohammed Abdulsada, Nicholas Syred, Antony Griffiths, Phillip Bowen and Steve Morris, Effect of Swirl Number and Fuel Type upon the Combustion Limits in Swirl Combustors, ASME Turbo-Expo conference in Canada, Vancouver 6-10 June 2011, **GT2011-45544**.
- [8] Mohammed Abdulsada, Nicholas Syred, Steve Morris and Phillip Bowen, Effect of Swirl Number and Fuel Type upon the Blow off Limits in Swirl Combustors. Conference paper accepted in The Fifth European Combustion Meeting held in Cardiff University, Cardiff, UK 28th June - 1st July 2011.
- [9] Mohammed Abdulsada, Nicholas Syred, Philip Bowen, Tim O'Doherty, and Anthony Griffiths, Effect of Swirl Number and Fuel Type upon the Blowoff Limits in Unconfined and Confined Swirl Combustors, PRO-TEM, TATA Conference Meeting, Newcastle, 25th-26th October, 2011 and in review for Journal Applied Thermal Engineering .
- [10] Mohammed Abdulsada, Nicholas Syred, Phillip Bowen, Antony Griffiths, Pure Hydrogen and Its Blends Advantages and Disadvantages as Fuel in the Gas Turbine Swirl Combustor, 50th AIAA Aerospace Sciences Meeting Including the New Horizons Forum and Aerospace Exposition, Nashville, Tennessee 9-12 January 2012, **AIAA 2012 -1120421**.

Note: Award Certificates and selected papers (*) are shown in Appendix I

TABLE OF CONTENTS

Abstract	i
Acknowledgements	iii
PhD Thesis Research Achievements	iv
Table of Contents	vi
List of Figures	xi
List of Tables	xix
Nomenclature	xx
Abbreviations	xxii
1 Introduction	1
1.1 World Energy Consumption	1
1.2 World Energy Production	4
1.3 World Energy Future	6
1.4 Gas Turbines	7
1.4.1 Gas Turbine Combustors	8
1.4.2 Combustion Performance	8
1.4.3 Operational Requirements and Combustor Design Factor	9
1.4.4 Types of Combustion Systems	10
1.5 Summary	11
1.6 Objectives	11
1.7 Thesis Structure	12

2	Characteristics of Gas Turbine Swirl Combustor	14
2.1	Introduction	14
2.2	Types of Combustible Mixtures	15
2.2.1	Non-Premixed Combustion	15
2.2.2	Premixed Combustion	16
2.2.3	Partially Premixed Combustion	17
2.3	Lean Premixed Mixture	17
2.4	Swirling Flow and It's The Effect upon Combustion	19
2.4.1	Swirl Flow Generation	20
2.4.2	Swirl Number	20
2.4.3	The Basic Swirl Stabilization Effect	22
2.5	Combustion Instabilities	25
2.5.1	Flashback	26
2.5.2	Blowoff	30
2.6	Fuel Blends	32
2.7	Summary	38

Part I CFD Simulation

3	Computational Modelling of Combustion	40
3.1	Introduction and CFD Definition	40
3.2	Benefit of CFD	42
3.3	CFD Analysis Steps	42
3.4	Planning CFD Analysis	46
3.5	Basic Equations	46
3.5.1	Mass Conservation	47
3.5.2	Momentum Equation	47
3.5.3	Energy Equation	49

3.5.4	General Transport Equation	50
3.5.5	Physical Behaviour and Boundary Conditions	50
3.6	Turbulence Modelling	51
3.6.1	What is Turbulence	53
3.6.2	Properties of Turbulence	56
3.6.3	Feature of Flows	56
3.6.4	Methods of Averaging	56
3.7	Turbulence Models	57
3.7.1	Choosing a Turbulence Model	57
3.7.2	Shear-Stress Transport (SST) k- ω Model	60
3.8	Modelling of Turbulent Combustion	61
3.8.1	Non-premixed Combustion Modelling	62
3.8.2	Premixed Combustion Modelling	64
3.8.3	Partially premixed Combustion Modelling	66
3.9	CFD Solver	67
3.9.1	ANSY 12 FLUENT	67
3.9.2	ANSY 12 Meshing	68
3.9.3	Mesh quality measurement	69
3.10	Summary	72
4	100 kW Tangential Swirl Combustor	73
4.1	Introduction	73
4.2	Burner Experimental Rig Setup	74
4.3	Burner CFD Modelling	76
4.4	Results and Discussion	80
4.4.1	Isothermal Validation	81
4.4.2	Non- Isothermal Validation	81
4.4.2.1	Non-Premixed Combustion	82

4.4.2.2	Premixed Combustion	85
4.4.2.3	Partially Premixed Combustion	98
4.5	Summary	103

Part II Experimental Analysis

5	Prototype Generic Swirl Combustor	104
5.1	Introduction	104
5.2	Basic Generic Swirl Burner Design	104
5.3	Design Evolution of Generic Swirl Burner	108
5.4	Fuel Blends	117
5.5	Turbulence Plates	118
5.6	Summary	120
6	Flashback Determination of Generic Swirl Burner	121
6.2	Flashback of Unconfined Conditions (Open Flame)	121
6.3	Flashback of Confined Conditions	130
7	Blowoff Determination of Generic Swirl Burner	137
7.2	Blowoff of Unconfined Conditions (Open Flame)	137
7.3	Blowoff of Confined Conditions	142

8	Comparisons of FB/BO and Operational Region for Burner	155
8.1	Introduction	155
8.2	FB/BF Operation Region Open Flame (Unconfined Burner)	156
8.3	FB/BF Operation Region of Confined Burner	163
8.4	Pure Hydrogen and Coke Oven Gas FB/BO Specialty	169
	8.4.1 Pure Hydrogen	169
	8.4.2 Coke Oven Gas	171
8.5	Summary	172
9	Conclusions and Recommendations for Future Work	175
9.1	Introduction	175
9.2	100 kW Tangential Swirl Burner	176
9.3	Generic Swirl Burner	178
9.4	Suggestions for Future Work Research	180
	References	182
	Appendix I	AI-1
	Award Certificates and Selected Papers	AI-1
AI.1	Certificates	AI-1
AI.2	Selected Papers	AI-3

LIST OF FIGURES

<i>Chapter 1</i>	Title	Page no.
Figure 1.1	World energy supply in percentage	4
Figure 1.2	World energy production in terajoules	5
Figure 1.2	Gas turbine conventional arrangements show combustor	8
<i>Chapter 2</i>		
Figure 2.1	Recirculation in a swirling jet adapted from Beer and Chigier	23
Figure 2.2	Velocity contours with combustion in a swirl burner	24
Figure 2.3	Stable partially mixed flame of swirling burner temperature contours	25
Figure 2.4	Burner assembly (left) damaged by combustion instability and new burner assembly (right)	27
<i>Chapter 3</i>		
Figure 3.1	Two-dimensional image of an axisymmetric water jet, obtained by the laser-induced fluorescence technique	52
Figure 3.2	2D and 3D basic mesh shape	68
Figure 3.3	Skewness calculation explanation shape	70
Figure 3.4	Aspect ratio comparison of two different cases	71
<i>Chapter 4</i>		
Figure 4.1	The perspex swirl generator	74
Figure 4.2	Schematic diagram shows the dimensions of the swirl burner	75
Figure 4.3	The swirl burner, fuel and air injection systems	77
Figure 4.4	Nozzle used to vary flame properties d=78mm	77

Figure 4.5	Burner confinements a) open and b) conical exit geometries	78
Figure 4.6	The geometry of the tangential swirl burner.	79
Figure 4.7	Tangential swirl burner mesh with injector	80
Figure 4.8	Comparison of axial velocity contours, a) Experimental (PIV), b) Simulation	81
Figure 4.9	Non-premixed case study for different inlet values of air with 25 l/min methane fuel	83
Figure 4.10	Non-premixed case study for different inlet values of air with 40 l/min methane fuel	84
Figure 4.11	Diagram of rig and constrictions used (35 mm total length of the constriction)	86
Figure 4.12	Comparison between experimental and CFD simulation for flashback and quasi stable regions in tangential swirl burner with injector (premixed only without quarl) (natural gas)	87
Figure 4.13	The modification of the burner neck to reduce the flashback occurrence	88
Figure 4.14	Comparison between experimental and CFD simulation for flashback and quasi stable regions in tangential swirl burner with injector (premixed only with quarl)	88
Figure 4.15	Comparison between CFD simulations for flashback map in tangential swirl burner with injector (premixed only with quarl and without quarl)	89
Figure 4.16	Comparison between experimental and CFD simulation for flashback and quasi stable flame regions in tangential swirl burner without injector (premixed flame with quarl)	90
Figure 4.17	Comparison between experimental and CFD simulation for flashback and quasi stable regions in the tangential swirl burner without injector (premixed without quarl)	90
Figure 4.18	Temperature contours distribution illustrating location of	91

	annular flame front in the boundary layer just before flashback $Q_a=400\text{L}/\text{min}$ $\phi=0.9$	
Figure 4.19	Variation of critical boundary velocity gradient, G_F , at flashback with % natural gas in air for laminar mixtures in comparison with swirl burners	92
Figure 4.20	CFD prediction for swirl burner, $S=0.86$, of A) Temperature contours, B) Temperature profiles just ahead of the flame front C) Axial velocity contours, D) Exit throat total velocity distribution. Critical boundary layer velocity gradient, g_f , from c) is $2,900\text{s}^{-1}$, air flowrate 700 l/min, {0-67} l/min fuel, $\phi =0.9$, just before flashback	94-95
Figure 4.21	CFD prediction for swirl burner, $S=0.86$, with fuel injector of A) Temperature contours, B) Temperature profiles just ahead of the flame front, C) Axial velocity contours, D) Exit throat total velocity distribution. Critical boundary layer velocity gradient, g_f , from c) is $5,200\text{s}^{-1}$, air flowrate 700 l/min, {25-40} l/min fuel, $\phi =0.9$, just before flashback	94-95
Figure 4.22	Flashback result without (A) and with (B) (fuel injector and confinement)	95
Figure 4.23	Flame images. A) No injector with nozzle, 700 l/min air, $\phi =0.54$, G) with injector and nozzle, $\phi =0.95$, $S=0.86$	96
Figure 4.24	Variation of critical boundary velocity gradient, g_f , with equivalence ratio without injector and with nozzle, $S=0.86$	96
Figure 4.25	Variation of critical boundary velocity gradient, g_f , with equivalence ratio with fuel injector and nozzle, $S=0.86$	97
Figure 4.26	Flashback Phenomena appearance with partial premixing ($Q_a=600\text{L}/\text{m}$ $Q_{fp}=40\text{L}/\text{m}$ $Q_{fd}=25\text{L}/\text{m}$ $\phi_p=1.1467$)	98-99
Figure 4.27	Stable swirling combustion, partially premixing	99

Figure 4.28	$Q_a=800\text{l/m}$ $Q_{fp}=40\text{l/m}$ $Q_{fd}=25\text{l/m}$ $\phi_p=0.86$ Near blowoff conditions with partial premixing	100
Figure 4.29	$Q_a=1600\text{L/m}$ $Q_{fp}=40\text{L/m}$ $Q_{fd}=25\text{L/m}$ $\phi_p=0.43$ Temperature contours illustrate irregular flame propagation into the mixing zone of the swirl burner causing flashback in a partially premixed case, also observed experimentally	101
Figure 4.30	Conical cup with confinement, Air=1600L/min, Diffusion fuel 25L/min, Premixed=40L/min $\phi_p =0.43$, $\phi_{total} = 0.69875$, fuel methane, Top diagram axial velocities, lower temperatures	102
Chapter 5		
Chapter 5		
Figure 5.1	The actual swirl burner, all parts	105
Figure 5.2	The assembled swirl burner $S=1.47$	106
Figure 5.3	Generic swirl burner diagram	106
Figure 5.4	Swirl burner dimensions	107
Figure 5.5	Experimental setup	107
Figure 5.6	Swirl insert of $S=1.47$	108
Figure 5.7	Blade swirler burner configuration	109
Figure 5.8	Schematic diagram of generic swirl burner with location of flame front	111
Figure 5.9	Swirl insert $S=1.04$	112
Figure 5.10	The assembled swirl burner $S=1.04$	112
Figure 5.11	Swirl burner fitted with open cylindrical confinement	113
Figure 5.12	Swirl burner fitted with conical cup exhaust and confinement	114
Figure 5.13	Schematic swirl burner diagram fitted with cylindrical confinement and the conical nozzle	115
Figure 5.14	Swirl burner exploded section fitted with cylindrical	115

	confinement and the conical cup nozzle	
Figure 5.15	Block diagram shows the stages of swirl burner design	116
Figure 5.16	The flashback protection Plates	119
Figure 5.17	Pressure difference verses air mass flow rate through the three swirl burners	120
Chapter 6		
Chapter 6		
Figure 6.1	The flashback stability limit of the three burners with different swirl numbers for five different fuels	122
Figure 6.2-a	Photo of flame surrounding central fuel injector at $S_A=1.47$, just before radial flashback	123
Figure 6.2-b	Photo of flame just before flashback through outer wall boundary layer, $S_B=1.04$	123
Figure 6.3	100%CH ₄ Flame in the swirl burner of $S=1.04$ $\dot{m}_f = 0.03g/s$, $\dot{m}_a = 0.6g/s$, $\phi = 0.858$ (about to flashback)	124
Figure 6.4	Attached flame of 30%H ₂ +70%CH ₄ , $\dot{m}_f = 0.7g/s$, $\dot{m}_a = 0.7g/s$, $\phi = 1.887$ (just before flashback) in the swirl burner $S=1.04$	124
Figure 6.5	Attached flame of coke oven gas $\dot{m}_f = 0.725g/s$, $\dot{m}_a = 10g/s$, $\phi = 1.1$ (just before flashback) for the swirl burner $S=1.04$	125
Figure 6.6	Coke oven gas stable flame in the swirl burner of $S=1.04$	125
Figure 6.7	Premixed hydrogen flame cannot see but detected by thermocouple	126
Figure 6.8	Rich hydrogen flame, $\dot{m}_f = 0.5g/s$, $\dot{m}_a = 11g/s$, $\phi = 1.5545$ for the swirl burner $S=1.47$	126
Figure 6.9	15%CO ₂ +85%CH ₄ flame in the swirl burner of $S=1.04$ $\dot{m}_f = 0.112g/s$, $\dot{m}_a = 1.318g/s$, $\phi = 1.55$	127
Figure 6.10-a	Flashback comparison between swirl burners $S_A=1.47$ and $S_B=1.04$ for 15%CO ₂	128

Figure 6.10-b	Flashback comparison between swirl burners $S_A=1.47$ and $S_B=1.04$ for 30%CO ₂	128
Figure 6.11	Lewis and Von Elbe critical boundary velocity gradient comparison for three swirl numbers (natural gas and methane) and laminar data	129
Figure 6.12	The steps of recognition the flashback flame in the confinement combustion	132
Figure 6.13	Flashback comparison between three types of flame for swirl burner=1.04 for pure methane (100%CH ₄)	133
Figure 6.14	Flashback comparison between three types of flame for swirl burner=0.8 for pure methane (100% CH ₄)	133
Figure 6.15	Flashback comparison between three types of flame for swirl burner number $S_B=1.04$ for (15%H ₂ +85%CH ₄)	134
Figure 6.16	Flashback comparison between three types of flame for swirl burner number $S_C=0.8$ for (15%H ₂ +85%CH ₄)	135
Figure 6.17	Flashback comparison between three types of flame for swirl burner number $S_B=1.04$ for (30%H ₂ +70%CH ₄)	135
Figure 6.18	Flashback comparison between three types of flame for swirl burner number $S_C=0.8$ for (30%H ₂ +70%CH ₄)	136
Chapter 7		
Chapter 7		
Figure 7.1	Flame shape for pure methane just before blowoff for the same fuel mass flowrate	138
Figure 7.2	Blowoff limits for different hydrogen-methane blends	140
Figure 7.3	30%CO ₂ +70%CH ₄ flame in the swirl burner of $S=1.04$ $\dot{m}_f = 0.088g/s$, $\dot{m}_a = 0.94g/s$, $\phi = \mathbf{0.8212}$ (near blowoff and no flashback)	141
Figure 7.4	30%H ₂ +70%CH ₄ flame in the swirl burner of $S=1.04$ $\dot{m}_f = 0.085g/s$, $\dot{m}_a = 2.15g/s$, $\phi = \mathbf{0.746}$ (near blowoff no flashback)	141
Figure 7.5	Blowoff comparison between three types of flame for	142

	swirl burner number $S_C=1.04$ for pure methane (100%CH ₄)	
Figure 7.6	Blowoff comparison between three types of flame for swirl burner number $S_C=0.8$ for pure methane (100%CH ₄)	143
Figure 7.7	Blowoff comparison between three types of flame for swirl burner number $S_C=1.04$ for (15% H ₂ +85%CH ₄)	144
Figure 7.8	Blowoff comparison between three types of flame for swirl burner number $S_C=0.8$ for (15% H ₂ +85%CH ₄)	144
Figure 7.9	Blowoff comparison between three types of flame for swirl burner number $S_C=1.04$ for (30% H ₂ +70%CH ₄)	145
Figure 7.10	Blowoff comparison between three types of flame for swirl burner number $S_C=0.8$ for (30% H ₂ +70%CH ₄)	145
Figure 7.11	30%H ₂ +70%CH ₄ mixture blowoff flame stages for $S_C=0.8$ for open cylindrical confinement ($\dot{m}_f = 0.35g/s$)	146-147
Figure 7.12	30%H ₂ +70%CH ₄ mixture blowoff flame stages for swirl burner number $S_C=0.8$ with cylindrical confinement and conical cup ($\dot{m}_f = 0.35g/s$)	148
Figure 7.13	30%H ₂ +70%CH ₄ mixture blowoff flame stages for $S_C=0.8$ with cylindrical confinement ($\dot{m}_f = 0.35g/s$)	149
Figure 7.14	30%H ₂ +70%CH ₄ mixture blowoff flame stages for swirl burner number $S_C=0.8$ with cylindrical confinement and conical cup($\dot{m}_f = 0.35g/s$)	150-151
Figure 7.15	30%H ₂ +70%CH ₄ mixture blowoff flame stages for swirl burner number $S_C=0.8$ with cylindrical confinement and conical cup($\dot{m}_f = 0.6g/s$)	151-152
Figure 7.16	Blowoff comparison between two types of flame for swirl burner number $S_C=1.04$ for coke oven gas	153
Figure 7.17	Blowoff comparison between two types of flame for swirl burner number $S_C=0.8$ for coke oven gas	154

Chapter 8		
Figure 8.1	Flashback/blowoff limits as a function of total mass flow and heat input for combination of methane and other gas, open flame for swirl number $S_B=1.47$	158
Figure 8.2	Flashback/blowoff limits as a function of total mass flow and heat input for combination of methane and other gas, open flame, for equivalence ratios up to 1 for swirl number $S_B=1.04$	160
Figure 8.3	Flashback/blowoff limits as a function of total mass flow and heat input for combination of methane and other gas, open flame, for swirl number $S_C=0.8$	162
Figure 8.4	Flashback/blowoff limits as a function of total mass flow and heat input, $S=1.04$, confined flame (cylindrical confinement)	164
Figure 8.5	Flashback/blowoff limits as a function of total mass flow and heat input, $S=1.04$, confined flame (cylindrical confinement & conical cup)	165-166
Figure 8.6	Flashback/blowoff limits as a function of total mass flow and heat input, $S=0.8$, confined flame (cylindrical confinement)	167
Figure 8.7	Flashback/blowoff limits as a function of total mass flow and heat input, $S=0.8$, confined flame (cylindrical confinement and conical cup)	168-169
Figure 8.8	Flashback limits comparison as a function of total mass flow for pure hydrogen for different swirl numbers	171
Figure 8.9	Flashback and blowoff limits comparison as a function of total mass flow for coke oven gas for different three swirl numbers	173

LIST OF TABLES

<i>Chapter 1</i>	Title	Page no.
Table 1.1	Short summary of fuel share in world energy utilization	2
<i>Chapter 2</i>		
Table 2.1	Fuel classification	34
<i>Chapter 3</i>		
Table 3.1	Formal classification of fluid flow equations	51
Table 3.2	Characteristics and features of turbulence models	58-59-60
Table 3.3	The relationship between skewness and mesh quality.	71
<i>Chapter 5</i>		
Table 5.1	Swirl burner possibilities design for different modifications	114
Table 5.2	Fuels blends tested and compositions, % by volume	117
Table 5.3	Fuels blends characteristics	117

NOMENCLATURE

Alphabetic Symbol

A	Model Constant	[-]
A	Area	[m ²]
AFR	Air to Fuel Ratio	[-]
C	Mean Reaction Progress Variable	[-]
D	Mass Diffusion	[m ² /s]
Da	Damköhler number	[-]
D, d	Diameter	[m]
D _q	Quenching Diameter	[m]
F	Mixture fraction	[-]
G _x	Axial Flux of Axial Momentum	[N]
G _θ	Axial Flux of Angular Momentum	[J]
G _f	Critical boundary velocity gradient after Lewis And von Elbe	[1/s]
g _f	Critical boundary velocity gradient derived from CFD	[1/s]
g _v	Critical boundary velocity gradient as Lewis And von Elbe	[1/s]
H	The flow passage height	[m]
K	Kinetic energy of turbulence	[m ² /s ²]
Ma	Mach Number	[-]
\dot{m}	Mass Flow Rate	[kg/s]
N	Number of products	[-]
P	The static Pressure	[N/ m ²]
Pe	Peclet number	[-]
Q	Flow rate	[m ³ /s]
Q _{EAS}	The Equiangle Skew	[-]
Q _{EVS}	The Equivolume Skew	[-]
R	Radius	[m]
Re	Reynolds number of air	[-]
r _{eff}	Effective Radius at the Middle of Pipe	[m]

S	Swirl Number	[-]
S_g	Geometrical Swirl Number	[-]
S_L	Laminar Flame Speed	[m/s]
S_M	Body Force	[kg/(m ² s ²)]
S_T	Turbulent Flame Speed	[m/s]
T	Time	[s]
T	The flow passage width between blades	[m]
T	Temperature	[K]
U	Premixed Flow Velocity	[m/s]
U	Axial velocity	[m/s]
V _c	Radial velocity	[m/s]
V _{exqua}	Total velocity	[m/s]
V	Velocity vector	[m/s]
W	Tangential velocity	[m/s]

Greek Symbol

α	Thermal diffusivity	[m ² /s]
R	Under-relaxation parameter	[-]
ε	Dissipation rate of turbulent kinetic energy	[m ² /s ³]
Γ	Exchange coefficient of diffusion Circulation	[m ² /s]
μ	Dynamic viscosity to relate stress to liner deformation	[kg/m/s]
Λ	Viscosity to relate stress to volumetric deformation	[kg/m/s]
ν	Kinematic viscosity	[m ² /s]
ρ	Density	[kg/m ³]
τ	Stress	[N/m ²]
ω	Specific dissipation rate	[s ⁻¹]
τ_{ij}	Viscous stress component acts in the j-direction on a surface normal to i-direction	[N/m ²]
ϕ	Equivalence ratio, General variable	[-]

ℓ, ℓ_t	Turbulence length scale	[m]
η	Kolmogorov length scale	[m]

Subscript

A	Air
i, j, k	refer to the three directions of a Cartesian coordinate system
I	Inlet Condition, random element
k	Kolmogorov scale
f	Fuel
fd	Diffused Fuel
fp	Premixed Fuel
o, e	Exit Condition, oxidizer
g	Geometric
p	Premixed
eff	Effective
ox	oxidizer stream inlet

Abbreviations

BO	Blowoff
CFD	Computational Fluid Dynamics
CIVB	Combustion Induced Vortex Breakdown
COG	Coke Oven Gas
CRZ	Central Recirculation Zone
CTRZ	Central Toroidal Recirculation Zone
DES	Detached Eddy Simulation
DNS	Direct Numerical Solution
FB	Flashback
FDM	Finite Difference Method
FEM	Finite Element Method

FVM	Finite Volume Method
GT	Gas Turbine
GTRC	Gas Turbine Research Centre
HHV	High Heating Value
ICE	Internal Combustion Engines
IRZ	Inner Recirculation Zone
LHV	Lower Heating Value
LES	Large Eddy Simulation
LPM	Lean Premixed Mixture
LPMC	Lean Premixed Combustion
PDF	Probability Density Function
PVC	Precessing Vortex Core
RFZ	Reverse Flow Zone
RNG	Renormalization-Group
RSM	Reynolds Stress Model
SST	Shear-Stress Transport
STP	Standard Temperature and Pressure
TDMA	Time Division Multiple Access

Chapter One

Introduction

CHAPTER ONE

INTRODUCTION

“If a man empties his purse into his head, no man can take it away from him; an investment in knowledge always pays the best interest.”

Benjamin Franklin

1.1 World Energy Consumption

The global demand for energy, and more especially clean energy, is increasing rapidly. There is a universal need for efficient technologies that will contribute to the sustainable development of the host countries and communities by providing employment, improving quality of life and protecting the environment. This energy solution must include the development of new clean, non-polluting and non-dangerous sources of energy for the environment and must necessarily guarantee sustainability on a human scale contrary to the current energy solutions [1-2].

The question here is how much energy needs to satisfy the desired needs and services, but who knows the answer? Looking into the past, trying to extrapolate into the future, mankind’s energy expenditure has grown differently in different areas:

- Energy used to procure food and water is now (say year 2000, per capita) five times larger than 10^6 years ago.
- Energy used for transportation is now sixty times larger than 500 years ago.
- Telecommunication technology; this scarcely existed 150 years ago.

Presently, we only use two final-user commercial-energy carriers: fuels and electricity. Most of the energy trade involves fuels, presently, in the past, and in the foreseeable future, as summarised in Table 1.1 [3].

Year 2000		Year 2020 prediction	
Primary Energy	Energy Carriers (end use)	Primary Energy	Energy Carriers (end use)
90% Fuels	84% Fuels	90% Fuels	82% Fuels
7% Nuclear	16% Electricity	5% Nuclear	18% Electricity
3% Hydro	Electricity production: <ul style="list-style-type: none"> • 66% Fuels • 17% Nuclear • 17% Hydro 	3% Hydro 2% Wind	Electricity production: <ul style="list-style-type: none"> • 65% Fuels • 10% Nuclear • 15% Hydro • 10% Wind, solar

Table 1.1 Short summary of fuel share in world energy utilization [3]

The substances collectively known as fuels (basically coal, oil, gas, bio fuels and synthetic fuels) are mainly used as convenient energy stores, because of their high specific energy-release when burnt with ambient air. The burning process, however, is not essential for the release of fuel-and-oxidiser energy; the same global process takes place in fuel cells without combustion. Fuels, as energy sources, are used for heat generation, for work generation, for cold generation, or for chemical transformations. Fuels are also used for non-burning purposes, as for the chemical synthesis of materials, mainly polymers (fibres, plastics, cosmetics, pharmaceuticals, mineral oils, etc.), but this is not considered here anymore. In summary, fuels may be used for the following [2]:

1. To produce heat in a burner (thermo-chemical converter). This heat may be used for direct heating, indirect heating (heat exchangers), for incandescent lighting, for feeding a thermal machine (heat engine, refrigerator, or heat pump) to produce power, cold, or more heat, or for materials processing.

2. To produce work (and heat) in a heat engine (mechanical-chemical converter). This work may be used to produce propulsion, or electricity, or cold, or more heat.
3. To produce electricity (and heat) in a fuel cell (electro-chemical converter). This electricity may be used to produce propulsion, cold, more heat, or for materials processing.
4. To produce materials (and heat) in a reactor (chemo-chemical converter); e.g. polymer synthesis, oils, perfumes.

Fuels may be considered as primary energy (i.e. directly extracted from natural sources and put on the market), as energy carriers or secondary-energy sources (i.e. manufactured fuels such as crude-oil distillates and synthetic fuels), or as final energy (bought by the end-user for final consumption).

Fuel consumption, both as primary energy (i.e. as found in nature) and as a final energy source (i.e. as input to the end user), is today the major contributor (near 90%) to energy use, both at source and at destination (up to the Middle Ages, animal power, water-mills and wind-mills were large contributors; in the far future, nuclear fusion might take over). The analyses of the utilisation of energy as a commodity (sources, transportation, storage and consumption) is sometimes called Energetics.

Fuels major share in world energy market (80% to 90%) means that the two terms, fuels and energy, can be used indistinctly both for primary and for final consumption. Beware, however, that some people use indistinctly 'electricity' and 'energy', without such a rational definition as above. On the other hand, it is worth considering that all terrestrial energy (except the minor contribution of gravitational tidal energy) is ultimately of nuclear origin: nuclear fission inside the Earth generates geothermal energy (also a minor share of the overall Earth energy budget), and nuclear fusion at the Sun provides the major energy input, which is partially converted in the short term (weeks) to hydraulic energy and wind energy, in the midterm (a year) to biomass energy, and in the very long term (million years) to fossil fuels. This is the dominant commercial source nowadays.

1.2 World Energy Production

Primary energy production (i.e. resource consumption) is computed from the budgets and estimates of industrial producers:

- Coal mines and coal importers
- Crude-oil extractors and importers
- Natural gas extractors and importers
- Nuclear energy generators
- Renewable energies: hydroelectric plants, wind-mill fields, solar energy fields, biomass industries, etc. Most of them, apart from many hydro-electric schemes are only economically viable through the application of government subsidies.

Crude oil and its derivatives still take the lead as a main source of energy production as it represents almost 1/3 of total energy production, as shown in Figure 1.1 and 1.2. Coal and natural gas share approximately the same figures and they occupy second rank in the energy resources.

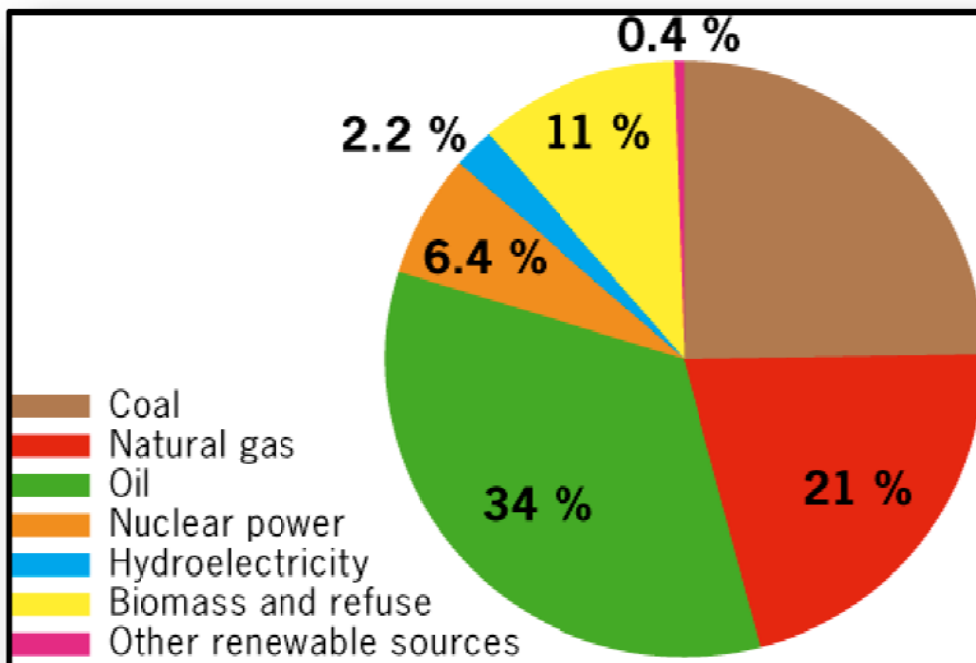


Figure 1.1: World energy supply in percentage [4]

Nowadays, using biomass as a fuel has become a strong alternative to traditional methods and is considered as a new effective source of fuel and this is confirmed when we see it contributes about 11% of the total amount of energy produced. Nuclear power represents half that of biomass and is still limited in developed countries and some developing countries because of the political influences, the technical difficulties and the risks surrounding use of nuclear energy. Using a water turbine to produce electricity contributes about 2.2% of the total amount of energy production. The other renewable energy produce the lowest amount of energy as they are still expensive compared to the other energy resources.

Figure 1.2 reveals that the energy production slope has somewhat increased since 2000 at a gradient above the normal range. This increase could result from the rapidly increasing use of computer technology as well from population growth.

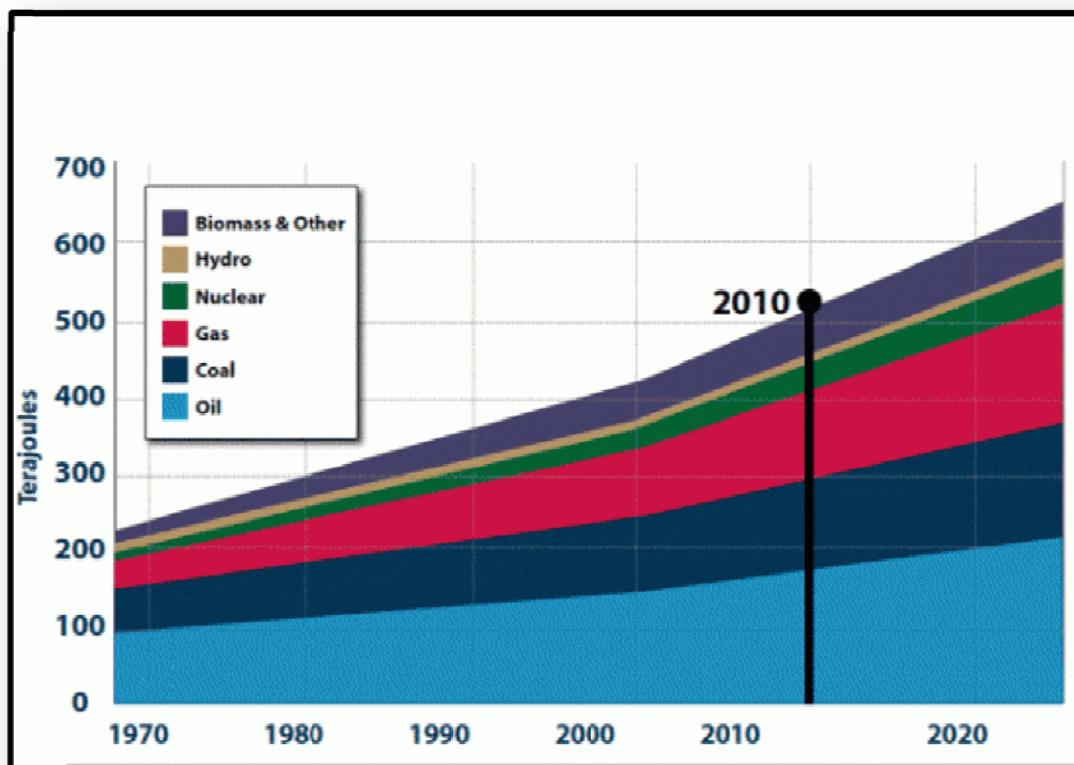


Figure 1.2: World energy production in terajoules [5]

Moreover, world energy production is increasing but not fast enough to prevent an energy crunch in the forthcoming future [6-7].

1.3 World Energy Future

The future of energy (as a human commodity) looks dark nowadays, even darker than the future of clean water and food. The key problem is that energy consumption is growing disproportionately to population growth (as food may be), at a much higher rate (because of the 'developed' way-of-life), with two associated consequences [8]:

- Environmental impact, because the largest share in energy production comes from fuel combustion, which generates global-warming gases and chemical pollution (global and local), and other energy sources do not show a clear alternative: nuclear fission has the unsolved problem of waste fuel and proliferation, and renewable energy sources have low power density and are not free of environmental impact (e.g. effects of wind mills on fauna and landscape).
- Scarcity of cheap resources, because readily-available oil, gas, and coal deposits, are being exhausted at a quicker pace than new reserves are found.

As a clear solution to this energy problem is presently not at hand, the most rational approach might be to push along several fronts, looking forward to solving some of the inconveniences (being alert for new possibilities), and weighting more on those showing better promise at the time being. In particular:

- New fossil fuel plants seem to be unavoidable for decades to come, at least. Cleaner and more energy-efficient combustion processes must be developed for the traditional fuels, e.g. using natural-gas combined-cycle plants with a thermal efficiency nearly double that of old coal-fired plants, capturing CO₂ emissions from traditional exhaust gases (e.g. using amine absorption/regeneration), or helped by the oxy-combustion process, or directly from the fuel by reformation of the fossil fuel to less-contaminant fuels before combustion (the drive towards the hydrogen economy), etc.
- New nuclear fission plants can alleviate in the short term the energy problem, their problem with nuclear waste perhaps being solved in the future, but their

remote risk of massive life destruction renders them too risky for wide-world proliferation (energy consumption in the future will increase most amongst presently underdeveloped societies). Power plants intrinsically safe, intrinsically non-proliferating, and making best use of fissionable material should be developed. Nuclear fusion research must be further encouraged, as being the only panacea on the horizon.

- New renewable plants must be promoted, even subsidised if one takes account of the social costs implied in traditional power plants (from human health to world politics), but not as a present panacea: nowadays, they cannot provide a complete substitute to fossil-fuel plants and will not be able to in the decades to come. Among renewable sources, the two approaches with a wider future are, first, biomass cultures for bio fuels (from non-alimentary plants), and second, thermal solar energy plants, although wind energy is developing faster, at present.

1.4. Gas Turbines

A gas turbine, also called a combustion turbine, is a rotary engine that extracts energy from a flow of combustion gas. It has an upstream compressor coupled to a downstream turbine, and a combustion chamber in-between, as shown in figure 1.3.

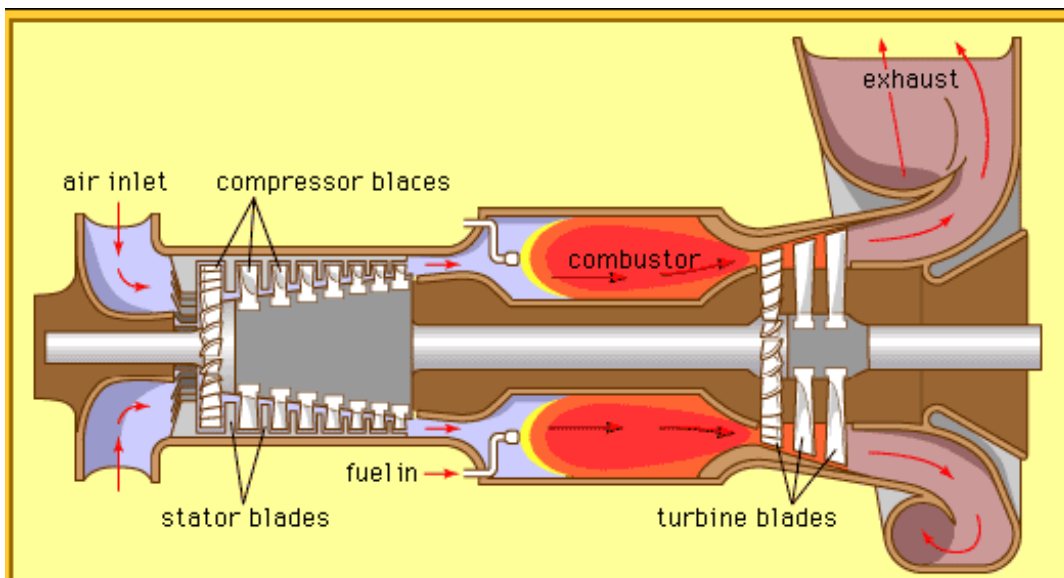


Figure 1.3 Gas turbine conventional arrangements showing combustor [9]

Energy is added to the gas stream in the combustor, where pressurized air is mixed with fuel and ignited. Combustion increases the temperature, velocity and volume of the gas flow. This is directed through a nozzle over the turbine's blades, spinning the turbine and powering the compressor.

Energy is extracted in the form of shaft power, compressed air and thrust, in any combination, and used to power aircraft, trains, ships, generators, and even tanks

1.4.1 Gas Turbine Combustor

The gas turbine combustor is considered to be one of the most complicated systems in gas turbine design. This complexity arises as the combustor connects the two other main parts, the compressor and the turbine. Furthermore, a designer of this system requires knowledge involving fluid dynamics, combustion and mechanical design. Recently, the complexity has increased rapidly because of new requirements of high efficiency, less undesirable emissions and alternative fuels. The designer of a combustion system needs to reach an optimum compromise between all conflicting requirements [8, 10].

These new requirements force researchers to use high levels of computational mathematics like computational fluid dynamics and software to increase the speed and accuracy of design.

The major goals of general gas turbine combustor design are:

- High combustion efficiency;
- Reduction of visible smoke;
- Reduction of oxides of nitrogen, NO_x; and
- Development of a design capable of withstanding the combustion temperatures through advanced materials and cooling designs.

These are some of the essential requirements for gas turbine design that need to be satisfied with an affordable cost.

1.4.2 Combustion Performance

Combustion stability, efficiency and lighting are ultimately inseparable. First of all combustion stability during the gas turbine operation demands that the combustion process

should burn fuel over a wide range of operating conditions in a stable manner and without any combustion problems that could arrest the burning process for any reason.

Secondly, the combustion efficiency should be very close to 100%.

Thirdly, no less important than the former elements, there should be a proper start system to ensure the engine reaches a self-sustaining speed. However, in an aircraft gas turbine there is the important additional requirement of rapid relighting of a combustor after a flame blowoff and relight (high altitude relight). The above three features of combustion (stability, efficiency, and ignition), are major aspects in a gas turbine.

1.4.3 Operational Requirements and Combustor Design Factors

Gas turbine requirements from combustors are high combustion efficiency (>99%) and low-pressure loss (2-8% of the compressor delivery pressure); such parameters will have no real effect on the cycle efficiency and the output power. On the other hand, it is quite important for the combustor to provide a suitable, near uniform turbine inlet temperature and velocity profile plus low undesirable emission throughout the period of operation.

The difficulties of the aforementioned points arise because of the different operational conditions through altitude change and power requirements (for aircraft engines). Atmospheric conditions change rapidly during ascent and descent phases of flight. The combustor needs to deal with these variations and maintain flame stability and appropriate turbine inlet temperature. For power turbines there are similar, but different considerations, ranging from fuel switching (natural gas to fuel oil and vice versa) and requirements for turndown, start up and shut down.

There are many types of fuel used in gas turbine combustors according to the application. These include natural gas, liquid distillate, diesel fuel, and residual fuel oil. The latter one is not widely used because of the high cost of pre-treatments. Some combustors work with dual firing. This means you can switch between two kinds of fuel according the operational requirements you might have.

The following summarises combustor design parameters [8, 10]:

- Outlet gas combustor temperature should be appropriate for the turbine blades (~ 1850K for aeronautical applications, 1750K for power applications).

- Temperature distribution through the turbine blades should be evaluated to avoid local failure at any stress point.
- Suitable air velocity (30-60m/s) and air / fuel ratio (60:1 to 120:1 for simple gas turbines cycle and 100:1 to 200:1 if heat exchangers are used) should be maintained.
- Carbon spot formation in the turbine blade should be avoided because it will cause erosion of the blade or block the cooling passages; aerodynamically it can cause vibration in either the combustor or turbine.
- The combustor should be stable for a wide range of chamber pressures and have the ability to be relit at high altitude and speed in the event of a flame blowoff.
- There should be avoidance of smoke in either industrial or aeronautical gas turbines.
- The amount of pollutants CO, UHC, and NO_x should be minimised.

An important feature is the connection and coupling between the compressor and combustion chamber and thus the inlet velocity and other conditions at entry.

Aircraft engines need small space and low weight, this will lead to use of light –gauge, heat resisting alloy, sheet working for maybe 10,000 hours between overhaul; industrial gas turbines conversely can perform for up to 100,000 hours between overhaul.

Any pressure drop through the combustor leads to both an increase in specific fuel consumption and reduction in specific power output.

1.4.4 Types of Combustion System

Combustion in the normal, open cycle, gas turbine is a continuous process in which fuel is burned in the air supply by the compressor; an electric spark is required only for initiating the combustion process and then the flame should be self-sustainable. The designer has many factors to consider first before making the optimum choice in consideration of them all. These include orientation, weight, frontal area, volume and emissions. There are many types of combustor to suit different applications including Can (or tubular) combustors, Can-annular (or tubo-annular) combustors, Silo combustors...etc.

Generally, industrial gas turbine designers are looking to new designs with dry low emissions (DLE) type of combustor, without adding any complexity of steam or water injection.

Thus, the increasing consumption of fossil fuels and their greenhouse emissions have increased the necessity for research to develop new and improve existing mechanisms for the generation of energy in a variety of industrial processes. Swirling flow combustors are widely used in almost all gas turbine combustors; they are not well understood and represent a fruitful area of research capable of giving considerable benefit to gas turbine combustor designers.

1.5. Summary

In detail, the aim of this project is to study and analyse flashback and blowoff limits characteristics of gas turbine swirl burners of variable swirl number and a wide range of hydrogen containing fuels. One version at a swirl number of 1.47 has been analysed numerically by CFD using computer software simulation (FLUENT), complimented by experimental data for a range of different fuels under fully premixed combustion conditions. The second one is a radial inlet swirl burner, which has been examined experimentally to find the flashback and blowoff limits for seven different premixed fuel blends for unconfined and confined conditions.

1.6. Objectives

This thesis covers two main areas as follows:

- Experimental and numerical studies of flashback in a tangential entry swirl burner, originally designed for the combustion of poor quality fuels. The work focussed on the flashback mechanism involving boundary layer flame propagation, determined by the critical boundary velocity gradient, derived both from experiments and CFD. The numerical simulation has confirmed and clarified experimental findings.
- Based upon the work described above a radial vaned swirl burner of variable swirl number has been designed and built; it has been examined experimentally under a wide range of conditions for flashback and blowoff behaviour as a function of geometry and swirl number. Up to seven different fuel blends have been investigated, ranging from pure methane to pure hydrogen, hydrogen/methane blends, methane/CO₂ blends and Coke Oven gas (COG). The data has been also

transformed into heating effect as a function of total gas throughput to allow direct comparison of thermal inputs under different operation conditions for all fuel blends. This allows determination of operational regimes of different fuels and levels of premixing permissible.

1.7 Thesis Structure

This thesis is divided into a number of chapters, which are as follows,

- **Chapter 1.** An introduction illustrates the basic principles of gas turbines including the problems of uncontrolled emissions and energy consumption.
- **Chapter 2.** This chapter comprehensively reviews previous work in the area and discusses phenomena including coherent structures in swirl flow, combustion technology, lean premixed combustion, fuel blends, flashback and blowoff.
- **Chapter 3.** Here, explanation is made of the numerical approach which has been used to model the swirling flow occurring both inside and outside of the burner. FLUENT software from ANS12 has been used. All the basic equations, the turbulence model, combustion models, and geometry mesh have been extensively discussed and clarified.
- **Chapter 4.** The numerical simulation for 100kW Tangential swirl Burner and the method of data analysis is explained with discussion of the results and the interaction between experimental and numerical studies. Discussion is made of the results obtained under isothermal, combustion and flashback conditions in order to apply them in real industrial situations.
- **Chapter 5.** This chapter outlines the methodology of design of the prototype radial vaned swirl burner, the rig setup and all the parts of the burner and the type of fuel blends used during the tests.
- **Chapter 6.** This chapter contains flashback determination of the radial vaned swirl burner for confined and unconfined conditions for different types of fuel blends with discussion of all the results.
- **Chapter 7.** This chapter describes blowoff estimation of the radial vaned swirl burner for confined and unconfined conditions for different types of fuel blends and contains discussion of all the results.

- **Chapter 8.** This chapter describes matching of flashback and blowoff results to produce curves explaining the possibilities of changing the fuel blend for a given gas turbine combustor from pure methane to another fuel blend with maximum premixing.
- **Chapter 9.** This chapter contains conclusions and further work, providing a summary of the key findings obtained with this project, suggesting several research programs that can be carried out for future experiments.

Chapter Two

CHARACTERISTICS OF A GAS TURBINE SWIRL COMBUSTOR

CHAPTER TWO

CHARACTERISTICS OF A GAS TURBINE SWIRL COMBUSTOR

“You will never do anything in this world without courage. It is the greatest quality of the mind next to honour.”

Aristotle

2.1 Introduction

Gradual and continuous evolutionary improvements have occurred with gas turbine combustion systems since they were discovered some 70 years ago. Dramatic changes have happened over the last quarter century as environmental aspects enter very strongly in the strategic plans of companies and scientists that are working in the field of gas turbine development.

Many parameters and phenomena affect combustors performance, efficiency and emissions. Gas turbine combustors are sophisticated combustion systems because they included many physical parameters and chemical characteristics that are interrelated. Designers of these important devices are looking for optimum designs that can offer high safety and maximum energy release with lower emissions with an acceptable cost.

Increasing interest in lean premixed fuel with swirl combustors has arisen because of its propensity to reduce NO_x emissions. This coupled with the use of hydrogen containing alternative fuels offers the possibility of reduced greenhouse gas emissions. Alternative fuels include hydrogen-enriched natural gas in various proportions, by-products of process industries such as coke oven gas and indeed pure hydrogen.

This gives rise to numerous areas of concern for operators and developers of gas turbines especially in the area of the combustor, which include flashback, temperature levels, blowoff, combustion instability, and fuel interchangeability. Flashback with hydrogen

containing fuels is of special concern with hydrogen enriched fuels, owing to the high flame speed of hydrogen, to such an extent that diffusion combustion is commonly employed resulting in higher NO_x emissions.

This chapter introduces some of these phenomena and features to explain their effects upon swirl combustor performance.

2.2 Types of Combustible Mixtures

Technically, most of the literature which has described the mixing processes in gaseous combustion systems can be divided into non-premixed, premixed and partially premixed. These are the main combustion mixture types.

2.2.1 Non-Premixed Combustion

In many combustion applications fuel and oxidizer enter separately into the combustion chamber where they mix and burn during continuous mutual diffusion; this can be called non-premixed combustion [11-12].

Classic examples are combustion in a furnace, diesel engine and some gas turbine applications. The non-premixed combustion reactions occur in the swirl stabilised combustion zone with the reactants being converted into products downstream. They then are diluted by secondary air to reduce the temperature at the exit of the combustor to values that are acceptable for the turbine blade material. In modern stationary gas turbines, liquid fuel is often pre-vaporized and partially premixed before entering the gas turbine combustion chamber. Similar partial premixing occurs with natural gas. Models used for partially premixed combustion are more relevant for describing the flame propagation and combustion processes occurring in these engines.

Sometimes non-premixed combustion (called diffusive combustion) is used. Diffusion is the rate controlling process.

The time needed for convection and diffusion, both being responsible for turbulent mixing is typically much larger than the time needed for combustion reactions to occur.

However, the non-premixed mixture in gas turbine combustors shows more stability in operation than other type of mixtures either experimentally [13] or in using CFD simulation [14].

In 1928 Burke and Schumann [15] showed that an important feature of calculation procedures was the introduction of a chemistry independent “conserved scalar” variable called the mixture fraction. All scalars such as temperature, concentrations, and density could then be uniquely related to the mixture fraction.

2.2.2 Premixed Combustion

In premixed combustion, fuel and oxidizer are mixed at the molecular level prior to ignition. Combustion occurs as a flame front propagating into the unburnt reactants. Premixed flames propagate in a mixture of fuel and air due to heat conducted from the burned hot products to fresh cold reactants. Premixed combustion often occurs in a thin reaction zone separating reactants and products. Turbulent premixed flames are particularly complicated due to very strong coupling of the flame with the small-scale structure of turbulence [11-12].

Premixed combustion is much more difficult to model than non-premixed combustion. The reason for this is that premixed combustion usually occurs as a thin, propagating flame that is stretched and contorted by turbulence. For subsonic flows, the overall rate of propagation of the flame is determined by both the laminar flame speed and the turbulent eddies. The laminar flame speed is determined by the rate that species and heat diffuse upstream into the reactants and burn. To capture the laminar flame speed, the internal flame structure would need to be resolved, as well as the detailed chemical kinetics and molecular diffusion processes. Since practical laminar flame thicknesses are of the order of millimetres or smaller, resolution requirements are usually unaffordable in terms of computer storage. The effect of turbulence is to wrinkle and stretch the propagating laminar flame sheet, increasing the sheet area and, in turn, the effective flame speed. The large turbulent eddies tend to wrinkle and corrugate the flame sheet, whilst the small turbulent eddies, if they are smaller than the laminar flame thickness, may penetrate the flame sheet and modify the laminar flame structure.

The essence of premixed combustion modelling lies in capturing the turbulent flame speed, which is influenced by both the laminar flame speed and the turbulence.

In premixed flames, the fuel and oxidizer are intimately mixed before they enter the combustion device. Reaction then takes place in a combustion zone that separates unburnt reactants and burnt combustion products.

Premixed combustion has been shown to cause many difficulties throughout the history of gas turbine combustors. These unwanted difficulties include instability, flashback, and blowoff.

2.2.3 Partially Premixed Combustion

Partially premixed combustion systems are premixed flames with some elements of non-uniform fuel-oxidizer mixtures (equivalence ratios). Such flames include premixed jets discharging into a quiescent atmosphere, lean premixed combustors with diffusion pilot flames and/or cooling air jets, and those with imperfectly mixed inlet flows [11-12].

Partially premixed combustion models are generally a simple combination of non-premixed model and premixed model. This means that the partially premixed combustion would carry the advantages and disadvantages of both types of mixture models.

Partially premixed flames exhibit the properties of both premixed and diffusion flames. They can occur under many circumstances including when an additional oxidizer or fuel stream enters a premixed system, or when a diffusion flame becomes lifted off the burner so that some premixing takes place prior to combustion.

2.3 Lean Premixed Mixture (LPM)

Lean fuel premixing is considered to be one of the most promising technologies for emission reduction in gas turbine combustion systems. Lean combustion is used widely in many applications, including gas turbines, boilers, furnaces, and internal combustion engines. This wide range of applications all attempt to use the advantage that combustion processes operating under fuel lean conditions can have very low emissions and very high efficiency. Pollutant emissions are reduced because flame temperatures are typically low, reducing thermal NO_x formation.

In addition, for hydrocarbon combustion, when lean combustion is accomplished with excess air, complete burnout of fuel generally results, reducing hydrocarbon and carbon monoxide emissions. Unfortunately, achieving these improvements and meeting the

demands of practical combustion systems is complicated by low reaction rates, extinction, instabilities, mild heat release, and sensitivity to mixing.

A number of internal structures appear in the flow field and are still not well understood including the central recirculation zone (CRZ) and precessing vortex core (PVC). There are numerous studies of the CRZ and PVC, both experimental and numerical, formed during combustion at different equivalence ratios and flow rates. They clearly show the need for more work in this area.

Amongst the most promising technologies used to reduce the impact and production of NO_x, lean premixing and swirl stabilised combustion are regarded as very good options. However, premixing is not perfect because usually fuel and air are mixed shortly before entering the combustion chamber, leading to a significant degree of unmixedness [16]. On the other hand, it has been found that the levels of swirl used in some combustors, coupled with the mode of fuel injection can induce the appearance of unwanted and undesirable regular fluid dynamic instabilities. Swirl stabilized combustion creates coherent structures that may produce low-frequency modes capable of coupling with natural frequencies of the equipment [17], exciting oscillations that can damage the system. Therefore, there is vast room for improvement for both technologies. Recent research [18-20] has focused on the use of both technologies for the improvement of the combustion process, adding passive and active mechanisms of suppression for the reduction of combustion related instabilities. New combustion systems based on ultra-lean premixed combustion have the potential for dramatically reducing pollutant emissions in transportation systems, heat, and stationary power generation [21]. However, lean premixed flames are highly susceptible to fluid dynamic and combustion instabilities, making robust and reliable systems difficult to design. Low swirl burners are emerging as an important technology for meeting design requirements in terms of both reliability and emissions for next-generation combustion devices.

They are also prone to flashback [22] as the flame may stabilise in the premixing zone, upstream of the combustion chamber. This regime of combustion can lead to severe damage of the injection device by increasing the wall temperature. Blowoff and re-ignition are also critical processes for gas turbine operation.

Instabilities during the gas turbine combustion are generally encountered when using lean premixed mixtures (LPM). LPM gas turbine engines employ swirling flows to stabilise the flame for efficient and clean combustion. One of the most important flow features produced by a swirl injector is a central recirculation zone (CRZ), which serves as a flame stabilization mechanism. Flows in this region are, in general, associated with high shear rates and strong turbulence intensities resulting from vortex breakdown. Although this type of flow has been comprehensively considered, there remain many uncertain issues, such as swirl generation, vortex breakdown, axisymmetry, and azimuthally instabilities. Dynamic combustion instabilities coupled with the effect of flow swirl have been discussed and analyzed to show the interaction of all these characteristics and their effects [17, 23-24].

2.4 Swirling Flow and It's the Effect upon Combustion

A swirling flow is defined as one undergoing simultaneous axial and vortex motions. It results from the application of a spiralling motion, a swirl velocity component (tangential velocity component) being imparted to the flow by the use of swirl vanes, axial-plus-tangential entry swirl generators or by direct tangential entry into the chamber [23].

Technologically, the use of swirl generators has been essential for the design of new equipment capable of reducing emissions, improving stability, whilst at the same time extending blowoff limits. The use of swirling flows is a well know technique to increase turbulent flame speed, reduce combustor size, avoid flashback and improve mixing of reactants in order to reduce emissions and increase power density [17, 25-26].

For more than two centuries, swirl burners have been used for the combustion of fuels like pulverised coal and coke. Nowadays, most large combustion systems use some form of swirl combustor [26-27].

Throughout the last few decades numerous experiments have been carried out to obtain a better understanding of the various underlying phenomenon.

The precessing vortex core (PVC) is one of these phenomena. This acts as a low frequency stirring mechanism, and often interacts strongly with the CRZ, which is the feature of swirling flows which give them their significant flame stabilization characteristics [17, 23, 28-29]. However, some coherent vortices and large scale structures appear in the flow under particular circumstances such as the use of high swirl, high flow rates or variable

equivalence ratios. There are still many uncertainties regarding the occurrence of some coherent structures, their influence and their relation to the important central recirculation zone (CRZ), where the mixing and flame stabilization process takes place. Details of this zone and mixing potential have been extensively investigated [30-31]. The CRZ is significant for improving mixing and preheating of the combustible mixture and air [32].

Numerical methods, particularly CFD analysis has been one of the familiar techniques used to analyse the swirling flow regime. Most of these simulations have found similar visualisations even when they have used different criteria. All methods have used the Navier–Stokes equations to solve the fluid flow equations.

Studies include:

- High-intensity swirling flow in a model combustor subjected to large density variations[33].
- Large-eddy simulation (LES) of a fuel-lean premixed turbulent swirling flame [34].
- The performance of a differential Reynolds-stress turbulence model has been assessed in predicting a turbulent, non-premixed combusting swirling flow of the type frequently found in practical combustion systems [14]. Calculations are also performed using the widely employed eddy-viscosity based $k-\varepsilon$ turbulence model in order to examine the relative performances of these two closure models.

2.4.1 Swirl Flow Generation

Three principal methods are used to generate swirl flow [23]:

1. Tangential entry (axial-tangential entry swirl generator),
2. Guided vanes (swirl vane pack or swirler),
3. Direct rotation (rotating pipe).

In the present work, the first method has been used to generate swirl flow.

2.4.2 Swirl Number

Swirling flows occurs as a result of the application of spiralling motion to the flow. The degree of swirl imparted to flow is characterised by the swirl number S . The swirl number is a non-dimensional number representing the ratio of axial flux of angular momentum to the axial flux of axial momentum times the equivalent nozzle radius [23]:

$$S = \frac{G_\theta}{G_x r} \quad 2.1$$

where:

$$G_\theta = \int_0^\infty (\rho u w + \rho \overline{u'w'}) r^2 dr \quad 2.2$$

and

$$G_x = \int_0^\infty (\rho u^2 + \rho \overline{u'^2} + (p - p_\infty)) r dr \quad 2.3$$

However, the above equations require knowledge of all the velocity and pressure profiles at every condition and giving a different swirl number at each point of the flow domain. This kind of calculation would be extremely difficult to undertake.

Syred and Beer in 1974 [35] proposed that this expression could be simplified for constant density environments, i.e. isothermal conditions, to a simple function of geometry:

$$S_g = \frac{\pi r_e r_{eff}}{A_t} \quad 2.4$$

where r_{eff} is the effective radius located at the middle of the inlet of the quarl, r_e is the radius on which the tangential inlets are attached with respect to the center of the combustor and A_t is the total area of the tangential inlet.

This geometrical swirl number does not account for phase changes that occur under combustion conditions, thus a further modification was introduced by Fick [26]. As the flow regime thermally expands under combustion conditions an increase in axial velocity occurs increasing the axial flux of axial momentum. This causes the swirl number to decrease in proportion to the ratio of the mean temperatures at the inlet and outlet thus:

$$S_{gcomb} = S_g \frac{T_i}{T_e} \quad 2.5$$

The swirl number can be accurately calculated by using velocity and pressure profiles. This would give local, precise values of swirl at various positions in the burner. This clearly provides better information about the swirl/pressure relationship and thus the behaviour of the flow. However, the main advantage of the above approximations is that it allows the designer to manipulate the test rig in order to achieve approximate levels of swirl that

generate the desired flow field phenomena without expensive measurement campaigns. More detailed explanations and derivations of the swirl number are found in [23, 35-36].

2.4.3 The Basic Swirl Stabilization Effects

The typical values of swirl number in gaseous and liquid fired swirling jets are between 0.5-2, cyclone combustors can range from 6-30, whereas dust separators normally operate with levels between 2 and 6. The basic effects of swirl on the subsequent flow field can be divided into three categories based on the level of swirl [23, 35, 37]:

1. Weak swirl, $S < 0.6$
2. Critical swirl, $S = 0.6$
3. Strong swirl, $S > 0.6$

The weak values of the swirl number lead to increases in the width of free and confined jet flows, also improving entrainment and decay. Radial pressure distributions are introduced due to centrifugal force field effects but do not give rise to significant axial pressure gradients and as such, weak values of swirl do not induce flow reversal. In other words the swirling jet is quasi two-dimensional as there is no significant coupling between the axial and tangential velocity components. As a result, axial pressure gradients are commonly omitted from analyses [23]. The radial pressure distribution at any axial station is defined by:

$$\frac{\partial p}{\partial r} = \frac{\rho w^2}{r} \quad 2.6$$

Whilst the level of swirl is increased (assuming a fully developed turbulent approach flow) a strong coupling between the velocity components evolves to ultimately reach a critical state and induces flow reversal along the central axis of the swirling jet. The standard parameters reported in the literature required to achieve a fully developed flow reversal are $S > 0.6$ with a Reynolds number exceeding the transition region, typically $Re = 18000$. The critical value of swirl is based on open channel flow thus if a physical pressure gradient is produced, as via a divergent or convergent exit geometry, the critical value is lowered.

The structure of the central reverse flow zone (CRFZ) is the most significant phenomenon in swirling combustion flows as it forms an aerodynamic flame holder whose size and shape can be easily influenced by both operating conditions and geometry. Thus the

procurement and resultant properties of the CRZ are flexible and can be integrated directly into burner design [23]. In short, the CRZ re-circulates hot combustion products upstream towards the low velocity regions where the local flow velocity can match the flame speed forming a highly stable flame, usually in the proximity of the burner exit. The result is a complex three dimensional flow generated at high degrees of swirl, which provides regions of high shear, increases reactant residence times, enhances flame stability and increases combustion intensity. Typical streamlines representative of this phenomenon are shown in Figure 2.1.

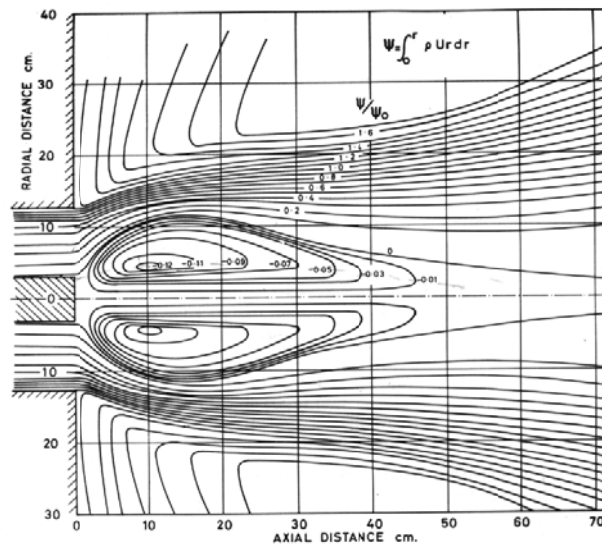


Figure 2.1 Recirculation in a swirling jet adapted from Beer and Chigier[36]

Similar CRZ contours has been derived through the CFD analysis in this project. They are similar as shown figure 2.2 below. The CRZ appears in the middle of the contours past the burner exit throat.



Figure 2.2 Velocity contours with combustion in a swirl burner

It is important to realise that the boundary of the RFZ is only well defined in a time-averaged sense. The flows with a high degree of swirl are not perfectly symmetrical about the central axis of the vortex in the flow stream.

The flame stabilization is an important issue in the combustion, the conventional methodology is to insert a bluff body and create a stagnation region with a CRZ for flame stabilization. One of the configurations used in this project uses an injector as a bluff body. CFD analysis reveals a stable partially mixed flame of this form of flow, for example Figure 2.3 reveals the corresponding temperature contours corresponding to the velocity contours of Figure 2.2.

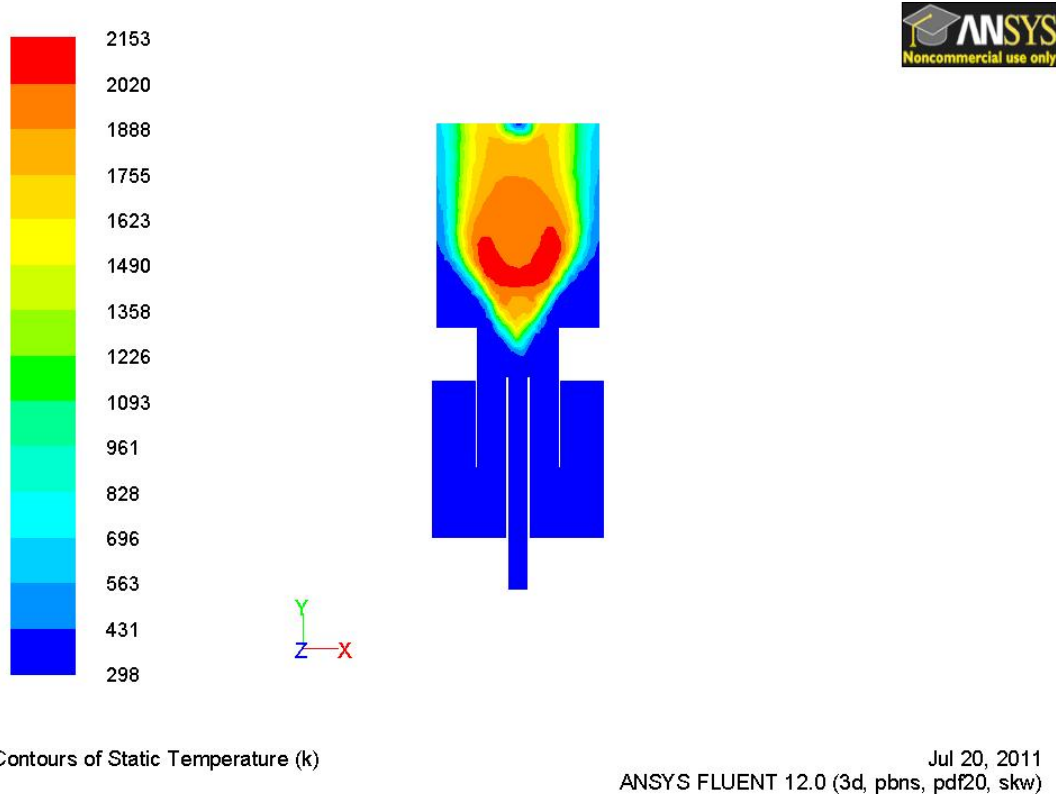


Figure 2.3 Stable partially mixed flame of swirling burner temperature contours

2.5 Combustion Instabilities

Combustion instability or “dynamic instabilities” refer to damaging oscillations driven by fluctuations in the combustion heat release rate. These undesirable oscillations can cause wear and damage to combustor components and, in some extreme cases, can cause breakages of components and resulting damage to downstream turbine components.

The gas turbine engines utilising swirling flows to stabilize the flame and employing lean premixed combustion commonly encounter these kinds of instabilities.

Flows in this region are, in general, associated with high shear rates and strong turbulence intensities resulting from vortex breakdown. Even though this type of flow has been comprehensively studied, there remain many uncertain issues, such as swirl generation, vortex breakdown, axisymmetry breaking, and azimuthal instability.

Laser-induced fluorescence and chemiluminescence [24], both phase-locked to the dominant acoustic oscillation, have been used to investigate such phenomena and relate them to thermo acoustic instabilities in a swirl-stabilized industrial scale gas turbine burner.

The observed sinusoidal phase averaged flame motion in axial (main flow) direction is analyzed using different schemes for defining the flame position.

Several studies have shown that these flames exhibit complex dynamic instabilities which lead to flashback and blowoff conditions, associated with local flame extinction.

The flashback phenomenon takes place when the flame retreats back to the mixing zone. This can be caused by several different phenomena including boundary layer propagation and vortex breakdown.

The extinction events are apparently due to the local strain rate irregularly oscillating above and below the extinction strain rate values near the attachment point. In other words, the flame extinction occurs when the time required for chemical reaction becomes less than the time required to produce adequate heat to raise the new mixture up to its ignition temperature.

The flashback and blowoff limits have been given most attention during this research programme for their effects on the combustion process and how to alter them to allow safe usage of alternative, high hydrogen content fuels in gas turbine combustors. It should be emphasised that applying a consistently uniform definition of flashback and blowoff is complicated by the manner in which the flame flashed back and blew off, this varied with burner configuration and equivalence ratio.

2.5.1 Flashback

One of the fundamental features of all premixed fuel combustion systems is a tendency towards flashback. Flashback occurs when the gas velocity (flow of incoming reactants' mixture speeding along some streamlines) becomes smaller than the turbulent flame burning velocity and the flame propagates upstream into the premixed passage (premixer or burner tube), this passage cannot withstand high temperature [38]. Thus, this will cause hardware damage as shown below, figure [39].

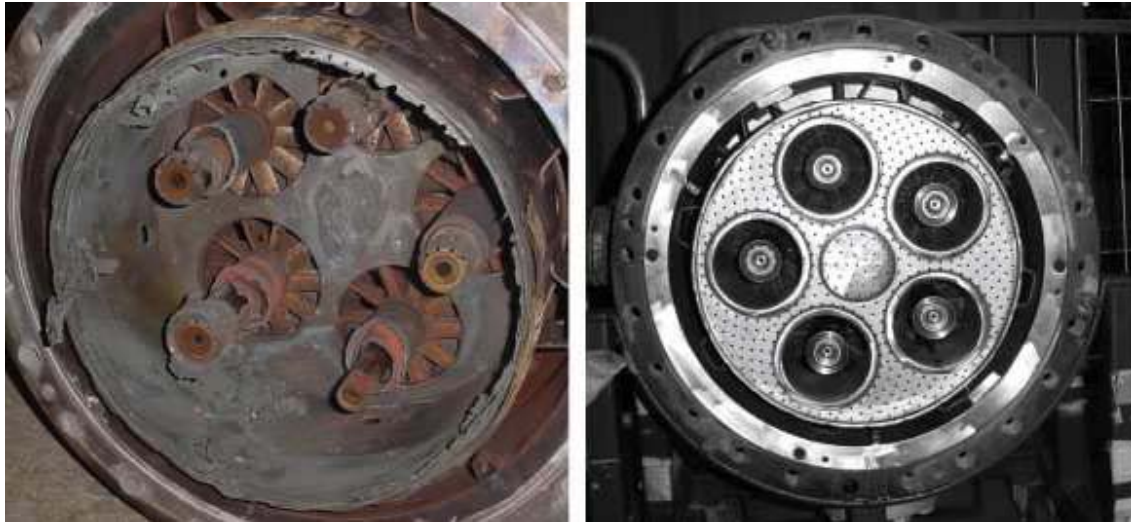


Figure 2.4: Burner assembly (left) damaged by combustion instability and new burner assembly (right) [39]

There are several types of flashback which can be identified, two important ones which are initially considered here include:

- Flashback occurring in the free stream (central flashback)
- Flashback occurring through the low-velocity flow in the boundary layer along the walls of the premixing section.

Either mechanism may involve homogeneous and/or heterogeneous reactions. Flashback occurs due to flow reversal in the bulk flow through the combustor. The flow reverse could be as a result of compressor surge, vortical motions, acoustic oscillations or combustion instability. Flashback can also occur in the absence of flow reversal if the turbulent flame speed through the gas in a premixing section is greater than the local bulk velocity [38].

Lean combustion tends to reduce flame velocity, but other factors associated with engine cycles, such as high temperatures, pressure, and turbulence levels and pre-ignition reactions in gas due to appreciable resident times at high temperature levels, cause increased flame speed. Therefore the flame velocity may be sufficiently high to cause the flashback [40].

The boundary layer flashback mechanism takes place through retarded flow in the boundary layer either along the burner nozzle exit or along the injector or bluff body.

The swirl strength is so strong that sometimes it causes the central recirculation flow to enter into the swirl chamber. As a result, the flame attached to the centre body propagates upstream and flashback occurs [21]. Excessive swirl may cause the central recirculation

flow to penetrate into the upstream swirl chamber and lead to the occurrence of flame flashback. A higher swirl number tends to increase the turbulence intensity, and consequently the flame speed. Thus, as the swirl number increases, the flame anchored by the centre recirculation flow may then propagate upstream periodically and lead to flame flashback [24].

The combination of swirl combustion and LPM technology increases the problem of flashback, especially when fuel blends include hydrogen [38, 41-42].

Flashback with lean premixed combustion is an especial problem with hydrogen, hydrogen fuel blends, as increases in flame speed by a factor of 20 are common, inferring that new or substantially modified combustors are needed, whilst dual fuelling is difficult (with say natural gas or fuel blends with hydrogen content > 40%) due to the very different requirements of the two fuels [43]. Clearly the effect of fuel composition variations upon flashback depends primarily on the corresponding change in turbulent flame speed S_T . However, the substantial variations in S_T that exist with variations in fuel composition are only beginning to be fully appreciated in the context of combustor design. Few comprehensive data sets or validated models currently exist for this phenomena.

In more detail, flashback can be caused by the following [38-42].

- I. Flame propagation in the boundary layer: This type of flashback is well known due to low flow velocities in the inner laminar sub layer of the boundary layer; this allows upstream flame propagation limited by quenching in the wall mixing zone [44]. Lewis and von Elbe [45] have suggested a relationship between laminar flame speed, S_L and the velocity gradient g_v at the wall divided by the quenching distance d_q :

$$g_v = \left[\frac{\partial u}{\partial r} \right]_{wall} \leq \frac{S_L}{d_q} \quad 2.7$$

Equation 2.7 indicates that when the flow velocity at distance d_q from the wall is lower than the flame velocity, flashback will take place leading to upstream flame propagation next to the wall. Lewis and von Elbe in their well known derivation for critical boundary velocity gradient for laminar Poiseuille flow in circular tubes showed the following:-

$$G_F = \frac{4V}{\pi r^3} \quad 2.8$$

Equation 2.8 has been extensively used to characterize flashback, especially with the use of ‘town gas’ containing significant proportions of hydrogen [44-46]. This equation 2.8 was derived by consideration of laminar pipe flow, but as admitted by the Lewis and von Elbe [45], is often used in the turbulent flow regime. This is of questionable validity but does give ready availability to a valuable databank for hydrogen based systems [45, 47]. Here, the differences between, g_f , derived from CFD must be emphasized. ‘ g_f ’ has been derived solely from CFD predictions of the boundary layers just upstream of the flame fronts just before flashback and is typically of order 10 times higher than the Lewis and von Elbe G_F .

- II. Turbulent flame propagation in the core flow: Flashback at the core can occur when turbulent flame velocity S_T becomes greater than the local flow velocity in the core flow. The turbulent burning velocity depends on the chemical kinetics and the turbulence structure, the length scales and the local velocity fluctuations. The interaction of turbulence and chemistry appear to be the biggest challenge encountered in any task to characterize the turbulent flame speed [44]. The highly corrugated structure of wrinkled swirling flames have an increasing number of surfaces above the surface of the laminar flame and this finally leads to an increase in the turbulent flame speed above the laminar value [48].
- III. Combustion instabilities: Combustion instabilities due to non-linear interaction of the pressure fluctuations and periodic heat release cause pulsations in combustion systems, which can intermittently create low velocity regions, allowing flashback. Boundary layer and core flow upstream flame propagation often comes from combustion instabilities [49].
- IV. Combustion induced vortex breakdown (CIVB): The rapid expansion at the burner exit plane creates a recirculation zone (CRZ) which acts as a flame holder. Different heat release patterns due to swirl number variation, different fuels or combustion instability can cause the CRZ to expand into a tulip shaped structure extending to the burner base plate, the flame then re-establishes itself on the new, extended CRZ boundary. Moreover, the flame can cause the vortex upstream to breakdown and

due to the adverse pressure gradient; a negative flow region appears to form ahead of it which leads to further upstream flow. The CIVB phenomenon is mainly caused by a variation in temperature ratio across the flame, in turn caused by a chemical reaction over a different range of fuel concentrations [50-53].

Flashback of the LPM combustor depends on other parameters such as the pilot fuelling rate and the geometry. A Peclet number [22, 50] model has been successfully applied to correlate flashback limits as a function of the mixing tube diameter, the flow rate and the laminar burning velocity. Using this model, a quench factor can be determined for the burner, which is a criterion for the flashback resistance of the swirler and which allows calculation of the flashback limit for all operating conditions on the basis of a limited number of flashback tests.

Also, flashback can be defined by Damköhler number and Wobbe number [54].

2.5.2 Blowoff

Blowoff takes place in gas turbine combustors due to a number of reasons, including the use of a very lean mixture or in some cases due to strong combustion instabilities, both of which can lead to flame extinction and blowoff. For low NO_x operation combustors tend to use lean mixture and, therefore, operate close to their blowoff limits. Blowoff can cause serious problem if the re-ignition system fails to relight the mixture again, especially under difficult conditions like low temperatures and pressures at high altitudes.

The crucial feature of a swirl burner is the formation of a central reverse flow zone (CRZ) which extends blowoff limits by recycling heat and active chemical species to the flame in the burner exit.

Numerous publications exist on calculating, measuring, and correlating the blowoff limits [55-65]. A wide range of different hypothesises and physical models have been established to explain the blowoff phenomenon. The blowoff problem becomes more serious when a swirl burner is employed with a lean premixed mixture. Typically, blowoff characteristics of bluff-body stabilized premixed flames have been determined for a given geometrical configuration in terms of flame blowoff equivalence ratio as a function of the gas-mixture approach velocity [55]. It is important to characterize not only the blowoff limits under

steady flow conditions, but also consider the blowoff occurrence in the existence of time-varying flow oscillations.

Determination of the flame blowoff equivalence ratio involves establishing a premixed flame at approximately stoichiometric conditions and slowly decreasing the fuel flow rate via flow controllers until flame blowoff occurs.

Mainly, flame extinction occurs when the time available for chemical reaction becomes less than the time required to generate sufficient heat to raise the fresh mixture up to its ignition temperature.

Lieuwen [60] suggests blowoff refers to the flame physically leaving the combustor and “blowing out” of the combustor. This issue is often referred to as “static stability”, when the flame cannot be anchored in the combustor. However, when the flame velocity increases the flame would blowoff at some point and likewise at the constant velocity and varying equivalence ratio the flame would also blowoff when the equivalence ratio reduces to a certain value. Some references have related the extinction and the chemical reaction time with Damköhler Number, Da , and calculated the blowoff time [60, 62], and hence the blowoff limits.

The Damköhler number is defined as the ratio of the residence and chemical kinetic times, τ_{res}/τ_{chem} . Noble et al. [62] defined the residence time as the ratio of a characteristic length scale (recirculation zone length), d , and a characteristic velocity scale, U_{ref} . The chemical time was defined as the ratio of the thermal diffusivity, α , and the square of the laminar flame speed, S_L . The complete Damkohler equation as defined by Noble et al. can be seen in the following equation.

$$Da = \frac{\tau_{res}}{\tau_{chem}} = \frac{S_L^2 d}{\alpha U_{ref}} \quad 2.9$$

In this study, the Damköhler number was modified slightly from Eq. 2.9 to eliminate the thermal diffusivity and incorporate the flame thickness, f_T . The resultant relationship can be seen below [62].

$$Da = \frac{\tau_{res}}{\tau_{chem}} = \frac{S_L d}{f_T U_{ref}} \quad 2.10$$

The characteristic velocity is derived from the following relationship:

$$U_{ref} = \frac{\dot{m}}{\rho A} \quad 2.11$$

Flame thickness and flame speed correlations are defined by the combustor inlet temperature, inlet pressure, the lower heating value of the fuel, and the equivalence ratio and by using CHEMKIN.

$$S_L = f(\phi, LHV, T, P) \quad (2.12)$$

$$f_T = f(\phi, LHV, T, P) \quad (2.13)$$

Results near blowoff show that increases in upstream mean velocity increase the blowoff equivalence ratio. This behavior is expected and is generally reflected in a decreasing Damköhler number with increasing velocity [66]. As increases in velocity decrease aerodynamic time scales, the chemical timescales must also be decreased, by an increase in flame temperature and therefore equivalence ratio, to maintain the same Da at blowoff [66].

Lean blowoff is normally considered to be the leanest fuel air mixture limit that will allow steady flame propagation. Flammability limits depend on the physiochemical properties of fuel-air mixture and on the combustion system configuration. Lean blowoff occurs when flame speed is lower than the flow velocity of the unburned combustible mixture.

Currently, blowoff is avoided by operating the combustor with a wide safety margin from the somewhat uncertain stability limit (i.e., at higher equivalence ratio). Reduction in this margin can potentially result in lower pollutant emissions and enable faster engine transients. The ability to sense blowoff precursors can therefore provide significant payoffs in engine reliability and operability, in enabling optimal performance over extended periods of time, in reducing maintenance costs and extending engine life. It has been demonstrated that blowoff stability margins can be monitored through suitable analyses of the flame's acoustic and optical signature [62-67].

2.6 Fuel Blends

The global energy landscape is experiencing major changes as present economic concerns grow. There is a necessity for higher efficiency and lower emissions in the perspective of safety, fuel supply costs, and greenhouse gas emissions. The demand for natural gas has significantly increased as Natural Gas Combined Cycle plants are highly efficient.

Moreover, the crucial need for electrical power supplies will push countries to look at any available natural fuel resources, such as liquid fuels and coal, as ways to meet the energy requirement and stability. In addition, reducing CO₂ emissions is important and can be most readily achieved by increasing energy conversion efficiency, by switching to more carbon neutral fuels or by CO₂ sequestration.. Finally, these pressures are drivers for many industries and refiners to examine the potential inherent value within process off-gases or process waste streams as a way to maintain or reduce energy operating expenses for themselves and regional power generators.

The focus here is on the role that gas turbines play in this changing environment that requires better flexibility to burn a wider range of fuels, this being a vital factor to the next generation of gas turbine power plants. Based on more than 50 years of experience, GE for instance, has developed gas turbine technology that is proven and a more efficient alternative to other technologies, whilst burning the widest range of alternative gas and liquid fuels [68].

The possible fuels which can be utilised in high efficiency gas turbines cover a very large range, and in this changing energy landscape, there is a growing interest in turning to non-traditional fuels, capitalising on the experience gained during the past five decades. As continuous flow machines with robust designs and flexible combustion systems, gas turbines have demonstrated distinctive capabilities to accept a wide variety of fuels.

The most common way to classify fuels is to split them between gaseous and liquid fuels, split by their calorific value. Table 2.1 shows such a classification for the gaseous fuels.

According to the data released from manufacturers of large gas turbines, the majority of gas turbine fuel is natural gas, followed by light distillate oil and other liquid fuel oils. Alternative fuels entered the world gas turbine fuel fairly recently to substitute for expensive liquid fuels. Alternative fuels often contain significant quantities of hydrogen as one of its constituents, due to the nature of the production process. This has the benefit of high calorific value, but the disadvantage of high flame speed and very fast chemical times. In the present work, a number of different gaseous fuels have been used ranging from pure methane, 15%, 30% hydrogen balanced methane by volume, pure hydrogen, 15%, 30% carbon dioxide balanced methane by volume, and coke oven gas. These gas mixtures have

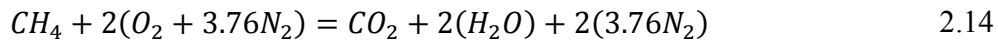
different properties, which need to be examined in the context of premixed combustion and gas turbines.

Classification	Typical composition	Lower heating value (kJ/Nm ³)	Typical specific fuel
Ultra/Low LHV gaseous fuels H₂ < 10%	CH ₄ < 10% N ₂ +CO > 40%	< 11,200	Blast furnace gas (BFG) Air blown IGCC Biomass gasification
High hydrogen gaseous fuels	H ₂ > 50% C _x H _y = 0-40%	5,500-11,200	Refinery gas Petrochemical gas Hydrogen power
Medium LHV gaseous fuels	CH ₄ < 60% N ₂ +CO ₂ = 30-50% H ₂ = 10-50%	11,200-30,000	Weak natural gas Landfill gas Coke oven gas Corex gas
Natural gas CH₄ = 90%	C _x H _y = 5% Inerts = 5%	30,000-45,000	Natural gas Liquefied natural gas (LNG)
High LHV gaseous fuels	CH ₄ and higher hydrocarbons C _x H _y > 10%	45,000-190,000	Liquid petroleum gas (butane, propane) Refinery off-gas
Liquid fuels	C _x H _y , with x > 6	32,000-45,000 (kJ/kg)	Diesel oil Naphtha Crude oils Residual oils Bio-liquids

Table 2.1: Fuel classification [68]

These blends can be divided into four groups as follows:

I. Pure methane CH₄: the properties of this gas are very close to natural gas even though they contain only 90% CH₄ mixed with other gases: some of them are inert gases which are relatively unaffected by the main properties of the fuel gas. The source of the natural gas affects the price according to its energy release and range of dilutants, inert or not. The higher calorific value of the pure methane is about 55 MJ/kg, which is relatively high and suitable for many gas turbines. Here, the research uses pure methane to represent natural gas in a small combustor. This has the considerable advantage of giving very consistent burning/combustion properties. The stoichiometric ratio of pure methane is an air to fuel ratio 17.16 by mass. The stoichiometric ratio is predicted from the basic combustion equation of methane.



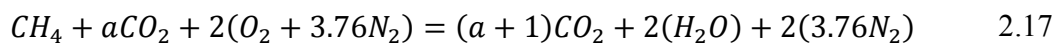
$$AFR_{stoich} = \frac{WEIGHT\ OF\ THE\ AIR}{WEIGHT\ OF\ THE\ FUEL} = \frac{2(M_{O_2} + 3.76M_{N_2})}{M_{CH_4}} \quad 2.15$$

The equivalence ratio represents the ratio of stoichiometric air to fuel ratio to the actual air to fuel ratio (actual air flow rate to actual fuel rate):

$$\phi = \frac{AFR_{stoich}}{(\dot{m}_{air}/\dot{m}_{fuel})} \quad 2.16$$

This means when $\phi = 1$ the mixture is at the ideal state but for values greater than 1 it means that the mixture is a rich mixture and for a value less than 1 the mixture would be a lean mixture.

II. Methane carbon dioxide blends: Methane balanced by carbon dioxide was investigated (by volume (5%CO₂+85%CH₄ and 30%CO₂+70%CH₄): CO₂ addition to pure methane reduces the calorific heating value and in turn the amount of heat produced from the mixture. One outcome of this research is that by adding CO₂ to methane one can reduce the flashback occurrence. This has been confirmed by CFD and experimental analysis. The combustion equation is below:



where a is the molar fraction of carbon dioxide to methane.

$$a = \frac{X_{CO_2}}{X_{CH_4}} \quad 2.18$$

For the current case of 15 and 30 % of CO₂ with methane, the stoichiometric ratios are 11.5 and 7.88 mass, respectively. CO₂ addition has been discussed extensively [69-72], all this work proved that adding CO₂ reduced the turbulent flame speed and reduced flame temperature and hence NO_x formation.

III. Pure hydrogen:

Hydrogen shows promise as an important energy carrier for the future. Hydrogen can be produced through electrolysis of water or via various thermo-chemical cycles [73-74]. Although these methods are not cost-effective, if the electricity required to convert water to hydrogen is provided by wind or solar power, then the hydrogen is produced without generating any pollution. On the other hand, hydrogen can be produced through coal gasification, or by steam reforming of natural gas, both of which are non-renewable fossil fuels but are abundantly available throughout the world. Combining the latter technologies with carbon capture and storage would provide a significant increase in sources of clean burning hydrogen whilst at the same time eliminating greenhouse gas emissions [73].

Hydrogen is a promising technology that when utilised produces no harmful emissions to the environment. Safety with hydrogenise the main issue, including flashback, high flame speed, tendency to explode under a wide range of air fuel mixtures. The stoichiometric ratio of hydrogen is 34.32 by mass.

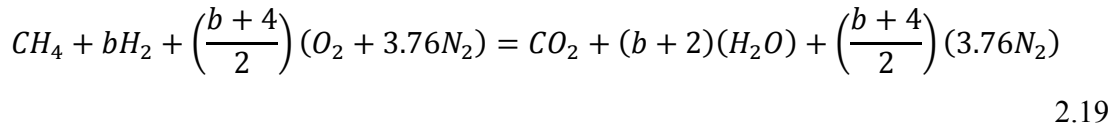
IV. Hydrogen methane blends:

Adding hydrogen to methane will produce a fuel which can produce fewer greenhouse gas emissions. There are two problems in using lean methane combustion: operation close to blowoff and flashback limits plus low values of laminar and thus turbulent burning velocities. Because hydrogen has a very low lean flammability limit with high burning velocities [75], hydrogen can be used to improve fuel characteristics (especially with methane) especially in the context of gas turbine combustor requirements.

Thus hydrogen–natural gas blends are receiving more attentions as alternative fuels for power generation applications to improve mixture performance and to reduce pollutant

emissions with lean combustion [76-80]. To overcome the difficulties of using pure hydrogen as a fuel (high flame speed, high propensity to flashback), substitution of some natural gas with some hydrogen has been proposed as a provisional solution towards a fully developed hydrogen economy [81].

For this programme of work, methane balance by hydrogen has been investigated (by volume 15%H₂+85%CH₄ and 30%H₂+70%CH₄): H₂ addition to pure methane increases the calorific heating value. The combustion equation of hydrogen mixtures is as follows:



where b is the molar fraction of hydrogen to methane,

$$b = \frac{X_{H_2}}{X_{CH_4}} \quad 2.20$$

For the current case of 15% and 30 % of H₂ substitution, the stoichiometric ratios are 17.53 and 18.03, respectively, by mass.

IV. Coke oven gas: (65%H₂+25%CH₄+6%CO+4%N₂), this is a complex gas containing hydrogen, methane, carbon monoxide and nitrogen. Coke oven gas contains large quantities of hydrogen and represents families of fuel gases whose behaviour is closer to that of hydrogen than methane. The stoichiometric air to fuel ratio is 15.15 by mass. Coke oven gas can behave aggressively in some situations and its combustion behaviour can be difficult to control.

Hydrogen addition to a fuel always imposes new design requirements for gas turbine combustors due to the higher flame speeds. Since flames typically stabilise in regions where the local flow velocity is near the local flame speed, the higher flame velocities can cause flame stabilisation to occur in undesirable parts of the combustor, causing damage.

The use of hydrogen in a large size, heavy duty gas turbine was studied by Chiesa et al. [74]. This unit was also designed to run on natural gas. Chiesa et al. proposed ways in which pure hydrogen could be used in existing gas turbines with little adjustment, although NO_x emissions suffered.

Combustion characteristics of premixed mixtures of hydrogen enriched methane have been studied by Schefer et al. [82-83] and Wicksall et al. [84]. The burner used a swirl-stabilized

flame to determine the effects of enriching methane with hydrogen under fuel-lean conditions. The OH concentration increased as a result of adding a reasonable amount of hydrogen to the methane/air mixture. Hydrogen addition resulted in a major change in the flame shape, indicated by a shorter and more intense appearing flame. Moreover, hydrogen addition notably improves flame stability: this depends on many factors and allows a reduced fuel/air ratio to give leaner premixed flames, a requirement for reduced NO_x emissions.

An experimental and numerical study are discussed in Jackson et al. [85] and show the influence of hydrogen on the response of lean premixed methane flames. Kido et al. [86] used a small amount of hydrogen as an additive to improve turbulent combustion performance of lean hydrocarbon mixtures.

2.7 Summary

In this chapter, a literature review has been carried out related to combustion characteristics of gas turbines and associated aspects of the flame stability such as flashback and blowoff, especially in the context of various alternative fuels. The following is concluded:

In this chapter, a literature review has been carried out related to combustion characteristics of gas turbines and associated aspects of the flame stability such as flashback and blowoff, especially in the context of various alternative fuels. The following is concluded:

- Alternative fuels and lean premixed combustion are considered one of the most promising concepts for substantial reduction of gas turbine emissions, especially NO_x, and CO₂ emissions, whilst maintaining high efficiency.
- Swirling flow and its effect upon premixed combustion and the significance of the swirl number and its relation with the type of flow and flames are all important topics.
- The main problem for all premixed combustion systems is the instability problem and the tendency of the combustible mixture toward flashback and blowoff.
- There are many possible fuel blends ranging over pure methane and various CO₂ and hydrogen blends.
- CO₂ dilution in methane combustion is a new research topic. It can be used for NO_x emission reduction as a way of reducing the flame temperature. The effect of CO₂

dilution in methane combustion on flashback limits is one topic studied in this thesis.

- Hydrogen combustion has attracted much attention recently because of the need for clean alternative energy source. H₂ is a carbon-free energy carrier, so it plays an important role in meeting the constraints on greenhouse gas emissions.
- The challenge when using H₂ is its high burning velocity that results in its high tendency to flashback or relocating the flame undesirably in regions of relative high velocity where methane flames will not stabilise.
- H₂/CH₄ hybrid fuel may have advantages over certain ranges of equivalence ratios.

Part I

CFD

Simulation

Chapter Three

COMPUTATIONAL MODELLING OF COMBUSTION

CHAPTER THREE**COMPUTATIONAL MODELLING OF
COMBUSTION**

"A successful research enables problems which once seemed hopelessly complicated to be expressed so simply that we soon forget that they ever were problems. Thus the more successful a research, the more difficult does it become for those who use the result to appreciate the labour, which has been put into it. This perhaps is why the very people who live on the results of past researches are so often the most critical of the labour and effort which, in their time, is being expended to simplify the problems of the future."

The famous British aerodynamicist M. Jones

3.1 Introduction and CFD Definition

Prediction of heat and mass transfer processes can be obtained by two main methods, experimental investigation and the theoretical calculation, based on mathematical models. Although the most reliable information is usually given by measurement, this is often impossible and always limited. The advantages of a theoretical approach comprise lower cost, greater speed, complete information throughout the whole domain of analysis and the ability to simulate realistic and/or ideal conditions [87]. However, it is useful to be aware of the drawbacks and limitations. As the computer analysis works out the implications of a mathematical description of some physical phenomena, it is clear that the validity of the models themselves limits the usefulness of a computation.

The basis of the numerical modelling of this project has been designed to fit with the principle of computational fluid dynamics. CFD can be simply defined as the analysis of systems involving fluid flow, heat transfer and associated phenomena such as chemical reactions by means of computer-based simulation. The technique is very powerful and

spans a wide range of applications; one of these applications is design of combustion chambers of gas turbine engines [88].

In this investigation the CFD code, ANSYS12.0, was utilised and this is the most recent version of the well-known software package. CFD packages are generally comprised of many programmes, three of them have been used in this analysis, the first one for geometry (**Geometry Modelling**) and the second one for mesh creation (**Mesh Generation**) and the last one is (**FLUENT**) for fluid mechanic, heat transfer, chemical reaction and combustion calculations. It obviously includes a definition of operating conditions etc...

The geometry modelling programmes used in this study allow physical geometries to be modelled. It does this via specific methods to draw and construct the geometry so as to prepare for the next step of meshing this geometry in ways which will give an efficient mesh. This is to allow interior flows and heat transfer to be efficiently and effectively modelled by a finite difference method, as used by FLUENT.

Geometries are created by constructing a series of major shapes and editing them using the programme tools and functions to create the final shape. Once the shape is created, it needs to be meshed efficiently.

A meshing programme is used to mesh complex geometries. There are many methods such as **Tetrahedrons** (unstructured), **Hexahedrons** (usually structured), **Pyramids** (where tet. and hex. cells meet) and **Prisms** (formed when a tet mesh is extruded) These methods can be used in many ways in this software. The number of elements and their shapes will determine the accuracy of the model. The more elements contained in the geometry, the more accurate the results will be. However, this will also be more computationally expensive in terms of time and memory.

FLUENT is a programme that uses the mesh created by the mesh generation programme, and applies the governing equations of fluid dynamics. Fluid dynamics is concerned with the dynamics of liquids and gases. The analysis of the behaviour of fluids is based upon the fundamental laws of applied mechanics. These laws are related to the conservation of mass-energy and the force momentum equations, [89]. Obviously, these equations vary depending on the properties of the flow in question and additional equations are solved for flows such as this one involving heat transfer and species transport. In addition, transport equations are solved if the flow is turbulent. These equations then will be replaced by

equivalent numerical descriptions that are solved by a finite volume method, to give solutions for the flow at discrete locations within the flow field, [12].

3.2 Benefit of CFD

The benefits of using computational fluid dynamics (CFD) techniques can be summarised as follows [12]:

- Crucial reduction of time and costs of new designs. Better and faster design or analysis leads to shorter design cycles. Time and money are saved. Products get to market faster. Equipment improvements are built and installed with minimal downtime. CFD is a tool for compressing the design and development cycle. Experimentation, the only alternative to simulation is very costly.
- New systems are often difficult to prototype. Often, CFD analysis shows you parts of the system or phenomena happening within the system that would not otherwise be visible through any other means. CFD gives you a means of visualising and enhancing understanding of your designs.
- Previous predictions can give the designer expectations for the result that he will predict. Because CFD is a tool for predicting what will happen under a given set of circumstances, it can answer many questions very quickly. All of this is done before physical prototyping and testing.
- Perform some impossible or dangerous experiments. For example, nuclear, biological, high intensity combustion systems and other types of experiments are so dangerous that sometimes they cost the lives of people.

3.3 CFD Analysis Steps

CFD codes are structured around the numerical algorithms that can tackle fluid flow problems. In order to provide easy access to their solving power, all commercial CFD packages include sophisticated user interfaces to input problem parameters and to examine the results. Hence, all codes contain three main elements: a pre-processor, a solver and a post-processor. Therefore, to look at fluid dynamic problems, it is important to consider these elements [12].

i. Pre-processor:

Pre-processing consists of the input of a flow problem to a CFD programme by means of an operator–friendly interface and subsequent transformation of this input into a form suitable for use by the solver. The user activities at the pre-processing stage involve [90]:

- ❖ Definition of the modelling goals:–
 - What specific results are required from the CFD model and how will they be used? What degree of accuracy is required from the model?
- ❖ Choice of the computational model:-
 - What are the boundary conditions?
 - Can a 2-D model be used or is 3-D required?
 - What type of grid topology is best suited to the model?
- ❖ Choice of physical model:-
 - Is the flow inviscid, laminar, or turbulent in nature?
 - Is the flow steady or unsteady?
 - Is heat transfer important?

Briefly, they could be listed more clearly in following steps:-

- Geometry Definition
- Grid Generation
- Selection of Physical and Chemical phenomena equations of the model
- Fluid Properties Definitions
- Boundary Conditions Specification

ii. Solver: There are three distinct streams of numerical solution techniques: finite differences, finite element and spectral methods. In outline, the numerical methods that form the basis of the solver perform the following steps [88, 91-93]:

- Approximation of the unknown flow variables by means of simple function.
- Discretisation by substitution of the approximations into governing flow equations and subsequent mathematical manipulations.
- Solution of algebraic equations.

The main differences between the three separate streams are associated with the way in which the flow variables are approximated and with the discretisation processes.

Finite difference methods: Finite difference methods (FDM) describe the unknowns ϕ of the flow problem by means of point samples at the node points of a grid of co-ordinate lines. Truncated Taylor series expansions are often used to generate finite difference approximations of derivatives of zero in terms of point samples of ϕ at each grid point and its immediate neighbours. Those derivatives appearing in the governing equations are replaced by finite differences yielding an algebraic equation for the values of ϕ at each grid point.

Finite Element Method: Finite element methods (FEM) use simple piecewise functions (e.g. linear or quadratic) valid on elements to describe the local variations of unknown flow variable ϕ . The governing equation is precisely satisfied by the exact solution ϕ . If the piecewise approximating functions for ϕ are substituted into the equation it will not hold exactly and a residual is defined to measure the errors. Next the residuals (and hence the errors) are minimised in some sense by multiplying them by a set of weighting functions and integrating. As a result, we obtain a set of algebraic equations for the unknown coefficients of the approximating functions. The theory of finite elements has been developed initially for structural stress analysis.

Spectral Methods: Spectral methods approximate the unknowns by means of truncated Fourier series or series of Chebyshev polynomials. Unlike the finite difference or finite element approach, the approximations are not local but valid throughout the entire computational domain. Again, we replace the unknowns in the governing equation by the truncated series. The constraint that leads to the algebraic equations for the coefficients of the Fourier or Chebyshev series is provided by a weighted residuals concept similar to the finite element method or by making the approximate function coincide with the exact solution at a number of grid points.

The Finite Volume Method: The finite volume method (FVM) was originally developed as a special finite difference formulation. It is the core of a commercial CFD code like FLUENT software. The numerical algorithm consists of the following steps:

- Formal integration of the governing equations of fluid flow over all the (finite) control volumes of the solution domain.

- Discretisation, which involves the substitution of a variety of finite-difference-type approximation for the terms in the integrated equation representing flow processes such as convection, diffusion and sources. This converts integral equation into system of algebraic equations.
- Solution of the algebraic equations by an iterative method.

The first step, the control volume integration, distinguishes the finite volume method from all other CFD techniques. The resulting statements express the (exact) conservation of relevant properties for each finite size cell. This clear relationship between the numerical algorithm and the underlying physical conservation principle forms one of the main attractions of the finite volume method and makes its concepts much simpler to understand by engineers than finite element and spectral methods. The conservation of a general flow variable ϕ , for example, a velocity component or enthalpy, within a finite control volume can be expressed as a balance between the various processes tending to increase or decrease it. In other words, we have:

$$\left[\begin{array}{c} \text{Rate of change} \\ \text{of } \phi \text{ in the} \\ \text{control volume} \\ \text{with respect} \\ \text{to time} \end{array} \right] = \left[\begin{array}{c} \text{Net flux} \\ \text{of } \phi \text{ due to} \\ \text{convection} \\ \text{into the} \\ \text{control volume} \end{array} \right] + \left[\begin{array}{c} \text{Net flux} \\ \text{of } \phi \text{ due to} \\ \text{diffusion} \\ \text{into the} \\ \text{control volume} \end{array} \right] + \left[\begin{array}{c} \text{Net Rate} \\ \text{of creation} \\ \text{of } \phi \text{ inside the} \\ \text{control volume} \end{array} \right]$$

CFD codes contain discretisation techniques suitable for the treatment of the key transport phenomena, convection (transport due to fluid flow) and diffusion (transport due to variations of ϕ from point to point) as well as for the source terms (associated with the creation or destruction of ϕ and the rate of change with respect to time). The underlying physical phenomena are complex and non-linear so an iterative solution approach is required. The most popular solution procedures are the TDMA line-by-line solver of the algebraic equations and the SIMPLE algorithm to ensure correct linkage between pressure and velocity. Commercial codes may also give the user a selection of further, more recent, techniques such as Stone's algorithm and conjugate gradient methods.

iii. Post-processor: As in pre-processor, a huge amount of development work has recently taken place in the post-processing field. Owing to the increased popularity of engineering workstations, many packages are now equipped with versatile data visualisation tools. These include:

- Domain geometry and grid display
- Vector plots
- Line and shaded contour plots
- 2D and 3D surface plots
- Particle tracking
- View manipulation (translation, rotation, scaling etc)
- Colour postscript output

3.4 Planning CFD Analysis

When using CFD to look at fluid dynamic problems, it is important to give considerations to the following steps [12].

Definitions of the modelling goals - What specific results are you looking for? How accurate do they need to be?

1. Definition of the modelling goals – What specific results are required from the CFD model and how will they be used? What degree of accuracy is required from the model?
2. Choice of the computational model: What are the boundary conditions? Can a two dimensional model be used or are three dimensions required? What type of grid topology is best suited to the model?
3. Choice of physical model - Is the flow inviscid, laminar, or turbulent in nature? Is the flow steady or unsteady? Is heat transfer important?
4. Determination of the solution procedure - How long will the problem take to converge on your computer? Can convergence be accelerated with a different solution procedure?

Consideration of these steps will reduce computer-processing time and contribute to the success of the modelling.

3.5 Basic Equations

The governing equations of fluid flow have made many assumptions to simplify the solution of the equation [12, 88, 90-92]:-

- The mass of fluid is conserved.
- The rate of change of momentum equals the sum of the forces on a fluid particle (Newton's second law).

- The rate of change of energy is equal to the sum of the rate of heat addition and the rate of work done on a fluid particle (first law of thermodynamics).

The basic equation can be summarised by the following equations:

3.5.1 Mass Conservation

The mass balance for a fluid element or the continuity equation states that the rate of increase of mass in a fluid element equals the net rate of flow of mass into the fluid element.

The continuity equation can be expressed as follows:

$$\frac{\partial \rho}{\partial t} + \frac{\partial(\rho u)}{\partial x} + \frac{\partial(\rho v)}{\partial y} + \frac{\partial(\rho w)}{\partial z} = 0 \quad 3.1$$

or in vector notation

$$\frac{\partial \rho}{\partial t} + \text{div}(\rho \mathbf{u}) = 0 \quad 3.2$$

where

ρ = density

t = time

u, v, w = velocity components in x, y and z respectively

\mathbf{u} = velocity vector

Equation 3.2 is the general form of the mass conservation equation and is valid for compressible fluids. The first term on the left-hand side is the rate of change in time of the density (mass per unit volume). The second term is concerned with the net flow of mass out of an elemental body of fluid and is called the convective term.

3.5.2 Momentum Equation

Newton's second law states that the rate of change of momentum of a fluid particle equals the sum of the forces acting on the particle.

Rate of increase of momentum of fluid particle = Sum of forces on fluid particle

It can distinguish two types of forces

1. Surface forces (pressure and viscous forces)
2. Body forces (gravity, centrifugal, coriolis, and electromagnetic forces)

Applying this to a fluid passing through an infinitesimal, fixed control volume yields the following equations:-

- The x-component of the momentum equation:

$$\rho \frac{Du}{Dt} = \frac{\partial(-p + \tau_{xx})}{\partial x} + \frac{\partial\tau_{yx}}{\partial y} + \frac{\partial\tau_{zx}}{\partial z} + S_{Mx} \quad 3.3.a$$

- The y-component of the momentum equation:

$$\rho \frac{Dv}{Dt} = \frac{\partial\tau_{xy}}{\partial x} + \frac{\partial(-p + \tau_{yy})}{\partial y} + \frac{\partial\tau_{zy}}{\partial z} + S_{My} \quad 3.3.b$$

- The z-component of the momentum equation:

$$\rho \frac{Dw}{Dt} = \frac{\partial\tau_{xz}}{\partial x} + \frac{\partial\tau_{yz}}{\partial y} + \frac{\partial(-p + \tau_{zz})}{\partial z} + S_{Mz} \quad 3.3.c$$

where

p = static pressure

τ = viscous stress

τ_{ij} = viscous stress component acts in the j-direction on the surface normal to i-direction.

S_{Mi} = body force in i-direction

The sign associated with the pressure is opposite to that associated with the normal viscous stress, because the usual sign convention takes a tensile stress to be the positive normal stress so that the pressure, which is by definition a compressive normal stress, has a minus sign.

The effects of surface stresses are accounted for explicitly; the source terms, S_{Mx} , S_{My} and S_{Mz} , in 3.3.a to 3.3.c, include contributions due to body forces only. For example, the body force due to gravity would be modelled by $S_{Mx}=0$, $S_{My}=0$ and $S_{Mz} = -pg$.

Momentum equation can be re-written in vector form:

$$\frac{\partial(\rho\mathbf{u})}{\partial t} + \text{div}(\rho\mathbf{u}\mathbf{u}) = -\text{grad } p + \text{div}(\tau) + \mathbf{F} \quad 3.4$$

where

ρ = density

p = static pressure

t = time

\mathbf{u} = velocity vector

τ = viscous stress

\mathbf{F} = body force vector

In a Newtonian fluid, the viscous stresses are proportional to the rates of deformation. The three dimensional form of Newton's law of viscosity for compressible flow involves two constants of proportionality: the dynamic viscosity, μ to relate stresses to linear deformations, and the viscosity, λ to relate stresses to the volumetric deformation. The viscous stress components are related to μ and λ . Substituting the values of viscous stress in the momentum equations yields the equations called Navier-Stokes equations:

$$\rho \frac{Du}{Dt} = -\frac{\partial p}{\partial x} + \text{div}(\mu \text{grad } u) + S_{Mx} \quad 3.5.a$$

$$\rho \frac{Dv}{Dt} = -\frac{\partial p}{\partial y} + \text{div}(\mu \text{grad } v) + S_{My} \quad 3.5.b$$

$$\rho \frac{Dw}{Dt} = -\frac{\partial p}{\partial z} + \text{div}(\mu \text{grad } w) + S_{Mz} \quad 3.5.c$$

3.5.3 Energy Equation

The energy equation is derived from the first law of thermodynamics, which states that the rate of change of energy of a fluid particle is equal to the rate of heat addition to the fluid particle plus the rate of work done on the particle.

$$\left[\begin{array}{c} \text{Rate of increase} \\ \text{of energy of} \\ \text{fluid particle} \end{array} \right] = \left[\begin{array}{c} \text{Net rate of} \\ \text{heat added to} \\ \text{fluid particle} \end{array} \right] = \left[\begin{array}{c} \text{Net rate of work} \\ \text{done on} \\ \text{fluid particle} \end{array} \right]$$

$$\begin{aligned} \rho \frac{DE}{Dt} = & -\text{div}(\rho \mathbf{u}) \\ & + \left[\frac{\partial(u\tau_{xx})}{\partial x} + \frac{\partial(u\tau_{yx})}{\partial y} + \frac{\partial(u\tau_{zx})}{\partial z} + \frac{\partial(v\tau_{xy})}{\partial x} + \frac{\partial(u\tau_{yy})}{\partial y} \right. \\ & \left. + \frac{\partial(u\tau_{zy})}{\partial z} + \frac{\partial(u\tau_{xz})}{\partial x} + \frac{\partial(u\tau_{yz})}{\partial y} + \frac{\partial(u\tau_{zz})}{\partial z} + \right] \\ & + \text{div}(k \text{grad } T) + S_E \end{aligned} \quad 3.6$$

$$E = i + \frac{1}{2}(u^2 + v^2 + w^2) \quad 3.7$$

This equation can be written in vector form:

$$\frac{\partial(\rho E)}{\partial t} + \text{div}(\rho E \mathbf{u}) = 0 = -\text{div}(\rho \mathbf{u}) + \Phi + \text{div}(k \text{grad } T) + S_E \quad 3.8$$

Φ Dissipation function represent the long stress term.

The dissipation function is non-negative since it only contains squared terms and represents a source of internal energy due to deformation work on the fluid particle. This work is extracted from the mechanical agency, which causes the motion and is converted into internal energy or heat.

3.5.4 General Transport Equation

It is clear that there are significant commonalities between the various equations. If a general variable ϕ is introduced, the conservative form of all fluid flow equations can usefully be written in the following form:

$$\frac{\partial(\rho\phi)}{\partial t} + \text{div}(\rho\phi\mathbf{u}) = \text{div}(\Gamma\text{grad } \phi) + S_\phi \quad 3.9$$

In words:

<i>Rate of increase of ϕ of fluid element</i>	+	<i>Net rate of flow of ϕ out of fluid element</i>	=	<i>Rate of increase of ϕ due to diffusion</i>	+	<i>Rate of increase of ϕ due to sources</i>
---	---	---	---	---	---	---

The equation 3.9 is the so-called transport equation of property ϕ . It clearly highlights the various transport processes: the rate of change term and the convective term in the left hand side and the diffusive term (Γ : diffusion coefficient) and the source term respectively on the right hand side.

3.5.5 Physical Behaviour and Boundary Conditions

There are two principal categories of physical behaviour [88]: Equilibrium problems and Marching problems.

Equilibrium problems are typically steady-state situations and are described by elliptic equations. A disturbance in the interior of the solution changes the solution everywhere else. Disturbance signals travel in all directions through the interior solution. The numerical techniques for elliptic problems must allow events at each point to be influenced by all its neighbours to ensure that the information propagates in all directions. Elliptic flows are sometimes referred to as recirculating flows. This study concentrates on such flows.

Marching problems are typically all unsteady flows and wave phenomena. These are described by parabolic or hyperbolic equations. Parabolic equations describe time-dependent problems involving significant dissipation (e.g. unsteady viscous flows or unsteady heat conduction). The prototype equation is the diffusion equation $\left(\frac{\partial^2\phi}{\partial t^2} = \alpha \frac{\partial^2\phi}{\partial x^2}\right)$.

Hyperbolic equations dominate the analysis of vibration problems and time-dependent processes with negligible dissipation. The prototype equation is the wave equation ($\frac{\partial^2 \phi}{\partial t^2} = c^2 \frac{\partial^2 \phi}{\partial x^2}$).

Table 3.1 summarizes the ‘formal’ classification of fluid flow equations. In practice, many fluid flows behave in a complex way.

	Steady flow	Unsteady flow
Viscous flow	Elliptic	Parabolic
Inviscid	Ma < 1 Elliptic Ma > 1 Hyperbolic	Hyperbolic
Thin shear layer	Parabolic	Parabolic

Table 3.1: Formal classification of fluid flow equations [88]

Patankar [87] underlined the fact that it would be more meaningful if situations were described as being parabolic or elliptic *in a given coordinate*. For example, an unsteady viscous flow problem is conventionally called parabolic, as it exists in at least one coordinate for which it is parabolic, it is actually parabolic in time, but elliptic in a space coordinate. Equation 3.8, for example, is elliptic by virtue of the gradient diffusion term. Boundary conditions are therefore required at all boundaries and iteration methods are necessary for solving the equations. In contrast, solution procedures for parabolic equations are generally of marching type. The flow is uninfluenced by downstream events and boundary conditions are required on only three sides of the solution domain.

3.6 Turbulence Modelling

3.6.1 What is Turbulence?

Turbulence is that state of fluid motion that is characterised by apparently random and chaotic three-dimensional vorticity. When turbulence is present, it usually dominates all other flow phenomena and results in increased energy dissipation, mixing, heat transfer, and drag. If there is no three-dimensional vorticity, there is no real turbulence. The reasons for this will become clear later; but briefly, it is the ability to generate new vorticity from

old vorticity that is essential to turbulence. Only in a three-dimensional flow is the necessary stretching and turning of vorticity by the flow itself possible [94].

For a long time scientists were not sure in which sense turbulence is “random”, but they were sure it was. Like anyone who is trained in physics, we believe the flows we see around us must be the solution to some set of equations, which govern them. But because of the nature of turbulence, it wasn’t clear whether the equations themselves had some hidden randomness, or just the solutions. In addition, if the latter, was it something the equations did to them, or a consequence of the initial conditions?

All of this began to come into focus as we have learned about the behaviour of non-linear dynamical systems in the past few decades. Even simple nonlinear equations with deterministic solutions and prescribed initial conditions were found to exhibit chaotic and apparently random behaviour. In fact, the completely new field of chaos was born in the 1980’s [95], complete with its new language of strange attractors, fractals, and Lyapunov exponents. Such studies now play a major role in analyzing dynamical systems and control, and in engineering practice as well.

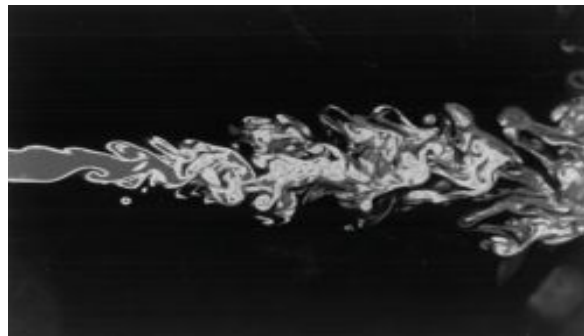


Figure 3.1: Two-dimensional image of an axisymmetric water jet, obtained by the laser-induced fluorescence technique [96]

Turbulence is not really chaos, at least in the sense of the word that the dynamical systems people use, since turbulent flows are not only time-dependent but space dependent as well. Nevertheless, as even the photos of simple turbulent jets and wakes, as in Figure 3.1, make clear, turbulence has many features that closely resemble chaos. Obvious ones include spatial and temporal intermittency, dissipation, coherent structures, sensitive dependence of the instantaneous motions on the initial and upstream conditions, and even the near-fractal distribution of scales. In fact, the flows we see themselves bear an uncanny resemblance to

the phase plane plots of strange attractors. No one would ever confuse a jet with a wake, but no two wakes seem to be quite alike either.

Because of the way chaos has changed our worldview; most turbulence researchers now believe the solutions of the fluid mechanical equations to be deterministic. Just like the solutions of non-linear dynamical systems, we believe turbulent solutions to be determined (perhaps uniquely) by their boundary and initial conditions. Moreover, like non-linear dynamical systems, these deterministic solutions of the non-linear fluid mechanics equations exhibit behaviour that appears essentially to be random. We call such solutions turbulent, and the phenomenon turbulence. Because of this chaotic-like and apparently random behaviour of turbulence, we will need statistical techniques for most of our study of turbulence.

The lack of a satisfactory understanding of turbulence presents one of the great remaining fundamental challenges to scientists — and to engineers as well, since most technologically important flows are turbulent. The advances in understanding over the past few decades, together with the advent of large-scale computational and experimental capabilities, present the scientist and engineer with the first real capabilities for understanding and managing turbulent flows [97].

3.6.2 Properties of Turbulence

1-Irregularity or randomness:

‘Turbulent fluid motion is an irregular condition of flow in which the various quantities show a random variation with time and space coordinates, so that statistically distinct average values can be discerned’ [98]. Average values of quantities exist with respect to time and space as at a given point in the turbulent domain a distinct pattern is repeated more or less regularly in time and at a given instant a distinct pattern is repeated more or less regularly in space.

2- Diffusivity:

The rapid mixing and increased rates of momentum, heat or mass transfer are typical features of turbulent flows. There are several elements involved:

Large Reynolds numbers: Turbulent flows always occur at higher Reynolds numbers. Turbulence often originates as instability of laminar flows if the Reynolds number becomes too large.

Three-dimensional vortex fluctuations: Periodicity in a velocity distribution involves the occurrence of velocity gradients, which correspond to a certain vortex, or eddying motion, the extent of which is determined by the periodicity. This eddying motion is found in a wide spectrum of sizes and a corresponding spectrum of fluctuation frequencies. Turbulence consists of many superimposed quasi-periodic motions; it is the ‘superposition of eddies of ever-smaller sizes’ [98]. The size of the largest eddies is determined mainly by the boundaries (size of the apparatus), whilst the size of the smallest eddies is limited by viscous forces. This lower limit is seen to decrease with increasing velocity of the average flow, with other conditions remaining the same [98]. The smaller an eddy, the greater, in general, the velocity gradient in the eddy and the greater the viscous shear stress that counteracts the eddying motion. So, for each turbulent flow, there will be a statistical lower limit to the size of the smallest eddy; there is a minimum scale of turbulence that corresponds to a maximum frequency in the turbulent motion. Large eddies are characterised by a length scale l and a velocity scale u , and the typical time scale of the large eddies is thus proportional to l/u . Furthermore, the kinetic energy is proportional to u^2 and this kinetic energy is extracted from the mean flow by interaction between turbulent fluctuations and mean flow. The smaller eddies do not extract their kinetic energy directly from the mean flow but are fed by a continuous decay of large eddies which break-up into smaller ones. These smaller ones in turn decay to even smaller eddies, until this cascade reaches the smallest scales of turbulent motion. In the classical turbulence theory, this process is known as energy cascade. The length and velocity scales of these smallest eddies are determined by the amount of kinetic energy transferred along the energy cascade from the large eddies towards the small eddies and by the viscosity of the fluid.

Dissipation: Turbulent flows are always dissipative. Viscous shear stresses perform deformation work, which increases the internal energy of the fluid at the expense of kinetic energy of turbulence. Turbulence, therefore, needs a continuous supply of energy to maintain a certain level. It is essential to distinguish between waves forming random motions that have insignificant viscous losses and therefore are non-dissipative, and turbulence that is essentially dissipative. The loss of kinetic energy of the large-scale eddies (macro-structure) is represented by the dissipation rate, which is independent of the microstructure (small eddies) and the fluid properties. It is fully determined by macro-

structure properties only. This is expressed by the following relationship, which is a fundamental result in turbulence theory and comes from Prandtl's mixing-layer theory [98]:

$$\varepsilon \sim \frac{u^3}{\ell} \quad 3.9$$

This relationship can be interpreted as the ratio of the kinetic energy of the macro-structure eddies and their lifetime. Within their lifetime, the large eddies lose their kinetic energy due to a break-up into smaller eddies. As argued above, the micro-structure scales are not only determined by the amount of kinetic energy transferred, but also by the molecular property of the fluid, the kinematic viscosity ν . As a result of dimensional analysis, the following expressions are obtained for the length scale ℓ , the velocity scale u , and the timescale t of the smallest eddies which are known as the Kolmogorov scales:

$$\eta_k = (\nu^3 / \varepsilon)^{1/4} \quad 3.10.a$$

$$u_k = (\nu \varepsilon)^{1/4} \quad 3.10.b$$

$$\tau_k = (\nu / \varepsilon)^{1/2} \quad 3.10.c$$

Since the dissipation rate is known in terms of macro-structure properties, one can easily deduce relationships between the various scales of the macro- and micro-structure.

Substitution of equation 3.9 into the expression 3.10.a, b, c yields:

$$\frac{\eta_k}{\ell} = Re_l^{-3/4} \quad 3.11.a$$

$$\frac{u_k}{u} = Re_l^{-1/4} \quad 3.11.b$$

$$\frac{\tau_k}{\ell} = Re_l^{-1/2} \quad 3.11.c$$

with the Reynolds number

$$Re_l = \frac{ul}{\nu} \quad 3.12$$

It is seen that the Reynolds number for the microstructure is equal to unity, i.e. convection and diffusion are equal:

$$Re_l = \frac{u_k \eta_k}{\nu} = 1 \quad 3.13$$

3-Continuum phenomenon:

Turbulence is a continuum phenomenon, governed by the equations of fluid mechanics. Even the smallest scales occurring in a turbulent flow are ordinarily far larger than any molecular length scale.

3.6.3 Feature of flows

Turbulence is not a feature of fluids but of fluid flows, i.e. the major characteristics of turbulent flows are not controlled by the molecular properties of the fluid. Most of the dynamics of turbulence is the same in all fluids, whether they are liquids or gases. If the Reynolds number is large enough, the turbulence is independent of the molecular properties of the fluid in which it appears.

3.6.4 Methods of averaging

Modelling of turbulent flows requires appropriate procedures to describe the effects of turbulent fluctuations of velocity and scalar quantities on the basic conservation equations previously presented.

As mentioned earlier, the problem of randomness is treated through statistical methods. All instantaneous quantities are decomposed into mean values and fluctuations with zero mean values:

$$u = \bar{u} + u' \quad 3.14.a$$

$$\phi = \bar{\phi} + \phi' \quad 3.14.b$$

$$p = \bar{p} + p' \quad 3.14.c$$

It has to be noted that in the particular case of the velocity, the component of fluctuations, 'u', brings a second notion, after the scale of turbulence introduced earlier, allowing us to describe quantitatively a turbulent motion, the notion of violence or intensity of turbulence:

$$I = \sqrt{\overline{(u')^2}} \quad 3.15$$

3.7 Turbulence Models

Turbulent flows are characterised by fluctuating velocity fields. These fluctuations mix transported quantities such as momentum, energy, and species concentration, and cause the transported quantities to fluctuate as well. Since these fluctuations can be of small scale and high frequency, they are too computationally expensive to simulate directly in practical engineering calculations. Instead, the instantaneous (exact) governing equations can be time-averaged, ensemble-averaged, or otherwise manipulated to remove the resolution of small scales, resulting in a modified set of equations that are computationally less expensive to solve. However, Turbulence variables, and turbulence models are needed to determine these variables in terms of known quantities. ANSYS FLUENT 12.0 provides the following choices of turbulence models [12]:

- Spalart-Allmaras model
- $k - \varepsilon$ models
 - Standard $k - \varepsilon$ model
 - Renormalization-group (RNG) $k - \varepsilon$ model
 - Realizable $k - \varepsilon$ model
- $k - \omega$ models
 - Standard $k - \omega$ model
 - Shear-stress transport (SST) $k - \omega$ model
- v2-f model
- Reynolds stress models (RSM)
- Detached eddy simulation (DES) model
- Large eddy simulation (LES) model

3.7.1 Choosing a turbulence model

The choice of turbulence model will depend on considerations such as the physics encompassed in the flow, the established practice for a specific class of problem, the level of accuracy required, the available computational resources, and the amount of time available for the simulation.

The following present general guidelines to enable choice of the appropriate turbulence model to be made, Table 2.2[88, 99-101]:

Model	Features
Spalart-Allmaras model	<ul style="list-style-type: none"> • Solves a model transport equation for the kinetic eddy (turbulent) viscosity. • One-equation model, not needed to calculate length scale. • Designed especially for aerospace and turbo-machinery applications, involving wall-bounded high-speed flows. • Boundary layer subjected to adverse pressure gradient.
Standard k-ϵ models	<ul style="list-style-type: none"> • Semi-empirical model based upon simplest of two transport equation models for the turbulence kinetic energy k and its dissipation rate ϵ. • Robust and suitable for initial iteration.
Renormalization-group (RNG) k - ϵ model	<ul style="list-style-type: none"> • Variant of standard k - ϵ models. • Has an additional term in ϵ equation to enhance strained flows. • Effect of swirl on turbulence is included to improve swirl flows. • More suitable for low Reynolds number.
Realizable k - ϵ model	<ul style="list-style-type: none"> • Variant of standard k - ϵ models. • Contains a new formulation for the turbulent viscosity. • A new transport equation for the dissipation rate, ϵ, has been derived from an exact equation for the transport of the mean-square vorticity fluctuation. • Accurate for spreading of both planar and rounded jets recommended for flows with

	boundary layers under strong adverse pressure, separation and recirculation.
Standard $k - \omega$ model	<ul style="list-style-type: none"> Solve for $k - \omega$ based on Wilcox model [102] <p>Specific dissipation rate:</p> $\omega = \frac{\varepsilon}{k}$ <ul style="list-style-type: none"> Includes modifications for low-Reynolds-number effects, compressibility, and shear flow spreading. Recommended for low Reynolds number flows, wall bounded boundary layer, and for transitional flows.
Shear-stress transport (SST) $k - \omega$ model	<ul style="list-style-type: none"> Variant of standard $k - \omega$ model Gradual change from the standard $k - \omega$ model in the inner region of the boundary layer to a high-Reynolds-number version of the $k - \varepsilon$ model in the outer part of the boundary layer. Modified turbulent viscosity formulation to account for the transport effects of the principal turbulent shear stress. More accurate and reliable for a wider class of flows, like adverse pressure in aerofoils, transonic shock waves, etc.
Reynolds stress models (RSM)	<ul style="list-style-type: none"> Five equations model. The RSM accounts for the effects of streamline curvature, swirl, rotation, and rapid changes in strain rate in a more rigorous manner than one-equation and two-equation models, it has greater

	<p>potential to give accurate predictions for complex flows.</p> <ul style="list-style-type: none"> • Run time and memory intensive.
--	---

Table 3.2: Characteristics and features of turbulence models

3.7.2 Shear-stress transport (SST) $k - \omega$ model

The shear-stress transport (SST) $k - \omega$ model was developed by Menter [103] to effectively blend the robust and accurate formulation of the $k - \omega$ model in the near-wall region with the free-stream independence of the $k - \omega$ model in the far field. To achieve this, the standard $k - \omega$ model is converted into a SST $k - \omega$ formulation. The SST $k - \omega$ model is similar to the standard $k - \omega$ model, but includes the following refinements:

- The standard $k - \omega$ model and the transformed $k - \omega$ model are both multiplied by a blending function and both models are added together. The blending function is designed to be one in the near-wall region, which activates the standard $k - \omega$ model, and zero away from the surface, which activates the transformed $k - \varepsilon$ model.
- The SST model incorporates a damped cross-diffusion derivative term in the ω equation.
- The definition of the turbulent viscosity is modified to account for the transport of the turbulent shear stress.
- The modelling constants are different.

These features make the SST $k - \omega$ model more accurate and reliable for a wider class of flows (e.g., adverse pressure gradient flows, airfoils, transonic shock waves) than the standard $k - \omega$ model. Other modifications include the addition of a cross-diffusion term in the $k - \omega$ equation and a blending function to ensure that the model equations behave appropriately in both the near-wall and far-field zones.

The transport equation for SST $k - \omega$ model is:

$$\frac{\partial}{\partial t}(\rho k) + \frac{\partial}{\partial x_i}(\rho k u_i) = \frac{\partial}{\partial x_j} \left(\Gamma_k \frac{\partial k}{\partial x_j} \right) + \overline{G_k} - Y_k + S_k \quad 3.16$$

$$\frac{\partial}{\partial t}(\rho \omega) + \frac{\partial}{\partial x_i}(\rho \omega u_i) = \frac{\partial}{\partial x_j} \left(\Gamma_\omega \frac{\partial \omega}{\partial x_j} \right) + \overline{G_\omega} - Y_\omega + D_\omega + S_\omega \quad 3.17$$

where:

$\overline{G_k}$ represents the generation of turbulence kinetic energy due to mean velocity gradients. $\overline{G_\omega}$ represents the generation of the specific dissipation rate due to mean velocity gradients. Γ_k and Γ_ω represent the effective diffusivity of k and ω . Y_k and Y_ω represent the dissipation of k and ω due to turbulence. D_ω represents the cross-diffusion term. S_k and S_ω are user-defined source terms. Calculations of all these terms have been fully explained and described in [12].

3.8 Modelling of Turbulent Combustion

Combustion requires that the fuel and oxidizer be mixed at the molecular level. This usually depends on the turbulent mixing process. During combustion, a fuel or any hydrocarbon mixture reacts with the oxidant, which is normally air, to form products of combustion. These products are not a result of one reaction but usually a sequence of chemical reactions. For instance, more than 1000 elementary reactions are involved in the combustion process of methane (CH₄), which is one of simplest hydrocarbon fuels.

Beside all the flow equations, the transport equations for the mass fraction m_j of each species j must be solved. The species equations can be written down by using the general transport [88]:

$$\frac{\partial(\rho m_j)}{\partial t} + \text{div}(\rho m_j \mathbf{u}) = \text{div}(\Gamma_j \text{grad } m_j) + S_j \quad 3.18$$

The volumetric rate of generation (or destruction) of species due to chemical reactions appears as the source (or sink) term S_j in each of their transport equations.

In simple chemical reaction system, infinitely fast chemical reactions are assumed and the intermediate reactions are ignored. The transport equations for the fuel and oxygen mass fraction may be written as below.

$$\frac{\partial(\rho m_f)}{\partial t} + \text{div}(\rho m_f \mathbf{u}) = \text{div}(\Gamma_f \text{grad } m_f) + S_f \quad 3.19$$

$$\frac{\partial(\rho m_o)}{\partial t} + \text{div}(\rho m_o \mathbf{u}) = \text{div}(\Gamma_o \text{grad } m_o) + S_o \quad 3.20$$

Under the assumption of equal diffusivities $\Gamma_f = \Gamma_o = \Gamma$, the species equations can be reduced to a single equation for the mixture fraction, f

$$f = \frac{Z_i - Z_{i,ox}}{Z_{i,fuel} - Z_{i,ox}} \quad 3.21$$

where Z_i is the elemental mass fraction for element i . The subscript “ox” denotes the value at the oxidizer stream inlet and the subscript fuel denotes the value at the fuel stream inlet. The reaction source terms in the species equations cancel, and thus f is a conserved quantity. Whilst the assumption of equal diffusivities is problematic for laminar flows, it is generally acceptable for turbulent flows where turbulent convection overwhelms molecular diffusion.

Combustion is normally divided into three main groups according to the type of mixing as follows:

8.3.1 Non-premixed combustion modelling

Fuel and oxidizer will not mix prior to combustion zone; this clearly means they will enter separately into combustion chamber. However, they will mix and burn during the combustion and the flame is called a diffusion flame.

In diffusion flames, flame response also critically depends on preferential diffusion processes which are generally characterised by the Lewis number, Le . The Lewis number is defined below:

$$Le = \frac{\alpha}{D} \quad 3.22$$

where α is the thermal diffusivity and D is the mass diffusion governed by Fick’s law. When $Le = 1$ the combustion process is said to be diffusively neutral and adiabatic as total energy conservation is maintained. When $Le < 1$ the mass transport exceeds heat loss resulting in an increase in combustion intensity. When $Le > 1$ the heat loss exceeds mass transport and the combustion intensity decreases accordingly.

Under certain assumptions, the thermochemistry can be reduced to a single parameter: the mixture fraction. The mixture fraction, denoted by f , is the mass fraction that originated from the fuel stream. In other words, it is the local mass fraction of burnt and unburnt fuel stream elements (C, H, etc.) in all the species (CO₂, H₂O, O₂, etc.). The approach is elegant because atomic elements are conserved in chemical reactions. In turn, the mixture fraction is a conserved scalar quantity, and therefore its governing transport equation does not have a source term. Combustion is simplified to a mixing problem, and the difficulties associated with closing nonlinear mean reaction rates are avoided. Once mixed, the

chemistry can be modelled as in chemical equilibrium, or near chemical equilibrium with the laminar flamelet model.

The non-premixed modelling approach has been specifically developed for the simulation of turbulent diffusion flames with fast chemistry. For such systems, the method offers many benefits over the eddy-dissipation formulation. The non-premixed model allows intermediate (radical) species prediction, dissociation effects, and rigorous turbulence-chemistry coupling.

The method is computationally efficient in that it does not require the solution of a large number of species transport equations. When the underlying assumptions are valid, the non-premixed approach is preferred over the eddy-dissipation formulation.

There are some restrictions on the mixture fraction approach that can be summarised as follows:

- The chemical system must be of the diffusion type with discrete fuel and oxidizer inlets (spray combustion and pulverized fuel flames may also fall into this category).
- The Lewis number must be unity. (This implies that the diffusion coefficients for all species and enthalpy are equal, a good approximation in turbulent flow).
- When a single mixture fraction is used, the following conditions must be met:
 - Only one type of fuel is involved.
 - Only one type of oxidizer is involved.
- When two mixture fractions are used, three streams can be involved in the system.

Valid systems are as follows:

- Two fuel streams with different compositions and one oxidizer stream.
 - Mixed fuel systems including gas-liquid, gas-coal, or liquid-coal fuel mixtures with a single oxidizer. In systems with a gas-coal or liquid-coal fuel mixture, the coal volatiles and char are treated as a single composite fuel stream.
 - Coal combustion in which volatile and char off-gases are tracked separately.
 - Two oxidizer streams with different compositions and one fuel stream.
 - A fuel stream, an oxidizer stream, and a non-reacting secondary stream.
- The flow must be turbulent.

8.3.2 Premixed combustion modelling

Fuel and oxidizer will fully mix prior to combustion zone; this means that they will enter as a mixture of air and fuel. Apart from some modern small, condensing gas boilers, few systems are fully premixed.

There are many limitations of using the premixed model; they can be summarised as follows:

- The segregated solver must be used. The premixed combustion model is not available with either of the coupled solvers.
- The premixed combustion model is valid only for turbulent, subsonic flows. These types of flames are called deflagrations. Explosions, also called detonations, where the combustible mixture is ignited by the heat behind a shock wave, can be modelled with the finite-rate model using the coupled solver.
- The premixed combustion model cannot be used in conjunction with the pollutant (i.e., soot and NOx) models. However, a perfectly premixed system can be modelled with the partially premixed model, which can be used with the pollutant models.
- It cannot be used to simulate reacting discrete-phase particles, since these would result in a partially premixed system. Only inert particles can be used with the premixed combustion model.

Premixed combustion is much more difficult to model than non-premixed combustion. As discussed above, the reason for this is that premixed combustion usually occurs as a thin, propagating flame that is stretched and distorted by turbulence. For subsonic flows, the overall rate of propagation of the flame is determined by both the laminar flame speed and the turbulent eddies. The laminar flame speed is determined by the rate that species and heat diffuse upstream into the reactants and burn.

The turbulent premixed combustion model, based on work by Zimont et al. [104-107], involves the solution of a transport equation for the reaction progress variable. The closure of this equation is based on the definition of the turbulent flame speed.

The flame front propagation is modelled by solving a transport equation for the density weighted mean reaction progress variable, denoted by c [105]:

$$\frac{\partial(\rho c)}{\partial t} + \nabla \cdot (\rho \vec{v} c) = \nabla \cdot \left(\frac{\mu_t}{Sc_t} \nabla c \right) + \rho S_c \quad 3.23$$

c = mean reaction progress variable

Sc_t = turbulent Schmidt number

Sc = reaction progress source term (s^{-1})

The progress variable is defined as a normalised sum of the product species,

$$c = \frac{\sum_{i=1}^n Y_i}{\sum_{i=1}^n Y_{i,eq}} \quad 3.24$$

where

n = number of products

Y_i = mass fraction of product species i

$Y_{i,eq}$ = equilibrium mass fraction of product species i

Based on this definition, $c = 0$ where the mixture is unburnt and $c = 1$ where the mixture is burnt. The value of c is defined as a boundary condition at all flow inlets. It is usually specified as either 0 (unburnt) or 1 (burnt).

The mean reaction rate in equation 3.23 is modelled as

$$\rho S_c = \rho_u S_T |\nabla c| \quad 3.25$$

where

ρ_u = density of burnt mixture

S_T = turbulent flame speed.

The turbulent flame speed is computed using a model of wrinkled and thickened flame fronts:

$$S_T = A(u')^{3/4} S_L^{1/2} \alpha^{-1/4} \ell_t^{1/4} = Au' \left(\frac{\tau_t}{\tau_c} \right)^{1/4} \quad 3.26$$

where

A = model constant

u' = root-mean-square (RMS) velocity (m/s)

S_L = laminar flame speed (m/s)

$\alpha = k / \rho c$ = molecular heat transfer coefficient of unburnt mixture (thermal diffusivity) (m²/s)

ℓ_t = turbulence length scale (m)

$\tau_t = \ell_t / \dot{u}$ = turbulence time scale (s)

$\tau_c = \alpha / S_L^2$ = chemical time scale (s)

The turbulence length scale ℓ_t is computed from

$$\ell_t = C_D \frac{(\dot{u})^3}{\varepsilon} \quad 3.27$$

where ε is the turbulence dissipation rate.

The model is based on the assumption of equilibrium small scale turbulence inside the laminar flame, resulting in a turbulent flame speed expression that is purely in terms of the large-scale turbulent parameters. The default values of 0.52 for A , and 0.37 for C_D are recommended by Zimont et al. [105], and are suitable for most premixed flames.

Non-adiabatic premixed combustion model is considered. The energy transport equation is solved in order to account for any heat losses or gains within the system. These losses/gains may include heat sources due to chemical reaction or radiation heat losses.

The energy equation in terms of sensible enthalpy, h , for the fully premixed fuel is as follows:

$$\frac{\partial}{\partial t}(\rho h) + \nabla \cdot (\rho \vec{v}) = \nabla \cdot \left(\frac{k + k_t}{c_p} \nabla h \right) + S_{h,chem} + S_{h,rad} \quad 3.28$$

$S_{h,rad}$ represents the heat losses due to radiation and $S_{h,chem}$ represents the heat gains due to chemical reaction:

$$S_{h,chem} = \rho S_c H_{comb} Y_{fuel} \quad 3.29$$

where

S_c = normalized average rate of product formation (s-1)

H_{comb} = heat of combustion for burning 1 kg of fuel (J/kg)

Y_{fuel} = fuel mass fraction of the unburnt mixture

8.3.3 Partially premixed combustion modelling

A system which includes the above two methods (non-premixed and premixed combustion) is called a partially premixed system. This type of system takes the benefits of both previous mentioned types of combustion. Examples of practical application are spark-ignition engines, lean-burn gas turbine combustors and many domestic central heating boiler burners.

The partially premixed model in FLUENT is a simple combination of the non-premixed model and the premixed model. The premixed reaction-progress variable, c , determines the

position of the flame front. Behind the flame front ($c = 1$), the mixture is burnt and the equilibrium or laminar flamelet mixture fraction solution is used. Ahead of the flame front ($c = 0$), the species mass fractions, temperature, and density are calculated from the mixed but unburnt mixture fraction. Within the flame ($0 < c < 1$), a linear combination of the unburnt and burnt mixtures is used.

The limitations of using a partially premixed model, the underlying theory, assumptions, and limitations of the non-premixed and premixed models apply directly to the partially premixed model. In particular, the single-mixture fraction approach is limited to two inlet streams, which may be pure fuel, pure oxidizer, or a mixture of fuel and oxidizer. The two-mixture-fraction model extends the number of inlet streams to three, but incurs a major computational overhead.

Both non-premixed and premixed systems are considered in this research. For the non-premixed systems, the nonpremixed model is used for simulation. Regarding the premixed systems, even though the premixed model is suitable for the simulation, it is preferable to use the partially premixed model to simulate the premixed combustion as it is possible to extend the analysis to perform pollutant analysis. The pollutant analysis is restricted with the premixed models but it can be performed with the partially premixed model.

3.9 CFD Solver

3.9.1 ANSYS 12 FLUENT

One of the most powerful computational fluid dynamics softwares available for optimisation of product development and processes is ANSYS 12 FLUENT. The broad physical modelling capabilities of this engineering design tool have been effectively applied to industrial applications ranging, for example, from flow over an aircraft wing to combustion in a furnace. The ability of the software to model internal combustion engines, aeroacoustics, turbomachinery and multiphase systems has served to broaden its reach.

Turbulence: Inside ANSYS FLUENT software, several popular k -epsilon and k -omega models are available, as is the Reynolds stress model (RSM) for highly swirling or anisotropic flows. Wall functions and enhanced wall treatment options allow for the best possible representation of all wall-bounded flows.

3.9.2 ANSYS 12 Meshing

For the purpose for CFD modelling, the software performs the computations at a range of discrete locations within the domain.

The purpose of meshing is to decompose the solution domain into an appropriate number of locations for an accurate result. The basic building blocks for a 2D and 3D mesh are shown in Figure 3.2:

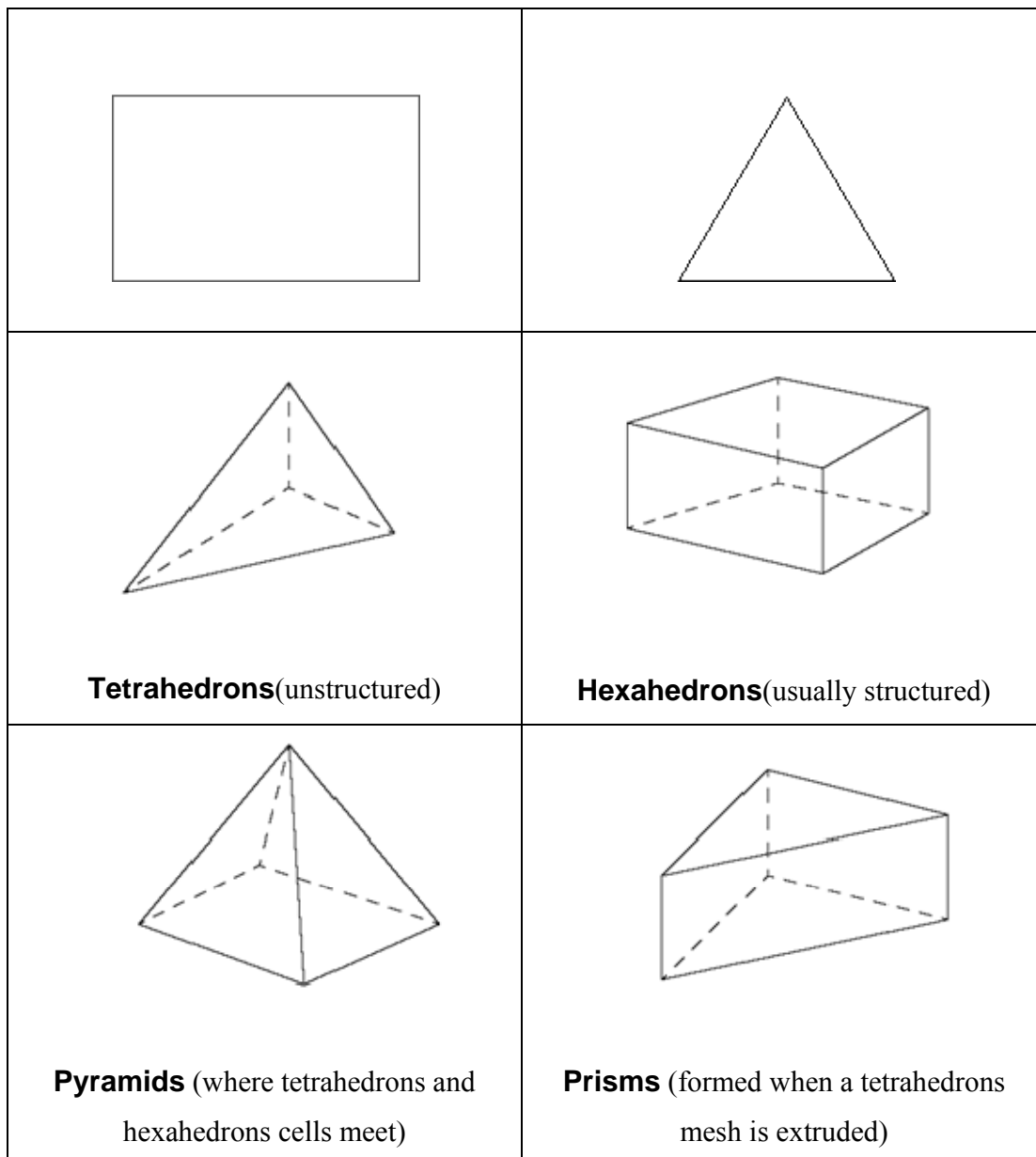


Figure 3.2: 2D and 3D basic mesh shape

3.9.3 Mesh Quality Measurement

Mesh metrics are available under mesh options to set and review mesh metric information and to evaluate mesh quality. Different physics and different solvers have different requirements for mesh quality. There is no doubt that mesh quality can have a great influence upon the accuracy of numerical simulations. Many factors influence mesh accuracy including the type of physics being simulated, details of the solution to the particular simulation, the method of discretization, and geometric mesh properties having to do with spacing, curvature, angles, smoothness, etc.

A mesh quality concerns the characteristics of a mesh that permit a particular numerical PDE simulation to be efficiently performed, with fidelity to the underlying physics, and with the accuracy required for the problem [108].

This definition hints at several issues. First off all, mesh quality depends on the particular calculation, which is undertaken and thus changes if a different calculation is performed. Second, a mesh should not create difficulties for the simulation. For example, inverted elements can cause a loss of fidelity or even cause the simulation to stop prematurely. The mesh should not cause the numerical solution to exhibit mesh imprinting. Third, the mesh should result in sufficiently accurate simulations, i.e., those that are in the asymptotic regime, and those, which reduce both global and local error below the required level. Ultimately, the mesh and discretization method together must enable the simulation to satisfy the requirement that the size of the error bars due to problem discretization are acceptable.

Genuinely, the shape of the cell including its skewness and aspect ratio has a significant impact on the accuracy of the numerical solution.

Skewness can be defined as the difference between the cell's shape and the shape of an equilateral cell of equivalent volume. Highly skewed cells can decrease accuracy and destabilize the solution. For example, optimal quadrilateral meshes will have vertex angles close to 90 degrees, whilst triangular meshes should preferably have angles of close to 60 degrees and have all angles less than 90 degrees.

There are two methods to determining the skewness [109]:

- Based on the Equilateral volume deviation:

$$skewness = \frac{\text{optimal cell size} - \text{cell size}}{\text{optimal cell size}} \quad 3.30$$

The above equation applies only to triangles and tetrahedral shapes.

- Based on the deviation from a normalized angle deviation:

$$skewness = \left(\frac{\theta_{max} - \theta}{180 - \theta} \right) \left(\frac{\theta - \theta_{min}}{\theta} \right) \quad 3.31$$

Where θ is the equiangular face/cell (60 for tetrahedrons and triangles, and 90 for quadrilaterals and hexahedrons), the equation applies to cell and face shapes and is used for prisms and pyramids.

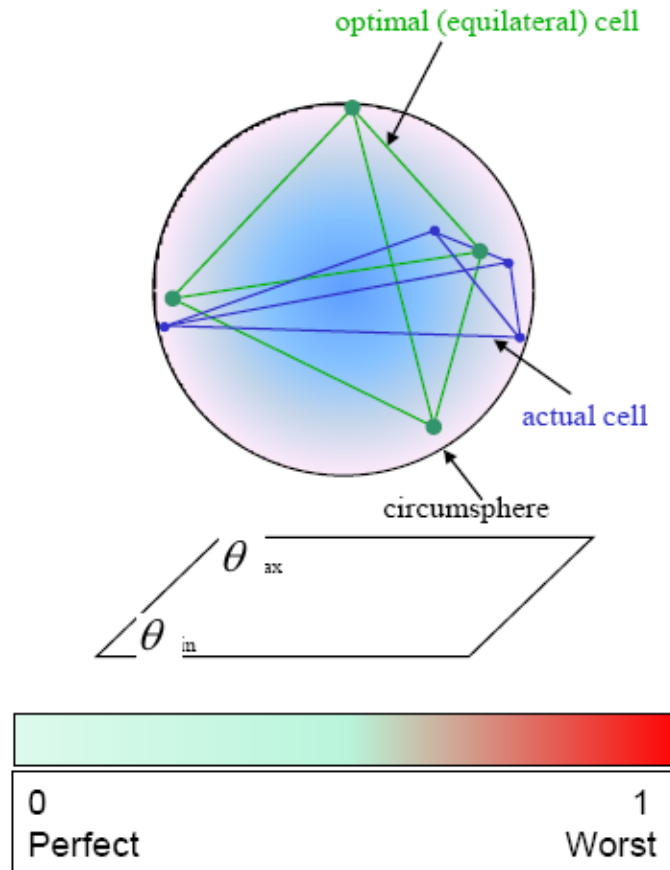


Figure 3.3: Skewness calculation explanation shape

Moreover, the classification of the mesh quality metrics is based on skewness:

0-0.25	0.25-0.50	0.50-0.80	0.80-0.95	0.95-0.98	0.98-1.00*
Excellent	very good	good	acceptable	bad	Inacceptable*

Table 3.3: The Relationship between skewness and mesh quality.

The aspect ratio is a measure of the stretching of the cell. For highly anisotropic flows, extreme aspect ratios may yield accurate results with fewer cells. However, a general rule of thumb is to avoid aspect ratios in excess of 5:1.

Aspect for generic triangles and quads is a function of the ratio of longest side to the shortest side of the reconstructed quadrangles equal to one (ideal) for an equilateral triangle or a square, as shown in Figure 3.4.

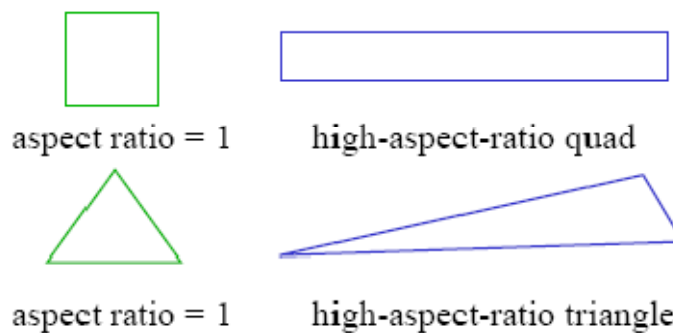


Figure 3.4: Aspect ratio comparison of two different cases

Points that have to be considered within each model to create an acceptable mesh include:

- FLUENT requires high quality mesh to avoid numerical diffusion.
- Several mesh quality metrics are involved in order to quantify the quality, however the skewness is the primary metric.
- The aspect ratio and cell size changes mesh metrics and are also very important.
- In worst case scenarios, and depending on the solver used (density based or pressure based), FLUENT can tolerate poor mesh quality. However, some applications may require higher mesh quality, resolution and good mesh distribution.
- The location of poor quality elements helps determine their effect.
- Indicators of overall mesh quality metrics are available in ANSYS Meshing.

3.10 Summary

In this chapter, CFD has been described as a potentially important tool in designing combustion systems in gas turbines. The following can be concluded:

- CFD is an important tool for analysing systems involving fluid flow, heat transfer and combustion.
- The commercial CFD packages contain three main elements: a pre-processor, a solver and, a post-processor.
- CFD codes target a solution to the main flow governing equations.
- There are many turbulent models that can be used by the FLUENT user, the one used in this work suited the requirements of prediction at relatively low flowrates and accuracy in the boundary layers
- FLUENT offers several models for chemical species transport and chemical reactions. The partially premixed combustion model was used
- The model preparation (models geometry draws method and mesh construction) plays an important role in the simulation accuracy and the solution convergence.

Chapter Four

100 kW

TANGENTIAL

SWIRL

COMBUSTOR

CHAPTER FOUR

100 kW TANGENTIAL SWIRL COMBUSTOR

“All truths are easy to understand once they are discovered; the point is to discover them.”

Galileo

4.1 Introduction

Lean premixed combustion using swirling flows is widely used in gas turbines and combustion processes due to the benefits of excellent flame stability and blowoff limits coupled with low NO_x emissions. Although flashback is not generally a problem with natural gas combustion, there are some reports of flashback damage with existing gas turbines, whilst hydrogen enriched fuel blends, especially those derived from gasification of coal and/or biomass, cause concerns in this area.

The objective of this model simulation is to analyse flames' characteristics such as flashback under atmospheric conditions and compare simulation data with experimental data [13]. The use of CFD technique such as FLUENT software allows the derivation of contours of velocity and other properties at different planes inside any flow system. This can be compared with experimental results; when good matching is achieved via model change this then allows the effects of geometrical changes to be investigated. Thus, this chapter describes a combined practical and modelling approach to study and reduce the effect of flashback in a pilot scale 100 kW tangential swirl burner, coupled with CFD modelling to guide experimental progress and facilitate analysis of the phenomena encountered. Natural gas is used as a fuel to establish baseline results and effects of different variables. The flashback phenomenon is studied experimentally via the derivation of flashback limits for a variety of different geometrical conditions and numerically to guide and facilitate analysis of the underlying processes. The use of a central fuel injector is shown to give substantial benefits in terms of flashback resistance by altering flow and flame patterns in the burner exit. The critical boundary velocity gradient is used for characterization of flashback, both via the original Lewis and von Elbe formula and via

new analysis using CFD and investigation of boundary layer conditions just in front of the flame front. Conclusions are drawn as to mitigation technologies.

4.2 Burner Experimental Rig Setup

A 100 kW Perspex swirl generator was used experimentally to study the isothermal phenomenon of the swirl flow, this is reported elsewhere [13]. An identical steel unit was used for combustion studies. These systems are based on a quarter-scale model of a 2 MW industrial scaled swirl burner/furnace system. Figures 4.1 and 4.2 show the photographs of the perspex prototype and a schematic geometry drawing, respectively. Two tangential entries together with variable width inserts allowed the use of different swirl numbers. The system was fed by a centrifugal fan providing air flow via flexible hoses and a bank of rotameters to measure the airflow rate.

Each inlet had an insert, Figure 4.1, that could be changed to alter the swirl number. Two different widths of inserts could be used, a pair of 75% of the diameter of the inlet, a 50% pair and a pair of 25%. In addition, a configuration with no insert (0%) could be used as well.



Figure 4.1: The Perspex swirl generator

Two different modes of natural gas injection were used for the prototype; a diffusive mode (non-premixed) with fuel normally injected along the central axis from the burner bottom, and a premixed mode with entry in both tangential inlets, located before the inserts used for varying the swirl number. Some studies were also undertaken with no fuel injector and fuel just injected through the bottom baseplate of the burner. Partial premixing was also extensively studied. Premixed gas injectors, extending across the inlet ducts, were located just before the inlets. Only one diffusive fuel injector was used in both experiment and simulation. This injector, 23.4 mm in diameter, was positioned 47.5 mm upstream of the burner nozzle to minimise flame impingement on it.

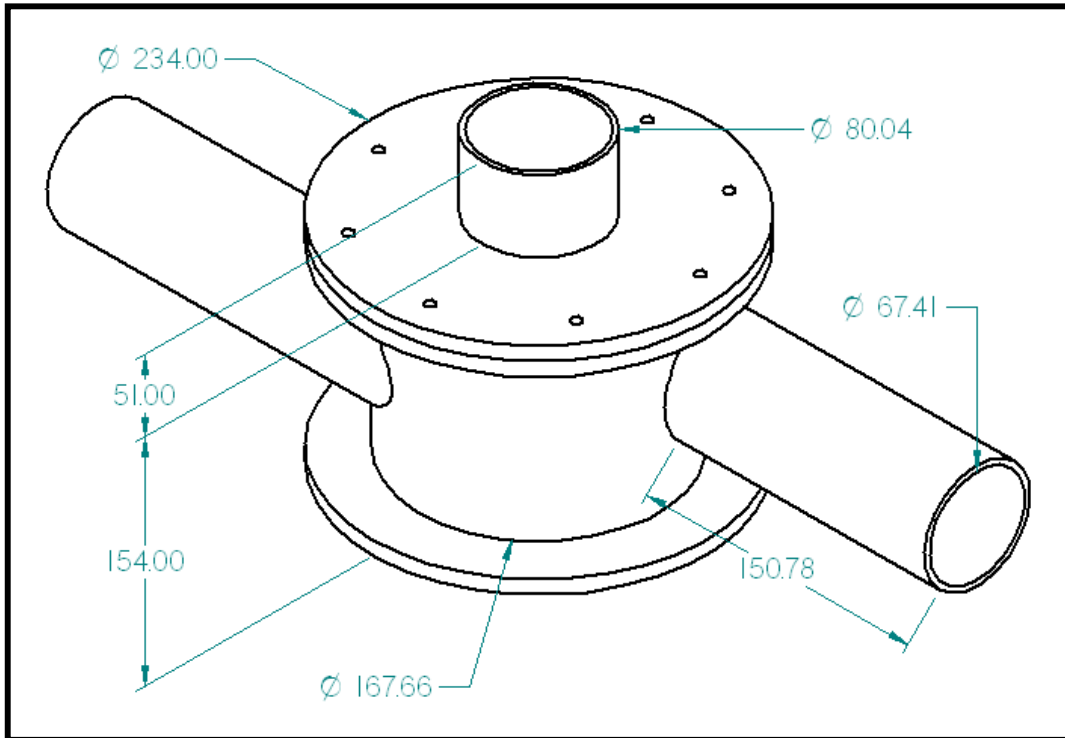


Figure 4.2: Schematic diagram of the swirl burner

Overall equivalence ratio ϕ is reported as well as the fuel proportion injected diffusively and that premixed in the tangential inlets. The format (25-80) here refers to 25 l/min diffusive natural gas injection, the 80 to that injected as premixed. Due to the high temperature variation, the Re is defined from the nozzle diameter and isothermal conditions.

According to previous experiments [110], some insert combinations at different Re showed the existence of different shapes of central recirculation zone and flame characteristics. The condition selected for CFD study was that characterised as [25-25], i.e. 25% blockage in each inlet, at a flowrate of 1400 l/min. This has been shown by [13, 17, 26], to be a very stable condition. The simulation carried out in this work performs as most of the cases that have been studied previously.

4.3 Burner CFD Modelling

CFD simulation needs multiple steps before analysing the model of study. These steps start from the defining of physical boundary conditions of the flow fields and then dividing the flow fields into smaller sub domains to discretize the governing differential equations, which are then solved inside each of these segments of the domain. Mesh characteristics in general influence the final solution. Making the correct decisions for the grid type and the method of constructing the mesh are extremely important. A higher number of cells increases the accuracy but at the same time increases solution time. Hence, selecting a suitable mesh method which gives acceptable results within an adequate time is difficult, particularly for complex systems. Figure 4.3 shows a schematic diagram of the actual tangential swirl burner including the main body, position of the 25% inserts in both tangential inlets and the central position of the injector.

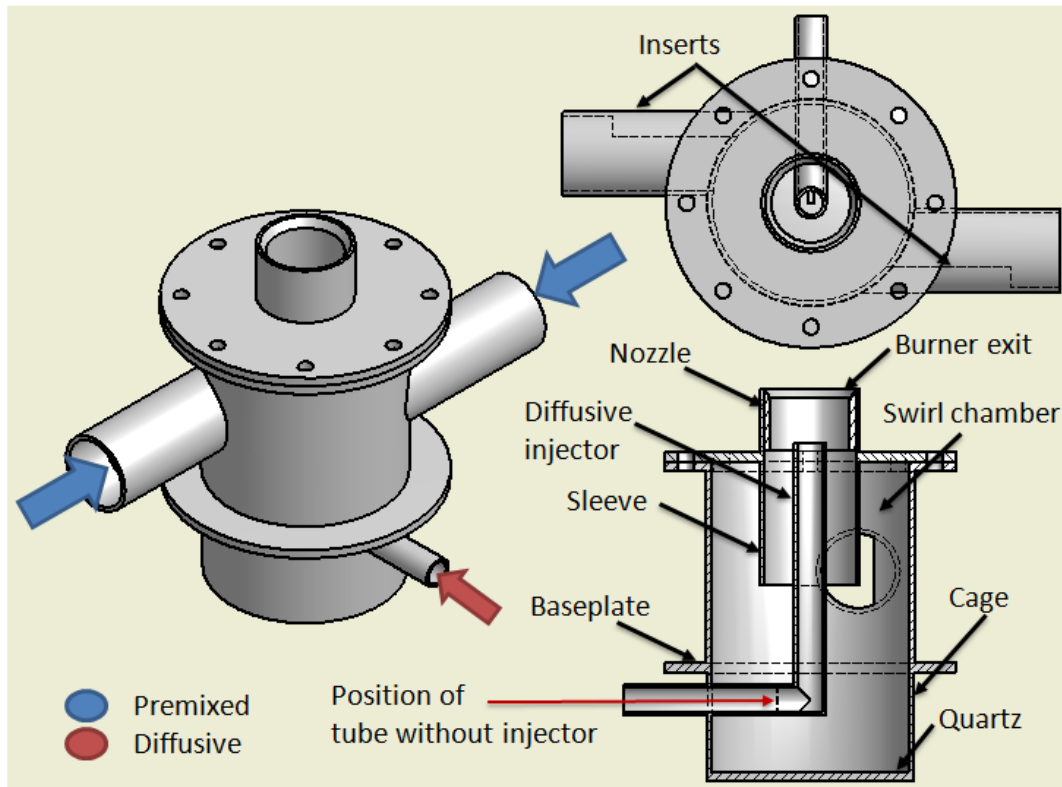


Figure 4.3: The swirl burner, fuel and air injection systems

The burner exit was varied from an open case with no nozzle to that with a quarl nozzle, Figure 4.4. Corresponding swirl numbers are 1.08 and 0.86, respectively. The quarl nozzle end edge is sloped by a 45° angle as clearly shown in Figure 4.4.

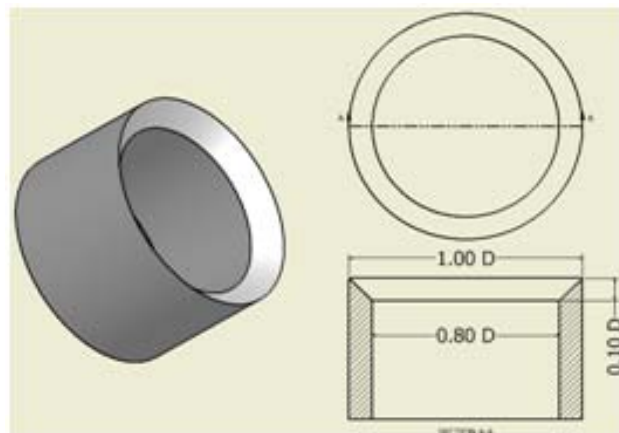


Figure 4.4. Nozzle used to vary flame properties. $D=78\text{mm}$

The exhaust sleeve extending back into the swirl chamber is designed to reduce flashback by increasing the radial velocity between the bottom of the nozzle and the baseplate of the burner. It was originally developed for a larger scale **2 MW** version of this unit [45].

The simulation has been carried out with the exhaust confinements only. The original design was fitted with two types of confinement: cylindrical and cylindrical with conical cup, as shown in Figure 4.5.

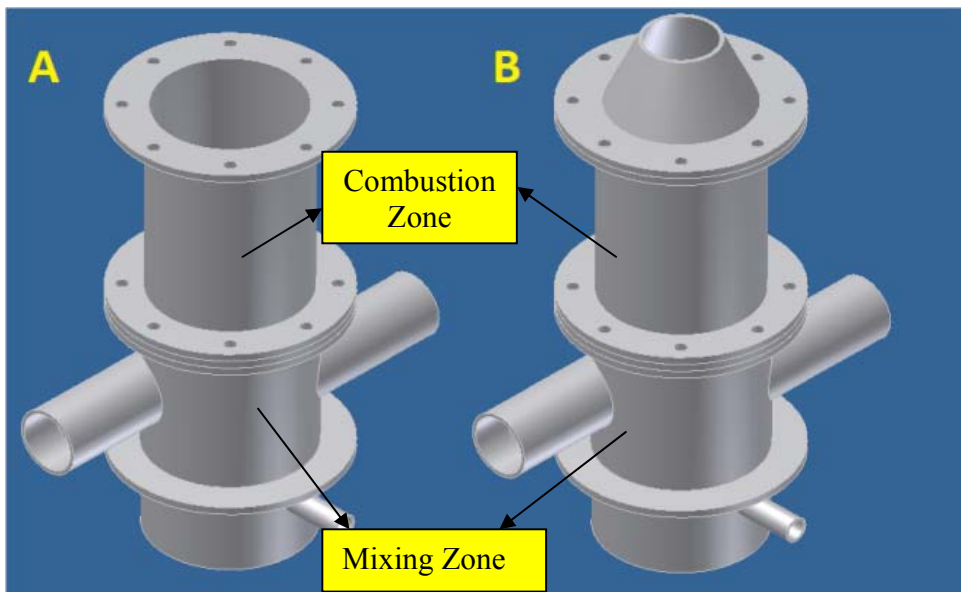


Figure 4.5: Burner confinements A) open and B) conical exit geometries

The tangential swirl burner used in this study is modelled as one part but consists of two connected zones: the premixed region and the combustion chamber. These two zones describe the flow fields in the system, as shown in Figure 4.5 A. The first zone is the mixing cylinder in which the air and fuel are mixed together and this section includes the tangential inlets which help to produce the turbulence. There is little combustion in this zone under the normal conditions. The other zone is the combustion chamber, which includes the burner exit and the confinement. Combustion is accomplished within this zone with the normal combustion.

The purpose of using different geometries for analysis was to recognize the position and evolution of flashback, as a function of different geometries and parameters which are known to be significant [13]. Geometrical variables included the effect of a fuel injector,

nozzle, two different confinements, with both premixed and partial premixed combustion being also investigated.

ANSYS 12.0 introduces three programs that are capable of carrying out the simulation. First of these programs is the **Design Modeller**, which is used to draw and design the geometry of the case under analysis, this programme has also the ability to import some graph files from other software. Figure 4.6 shows the geometry of the tangential swirl burner after been plotted.

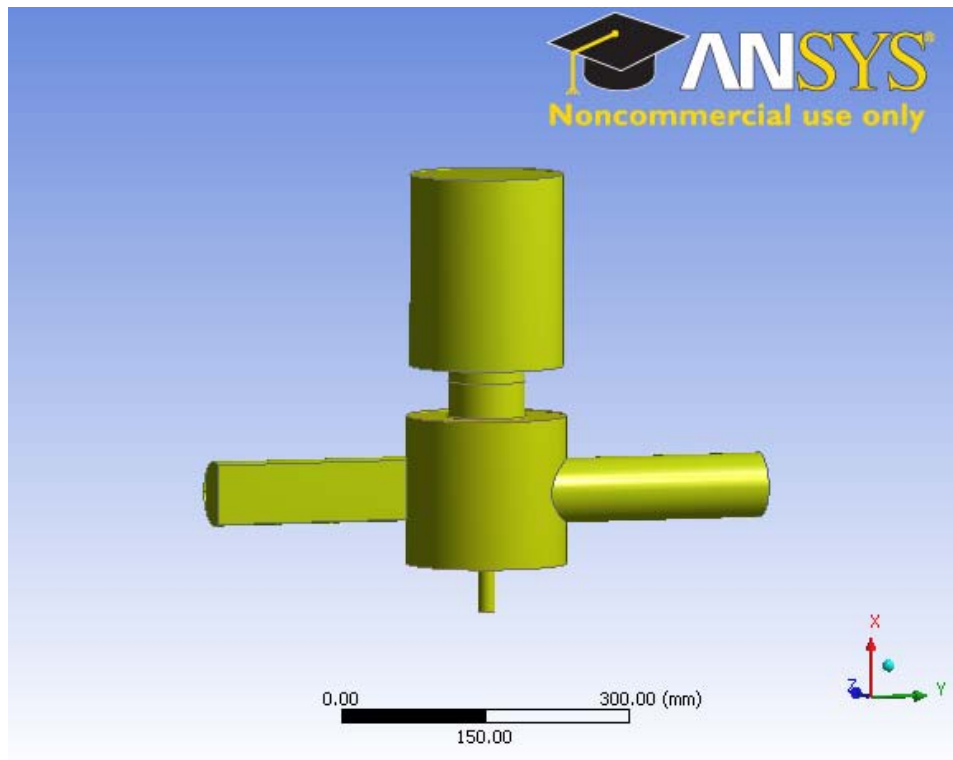


Figure 4.6: The geometry of the tangential swirl burner

Secondly, after the design has been prepared, the **Mesh Programme** is ready to create the mesh. A hexahedral has been mostly used to create the system mesh as this is known to give more accurate, faster and more stable solutions. Only some regions have used a tetrahedral mesh, which is difficult to mesh using the former method as shown in Figure 4.7.

Hence, the mesh generation type and the mesh density are unstructured and the solution results independent of the mesh results. The total number of cells in this model was 44518cells.

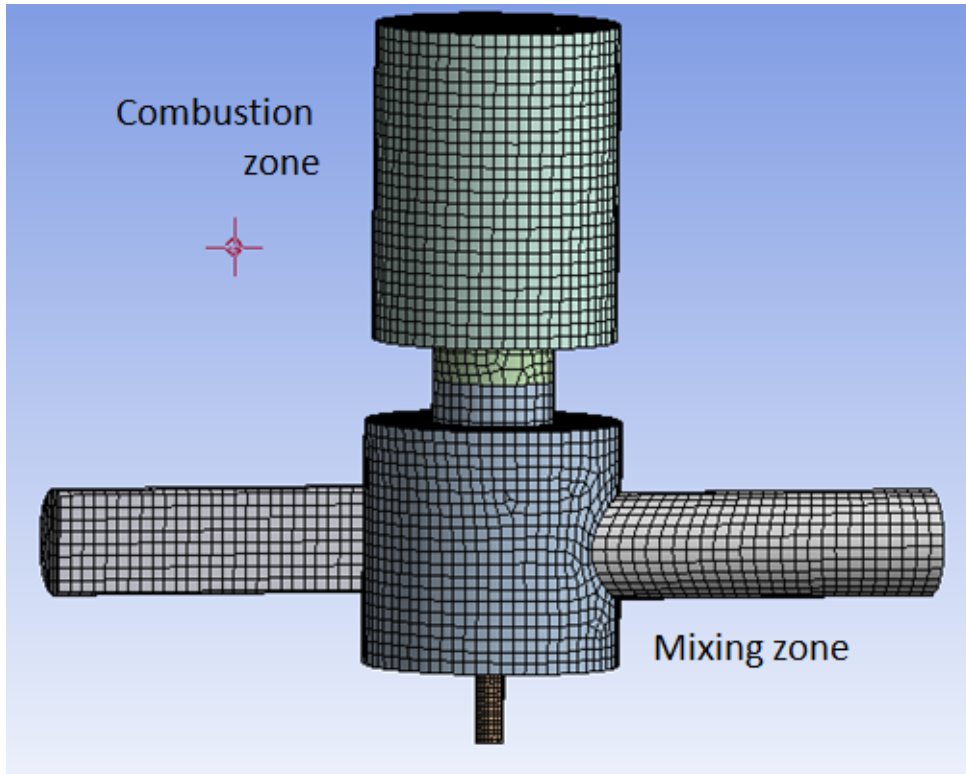


Figure 4.7: Tangential swirl burner mesh with injector

The main problem with this model was the number of cells, which affects the time for the solution to become converged and causes difficulties due to combustion effects and obtaining convergence with swirling flows.

Eventually, after the model mesh is set up, the next step is to take the model to the FLUENT software. A critical factor is the choice of turbulence model. Because of the relatively low Reynolds Numbers and the importance of the boundary layer flows, the SST- $k-\omega$ model was used. After a numerical simulation comparison with standard, RNG and Realizable $k-\epsilon$ model and standard $k-\omega$ model was made, a very similar result for isothermal flow was found. Reynolds stress models could not be used successfully because of computer memory limitations. Convergence was accepted as being completed when the residual curve reached 10^{-5} .

Here it should be noted that flashback occurs when vortex breakdown has not occurred and there are not significant central recirculation zones (CRZ) present. If such CRZs were present, a full Reynolds Stress turbulence model would probably be needed.

4.4 Results and Discussion

Before going through the results, it should be mentioned that the simulation has only been made for the swirl burner with cylindrical confinements with and without the fuel injector. In some cases the conical cup has been added to the confinement, as shown in Figure 4.5.B. Isothermal and combustion conditions have been simulated.

4.4.1 Isothermal Solution

Isothermal conditions with no combustion were used to calibrate the system and indicate the size of the central recirculation zone (CRZ), although it is well known that there are also 3D time dependant coherent structures present and thus the results are only of an indicative nature. During the simulation, various types of solvers were investigated and conclusions drawn as to which were the most effective. Based on the experimental results obtained at 1400 l/min flowrate, results were obtained using the $k - \omega$ model. Figure 4.8-a and b show the CRZ velocity contours formed (no injector). Although there are differences there are many similarities in the location of the CRZ and the shear flows which supports the predictive work with combustion, as it is well known that 3-dimensional time dependant effects are suppressed often with combustion [35].

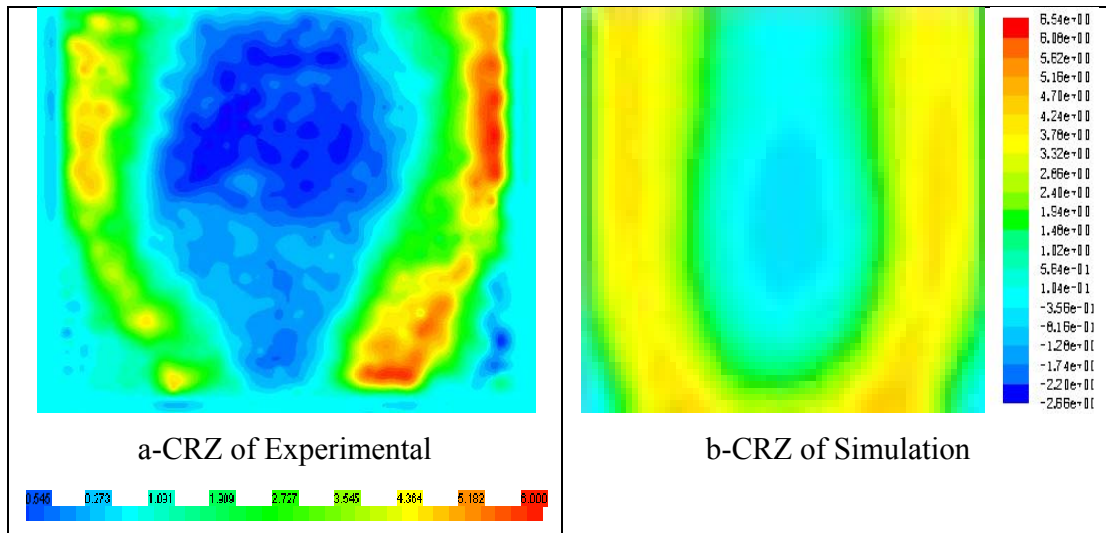


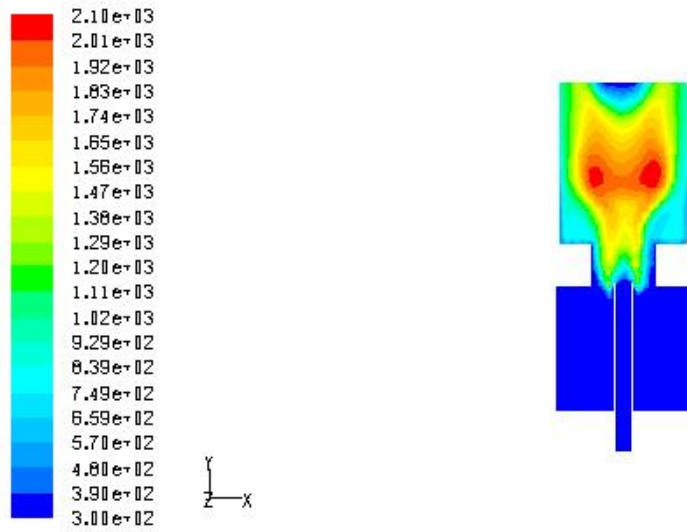
Figure 4.8: Comparison of axial velocity contours,
a) Experimental (PIV), b) Simulation

4.4.2 Non-Isothermal Solution

Three types of non-isothermal solutions have been studied: non-premixed, premixed and partially premixed combustion, as discussed previously. The crucial feature of swirl burners is normally the formation of a central reverse flow zone (CRZ) which extends blowoff limits by recycling heat and active chemical species to the root of the flame in the burner exit. However, unless its size and shape are properly controlled, problems can arise. The CRZ can for instance readily extend back into the burner at high swirl numbers, even surrounding the fuel injector and facilitating early flashback [49, 111-112]. However, for certain flashback cases at lower swirl numbers, $S < 1.2$, the situation was different and the CRZs formed at flashback were either very weak and located downstream or nonexistent, i.e. vortex breakdown had not occurred. Under these conditions, flashback occurred via different circumstances compared to higher swirl numbers where flashback was clearly associated with the presence of a CRZ.

4.4.2.1 Non-Premixed combustion (Diffused flame only)

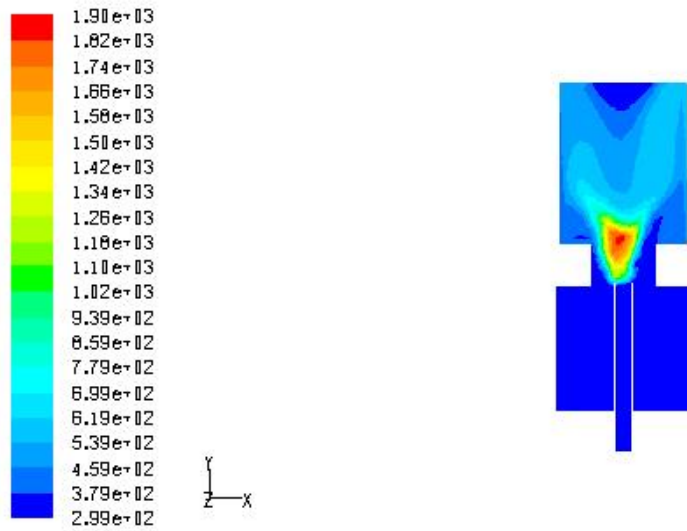
In non-premixed combustion, fuel and oxidizer enter the reaction zone in distinct streams. This means the fuel will enter the combustion zone through the injector and the oxidizer (atmospheric swirling air) will come through the two tangential inlets. This type of combustion produces very stable flames with no flashback possibility, irrespective of the type of fuel. Figures 4.09 and 4.10 show a typical example of diffusion combustion. Figure 4.09 shows cases of one lean and the other very lean combustion with methane, whilst Figure 4.10 shows cases with rich and lean combustion at higher fuel flowrates. There is little evidence of the existence of a CRZ in any of the case as vortex breakdown has not apparently occurred. Visually this is clear from the flames observed experimentally.



Contours of Static Temperature (k)

Feb 10, 2009
FLUENT 6.3 (3d, pbns, pdf19, skw)

$$Q_a=600\text{L/min } Q_f=25\text{L/min } \phi=0.717$$

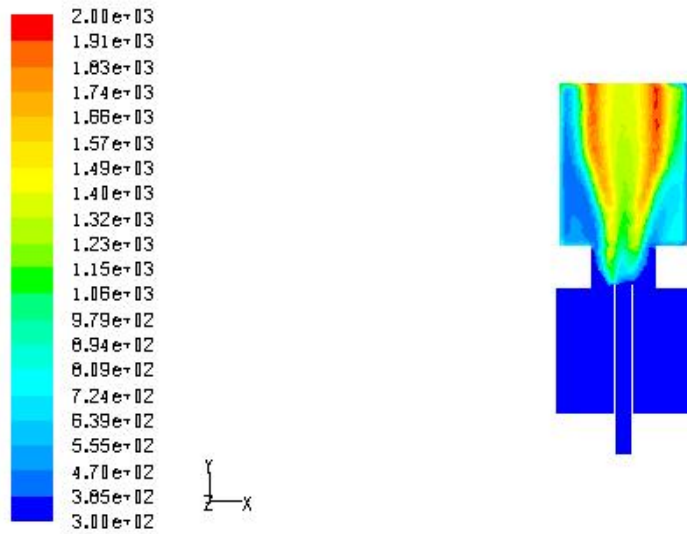


Contours of Static Temperature (k)

Feb 10, 2009
FLUENT 6.3 (3d, pbns, pdf19, skw)

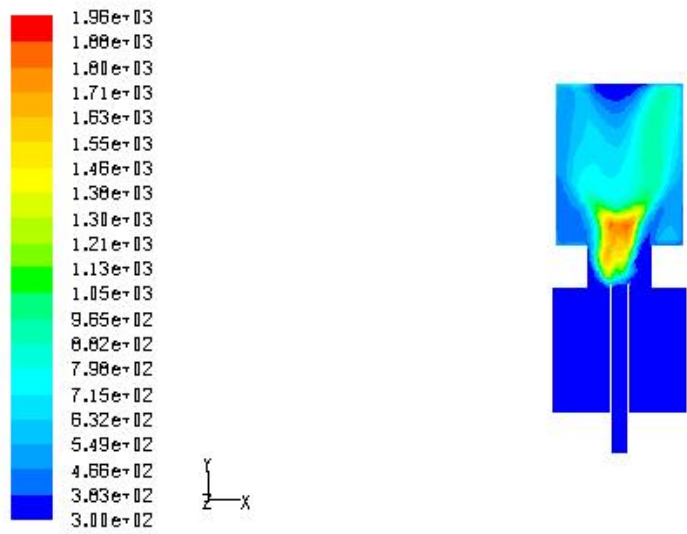
$$Q_a=2200\text{L/min } Q_f=25\text{L/min } \phi=0.1955$$

Figure 4.9: Non-premixed case study for different inlet values of air with 25L/min methane fuel



Contours of Static Temperature (k) Feb 10, 2009
FLUENT 6.3 (3d, pbns, pdf19, skw)

$$Q_a=600\text{L/min } Q_f=40\text{L/min } \phi=1.147$$



Contours of Static Temperature (k) Feb 10, 2009
FLUENT 6.3 (3d, pbns, pdf19, skw)

$$Q_a=2200\text{L/min } Q_f=40\text{L/min } \phi=0.31273$$

Figure 4.10: Non-premixed case study for different inlet values of air with 40L/min methane fuel

Through the previous mentioned graphs, it can be easily recognized that when the quantity of air increases the total temperature decreases and this is normal. The other problem is high NO_x generation due to hot spots formed with diffusion combustion.

4.4.2.2 Premixed combustion

There are many difficulties surrounding this kind of combustion, like instabilities, flashback and blowoff. Premixed combustion with a lean mixture offers lower NO_x due to the reduced average temperature.

Lean combustion tends to reduce average flame velocities, but other factors associated with engine cycles, such as high temperatures, pressure, turbulence levels and pre-ignition reactions in the gases due to appreciable residence times at high temperature cause increased flame speeds, encouraging flashback.

During the experiments and simulation of premixed combustion, the flashback and blowoff problems are clearly dominant as the engine must operate between these two limits. This study focuses on this problem and primarily on flashback and how geometrical changes can be used to control it. The CFD analysis indicates that for the flashback cases investigated a Rankine tangential velocity distribution (free/forced) is produced, with or without the fuel injector, although the CRZ is often absent or located downstream of the flame stabilization region.

The experimental work showed flashback was occurring through the outer exit wall boundary layer [13]. There were elements of three dimensionality and time dependence associated with this process for the cases without the fuel injector, as discussed later. Recognizing the limitations of both experimental and time dependant CFD techniques with flame propagation in thin wall boundary layers, a time averaged 3D CFD analysis was used as an aid to understand the complex flows developing and occurring inside the burner under combustion conditions. As flashback occurred via the outer wall boundary, CFD was used to characterize the flow and wall boundary layers just upstream of the flame front and thus understand the mechanisms that allow flashback to occur. This also allowed the derivation of actual critical boundary velocity gradients when flashback occurred.

Comparison between cases was performed using the average radial velocity of the flow (passing from the outer swirl chamber through the gap between the baseplate and the

backwards facing exhaust extension) Figure 4.11, and the equivalence ratio, to recognize regions of flashback for both premixed and diffusive-premixed conditions.

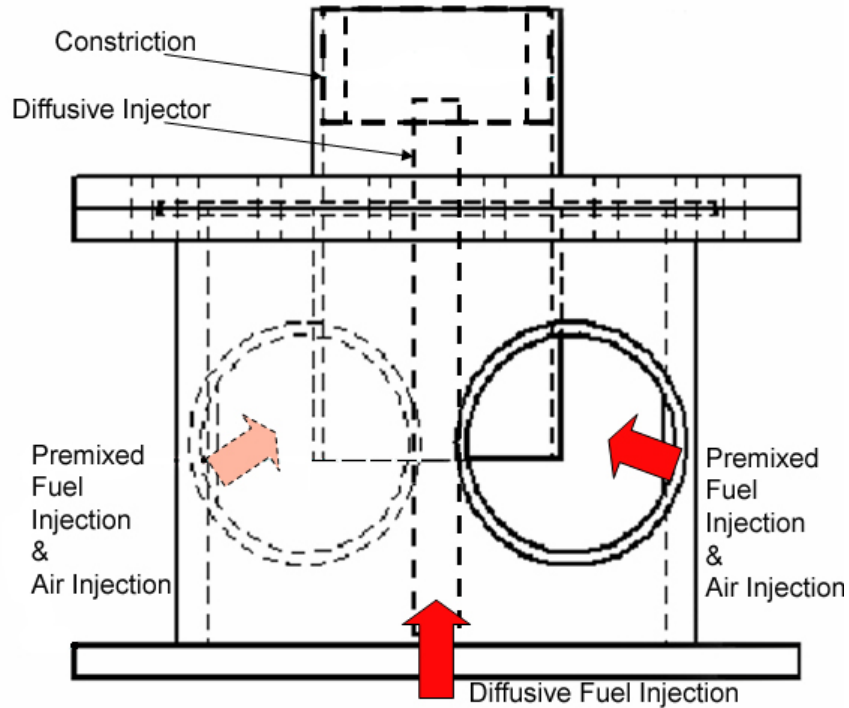


Figure 4.11: Diagram of rig and constrictions used (35 mm total length of the constriction)

The following simulations were carried out with natural gas to compare against experiments [13]. The experiments initially used premixed combustion for different cases as follows; corresponding CFD simulations were also performed:

- 1- **Tangential Swirl Burner with injector (premixed only without quarl)**
- 2- **Tangential Swirl Burner with injector (premixed only with quarl)**
- 3- **Tangential Swirl Burner without injector (premixed only with quarl)**
- 4- **Tangential Swirl Burner without injector (premixed only without quarl)**

Each case has been run under different values of equivalence ratio over different values of mass flowrate of air and fuel until the simulation reaches convergence. Judgements are then made as to when the simulation is predicting flashback and how that compares to the experiments.

According to the experiment and simulation, two types of flashback have been observed. With the first type, the flame retreated back along the injector (type 1: central flashback at higher swirl numbers). The other process was when the flame propagated back in the boundary layer of the burner exit (nozzle) due to low velocity of flow mixture and governed by the critical boundary velocity gradient (type 2: boundary layer flashback, occurs at lower swirl number $S \leq 1.2$).

Figure 4.12 shows a comparison of flashback occurrence with the fuel injector for premixed combustion [13]. Both the experiments and simulation have been carried out without the quarl. The graph shows fair agreement between experiment and numerical simulation. Flashback of type 1 has been observed during the simulations and the experiment.

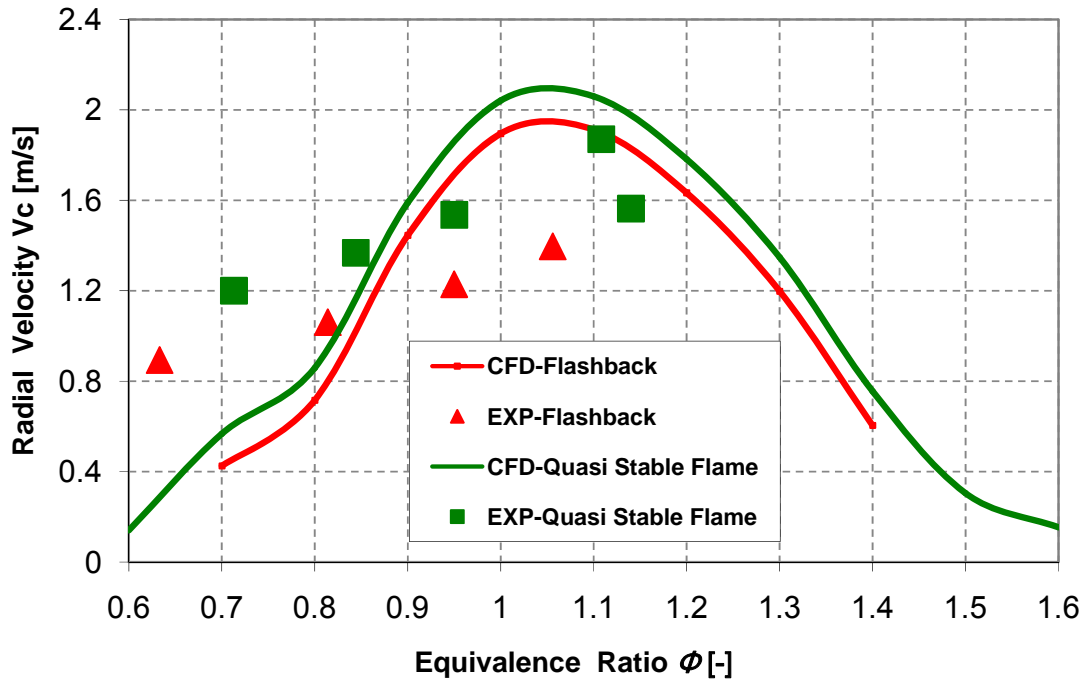


Figure 4.12: Comparison between experimental and CFD simulation for flashback and quasi stable regions in tangential swirl burner with injector (Premixed only without quarl) (Natural gas)

The next simulation added a quarl (Figure 4.13) to the burner exit in order to reduce the swirl number and follow industrial practice. The quarl nozzle has reduced the experimental occurrence of flashback.



Figure 4.13: The modification of the burner neck to reduce the flashback occurrence. Figure 4.14 shows a comparison between the experiment and simulation for the next case with the quarl nozzle. Agreement between the simulation and experiments are closer than for the previous figure without the quarl nozzle. There is a considerable reduction of the flashback region for both experiment and simulation as shown by Figure 4.15.

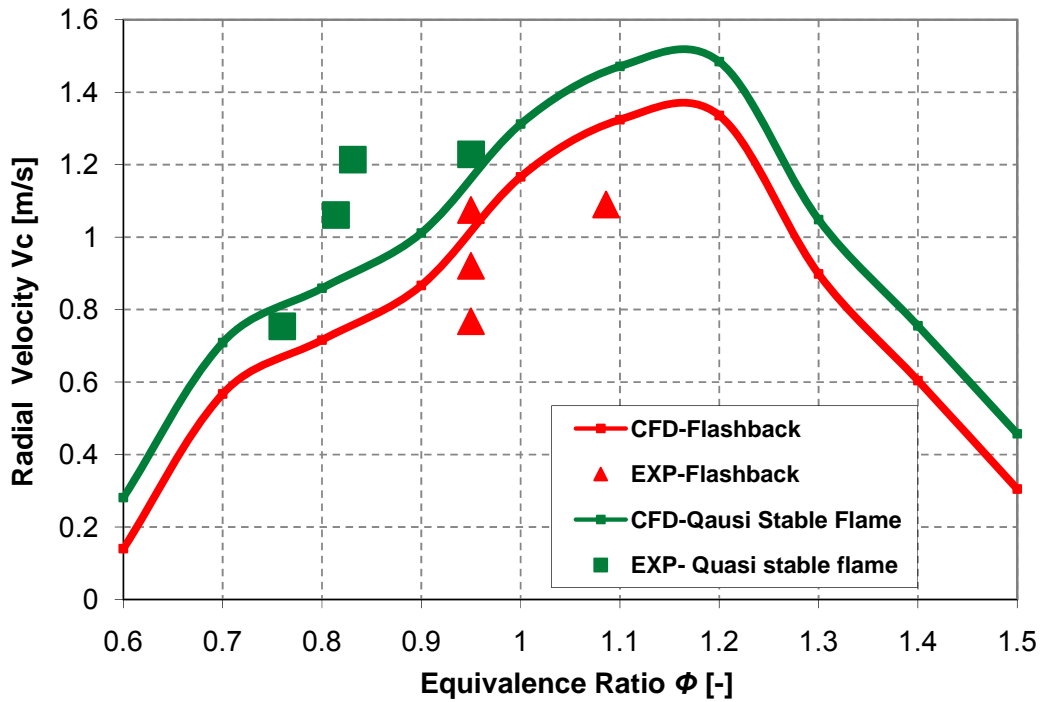


Figure 4.14: Comparison between experimental and CFD simulation for flashback and quasi stable regions in tangential swirl burner with injector (Premixed only with quarl)

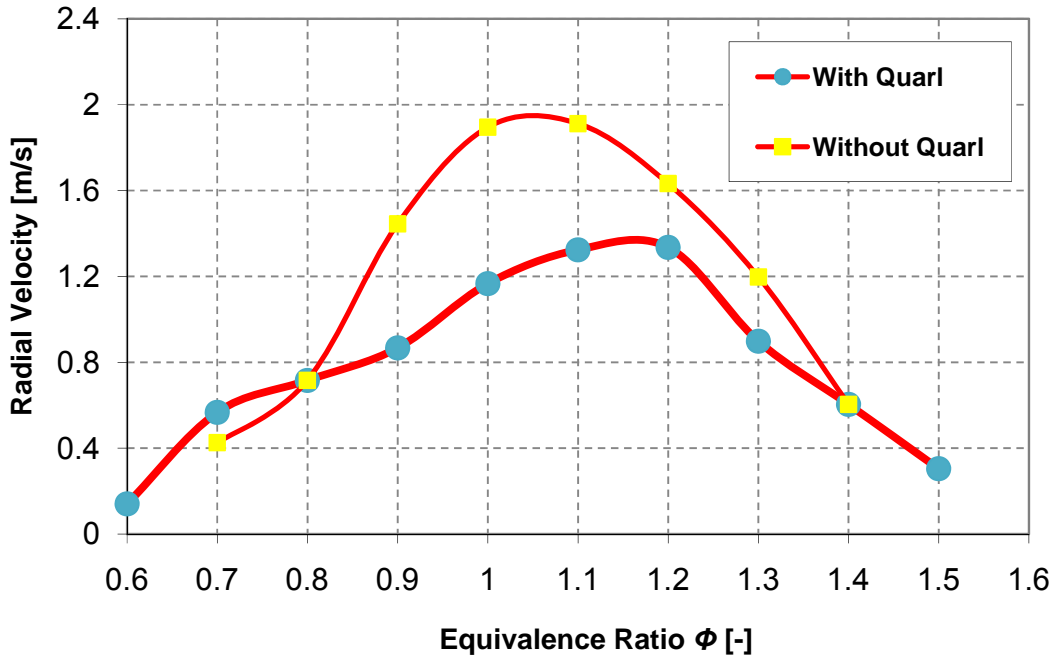


Figure 4.15: Comparison between CFD simulations for flashback map in tangential swirl burner with injector (premixed with quarl and without quarl)

Moving to premixed combustion without injector, simulations have given, in general, poor results. This can be seen clearly via the two cases that have been studied. Results for premixed combustion without injector and without quarl are shown in Figure 4.16.

Similar results were obtained with or without the use of a quarl exhaust, Figure 4.17. The reason for the poor simulations appears to be due to the presence of time dependent coherent structures when the central fuel injector is removed. The central fuel injector appears to suppress coherent structures such as vortex breakdown and the precessing vortex core (PVC).

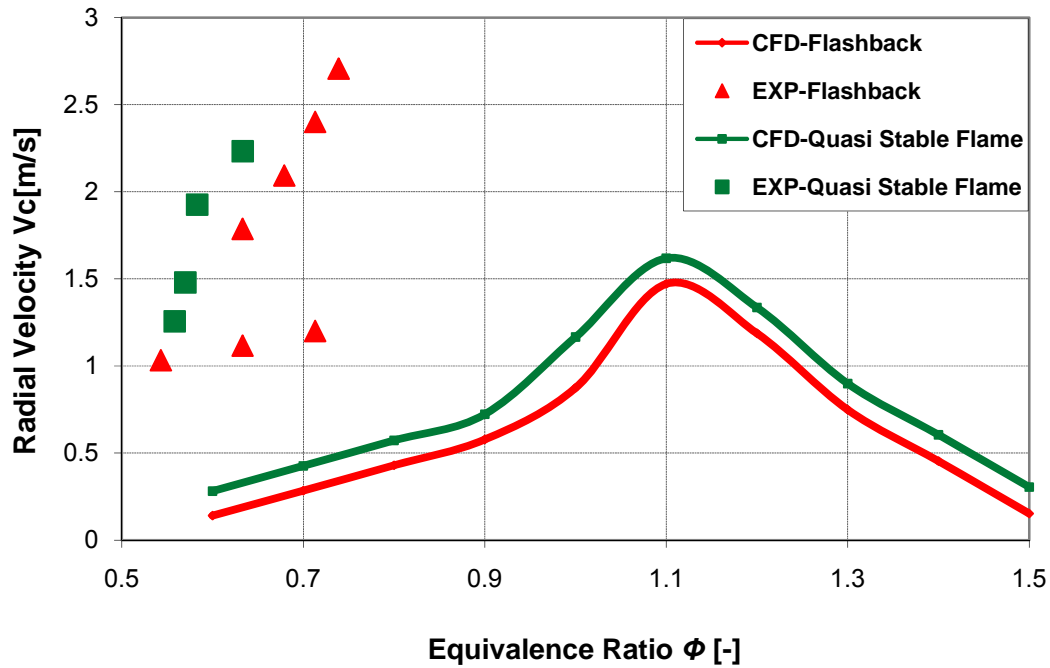


Figure 4.16: Comparison between experimental and CFD simulation for flashback and quasi stable flame regions in tangential swirl burner without injector (premixed flame with quarl)

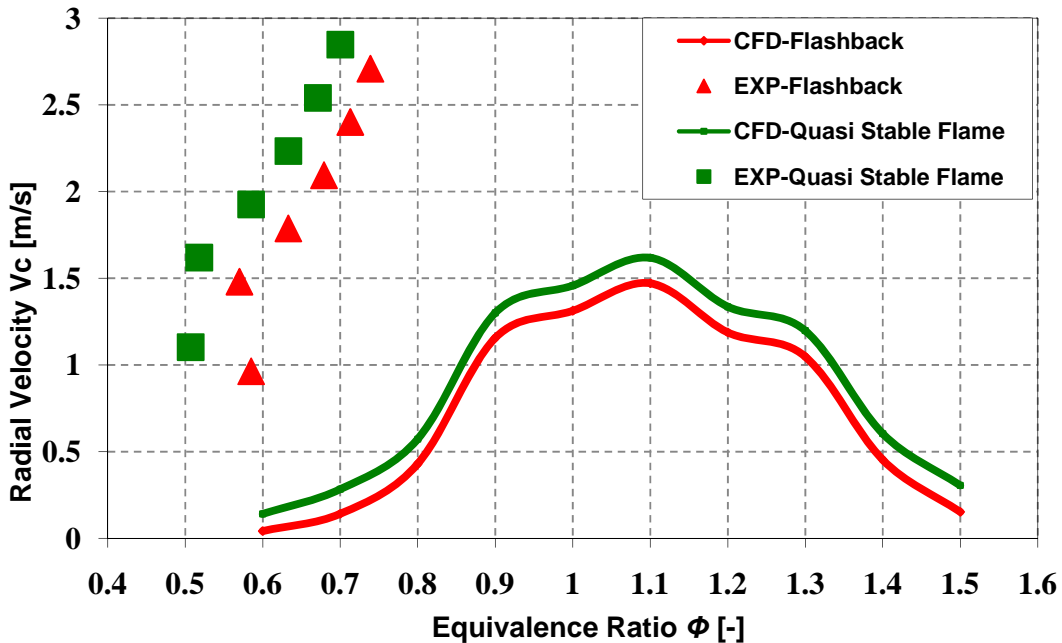


Figure 4.17: Comparison between experimental and CFD simulation for flashback and quasi stable regions in the tangential swirl burner without injector (premixed without quarl)

Figure 4.18 shows a typical example of flashback type 2 in the outer wall boundary layer with a stable annular kernel of a flame being located in the boundary layer of the exhaust nozzle just before flashback.

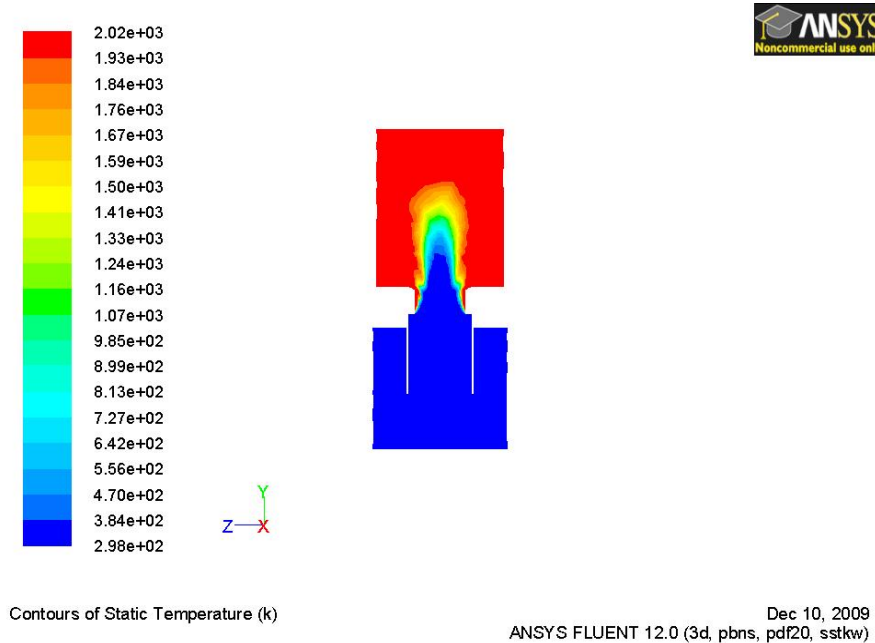


Figure 4.18: Temperature contours distribution illustrating location of annular flame front in the boundary layer just before flashback $Q_a=400\text{L}/\text{min}$ $\phi=0.9$.

Flashback analysis has been a subject of considerable interest especially before the widespread supply of natural gas superseded town gas, which typically had 20% or more hydrogen content, causing problems of ‘light back’ or flashback in the then existing burners, [45-46]. Lewis and von Elbe developed their well known Equation 2.8 for critical boundary velocity gradient for laminar Poiseuille flow in circular tubes and it was extensively used to characterize flashback, especially with ‘town gas’ containing significant proportions of hydrogen [45-47]. Equation 2.8 was derived by consideration of laminar pipe flow, but as admitted by Lewis and von Elbe [45-46], is often used in the turbulent flow regimes. This is of questionable validity but does give ready availability to a valuable databank for hydrogen based systems [45-46]. Some of the results are shown plotted with the standard Lewis and von Elbe definition of G_F Equation 2.8 in Figure 4.19. Here the differences between g_f , derived from CFD, must be emphasized. ‘ g_f ’ has been derived solely from CFD predictions of the boundary layers just upstream of the flame

fronts just before flashback and is typically of order 10 times higher than the Lewis and von Elbe G_F . This is discussed later.

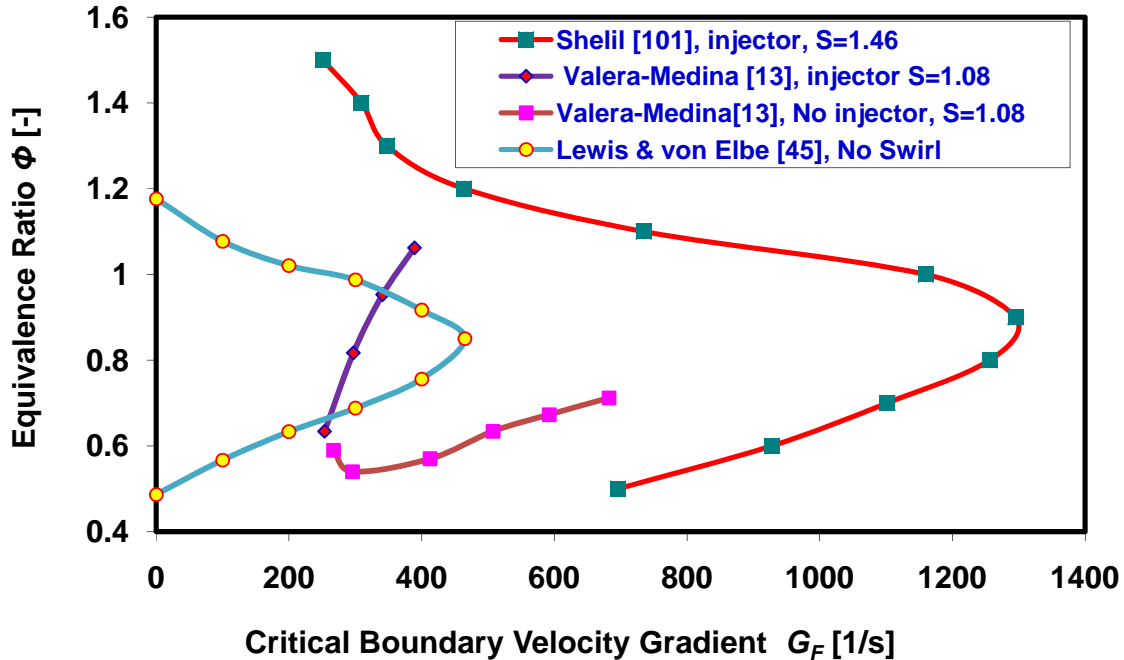


Figure 4.19: Variation of critical boundary velocity gradient, G_F , at flashback with % natural gas in air for laminar mixtures in comparison with swirl burners.

Figure 4.19 compares typical flashback results in terms of G_F for laminar flow in a 13mm diameter tube against the swirl burner of this paper (78 mm exit diameter, $S=1.08$) and also the smaller swirl burner of Shelil [101, 113], $S=1.47$ (see Chapter 5 for more details). With the injector the $S=1.08$ swirl burner system beneficially flashes back at lower values of G_F for values of ϕ between 0.6 and 0.9, presumably because of the much thinner boundary layers and hence higher real velocity gradients. Without the injector, values of G_F are always higher and reflect the worsened flashback behaviour. Shelil's results show the effect of higher swirl numbers and the consequent large tulip shaped CRZ which extends back over the fuel injector. These factors considerably worsened the occurrence of flashback for methane over all measured conditions.

The equations of Lewis and von Elbe [45] were modified by Wohl et al. [47] to account for turbulent flow in pipes, but the formulae are not easily extendable to swirling flow systems

as detailed knowledge of the flow field next to the boundary layer was required. As little experimental information is available in this region [35, 114], it was decided to use CFD to investigate the critical boundary velocity gradients, g_f , for comparison with those produced by the Lewis and von Elbe formula G_f . g_f was derived directly from the CFD prediction which were particularly focused on the boundary layer region. Boundary layer thickness could be readily measured and near wall velocity derived from the CFD to give values of real ' g_f '.

Some typical results are shown in Figures 4.20 and 4.21. This CFD analysis corresponds with the experimental one in Figures 4.22A and 4.22B [13], whilst the flame front corresponds with those shown in Figures 4.23A and 4.23G [13]. Comparing these flames with the temperature predictions shows considerable similarities (Figures 4.20A, 4.20B and 4.21A, 4.21B). This is especially striking with the fuel injector present where the two flame fronts can be seen both in the photo and predictions.

The axial velocities, Figure 4.20C, show that no CRZ exists without the injector when flashback starts. This seems to be a point of transition after the CRZ has disappeared and before any vortex breakdown occurs, a point for future investigation. The flame can be seen to be extending down the nozzle in a thin annular boundary layer, Figure 4.20A. Figure 4.20D shows the total velocity profile across the burner exit just below the flame front and allows derivation of a value of ' g_f ' of $2,900\text{s}^{-1}$ in the outer laminar sub-layer next to the wall. The total velocity has been used for analysis as high speed camera results [13] indicated that flashback was occurring via flame propagation in a spiral shape, indicating that all velocity components were important.

The axial velocities with the injector, Figure 4.21C, show that the central core flame is retained at the tip of the injector by a small bluff body CRZ, the main CRZ developing downstream of the nozzle. In the burner exit throat the burning gases accelerate the flow creating a region of high velocity flow that affect the outer flow region and especially the boundary layer, Figure 4.21D. Here maximum velocities are 7m/s as opposed to 5m/s without the injector. As a consequence ' g_f ' in the outer laminar sub layer becomes $5,200\text{s}^{-1}$ and the reason for the better flashback resistance for the cases with the fuel injector becomes apparent, Figure 4.22.

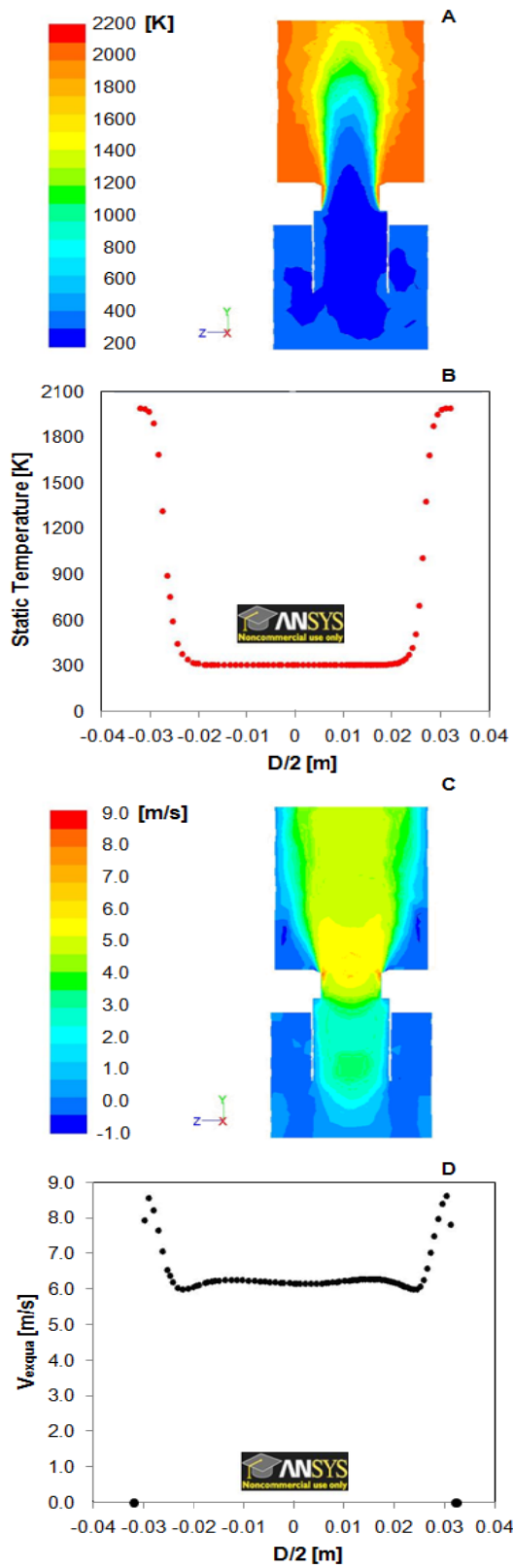


Figure 4.20

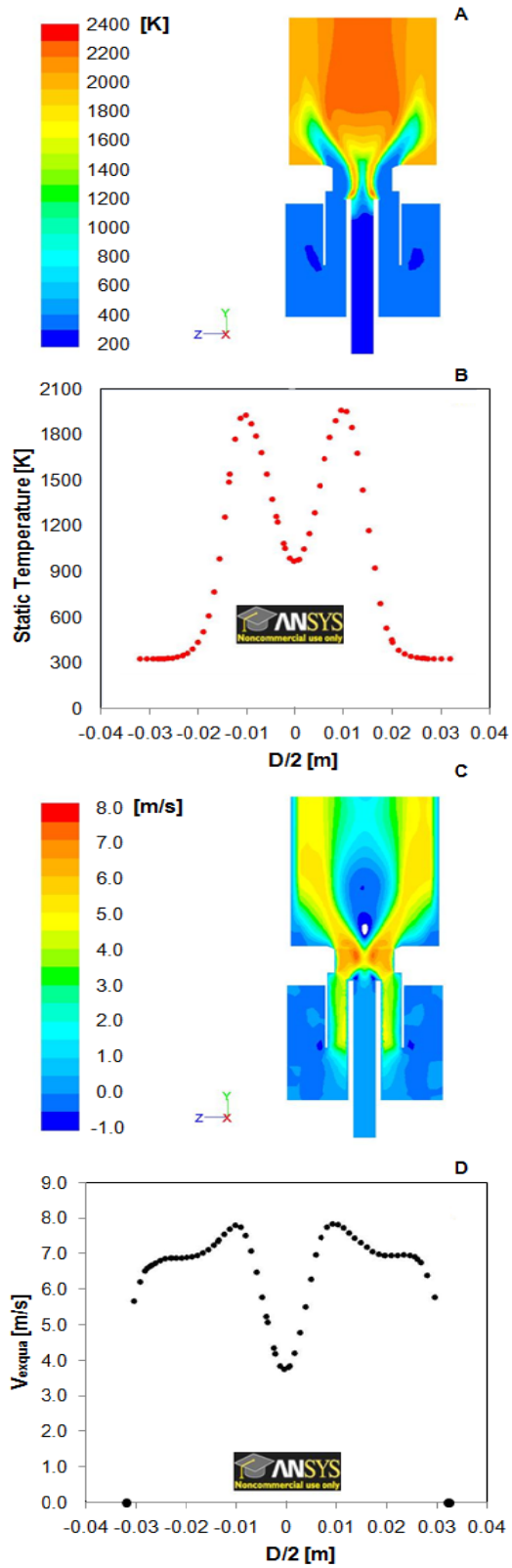


Figure 4.21

Figure 4.20: CFD prediction for swirl burner, $S=0.86$, of A) Temperature contours, B) Temperature profiles just ahead of the flame front C) Axial velocity contours, D) Exit throat total velocity distribution. Critical boundary layer velocity gradient, g_f , from c) is $2,900s^{-1}$, air flowrate 700 l/min, {0-67} l/min fuel, $\phi =0.9$, just before flashback

Figure 4.21: CFD prediction for swirl burner, $S=0.86$, with fuel injector of A) Temperature contours, B) Temperature profiles just ahead of the flame front, C) Axial velocity contours, D) Exit throat total velocity distribution. Critical boundary layer velocity gradient, g_f , from c) is $5,200s^{-1}$, air flowrate 700 l/min, {25-40} l/min fuel, $\phi =0.9$, just before flashback

Careful examination of the CFD results indicates that the fuel injector is slightly thinning the wall boundary layer and hence increasing g_f . Typically without the fuel injector, the boundary layer occupies up to $\sim 18\%$ of radius, slightly reducing to 15% with the injector, although the main effect is due to the higher near wall velocities with the injector, compare Figure 4.20D and 4.21D.

The CFD data has been gathered together with the curves of Figures 4.22A and 4.22B as well as other data [13] to derive more realistic critical boundary velocity gradients over a range of equivalence ratios.

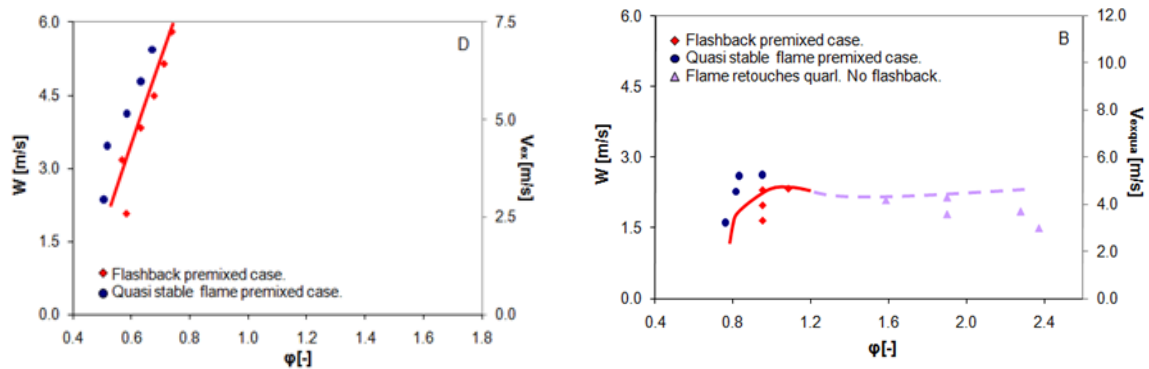


Figure 4.22: Flashback result without (A) and with (B) (fuel injector and confinement)

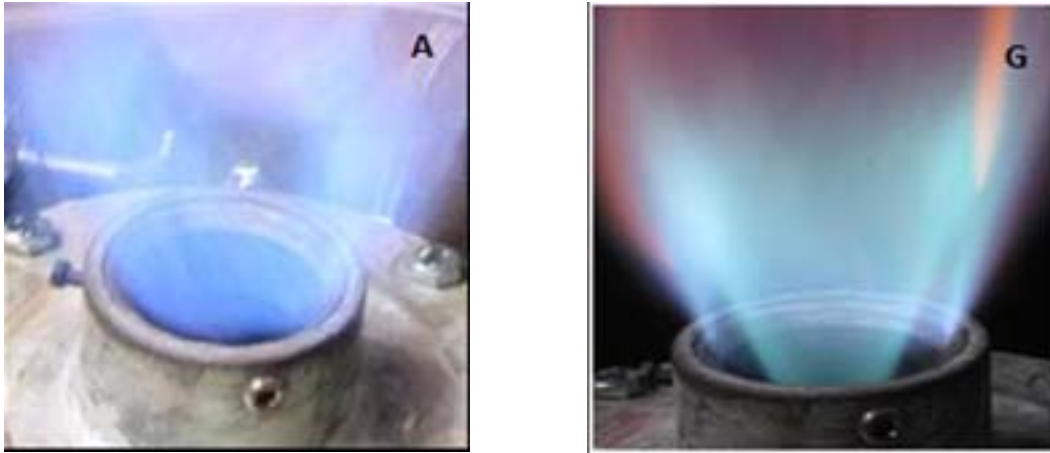


Figure 4.23: Flame images. A) No injector with nozzle, 700 l/min air, $\phi = 0.54$, G) with injector and nozzle, $\phi = 0.95$, $S=0.86$

The CFD simulation has been run as described earlier and a complete flashback loop derived, Figure 4.24,; for the case $S=0.86$; nozzle fitted and no injector. Available experimental data has been compared with CFD simulations at the same air and fuel flowrates with flames which CFD indicates are stabilized downstream, thus allowing values of g_f to be derived from the CFD predictions in the burner exit. The CFD results for a given equivalence ratio predict flashback occurrence at much lower exit velocities than found experimentally with correspondingly lower values of g_f . Figure 4.25 shows results as Figure 4.24 but with the fuel injector.

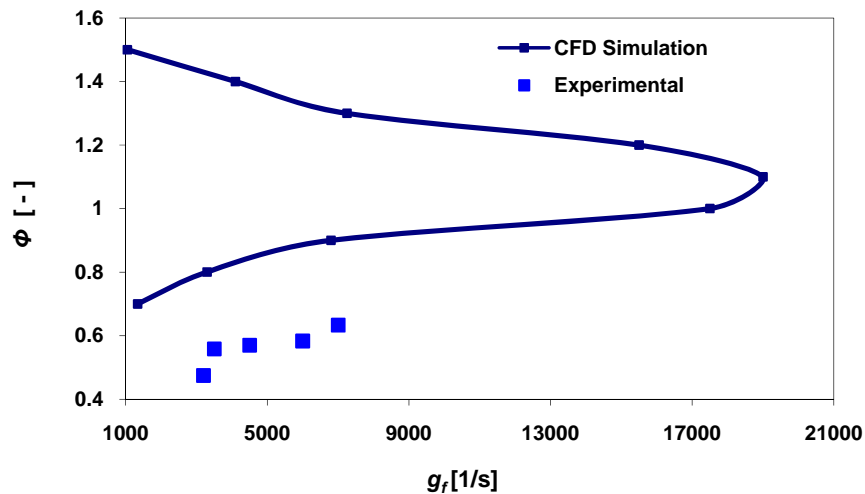


Figure 4.24: Variation of critical boundary velocity gradient, g_f , with equivalence ratio without injector and with nozzle, $S=0.86$.

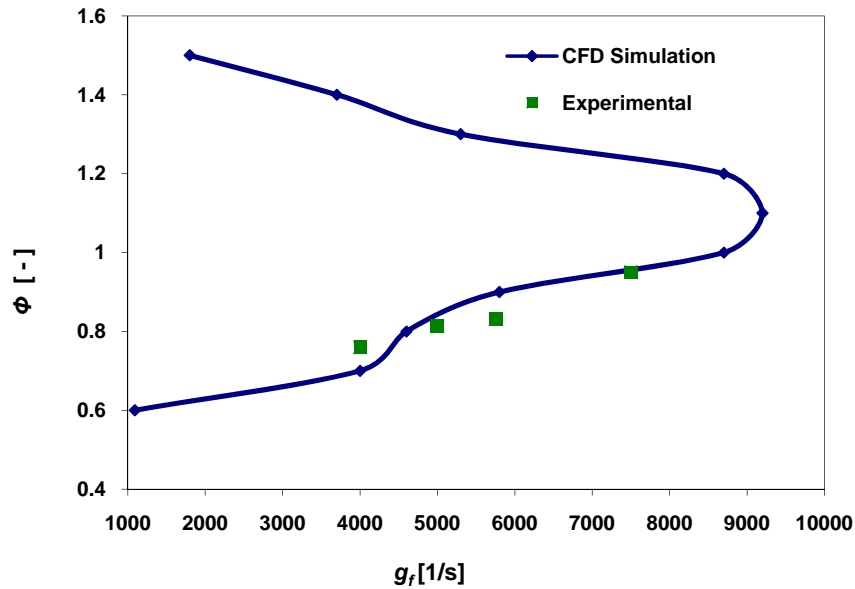


Figure 4.25: Variation of critical boundary velocity gradient, g_f , with equivalence ratio with fuel injector and nozzle, $S=0.86$.

Here the experimental and CFD results match well. The reasons for this lies in the use of the central fuel injector which occupies 46% of the exit diameter and interferes/prevents the formation of coherent structures in this area which can cause considerable regular time dependant motion [17, 35, 47], thus making the predictions better able to represent the real system. The reasons for the poorer predictions of Figure 4.21 without the injector are not clear, but the combustion, turbulence models and possible time dependence effects need to be investigated further. In terms of absolute values of g_f , they range from 3000 to 7000 for $0.475 < \phi < 0.633$ for the case without the injector, Figure 4.24, and from 4000 to 7500 for $0.76 < \phi < 0.95$ with the injector, Figure 4.25. Although the experimental data for the 2 cases cover different equivalence ratio ranges, it can be seen that for a given equivalence ratio values of g_f are significantly lower with the injector showing much better flashback resistance. Similarly Figure 4.24 and 4.25 show for the same air flowrate that the injector allows operation at a higher value of ϕ (for $\phi < 1.1$) before flashback occurs.

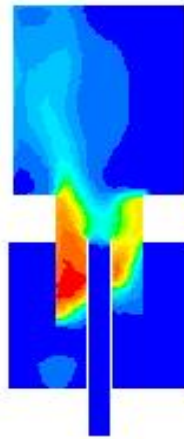
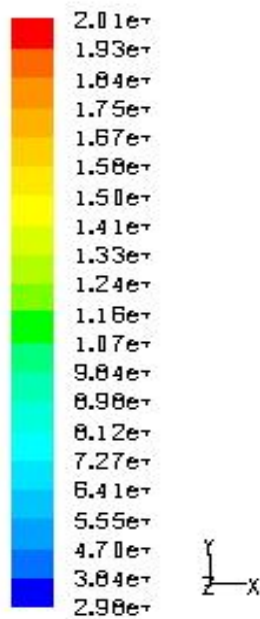
These results need further experimental validation, but nevertheless show that new methodologies need to be developed to characterize the critical boundary velocity gradient when flashback occurs.

4.4.2.3 Partially Premixed combustion (Diffused & premixed)

Partially premixed combustion systems are premixed flames with some diffused fuel. Such flames include premixed jets discharging into quiescent atmospheres, lean premixed combustors with diffusion pilot flames and/or cooling air jets, and imperfectly mixed inlets. The partially premixed model is a simple combination of non-premixed model and premixed model.

Partially premixed flames exhibit the properties of both premixed and diffusion flames. They occur when an additional oxidizer or fuel stream enters a premixed system, or when a diffusion flame becomes lifted off the burner so that some premixing takes place prior to combustion.

Whenever there is premixed combustion there is possibility of flashback occurrence; Figure 4.26 illustrates this with two examples. Figure 4.27 shows a typical example of a stable flame whilst in the case of high flowrate the flame tends to blowoff as shown in Figure 4.28.



Contours of Static Temperature (k)

Mar 01, 2009
FLUENT 6.3 (3d, pbns, pdf20, skw)

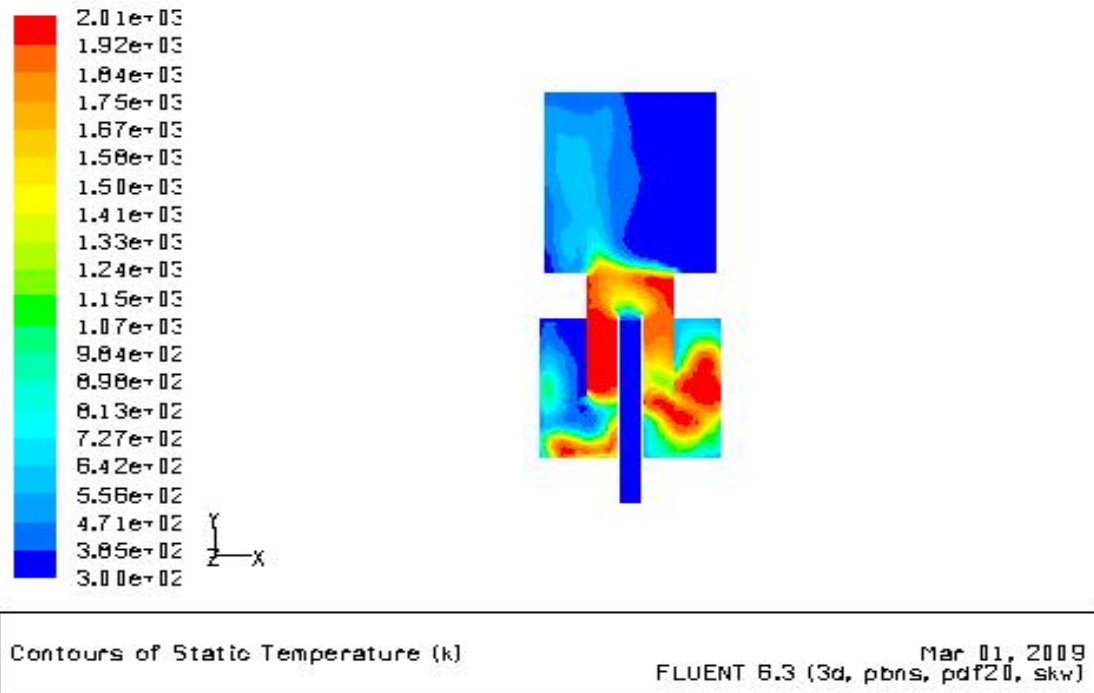


Figure 4.26: Flashback Phenomena appearance with partial premixing ($Q_a=600\text{L/m}$
 $Q_{fp}=40\text{L/m}$ $Q_{fd}=25\text{L/m}$ $\phi_p=1.1467$)

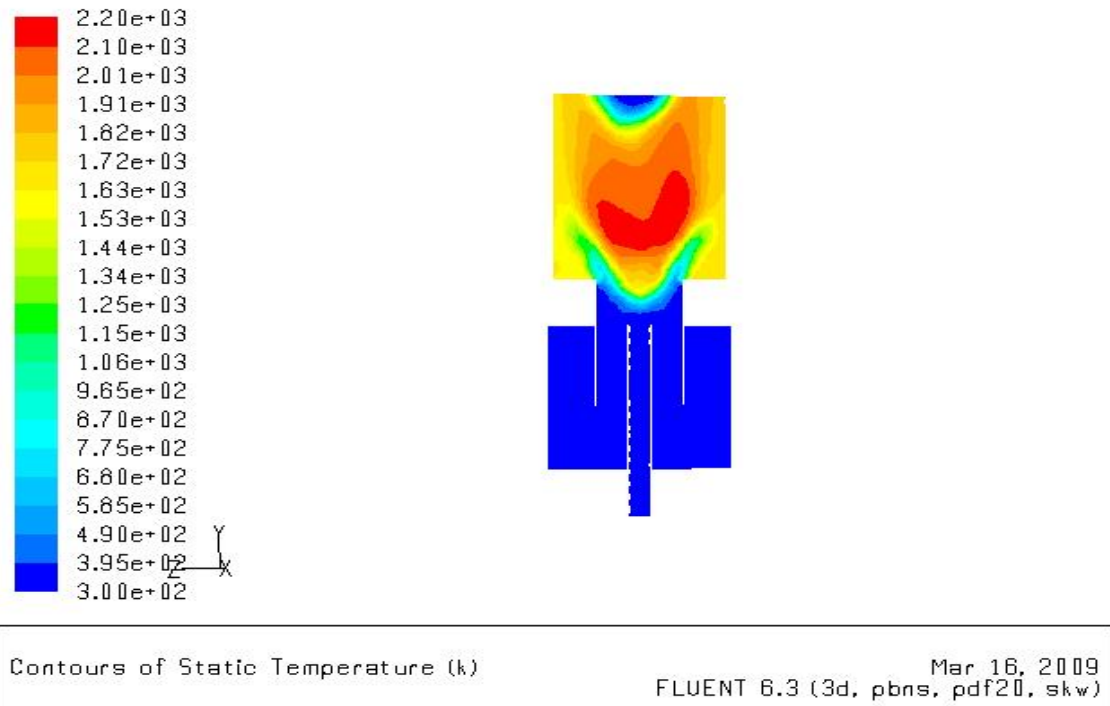


Figure 4.27: Stable swirling combustion, partially premixing
 $Q_a=800\text{L/m}$ $Q_{fp}=40\text{L/m}$ $Q_{fd}=25\text{L/m}$ $\phi_p=0.86$

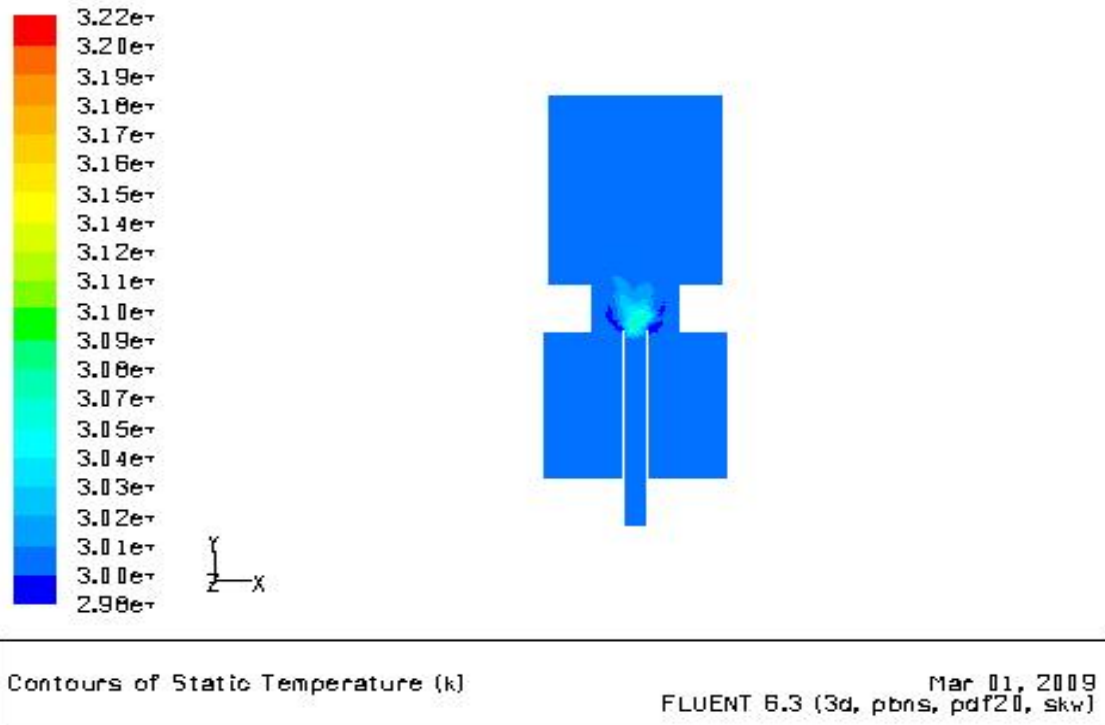


Figure 4.28: Near blowoff conditions with partial premixing

$$Q_a=1600\text{L/m } Q_{fp}=40\text{L/m } Q_{fd}=25\text{L/m } \phi_p=0.43$$

Other work with premixed methane air flames at a swirl number of 1.47 has shown that a central recirculation zone (CRZ) develops a tulip shape whose neck extends back over the central fuel injector. As the flame then stabilizes on the boundary of the CRZ, the flame propagates to the burner backplate. Subsequently, the annular flames in the swirl chamber can flashback radially to the inlets[101, 113]. Similar behaviour has been observed with partially premixed natural gas flames in swirl burners [13, 110].

Under some conditions, it was found that the system developed an asymmetric combustion process extending into the burner; eventually this will lead to flashback in the whole system as shown in Figure 4.29. This simulates what happens in practice as the combustion process in the model converges to solution where combustion finally stabilizes in the upstream mixing chamber, although it is recognized that the CFD model is not time dependant.

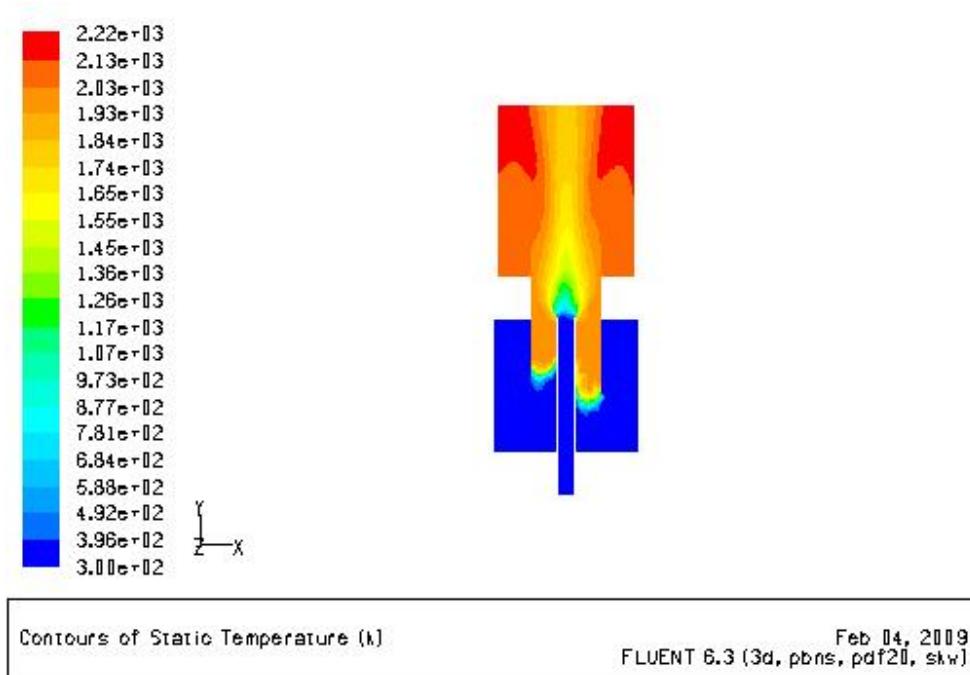
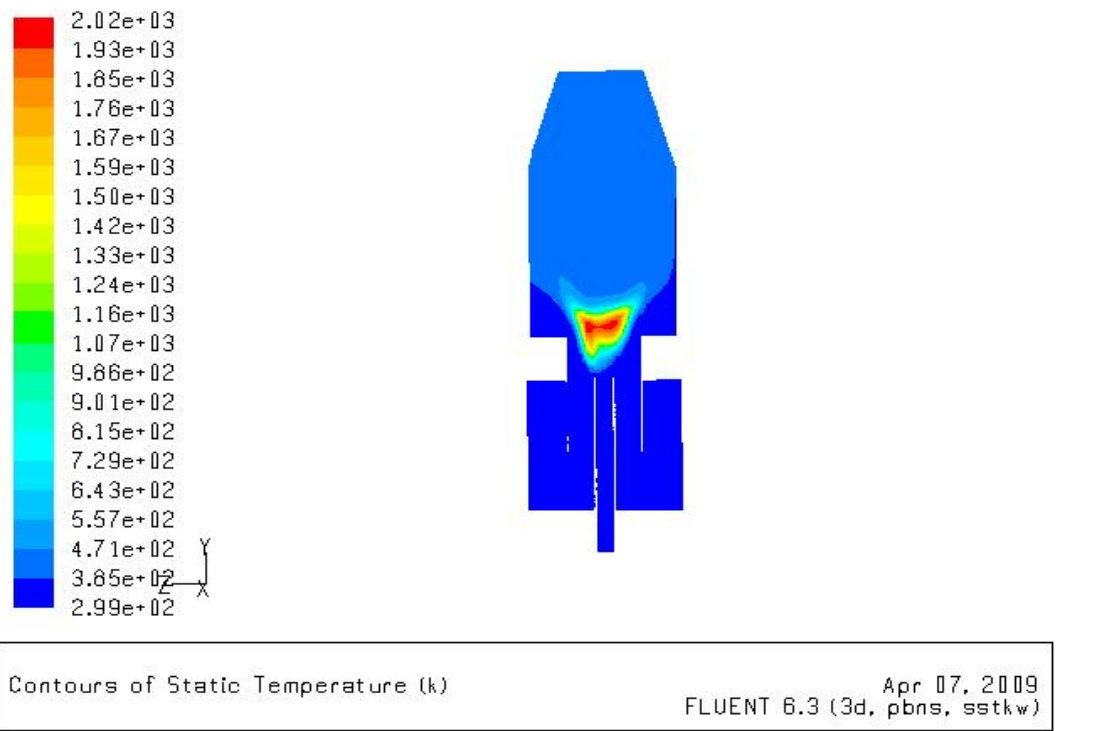
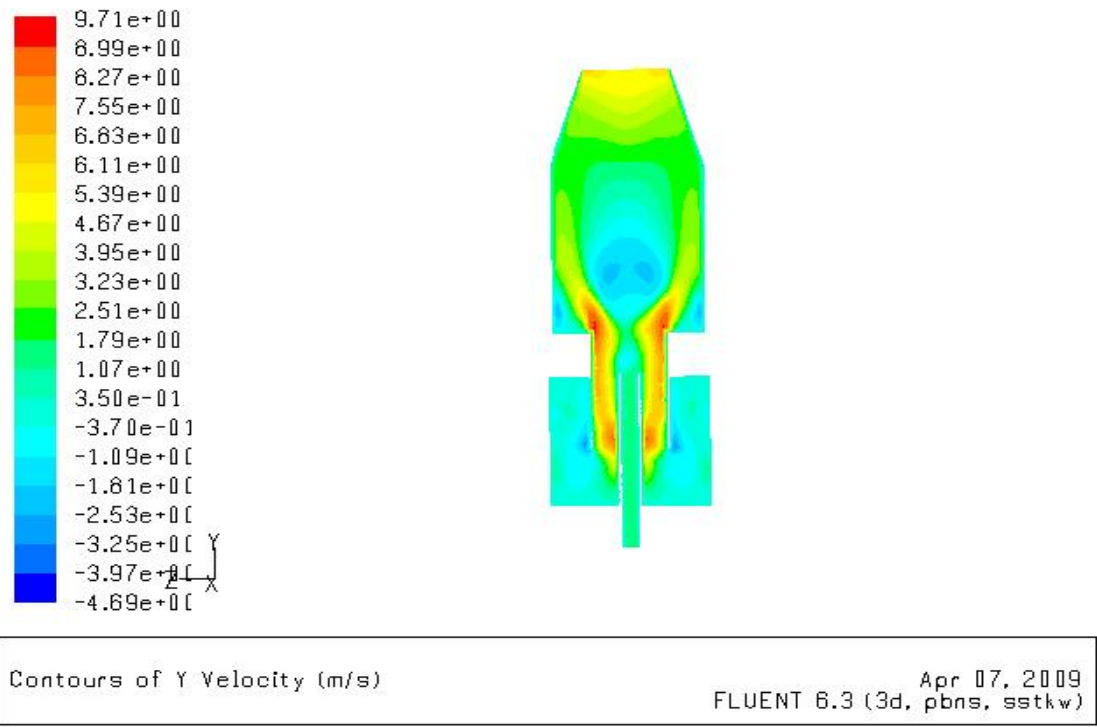


Figure 4.29: Temperature contours illustrate irregular flame propagation into the mixing zone of the swirl burner causing flashback in a partially premixed case, also observed experimentally

This was observed during the experimental trials.

Finally, the Figures 4.30 show the velocity and temperature maps respectively for case of a conical exhaust cup fitted over the end of the confinement; this is the configuration of Figure 4.5B.



**Figure 4.30: Conical cup with confinement, Air=1600L/min, Diffusion fuel 25L/min, Premixed=40L/min $\phi_p = 0.43$, $\phi_{total} = 0.69875$, fuel methane
Top diagram axial velocities, lower temperatures**

This model appears to predict flashback quite well when the fuel injector is present, not so when it is absent. Clearly more experimental work is needed to extend the flashback experimental results with the injector to cover the full range of very rich to very lean equivalence ratios. Without the injector fundamental examination of the modelling process is needed to try to elucidate the reasons for the differences between the modelling and the experimental results. It may well be that use of Reynolds Stress turbulence or LES model is needed, although there are very serious problems of convergence, large under relaxation factors are needed as well as possibly improved grid resolution and changes to the combustion model.

4.5 Summary

This chapter has focussed on the CFD Analysis of a 100 kW Tangential swirl Combustor using experimental measurements from a previous PhD student. The analysis has focused on the following points with the stated deductions:

- Simulation of non-premixed, premixed and partially premixed combustion.
- Simulation of the rig with cylindrical and conical cup exhausts confinements with a swirl number around one.
- Comparison of the simulation flashback results with the experimental result shows that CFD can give useful results when there is a fuel injector present.
- Non-premixed combustion gives the most stable simulation solution, being the easiest to converge.
- Premixed combustion and partially premixed combustion cause flashback problem which ideally need to be simulated to enable their occurrence to be avoided.
- Flashback along boundary layer of the burner exit has been described using a critical velocity gradient approach.
- Conditions close to blowoff have also been simulated.

Part II

Experimental

Analysis

Chapter Five

PROTOTYPE

GENERIC

SWIRL

BURNER

CHAPTER FIVE

PROTOTYPE GENERIC SWIRL COMBUSTOR

“The important thing is not to stop questioning. Curiosity has its own reason for existing. One cannot help but be in awe when he contemplates the mysteries of eternity, of life, of the marvellous structure of reality. It is enough if one tries merely to comprehend a little of this mystery every day. Never lose a holy curiosity.”

Albert Einstein

5.1 Introduction

Swirl combustors are a well-known technology [23], their main attribute being the generation of aerodynamically stabilized central recirculation and reverse zones, which recycle hot chemically active reactants to the flame root, producing excellent flame stability and wide blowoff limits [17]. The tangential swirl combustor has been analysed numerically in the preceding chapter, Chapter 4, and compared with the experimental analyses [13]: it was constructed to investigate the tangential swirl burner characteristics. When hydrogen related fuels and mixes are considered the existing prototype was too large and would have consumed too much expensive fuel, which had to be supplied in bottles under pressure. Thus a smaller (28 mm exhaust diameter as opposed to 78 mm with the earlier unit) generic swirl burner was designed and manufactured to meet the operational design requirements. The new design was broadly based upon the preceding one, but with modifications to allow it to be fitted in the future to the Cardiff University GTRC pressurized rig. The following section describes this unit.

5.2 Basic Generic Swirl Burner Designs

The generic swirl burner was used to examine flame stability limits at atmospheric conditions (1 bar, 293 K) at Cardiff University’s Gas Turbine Research Centre (GTRC). A single tangential inlet feeds an outer plenum chamber which uniformly distributes premixed air/fuel to the insert and slot type radial tangential inlets, then into the burner body and

finally the burner exhaust, where the all important flame stabilizing central recirculation zone forms. The central fuel injector (not used for fuel injection here) extends through the whole body of the plenum and swirl burner body to the exhaust. Figure 5.1 shows a photo of the burner components and Figure 5.2 shows the assembled burner. In sequence, Figure 5.3 and Figure 5.4 show the swirl burner section drawings and the swirl burner dimensions.

Air and fuel mass flow rate are measured simultaneously using suitably ranged Coriolis flow meters, which have an accuracy of $\pm 0.35\%$ for mass flow rate measurement [115]. Equivalence ratio calculation based on mass flow rates gave errors of $\pm 0.48\%$. The complete arrangement of the atmospheric experimental rig is shown by the photo in Figure 5.5 [42-43, 116-117].

The burner is designed to produce premixed, non-premixed and partially premixed flames. It is able to handle different types of fuels. In this research, only premixed combustion is considered to examine flashback and blowoff characteristics with a variety of different fuels.

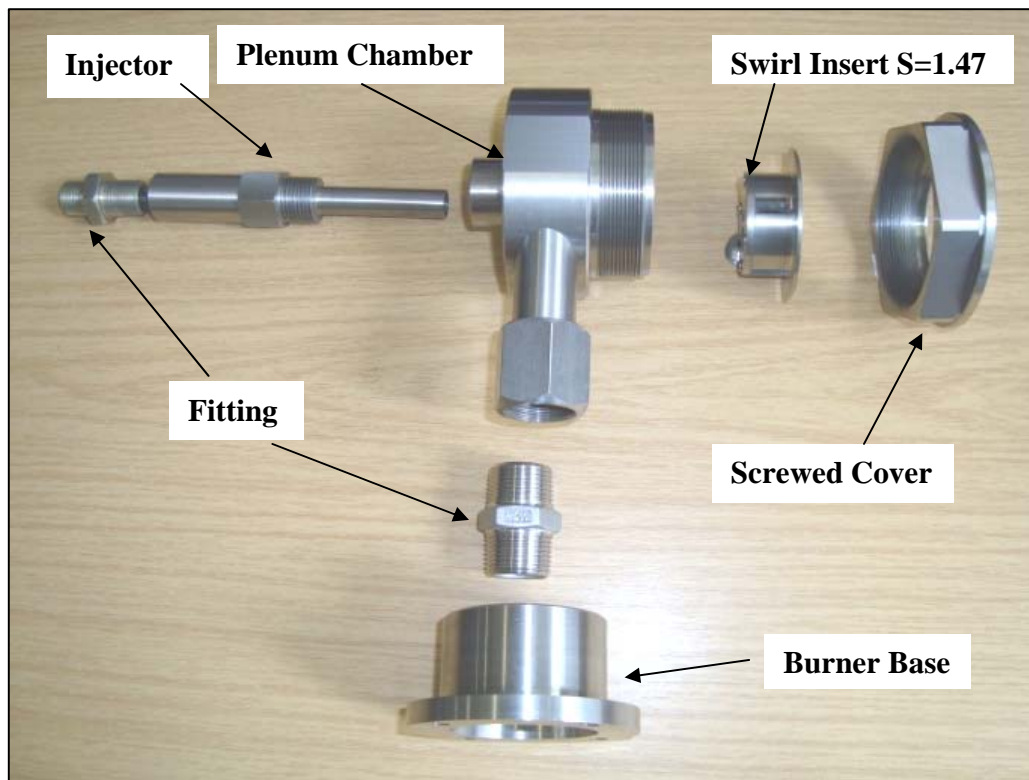


Figure 5.1: The actual swirl burner, all parts



Figure 5.2: The assembled swirl burner $S=1.47$

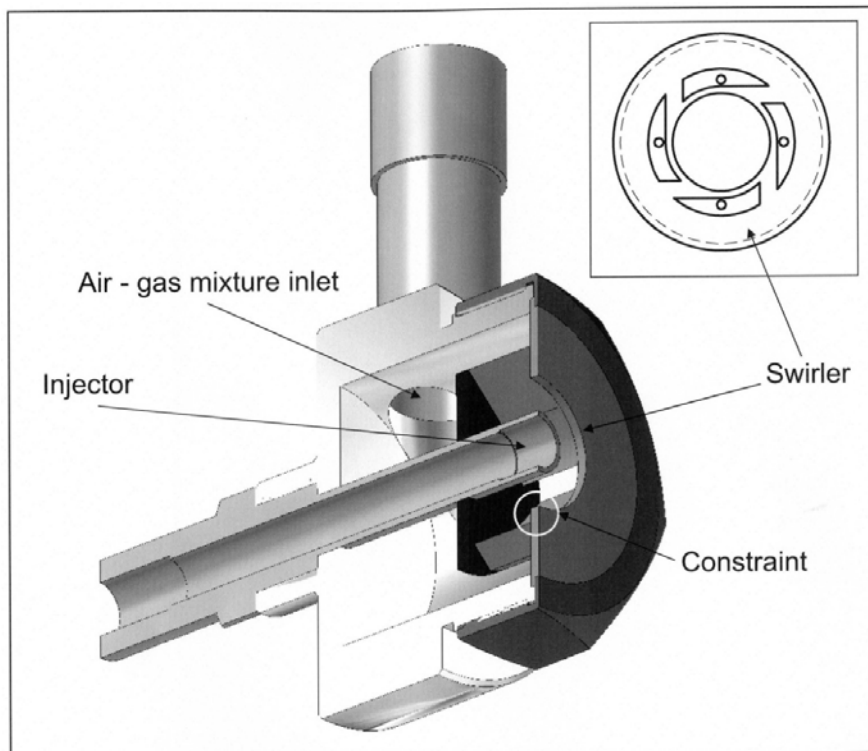


Figure 5.3: Generic swirl burner diagram

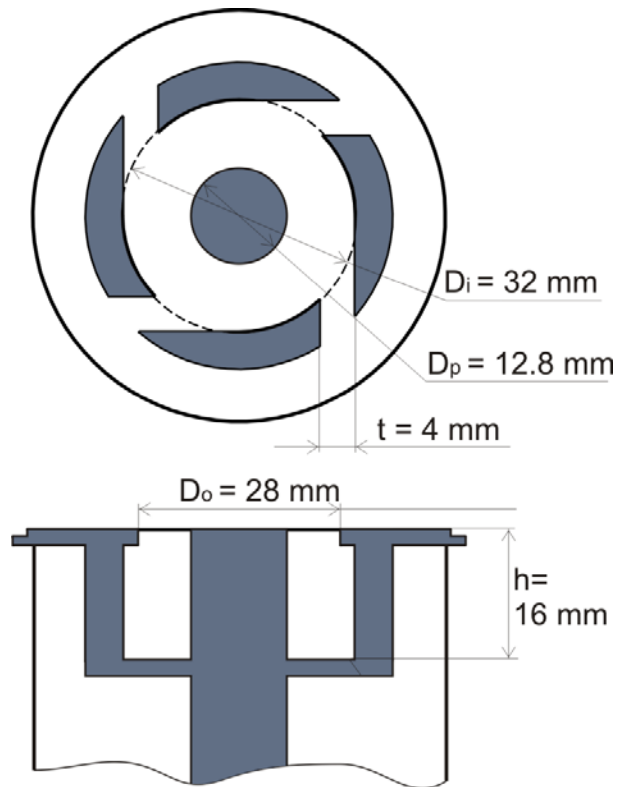


Figure 5.4: Swirl burner dimensions

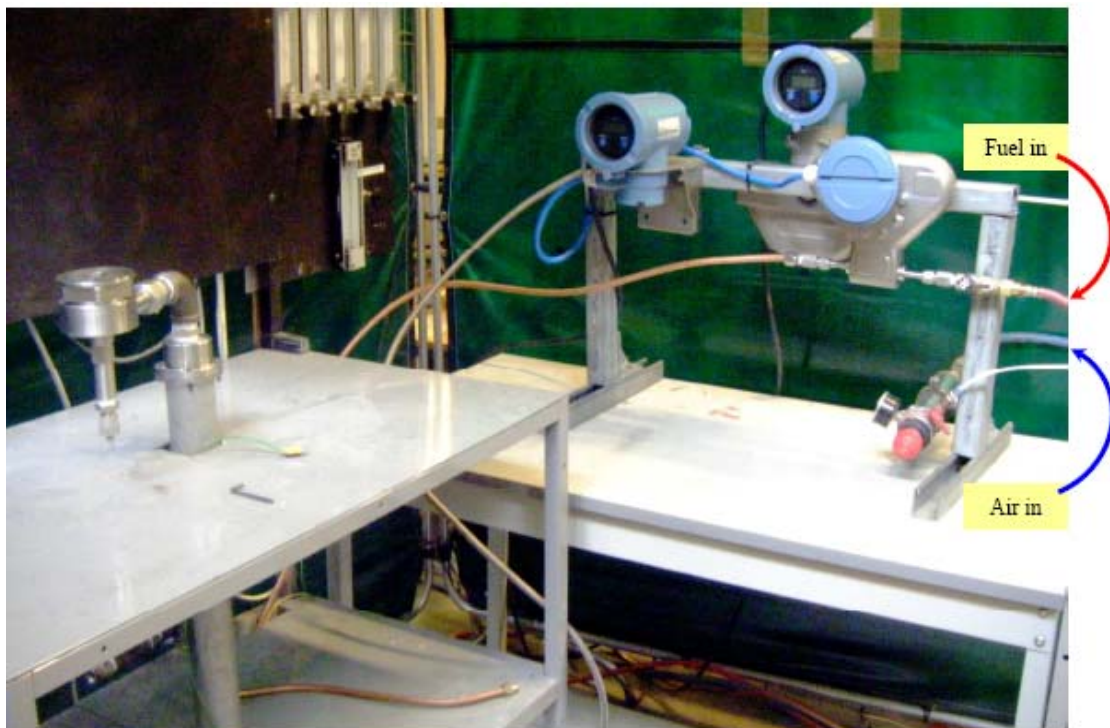


Figure 5.5: Experimental setup

5.3 Design Evolution of the Generic Swirl Burner

The above swirl burner design has been improved many times during the research process. These improvements can be summarised as follows.

- I. The initial burner had a swirl number of $S=1.47$ without an exhaust nozzle (just a short orifice). It is shown assembled above in Figure 5.2. The swirl number was varied by altering the area and number of the radial tangential inlets, which are shown in Figure 5.6.



Figure 5.6: Swirl insert for $S=1.47$

The $S=1.47$ swirl insert consists of four tangential inlets fed from the main plenum chamber. This piece can be easily removed and swapped for another insert with a different swirl number.

The factor used to measure the degree of swirl generation is the swirl number (S), which has been defined comprehensively in Chapter 2. The swirl number is one of the main parameters used to characterize swirl flow. The flow inside the swirl burner is complex and this complexity makes Equation 2.9 difficult to apply. The geometrical swirl number has been used as an approximation to the swirl number of equation 2.9 with awareness of the following assumptions.

1. Isothermal conditions

2. Assumptions of a uniform axial velocity profile in the exhaust
3. All the angular momentum of the flow entering the outer swirl chamber is fully transmitted to the flow in the outer swirl chamber and there are correspondingly minimum frictional or similar losses

This leads to the following equations for the swirl number of the unit shown in Figure 5.7 below.

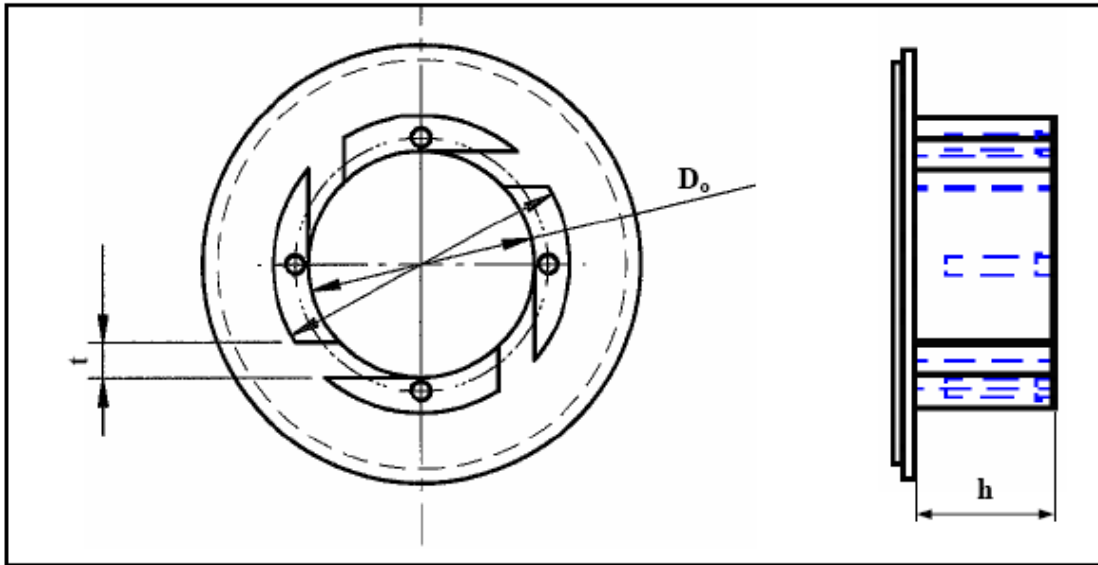


Figure 5.7: Blade swirler burner configuration

$$S_g = \frac{G_\theta}{G_x d/2} = \frac{\dot{m}_i w_i r_{eff}}{\dot{m}_o u_o r_o}$$

$$\dot{m}_i = \dot{m}_o$$

$$\therefore S_g = \frac{w_i r_{eff}}{u_o r_o}$$

$$= \frac{\left(\frac{Q}{A_i}\right) r_{eff}}{\left(\frac{Q}{A_o}\right) r_o}$$

$$\begin{aligned}
&= \frac{A_o r_{eff}}{A_i r_o} \\
A_o &= \pi(r_o^2 - r_p^2) \\
A_i &= 4. t. h \\
r_{eff} &= \left(r_i - \frac{t}{2}\right) \\
\therefore S_g &= \frac{\pi(r_o^2 - r_p^2) \left(r_i - \frac{t}{2}\right)}{(4. t. h) r_o} \tag{5.1}
\end{aligned}$$

Where,

r_o is the radius of the swirl burner at the exit (diameter D_o),

r_i is the radius of the swirl burner at the inlet (in this case $r_o = r_i$)(diameter D_i),

r_p is the radius of the internal pipe (injector outside radius) (diameter D_p),

t is the flow passage width between the blades and,

h is the height of flow passage

According to Equation 5.1 the geometrical swirl number of the initial design gives a swirl number of 1.47.

However, there are three types of velocity that can be recognized in the swirl burner. These velocities are axial velocity, radial velocity and tangential velocity. The velocity vectors are presented in the schematic burner drawing, Figure 5.8. Based on the experimental data, u , v and w were calculated from the known mass flow rate and gas mixture density. Axial, radial and tangential velocities in the inlets are presented in the following three equations:

$$u = \frac{\dot{m}}{\pi. \rho. (r_o^2 - r_i^2)} \tag{5.2}$$

$$v = \frac{\dot{m}}{\pi. \rho. h. (r_p + r_i)} \tag{5.3}$$

$$w = \frac{\dot{m}}{4. \rho. h. t} \tag{5.4}$$

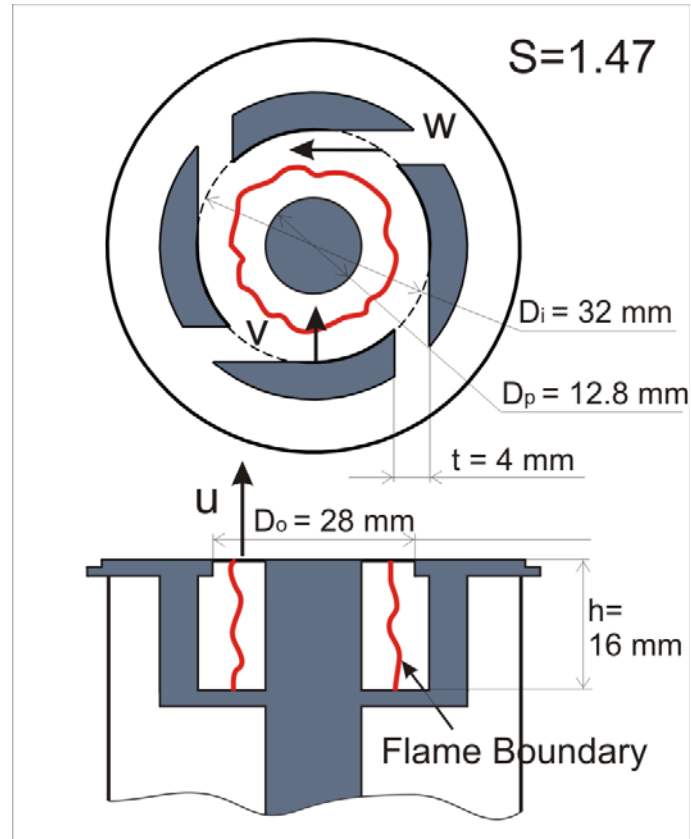


Figure 5.8: Schematic diagram of generic swirl burner with location of flame front

- II. The first enhancement to this design has been made by changing the swirl number from 1.47 to $S=1.04$. The new swirl insert has three main differences from the original design. The first difference is an increase in the number of swirl tangential inlets from 4 to 9, which delivers a mean increase in the premixed mixture (fuel/air) mass flow through the burner. Secondly, there was a reduction in the height of the swirl inset from 16 mm to 13 mm, which increased the volume of the mixing chamber prior to the combustion zone. Eventually, based on other work [43, 117], an exhaust nozzle extension $0.5D_o$ long was added with a tapering ‘Quarl’ end, Figure 5.9. The assembled burner is as shown in Figure 5.10. These changes lead to a reduction in the swirl number from 1.47 to 1.04. This improved the flashback limits, as will be shown in the following chapters.



Figure 5.9: Swirl insert S=1.04



Figure 5.10: The assembled swirl burner S=1.04

- III. The third change has been accomplished by a small change in the swirl insert, as shown in Figure 5.9. The swirl insert blades were made even smaller to increase the

tangential inlet area. The swirl number was reduced from 1.04 to 0.8 and lead to a significant improvement in the blowoff limits as discussed later.

- IV. The next design modification was to remove the tapered end ring and directly fit an open cylindrical exhaust confinement as shown in Figure 5.11[118]. The diameter of cylindrical confinement was equal to the diameter of the mixing chamber and doubles the length [119]. This gave a small improvement in the flashback limit and a good enhancement to the blowoff limits under certain mixing and operational conditions. Adding cylindrical confinements gives operational conditions more representatives of gas turbine combustors.

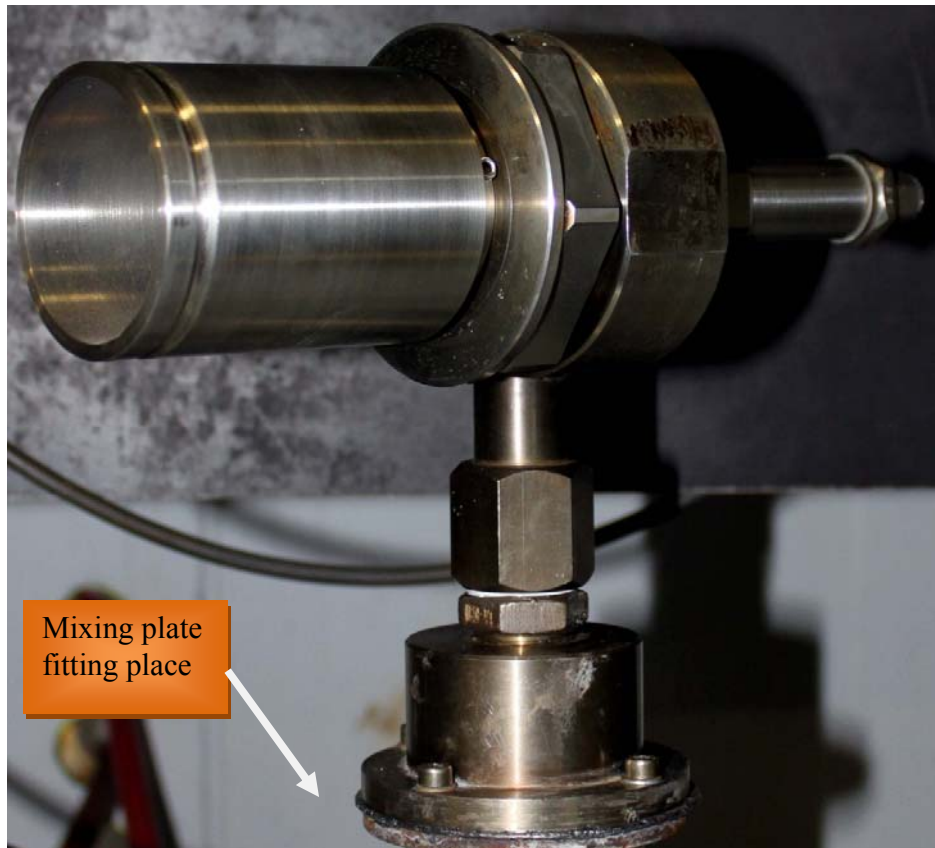


Figure 5.11 Swirl burner fitted with open cylindrical confinement

- V. Adding a conical cup nozzle at the end of the cylindrical confinement is the last enhancement that has been made, as shown in Figure 5.12. The diameter of the exit nozzle of the conical cup is equal to the diameter of the main nozzle exit and about

the same length [13, 119]. This has made a considerable enhancement in the blowoff limits for all fuels tested.

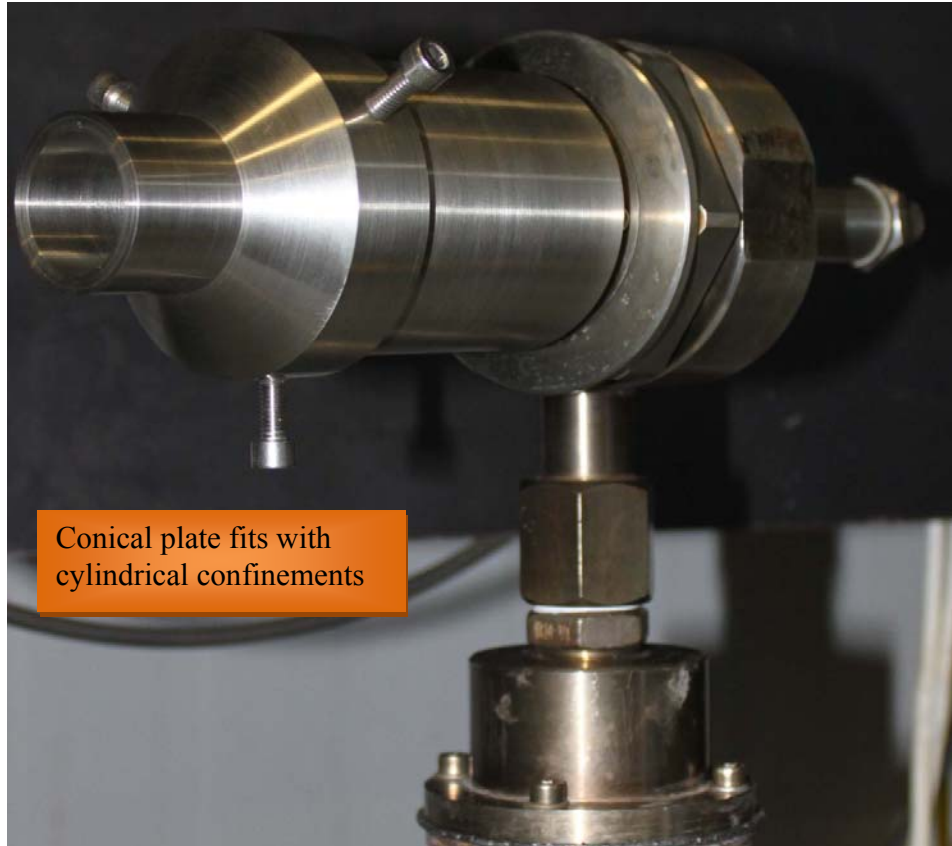


Figure 5.12: Swirl burner fitted with conical cup exhaust and confinement

All the above changes to the original design gave rise to three swirl burners with different swirl numbers. Two of those swirl burners can use a confinement as well as the conical cup. This is summarised in the following table, Table 5.1.

Swirl Burner name	A	B	C
Geometrical swirl number	1.47	1.04	0.8
Exhaust nozzle	No	Yes	Yes
Confinements	No	Yes	Yes
Conical cup with Confinements	No	Yes	Yes

Table 5.1: Swirl burner design with different modifications

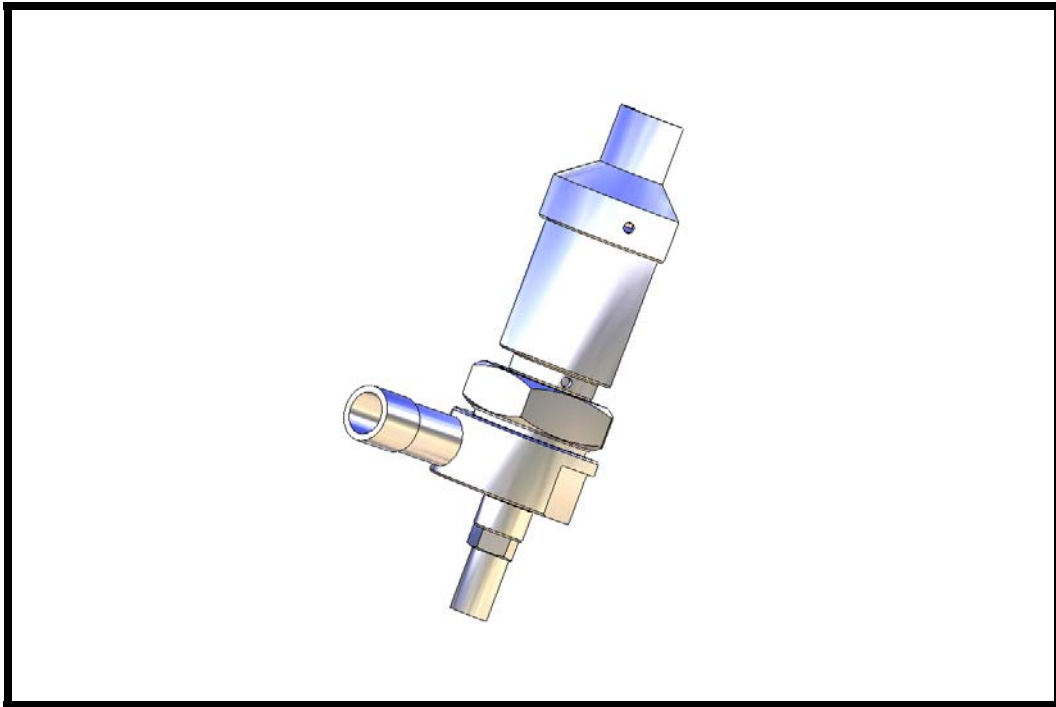


Figure 5.13: Schematic swirl burner diagram fitted with cylindrical confinement and the conical nozzle

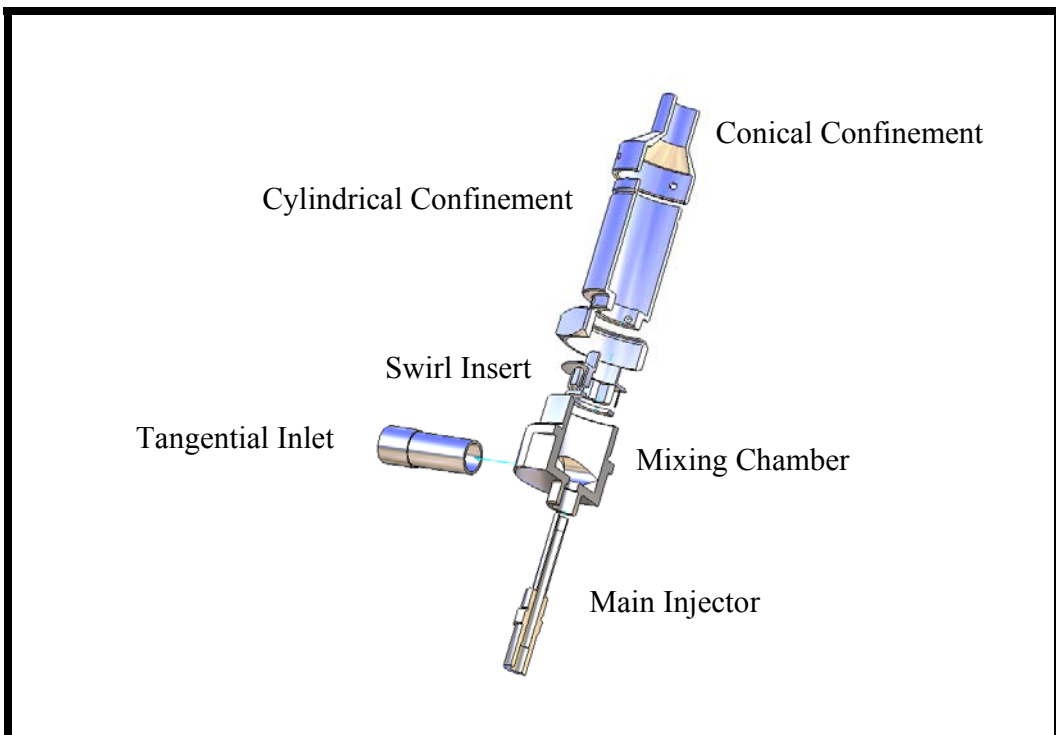


Figure 5.14: Swirl burner exploded section fitted with cylindrical confinement and the conical cup nozzle

These swirl burner arrangements can be expressed in a block diagram as shown in Figure 5.13. This clarifies and explains the design and improvements that have been made whilst undertaking this thesis programme.

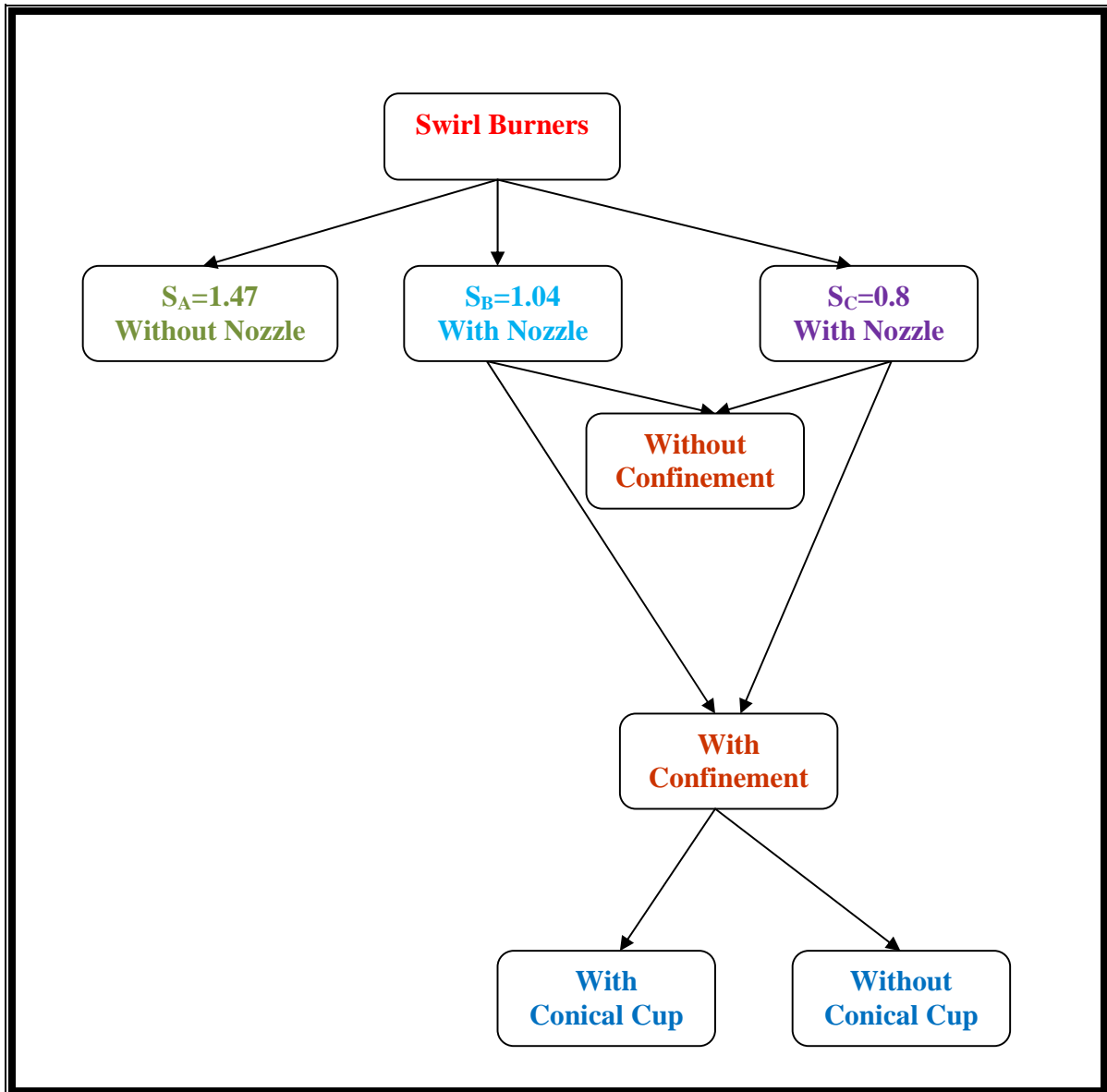


Figure 5.15: Block diagram shows the stages of swirl burner design

5.4 Fuel Blends

Seven different fuels and fuel blends ranging from pure fuel to different strengths of fuel mixture have been used to observe flashback, blowoff and the other characteristics of combustion inside the above mentioned swirls burners [5-9, 12]. These can be summarised in Table 5.2.

Fuel Name	Gas Percentage				
	%CH ₄	%H ₂	%CO	%N ₂	%CO ₂
Pure Methane	100	0	0	0	0
Pure Hydrogen	0	100	0	0	0
15%H ₂ /85%CH ₄	85	15	0	0	0
30%H ₂ /70%CH ₄	70	30	0	0	0
Coke Oven Gas	25	65	6	4	0
15%CO ₂ /CH ₄	85	0	0	0	15
30%CO ₂ /CH ₄	70	0	0	0	30

Table 5.2: Fuels blends tested and compositions, % by volume

The fuel mixtures in the above table have been given in volume per cent. Some other important characteristics of the pure fuels and the fuel blends have been used in further calculations, such as higher and lower calorific values, stoichiometric ratio and the maximum adiabatic temperature, as shown in Table 5.3.

Characteristic Fuel Name	HHV [MJ/kg]	LHV [MJ/kg]	Stoichiometric Ratio by mass	Maximum Temperature T _{max} [K]
Pure Methane	55.5	50.1	17.2	2237
Pure Hydrogen	141.9	120.1	34.2	2406
15%H ₂ /85%CH ₄	57.36	51.6	17.53	2245
30%H ₂ /70%CH ₄	59.89	53.66	18.02	2253
Coke Oven Gas	43.74535	47.578	15.15	2300
15%CO ₂ /CH ₄	54.018	49.018	11.5	2200
30%CO ₂ /CH ₄	52.6779	47.6	7.88	2018

Table 5.3: Fuels blend characteristics

Where possible and within the flow limits of the rig in terms of air and fuel gas supply, flashback limits have been derived for the three different swirl numbers (Table 5.1) and for up to the eight different fuels shown in Table 2.2. Because of the high turbulent flame speed of hydrogen it was not possible to obtain complete flashback or blowoff loops for all gas fuel mixtures, this being beyond the capability of the rig at the moment.

As shown above, the high cost of fuel (resulting from high hydrogen content) meant that the experimental data gathering was only repeated twice. This situation was not ideal but since experiments were repeatable at least once it was considered statistically acceptable.

5.5 Turbulence Plates

The burner is fed a premix of fuel and air via a mixing plate/flashback protector, 50 mm in diameter, which is fitted inside the mixing chamber shown in Figure 5.11. Two plates are used for experiments. The first is shown in Figure 5.16 (a) and produces finer grain turbulence via the 82 holes, each of 1 mm diameter; it is made of brass, blockage ratio 96.6%. The second plate is shown in Figure 5.17 (b) and is made of stainless steel with 53 holes, each of 1.5 mm diameter, blockage ratio 95% [101, 120]. The preheated air and fuel gas supply are connected to a mixing chamber upstream of this plate. The air is delivered through a large air compressor to reach its maximum pressure, 7 bar, at the flashback protector plates, whilst the fuel is fed from the fuel gas bottle at up to 4 bar. Both fuel and air are mixed prior to the mixing chamber and before they come through the flashback protector plate. The central fuel injector is used to supply a diffusive pilot flame to aid stability whilst adjusting the operating conditions.

During the experiments, the brass plate was damaged by flashback during pure hydrogen flame experiments. The experiments continued with another plate made of steel.

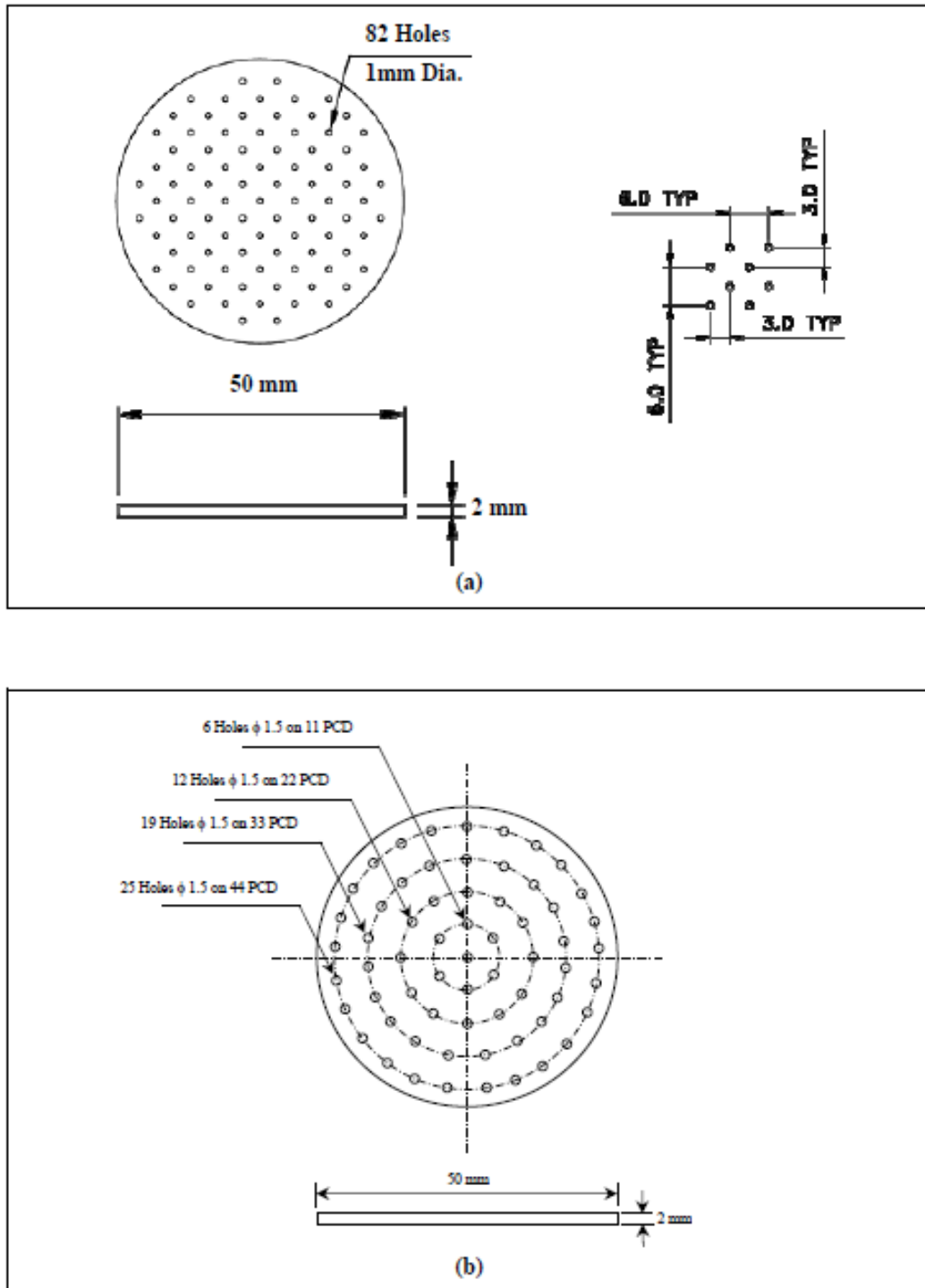


Figure 5.16: The flashback protection Plates

The typical pressure loss coefficient at $S_B=1.04$ is nearly half that at $S_A=1.47$ and is about 10% lower again at $S_C=0.8$. This is measured using the steel flashback protection plate as shown in Figure 5.17.

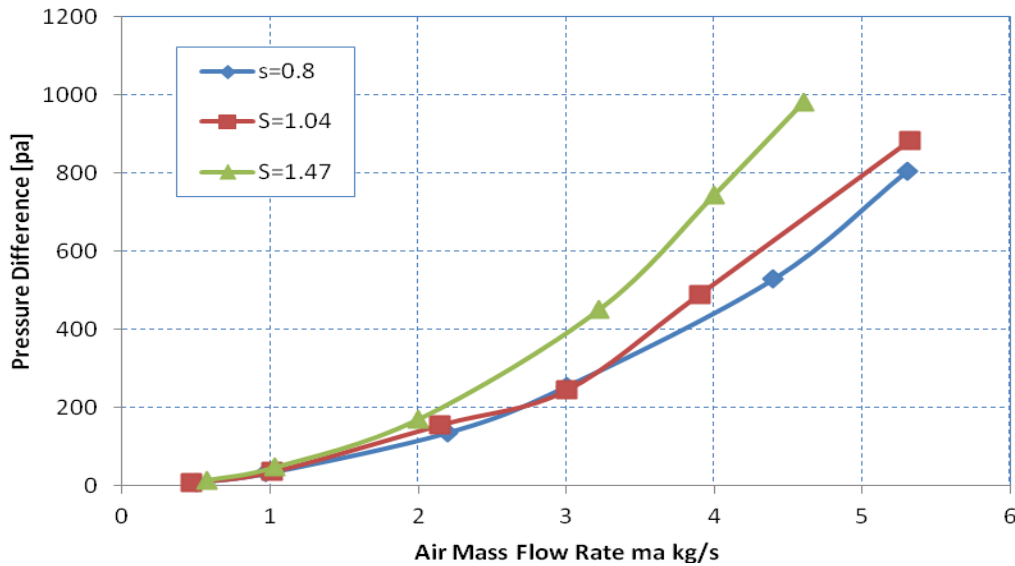


Figure 5.17: Pressure difference versus air mass flow rate through the three swirl burners

5.6 Summary

Chapter Five gives a clear picture regarding the generic swirl burner that has been designed, manufactured and developed at GTRC, Cardiff University. The requirements and process can be summarised as follows:

- The need to design a small test generic swirl burner to use different swirl numbers and that will be suitable for laboratory experiments with many different fuels.
- Understanding that the swirl insert played a very important role in the design.
- The swirl number calculation is based on the geometrical swirl number.
- Developing the design by using complementary cylindrical confinements to more closely simulate gas turbine practice.
- Extending experiments to cover more than one type of fuel to investigate the relationship between swirl number and alternative fuel composition.
- Strengthening the flashback protection plate in order to mitigate the flashback occurrence.

Chapter Six

**FLASHBACK
DETERMINATION
OF GENERIC
SWIRL
COMBUSTOR**

CHAPTER SIX**FLASHBACK DETERMINATION OF GENERIC SWIRL COMBUSTOR**

“People all over the world are brothers either because they share the same faith or they counterpart in their creation.”

Ali Bin Abi Talib

The phenomenon of flames often suddenly retreating back to the air/fuel mixing zone is called flashback. Flashback can be very dangerous, damage expensive equipment and may cause serious accidents.

As discussed earlier in this thesis, flashback has been experimentally studied and analyzed over a wide range of different gas fuel mixtures by using three types of swirl burners having three different swirl numbers.

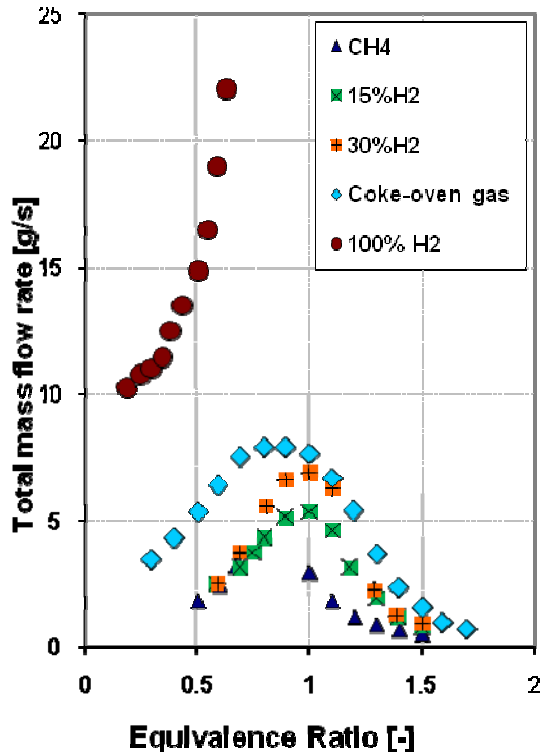
6.1 Flashback for Unconfined Burners (Open Flames)

The setup of the experiments in this thesis has been discussed in Chapter 5. All the tests have been carried out under atmospheric conditions.

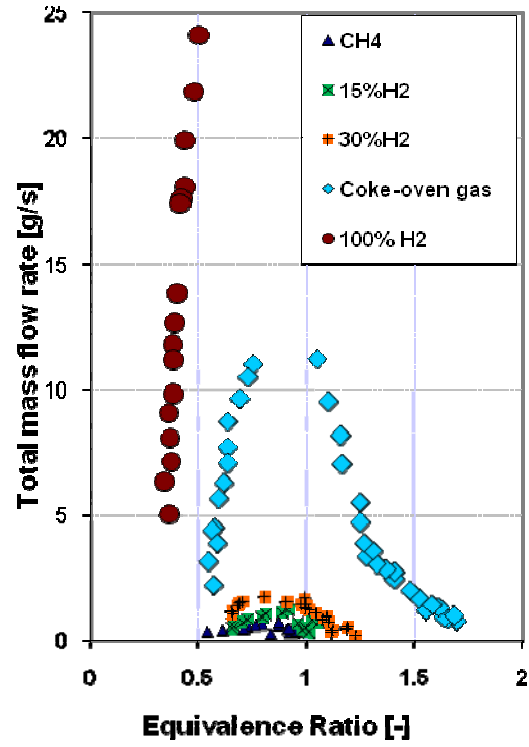
Flashback has been observed for the open flame by watching the flames location and how its position changes. Typically the flame retreated violently back into the swirl chamber and beyond with a loud noise. This is especially true with fuel blends containing a high percentage of hydrogen. This method has been complemented by using a thermocouple to measure the temperature and temperature changes of the mixing chamber.

The targets of all the tests have been to build up a picture of the flashback limits for each fuel for specific swirl numbers.

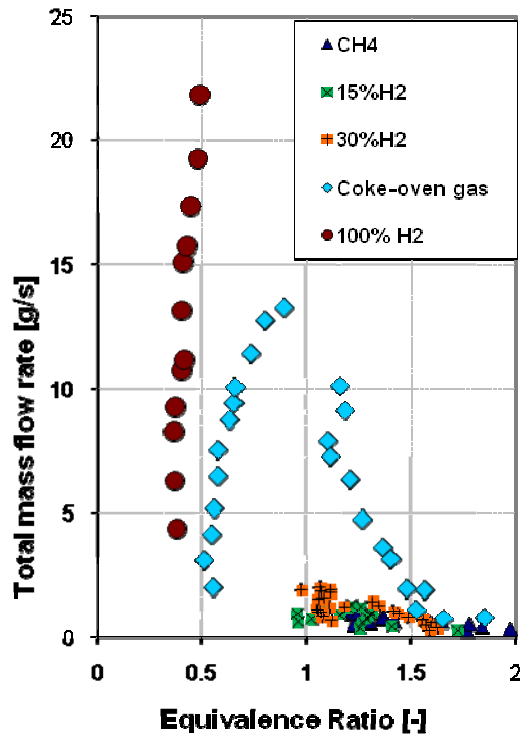
Three families of flashback curves are shown in Figure 6.1 below, for swirl numbers of $S_A=1.47$ see Figure 6.1.a, for $S_B=1.04$, Figure 6.1.b and Figure 6.1.c for $S_C=0.8$. Fuel blends used a range from pure methane, methane with 15%, 30% hydrogen, coke oven gas with 65% hydrogen, 25% methane, 6% CO, and pure hydrogen, as discussed in Chapter 5.



a) $S_A=1.47$



b) $S_B=1.04$



c) $S_C=0.8$

Figure 6.1: The flashback stability limit of the three burners with different swirl numbers for five different fuels
Note: All data has been taken under atmospheric conditions

Associated flame photographs at conditions just before flashback for pure methane are shown in figures **6.2.a** ($S_A=1.47$) and **6.2.b** ($S_B=1.04$).

The comparison is extremely interesting and reveals different flashback mechanisms for the three different swirl numbers. With $S_A=1.47$, the central recirculation zone (CRZ) extends over the central fuel injector to the base plate for all fuels, with an associated flame front on the CRZ boundary.

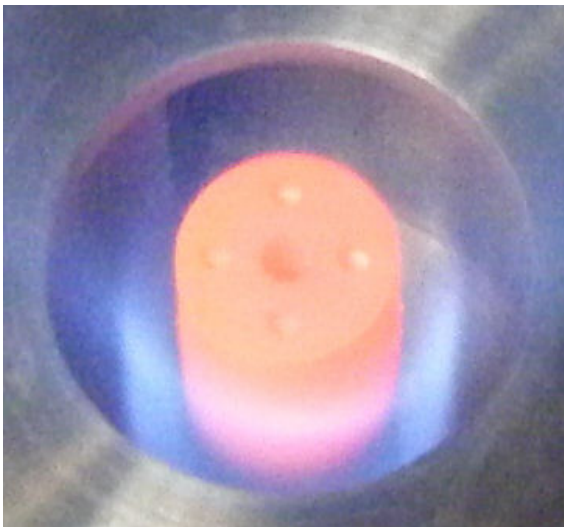


Figure 6.2.a: Photo of flame surrounding central fuel injector at $S_A=1.47$, just before radial flashback



Figure 6.2.b: Photo of flame just before flashback through outer wall boundary layer, $S_B=1.04$

At $S=1.47$, flashback occurs when the radial velocity in the swirl chamber around the area of the CRZ (surrounding the fuel injector, Figure **6.2.a**) drops to such a level that the near radial flame front can flashback to the inlets and often into the plenum chamber. Conversely with $S_B=1.04$ and $S_C=0.8$, flashback occurs by a different mechanism via flashback in the outer wall boundary layer of the exhaust nozzle, then being controlled by the critical boundary velocity gradient as initially defined by Lewis and von Elbe. A comparison of different flame shapes at $S_A=1.47$ and $S_B=1.04$ is shown in Figure **6.2.a** and **6.2.b**. More clearly, Figure **6.3** shows a common example of wall boundary layer flashback for methane in the swirl burner with $S_B=1.04$. It can be easily recognized from the two photograph views detailing how the flame is attached the inner surface of the nozzle exit.

Flashback will occur and the flame will pass down into the swirl chamber in front of the exhaust, sometimes further upstream to the flashback protector plate.



Side View



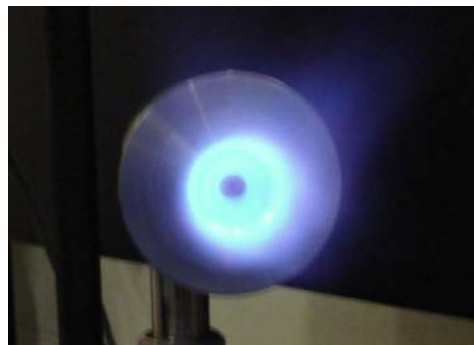
Top View

Figure 6.3: 100%CH₄ Flame in the swirl burner of $S=1.04$ $\dot{m}_f = 0.03\text{g/s}$, $\dot{m}_a = 0.6\text{g/s}$, $\phi = 0.858$ (about to flashback)

Flashback is affected crucially by the fuel blends. It has been observed that the flashback becomes more violent when the percentage of hydrogen is increased in the blends. In terms of flashback limits for methane and methane containing up to 30% hydrogen, Figure 6.1 shows that a value of $S_B=1.04$ and $S_C=0.8$ produces flashback which occurs at mass flow (and hence velocity levels) up to 1/3 of those found for $S_A=1.47$. Figure 6.4 shows a classic wall boundary layer flashback in the swirl burner $S_B=1.04$, the flashback occurred after the flame attached the burner exit sleeve (nozzle).



Side view



Front view

Figure 6.4: Attached flame of 30%H₂+70%CH₄, $\dot{m}_f = 0.07\text{g/s}$, $\dot{m}_a = 0.7\text{g/s}$, $\phi = 1.887$ (just before flashback) in the swirl burner $S=1.04$

A precise inspection of the flames of fuels containing hydrogen shows that the flame colour becomes brighter compared to pure methane flames. Loud noises often accompany flashback occurrence.

However, with coke oven gas more complex behaviour occurs, a typical example of the stable flame shape and the flame shape before flashback occurrence can be seen in Figures 6.5 and 6.6, respectively.



Figure 6.5: Attached flame of coke oven gas $\dot{m}_f = 0.725\text{g/s}$, $\dot{m}_a = 10\text{g/s}$, $\phi = 1.1$ (just before flashback) for the swirl burner $S=1.04$



$\dot{m}_f = 0.21\text{g/s}$, $\dot{m}_a = 2.0\text{g/s}$,
 $\phi = 1.593$

$\dot{m}_f = 0.245\text{g/s}$, $\dot{m}_a = 2.6\text{g/s}$,
 $\phi = 1.43$

Figure 6.6: Coke oven gas stable flame in the swirl burner of $S=1.04$

The swirl number $S_A=1.47$ gives better flashback resistance between equivalence ratios of 0.55 to 1.21 for coke oven gas, as shown in Figure 6.1.

The respective flashback curves cross at an equivalence ratio ~ 0.55 , whereafter, the flashback limits are better for the swirl number $S_B=1.04$ and $S_C=0.8$. Indeed flashback could scarcely be detected for equivalence ratios less than 0.5 for the two lower swirl numbers. Pure hydrogen gave similar trends to coke oven gas, although results for all swirl numbers were much closer over the range of equivalence ratios tested. Indeed the range of equivalence ratios tested was restricted to being below 0.6 and above 2 due to the very large hydrogen and air flow rates required compared to those for methane. Moreover, pure hydrogen flashback detection caused some difficulties as well. Mainly the lean hydrogen flames were invisible and could not be seen. Figure 6.7 shows one of these flames. Flame flashback was then detected by thermocouple. In contrast, the rich hydrogen flame can be seen and recognized clearly as shown in Figure 6.8.

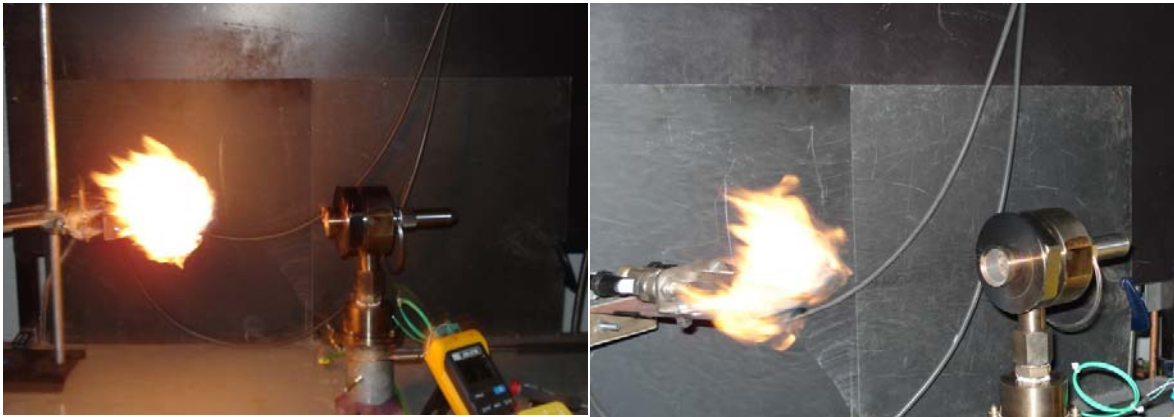


Figure 6.7: Premixed hydrogen flame cannot be seen but is detected by thermocouple
(Propane torch used to attempt to visualize the hydrogen flame)



Figure 6.8: Rich hydrogen flame $\dot{m}_f = 0.5 \text{ g/s}$, $\dot{m}_a = 11 \text{ g/s}$, $\phi = 1.5545$ for the swirl burner at $S=1.47$. Note use of propane torch again.

More detailed inspection of the results with pure hydrogen for $S_B=1.04$ and $S_C=0.8$, Figure 6.1.b and 6.1.c, indicated that the flashback limit for $S_C=0.8$ was slightly better than $S_B=1.04$: at $S_C=0.8$ swirl number it produces less of a pressure drop and it is clearly favoured. No significant differences between the flashback trends with methane, methane/hydrogen blends and coke oven gas could be found for these two swirl numbers.

The effects on flashback of CO_2 addition to methane were also studied, experiments being carried out with 15%, 30% of CO_2 blends with CH_4 to check the flashback effect at atmospheric conditions. During these experiments, flashback was often eliminated and thus only a few points were determined. Figure 6.9 shows a stable 15% CO_2 +85% CH_4 flame.

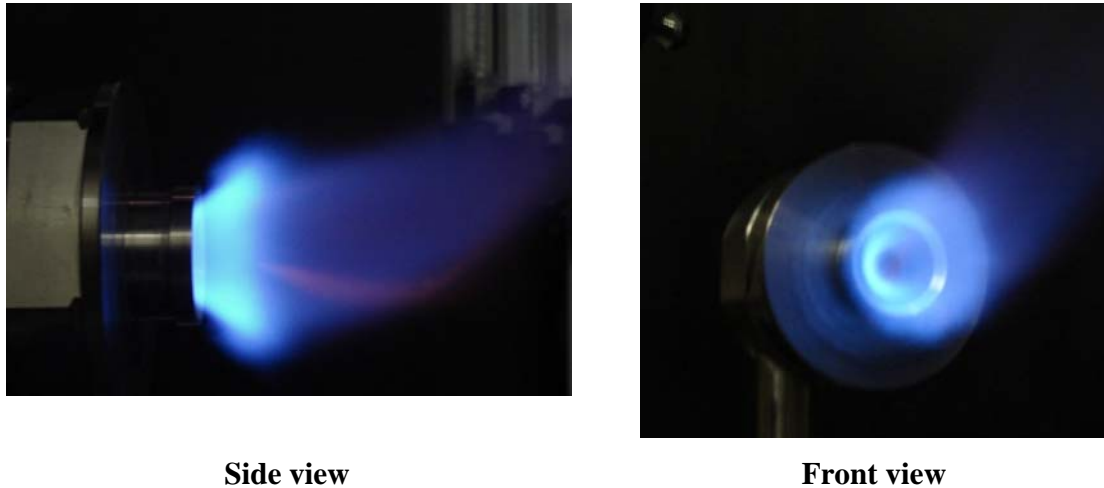


Figure 6.9: 15% CO_2 +85% CH_4 Flame in the swirl burner of $S=1.04$ $\dot{m}_f = 0.112\text{g/s}$,
 $\dot{m}_a = 1.318\text{g/s}$, $\phi = 1.55$

A comparison of flashback has been made between the two swirl numbers $S_A=1.47$ and $S_B=1.04$; flashback points for 15% and 30% CO_2/CH_4 blends are shown in Figure 6.10-a and 6.10-b for both swirl numbers. These curves show that $S_B=1.04$ virtually eliminates flashback. This confirms the differences in flashback mechanisms between the two swirl numbers. Generally, CO_2 addition decreases the turbulent burning velocity, thus making flashback more difficult. Unfortunately, CO_2 addition worsens the blowoff limits and thus is normally undesirable.

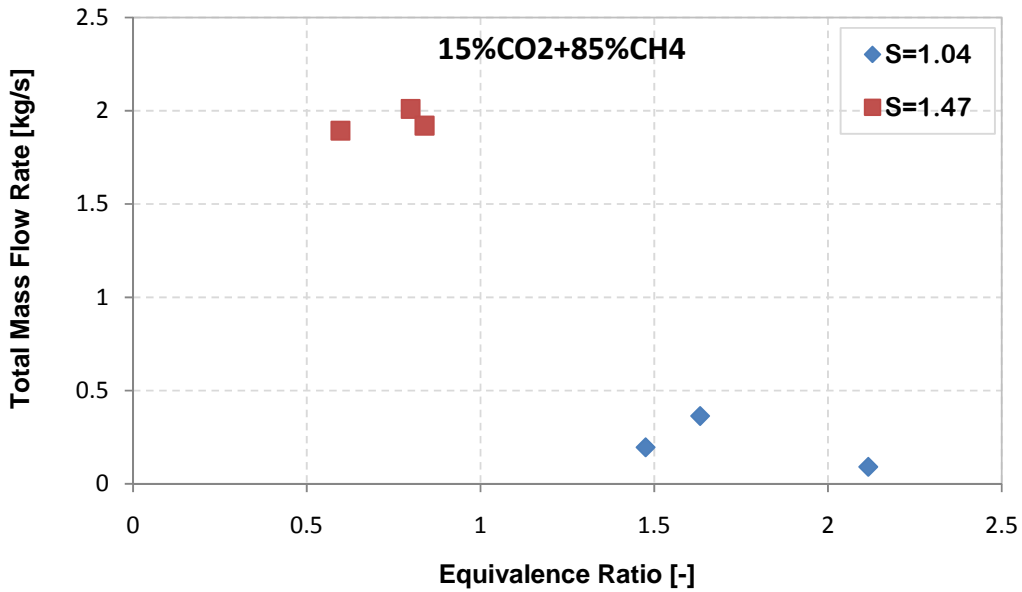


Figure 6.9-a: Flashback comparison between swirl burners $S_A=1.47$ and $S_B=1.04$ for 15%CO₂

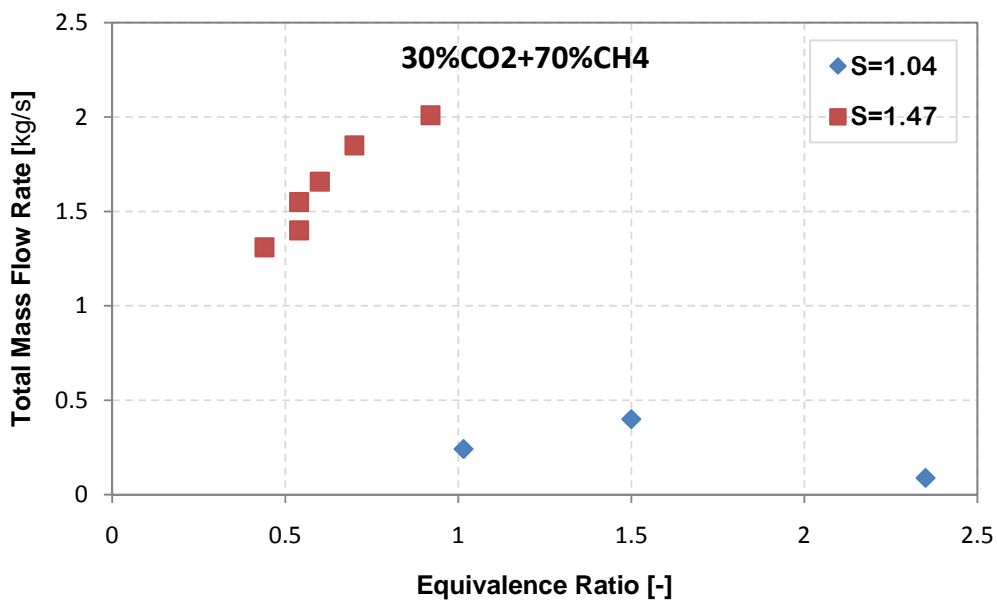


Figure 6.10-b: Flashback Comparison between Swirl Burners $S_A=1.47$ and $S_B=1.04$ for 15%CO₂

Another interesting result was that the peaks of the flashback curves all occurred at weak equivalence ratios as opposed to the expected values around the stoichiometric ratio. This effect is thought to be due to changes in the recirculation zone occurring as the equivalence ratio approaches 1. This is also illustrated by Figure 6.11, where all the methane data has been plotted as a function of critical boundary layer gradient at flashback, G_f : also included is laminar data on natural gas. The swirl burners at $S_B = 1.04$ and 0.8 are flashing back at lower values of G_f than the laminar results (albeit at a higher system pressure drop), whilst for $S_A = 1.46$ values of G_f are significantly higher. Overall $S_C = 0.8$ gives the best flashback limits for methane based fuels.

However, the opposite occurs for fuels with hydrogen content in the range $30\% \leq H_2$ content $\leq 65\%$ with the critical boundary velocity gradient being higher at lower swirl numbers, reflecting the previously discussed results.

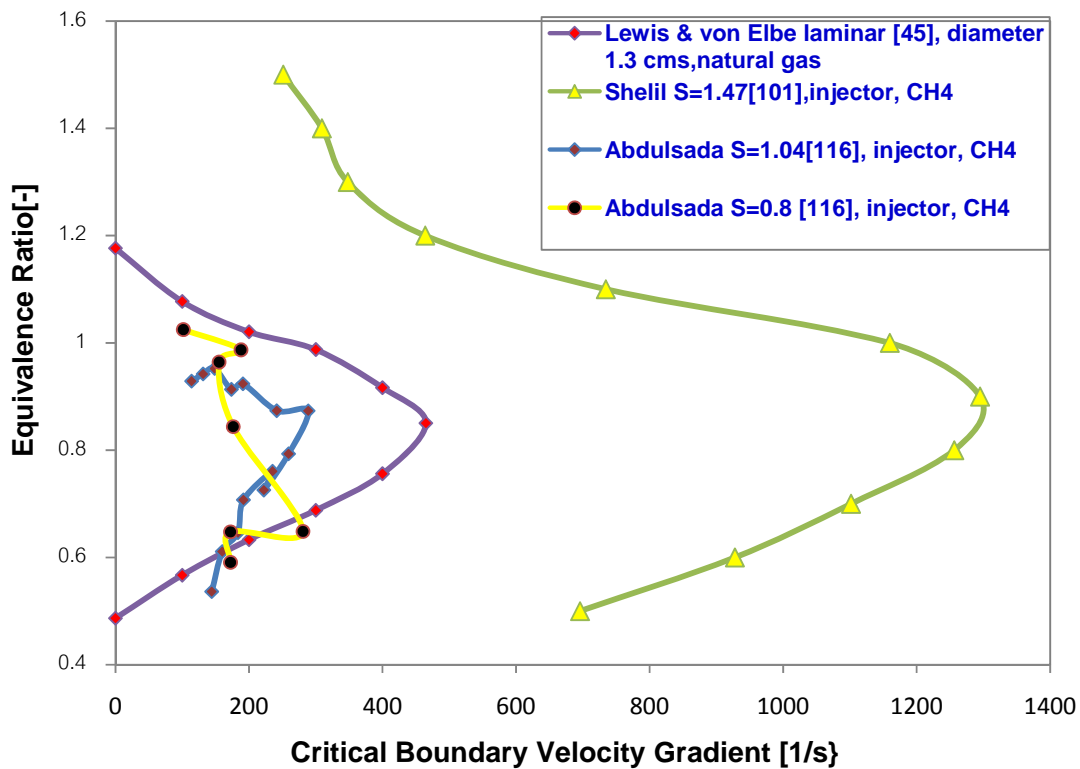


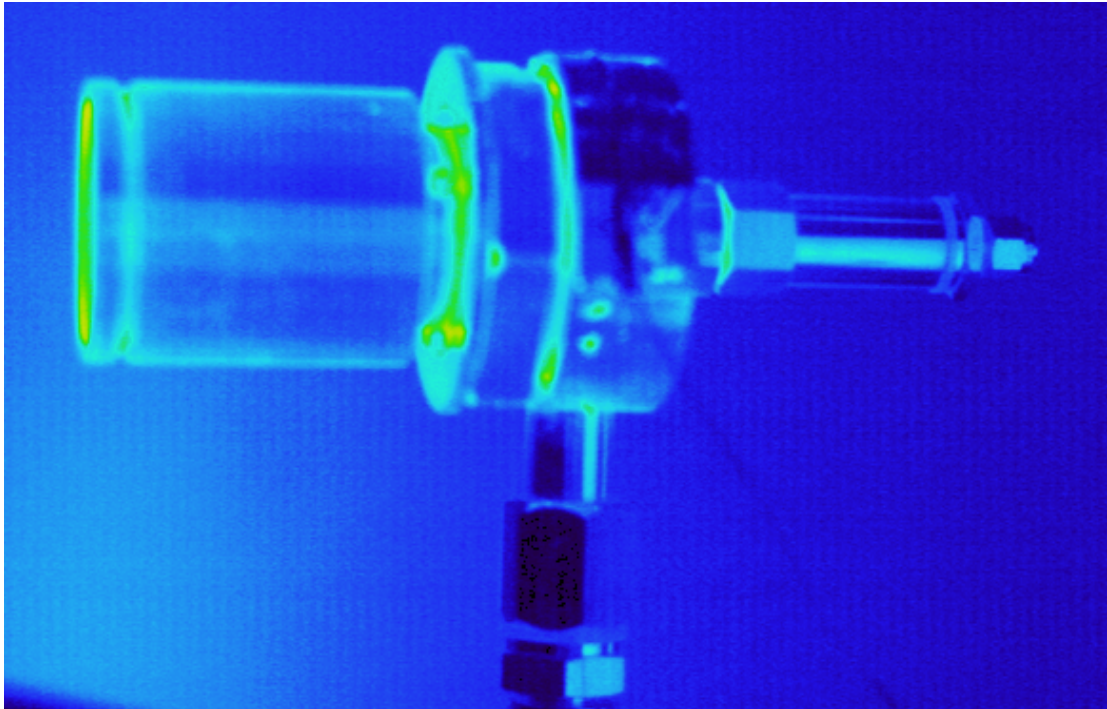
Figure 6.11: Lewis and Von Elbe critical boundary velocity gradient comparison for three swirl numbers (natural gas and methane) and laminar data

6.2 Flashback for Confined Burners

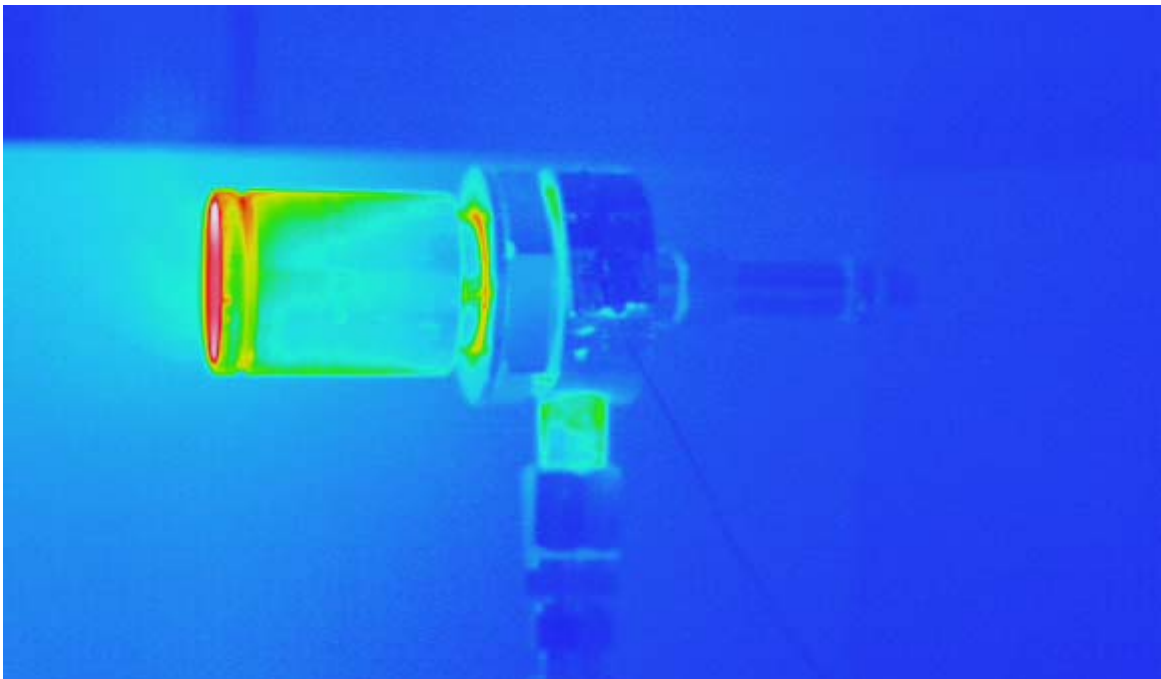
Cylindrical confinements and conical extension have been fitted to the burner rig as mentioned in Chapter 5. Experiments were carried out with both arrangements of the confinements, essentially by adding or removing the conical cup exhaust. Results have shown different behaviours for various gases and swirl numbers; some of them have improved and others worsened, whilst others have not shown any noticeable change.

The whole set of experiments have been done for only two of three burners ($S_B=1.04$ and $S_C=0.8$). $S_A=1.47$ was excluded because of technical difficulties in connecting the cylindrical confinement and conical cup exhaust. Moreover, hydrogen flame flashback and blowoff tests encountered some complexities due to the maximum air flow rate needed to cover all the required range of equivalence ratios. The other critical difficulty was when the flashback point became too close to the blowoff limit, making their measurement very difficult.

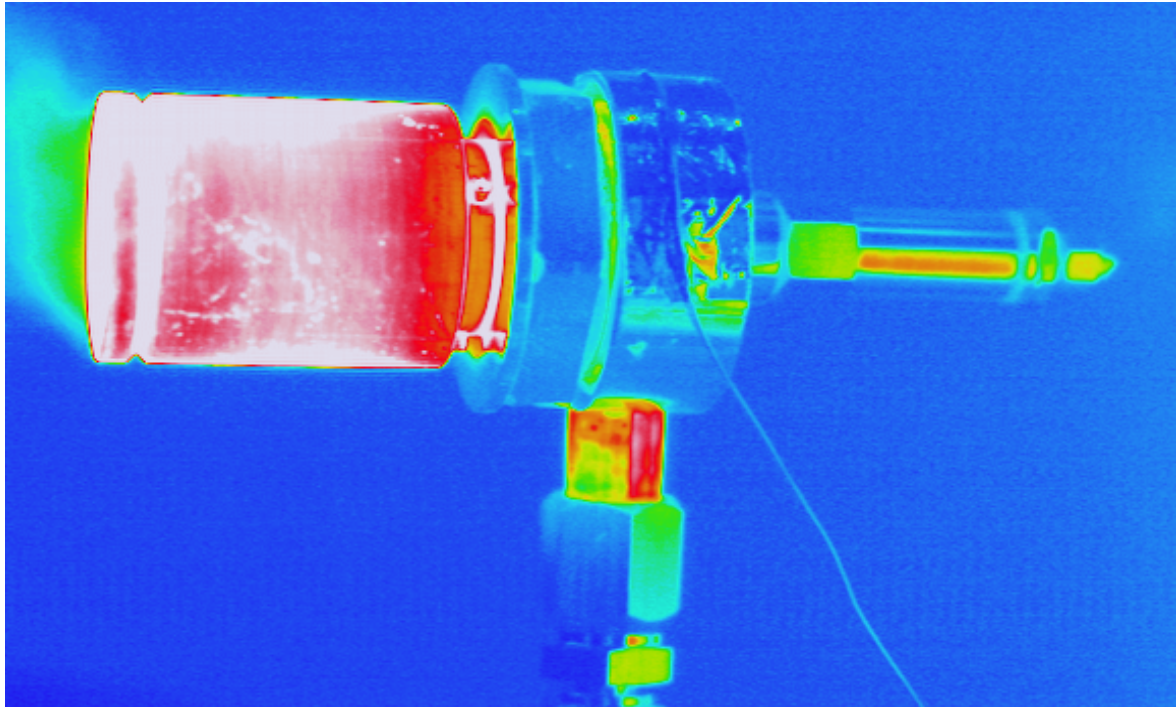
A thermal imaging camera has been used to detect flashback in the cylindrical confinements for some cases as it is difficult to recognize flashback occurrence, especially when it is noiseless and at high mass flow rates. Figure 6.12 shows the steps involved in recognizing if the flame is a stable flame or has flashed back. Figure 6.12.a shows the thermal image of a non-combustion picture of the burner with the confinement. In the second image, Figure 6.12.b, we can observe the normal combustion with a stable flame and there is no hot red spot prior to the swirl chamber. The last image, as shown in Figure 6.12.c, shows flashback occurrence. It could easily be recognized that the tube which is situated before the mixing chamber has become red, indicating flashback beyond the inlets to the unit.



a-Normal Thermal Image without any combustion



b-Thermal Image of Stable Combustion



c- Thermal Image for the Flashback Case

Figure 6.12: The steps of recognition of the flashback flame in the confinement combustion

Pure methane flashback results show differences between the two burners, as shown in Figure 6.13 and 6.14, respectively. Figure 6.13, for swirl number $S_B=1.04$, shows clearly the confinement and conical cup have almost the same trend line/curve for flashback. These flashback curves are clearly moved into the rich equivalence ratio region of the graph compared to those of the open flame. In contrast, Figure 6.14, for the swirl number $S_A=0.8$, shows there is little difference between the three different geometrical systems (open flame, cylindrical confinement and conical cup) in terms of flashback curves.

For the two types of confinement the results are quite close together; however the lower pressure drop gives the advantage to $Sc=0.8$.

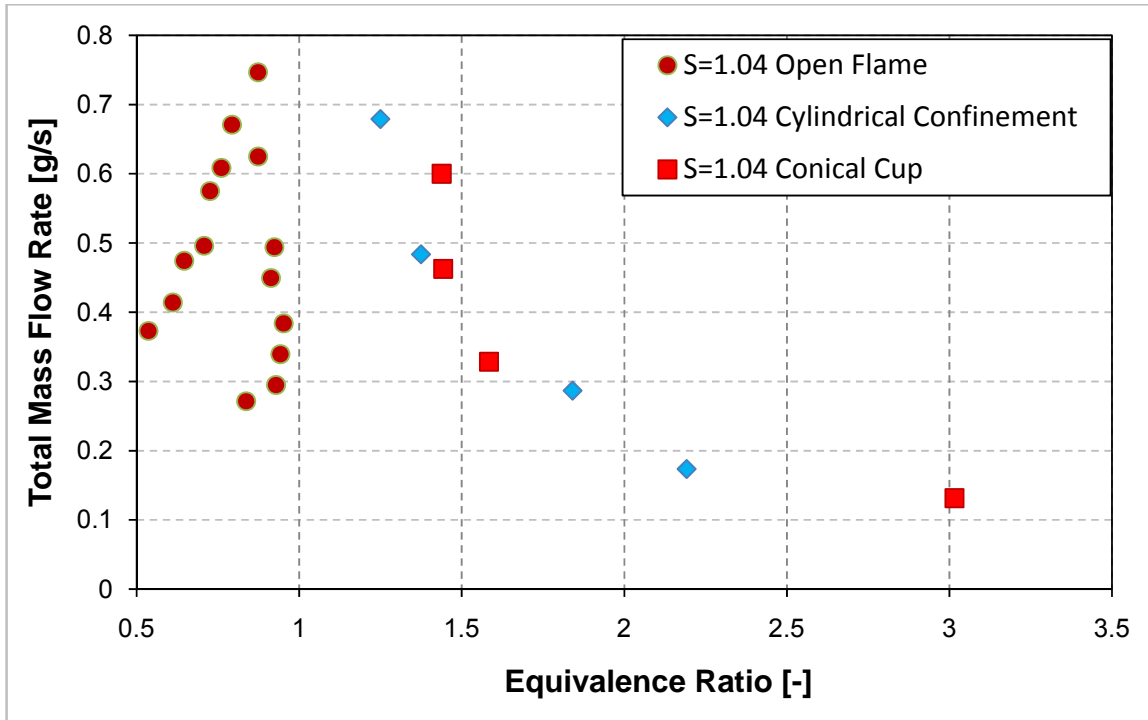


Figure 6.13: Flashback comparison between three types of flame for swirl burner=1.04 for pure methane (100%CH₄).

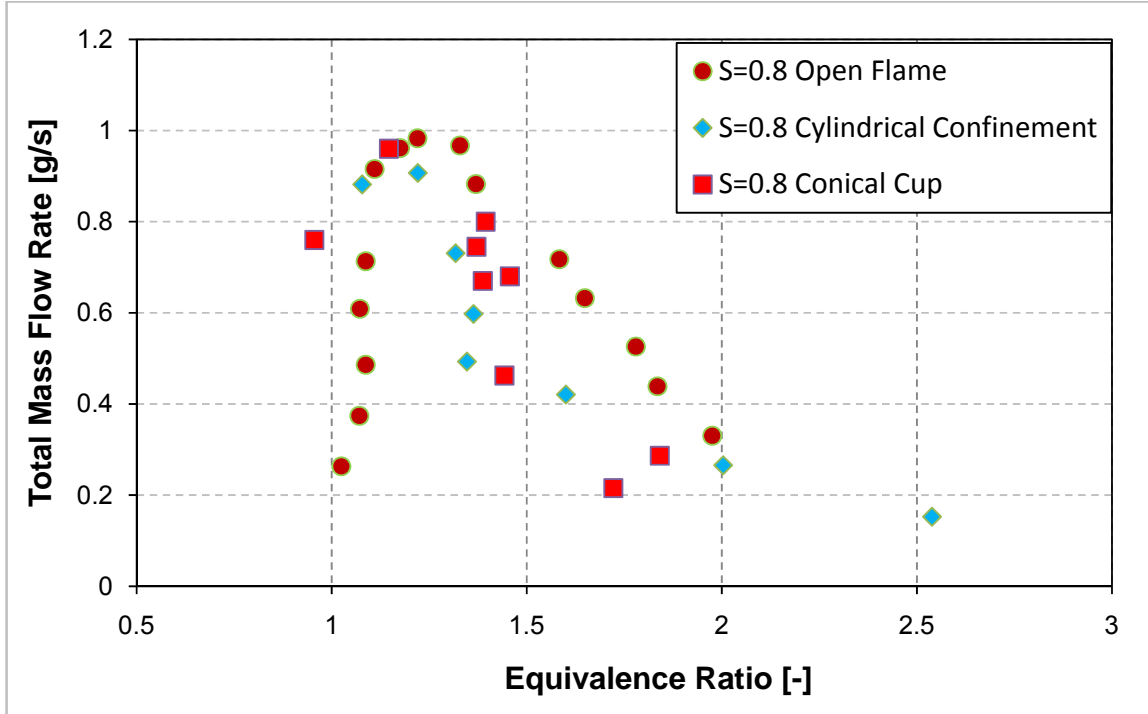


Figure 6.14: Flashback comparison between three types of flame for swirl burner=0.8 for pure methane (100% CH₄).

The results for the fuel containing 15%H₂ balanced by pure methane is shown in Figure 6.15 for $S_B=1.04$. This shows that the cylindrical confinement narrows the area of the flashback and this is significantly better than the open flame case. It is also somewhat better than the cylindrical confinement and conical cup exhaust case.

For the swirl number $S_B=0.8$ the open confinement gives the best flashback limit, followed by the open flame and then the cylindrical confinement with the conical cup exhaust, which is up to 30% worse in flashback limit terms compared to the case with the open cylindrical confinement, Figure 6.16.

Again there are similar outcomes to the two previous cases for the (30%H₂+70%CH₄) mixture for swirl numbers $S_B=1.04$ and $S_C=0.8$, Figures 6.17 and 6.18 respectively. The open confinement again gives the best flashback limits for the swirl number $S_C=0.8$, followed by the open flames, then the cylindrical confinement with conical cup. Similar results pertain for $S_B=1.04$, although the $S_C=0.8$ appears to be the best.

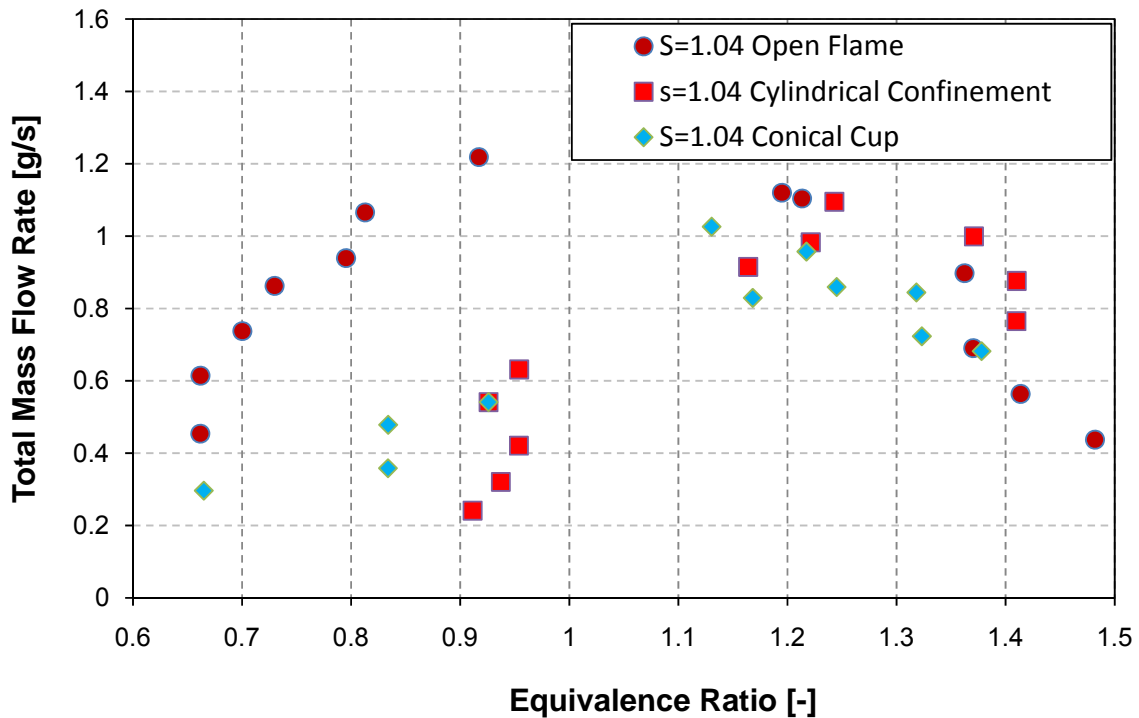


Figure 6.15: Flashback comparison between three types of flame for swirl burner number $S_B=1.04$ for (15%H₂+85%CH₄)

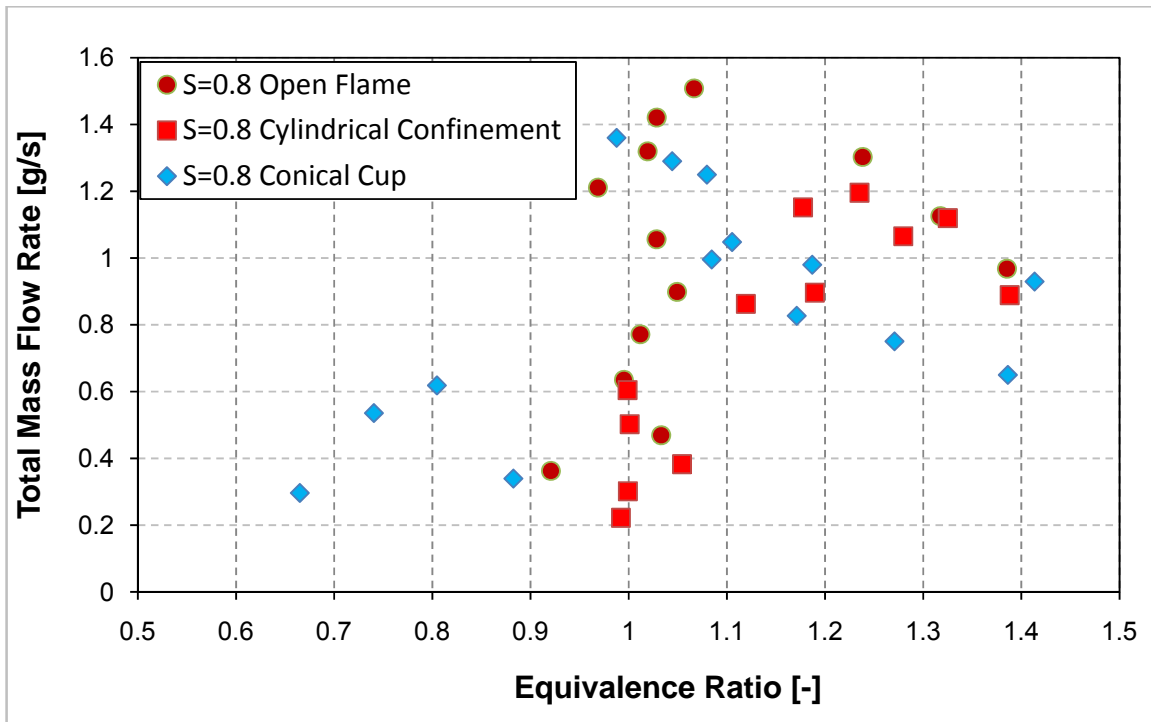


Figure 6.16: Flashback comparison between three types of flame for swirl burner number $S_C=0.8$ for (15%H₂+85%CH₄)

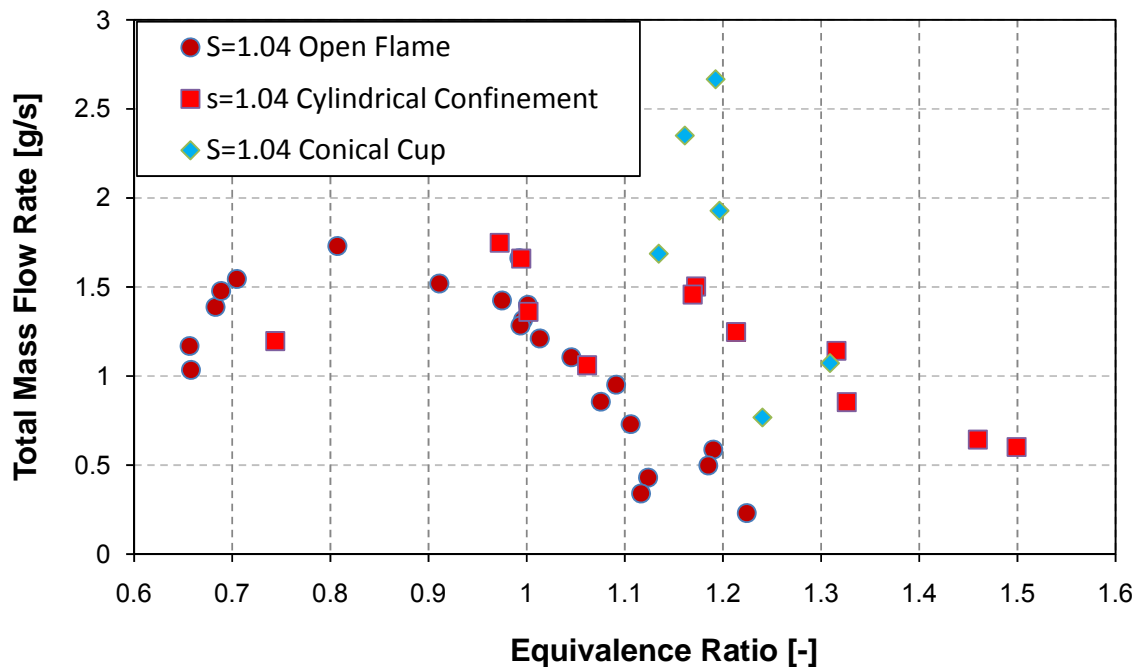


Figure 6.17: Flashback comparison between three types of flame for swirl burner number $S_B=1.04$ for (30%H₂+70%CH₄)

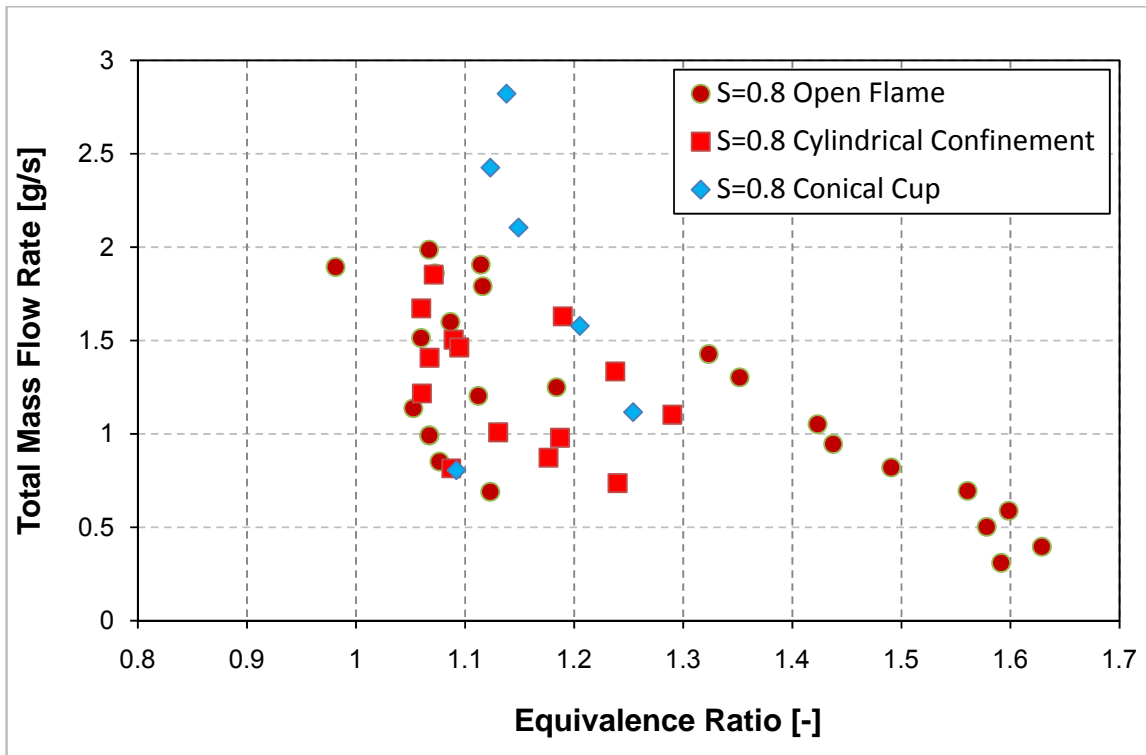


Figure 6.18: Flashback comparison between three types of flame for swirl burner number $S_C=0.8$ for (30%H₂+70%CH₄)

The experiments could be readily conducted with up to 30% of hydrogen balanced with methane, but when the coke oven gas (which contains 65% of H₂) was used, no flashback data could be obtained with the confinements. The main reason for this was because the flashback points become too close to the blowoff points whilst there was insufficient air and fuel to move the operational region to areas where flashback limits could be obtained. In other words, for lean premixed combustion (equivalence ratio less than 1) the flashback points match the blowoff points and the combustion was unstable and violent. Coke oven gas flashback curves have thus not been obtained for the cylindrical confinements with or without the conical cup. Similar difficulties were encountered with pure hydrogen with the two confinements. Other fuel gas containing (60%H₂+40%CH₄) has been used to confirm these findings.

In consequence, fundamental work is needed to understand this problem so as to be able to design combustors capable of avoiding flashback. Confinements are obviously needed, but considerable geometrical changes are feasible and need to be investigated.

Chapter Seven

BLOWOFF

DETERMINATION

OF GENERIC

SWIRL

COMBUSTOR

CHAPTER SEVEN**BLOWOFF DETERMINATION OF GENERIC SWIRL COMBUSTOR**

"Science is a wonderful thing if one does not have to earn one's living at it."

Albert Einstein

The phenomenon of the flame extinction and disappearance or extinction is called blowoff. Unexpected blowoff could be potentially disastrous for gas turbine engine operation. Extreme lean mixtures are often the cause of blowoff.

Wide blowoff limits are enormously important for gas turbine operation. Blowoff limit is affected by many characteristics like fuel type, geometrical swirl number and combustion process such as non-premixed, premixed or partially premixed (diffused and premixed).

However, it is crucial for gas turbine designer to look at the blowoff limits of the fuel for specific burner design under specific conditions of operation. For the following sections of this chapter the blowoff limits of different fuel blend gases for all three swirl burners will be considered for unconfined and confined systems under atmospheric conditions.

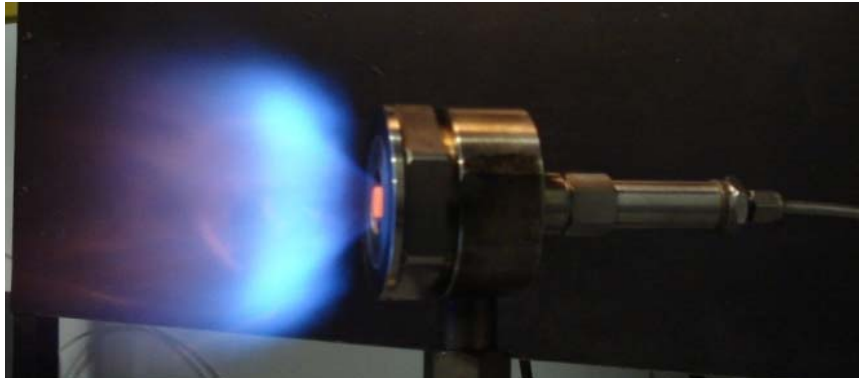
7.1 Blowoff for Unconfined Burners (Open Flame)

By using the same process that has been used in this project for flashback, blowoff limits have been experimentally derived and plotted. The blowoff is observed by viewing the flame; when the flame disappears this means the flame has reached the blowoff point.

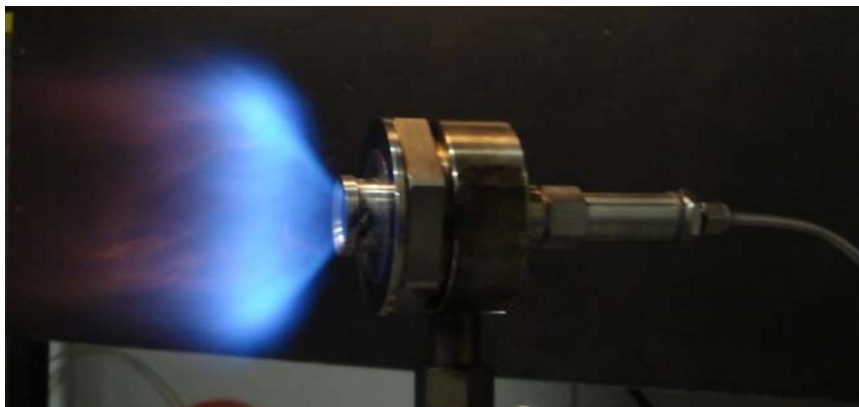
Pictures in Figures **7.1-a, b, c** below show how swirl number and burner exit shape can affect the flame shape just before blowoff for pure methane.

The flame shapes shown in Figures **7.1-a** and **7.1-b**, for swirl numbers of $S_A=1.47$ and $S_B=1.04$ are typical of those just before blowoff (which occurs very suddenly). Reduction in swirl number to $S_C=0.8$ gives a slower gradual blowoff process and improved the blowoff limits, Figure **7.1-c**. The change in flame shape is very noticeable from Figures **7.1 a** to **b**, to **c**, and appears to arise from changes in the shape of the CRZ formed in the

exhaust of the burner. The flame is normally located (with methane) towards the outer boundary of the shear flow surrounding the CRZ, past the burner (near the inner boundary in the burner exit, see Figure 7.1 a) and as the swirl number is reduced from 1.47, Figure 7.1.a, to 1.04, Figure 7.1.b, and to 0.8, Figure 7.1.c, the CRZ shape alters considerably and hence the flame shape.



a: $S_A=1.47$ $\dot{m}_f = 1.0$ g/s, $\dot{m}_a = 7.35$ g/s $\phi = 2.34$



b: $S_B=1.04$, $\dot{m}_f = 1.0$ g/s, $\dot{m}_a = 9.0$ g/s $\phi = 1.91$



c: $S_C=0.8$ $\dot{m}_f = 1.0$ g/s, $\dot{m}_a = 17$ g/s $\phi = 1.012$

Figure 7.1: Flame shape for pure methane just before blowoff for the same fuel mass flowrate

As the hydrogen content of the fuel blend was increased the shape of the flames near blowoff subtly changed as the higher turbulent burning velocities allowed the outer flame boundary to locate at larger radii early in the flame stabilization process, very close to or in the burner exhaust. This caused corresponding changes in the downstream flame shape.

Analysed blowoff data for the range of fuels tested is shown in Figure 7.2, below, as a function of equivalence ratio. Significant data for pure hydrogen blowoff could not be obtained due to rig limitations on hydrogen flowrate.

Swirl numbers, $S_A=1.47$, gave the worst blowoff limits for all fuels, although coke oven gas with 65% hydrogen content gave a dramatic improvement. The most interesting feature was the differences between blowoff limits for $S_B=1.04$ and $S_C=0.8$. The swirl burner with a swirl number of $S_C=0.8$ gave much improved blowoff limits with pure methane and fuel blends containing up to 30% hydrogen. Both swirl numbers gave very similar results for blowoff with coke oven gas.

The swirl number of $S_A=1.47$ gives the worst blowoff limits (and a pressure drop which is twice that of the $S_B=1.04$ case) as shown in Figure 7.2. Increasing hydrogen fuel content dramatically improves the blowoff limits. Coke oven gas (COG), contains 65% H_2 , 25% CH_4 , 6% CO and 4% N_2 and had the best blowoff limits; rig limitations precluded obtaining the pure H_2 blowoff limits. Interestingly COG results produced curves that had similar slopes and shape for all swirl numbers. This did not occur with pure methane and fuel blends up to 30% hydrogen for swirl numbers of $S_A=1.47$ and $S_B=1.04$.

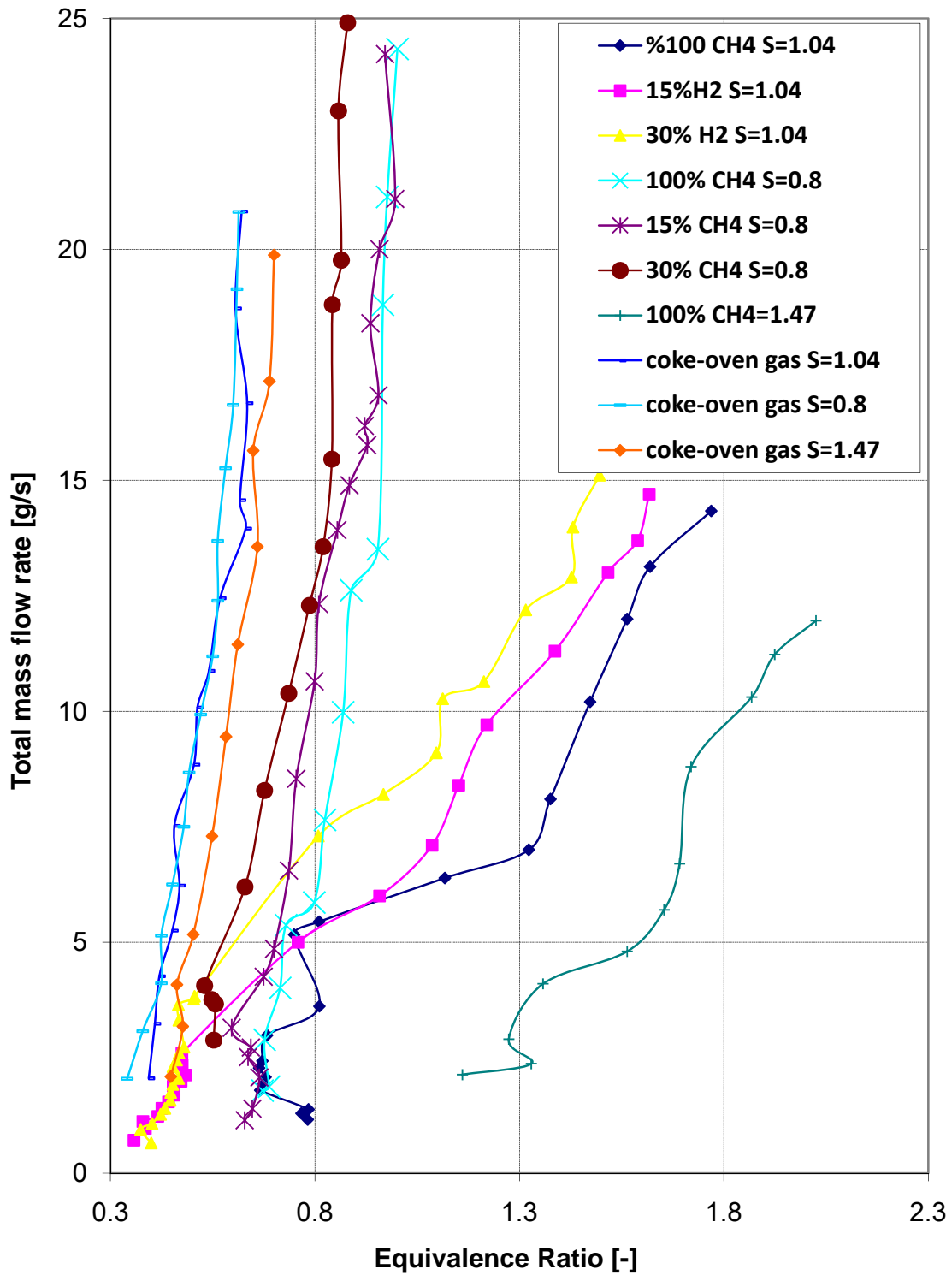
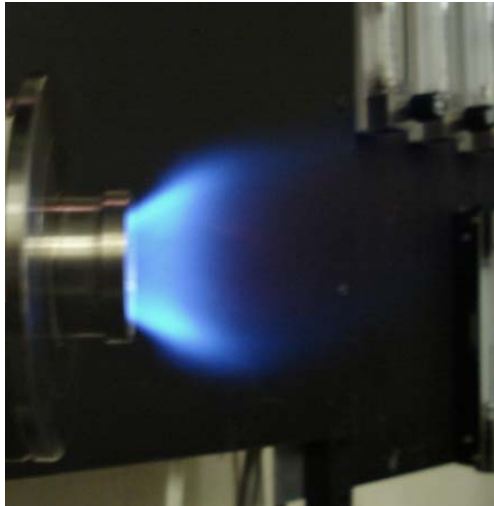
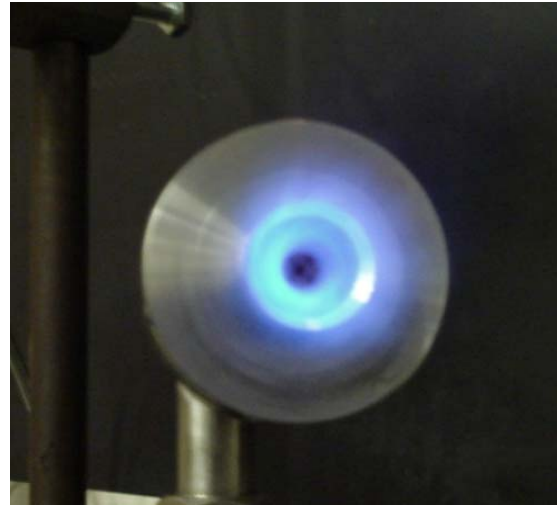


Figure 7.2: Blowoff limits for different hydrogen-methane blends

For different fuel blends similar blowoff behaviour occurred, but at different values of equivalence ratio for a given mass flowrate. Figures 7.3 and 7.4 show side view and front view of the blowoff of two different fuel blends, for 30%CO₂+70%CH₄ and 30%H₂+70%CH₄ respectively, with a swirl number $S_B=1.04$. Comparing Figure 7.1 b (pure methane) with Figure 7.4 shows subtle differences in flame shape due to the 30% H₂ content of the fuel in Figure 7.4.

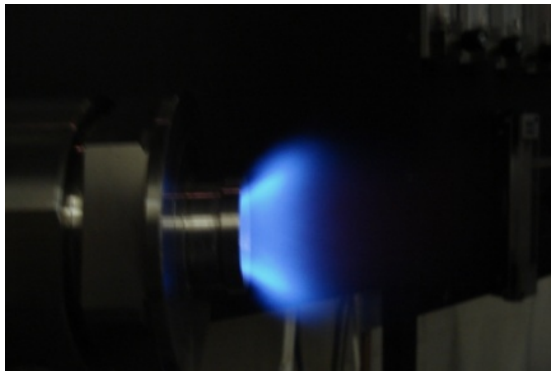


Side view

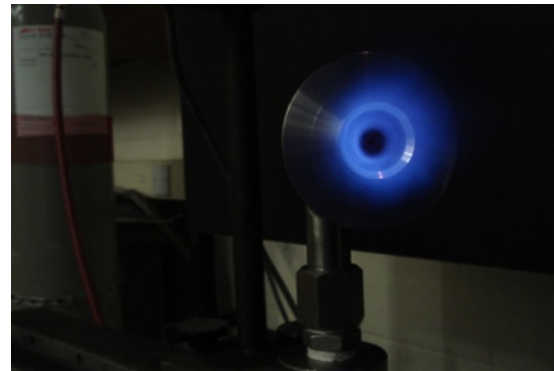


Front view

Figure 7.3: 30%CO₂+70%CH₄ Flame in the swirl burner of $S=1.04$ $\dot{m}_f = 0.088\text{g/s}$,
 $\dot{m}_a = 0.94\text{g/s}$, $\phi = 0.8212$ (near blowoff and no flashback)



Side view



Front view

Figure 7.4: 30%H₂+70%CH₄ Flame in the swirl burner of $S=1.04$ $\dot{m}_f = 0.085\text{g/s}$,
 $\dot{m}_a = 2.15\text{g/s}$, $\phi = 0.746$ (near blowoff no flashback)

7.2 Blowoff with the Confinements Attached to the Burner

The two types of confinement considered are cylindrical confinement with open exhaust and cylindrical confinement with conical cup exhaust, as discussed in Chapter 5. There was a remarkable effect with the confinements in terms of improving the blowoff limits.

First of all, Figures 7.5 and 7.6 show pure methane blowoff limits for $S_B=1.04$ and $Sc=0.8$. The first significant result is the general improvement of blowoff limits moving from the unconfined to the burner with the confinement. With the confined burner up to 10% improvement for low total mass flowrate (5g/s) occurred and this value rose up to 70% for higher total mass flowrate (15g/s) as shown in Figure 7.5 for $S_B=1.04$. Figure 7.6 shows improved results for $S_C=0.8$ compared to $S_B=1.04$. For total mass flowrate (5g/s) the blowoff enhancement for the confined compared to the unconfined burner is up to 40% and for 12g/s total mass flowrate the improvement is up to 70%. In both cases the confinement with the cylindrical cup exhaust is slightly better than the open confinement. However, the advantage lies with the open confinement due to its superior behaviour with flashback.

The scientific explanation for this improvement of blowoff limits is because the confinement remains warm and prevents entrainment of cold air into the flame and CRZ. Thus, essentially the confinements suppress flame quenching, not unexpectedly.

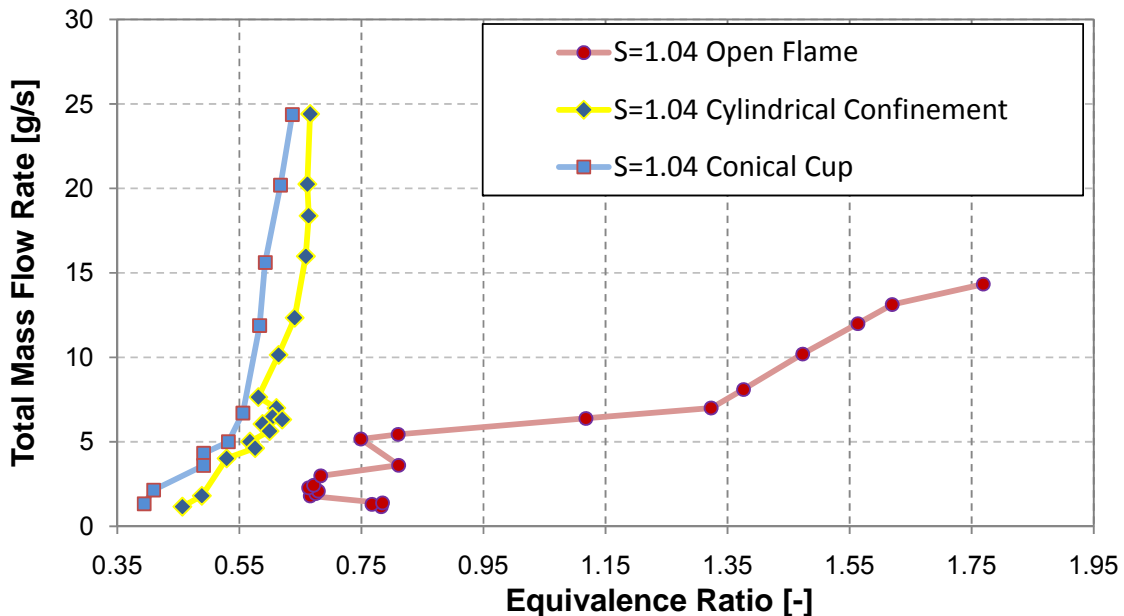


Figure 7.5: Blowoff comparison between three types of flame for swirl burner number $S_B=1.04$ for pure methane (100%CH₄)

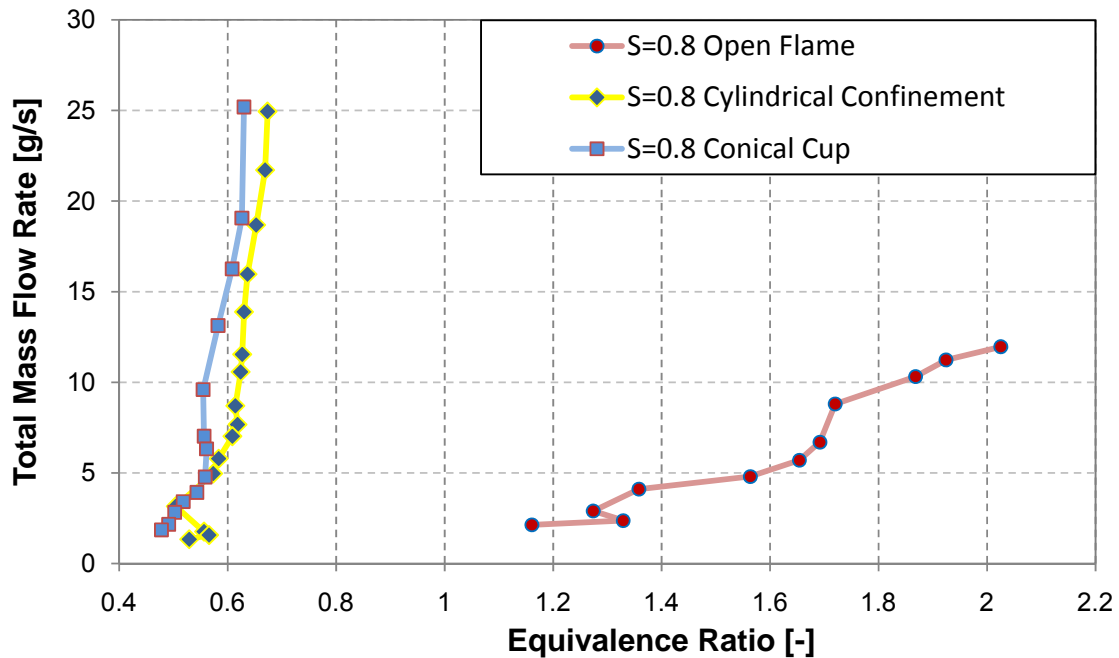


Figure 7.6: Blowoff comparison between three types of flame for swirl burner number $S_C=0.8$ for pure methane (100%CH₄)

The use of the open ended confinement in a gas turbine combustor would be difficult as the flow needs to be focussed towards the turbine inlet. An offset confinement exhaust is one possibility; others include annular exhaust passages such that where the high temperature flow leaving the confinement is forced into an annulus next to the outer wall.

The 15% hydrogen fuel blends blowoff maps are shown in Figures 7.7 and 7.8 for swirl numbers $S_B=1.04$ and $S_C=0.8$ respectively. Both Figures 7.7 and 7.8 show the enhancement of blowoff with the confinements. The results with $S_C=0.8$ are significantly improved compared to $S_B=1.04$ for the open flame case (unconfined burner).

Comparing Figures 7.5, 7.6, 7.7 and 7.8 to determine the effect of fuel blend change from pure methane (100%CH₄) to 15%H₂+85%CH₄ shows little change due to the use of the confinement when equivalence ratio is considered. However, as discussed later when the effect of the different heating value of the various gas mixtures is taken into account, differences do arise in terms of the thermal input to the combustor (the important parameter in gas turbine systems).

Figures 7.9 and 7.10 show the blowoff limit maps for 30% hydrogen balanced with methane for the swirl number cases $S_B=1.04$ and $S_C=0.8$ respectively.

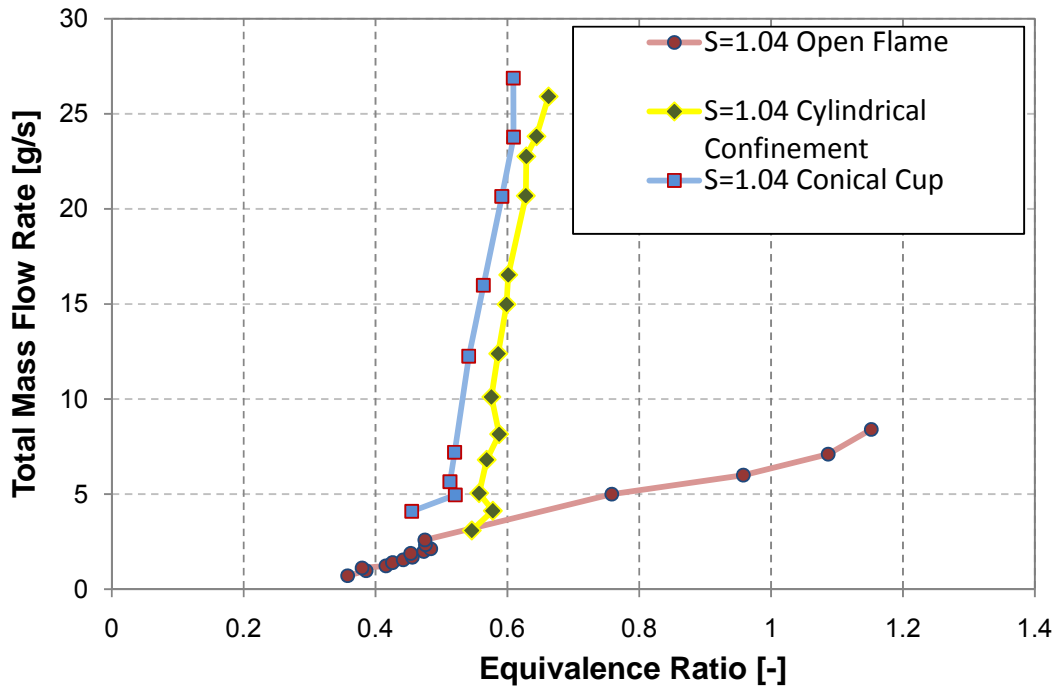


Figure 7.7: Blowoff comparison between three types of flame for swirl burner number $S_C=1.04$ for (15% H₂+85%CH₄)

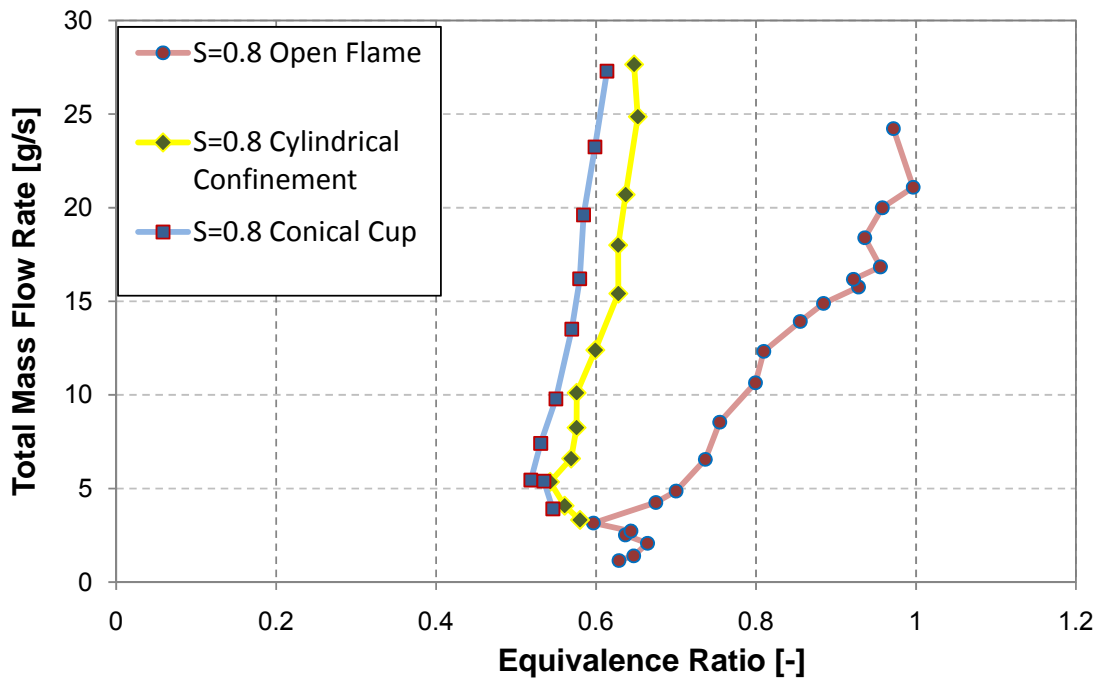


Figure 7.8: Blowoff comparison between three types of flame for swirl burner number $S_C=0.8$ for (15% H₂+85%CH₄)

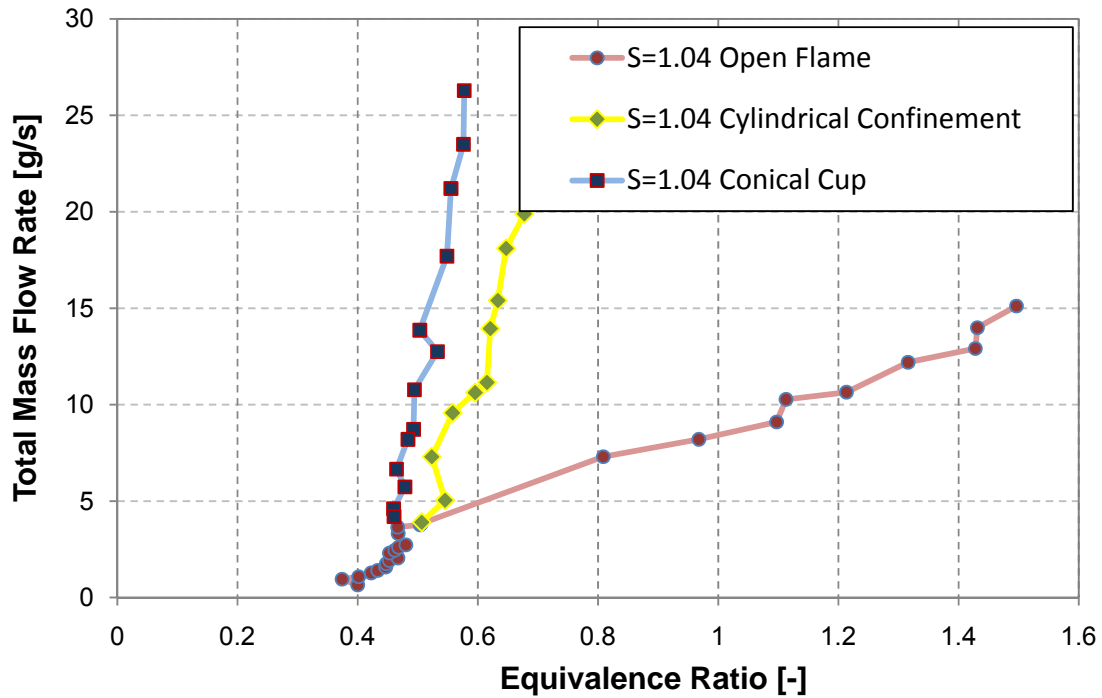


Figure 7.9: Blowoff comparison between three types of flame for swirl burner number $S_C=1.04$ for (30% H₂+70%CH₄)

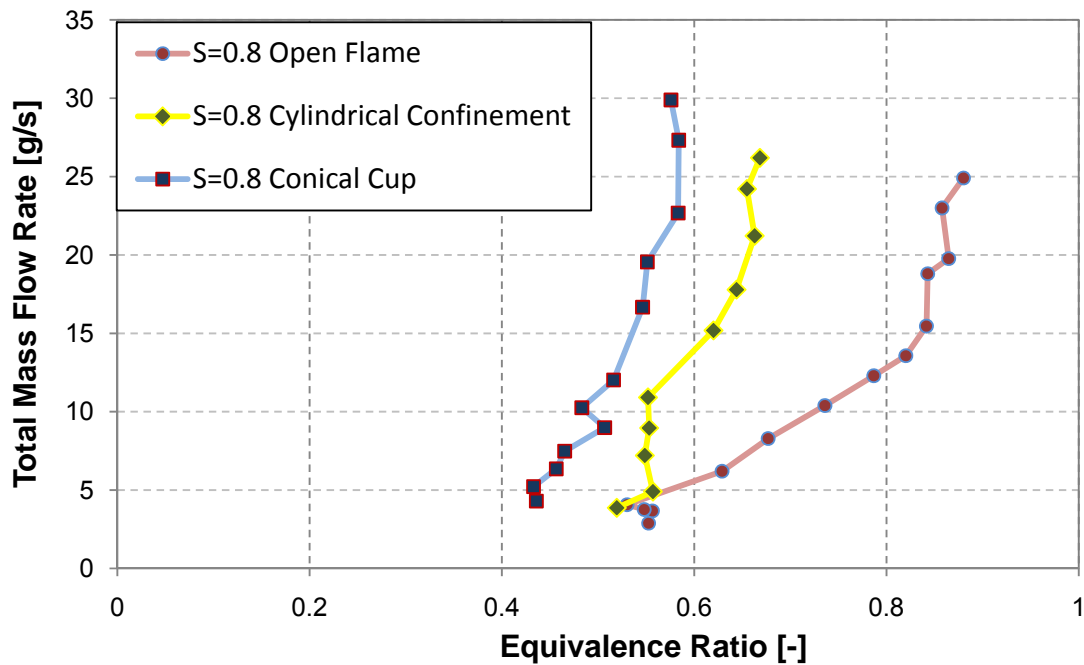


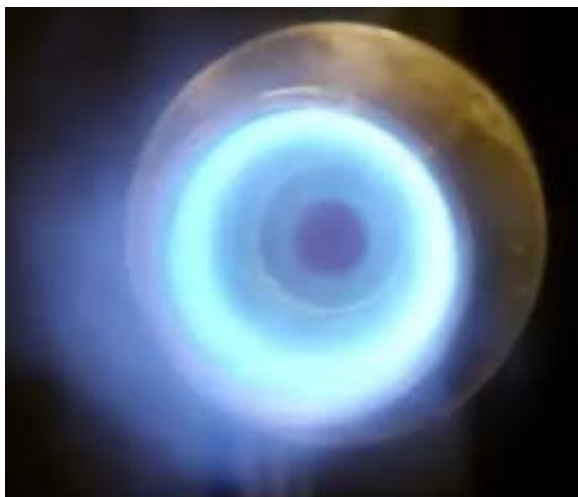
Figure 7.10: Blowoff comparison between three types of flame for swirl burner number $S_C=0.8$ for (30% H₂+70%CH₄)

More details regarding the blowoff limits for the 30% hydrogen mixture can be observed from a video of the blowoff. Figures 7.11 and 7.12 show two series of images derived from the videos that show stages of the blowoff process.

At a value of $\dot{m}_f = 0.35 \text{ g/s}$ of fuel, air has been increased gradually until the flame reached the point of blowoff for both cases (cylindrical confinement and that with conical cup).

Images 1 and 2 from Figure 7.11 (cylindrical confinement) show a blue flame which is primarily located close to the outer wall of the confinement and extends down into the burner exhaust nozzle. Image 2 clearly shows there is little combustion in the centre of the flow in the burner exhaust nozzle. Moving onto image 3, the flame can be seen to be becoming smaller and less intense in the burner exhaust region (darker blue), whilst still maintaining fairly intense combustion in the confinement. Finally with image 4 the combustion becomes less intense generally (becoming a deeper shade of blue) and loses stabilization inside the burner exhaust nozzle, the flame contracting in size. This leads to final blowoff.

The point when the flame disappears is defined as the blowoff point. The blowoff in this case was very gradual and smooth.



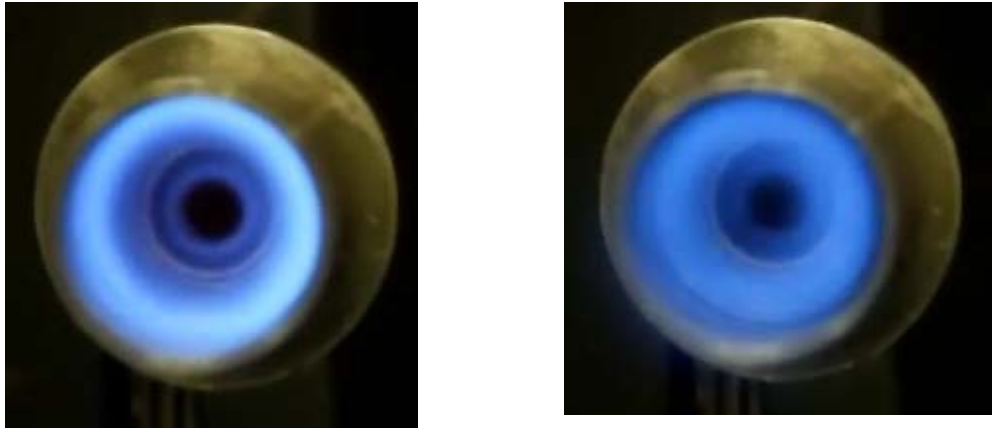


Figure 7.11: 30% H_2 +70% CH_4 Mixture - blowoff flame stages for swirl burner number $S_c=0.8$ for open cylindrical confinement ($\dot{m}_f = 0.35g/s$).

The next photographs, shown in Figure 7.12, represent the confinement case by adding the conical cup to the end of the cylindrical confinement.

With the same quantity of fuel, image 1 shows a stable fuel rich flame extending past the confinement; image 2 shows how a central vortex core region is starting to form with fuel gases burning on its periphery. This is a noisy process with the flame still extending past the end of the confinement. In contrast, image 3 shows the disappearance of the flame burning on the boundary of the central vortex core whilst the flame locates near the wall of the confinement and that of the conical cup exhaust. Image 4 shows the flame is now stabilized inside the confinement, against the outer wall, with no visible combustion in the burner exhaust nozzle. This condition is close to blowoff, which would probably occur in due course as the confinement cooled. Image 5 represents the final image just before blowoff; this is typical of this type of system, the flame stabilizes on the boundary of the central vortex core right the way back through the burner exhaust nozzle to the fuel injector. There is still some combustion in the cylindrical confinement. This condition causes poor combustion and soon leads to blowoff.

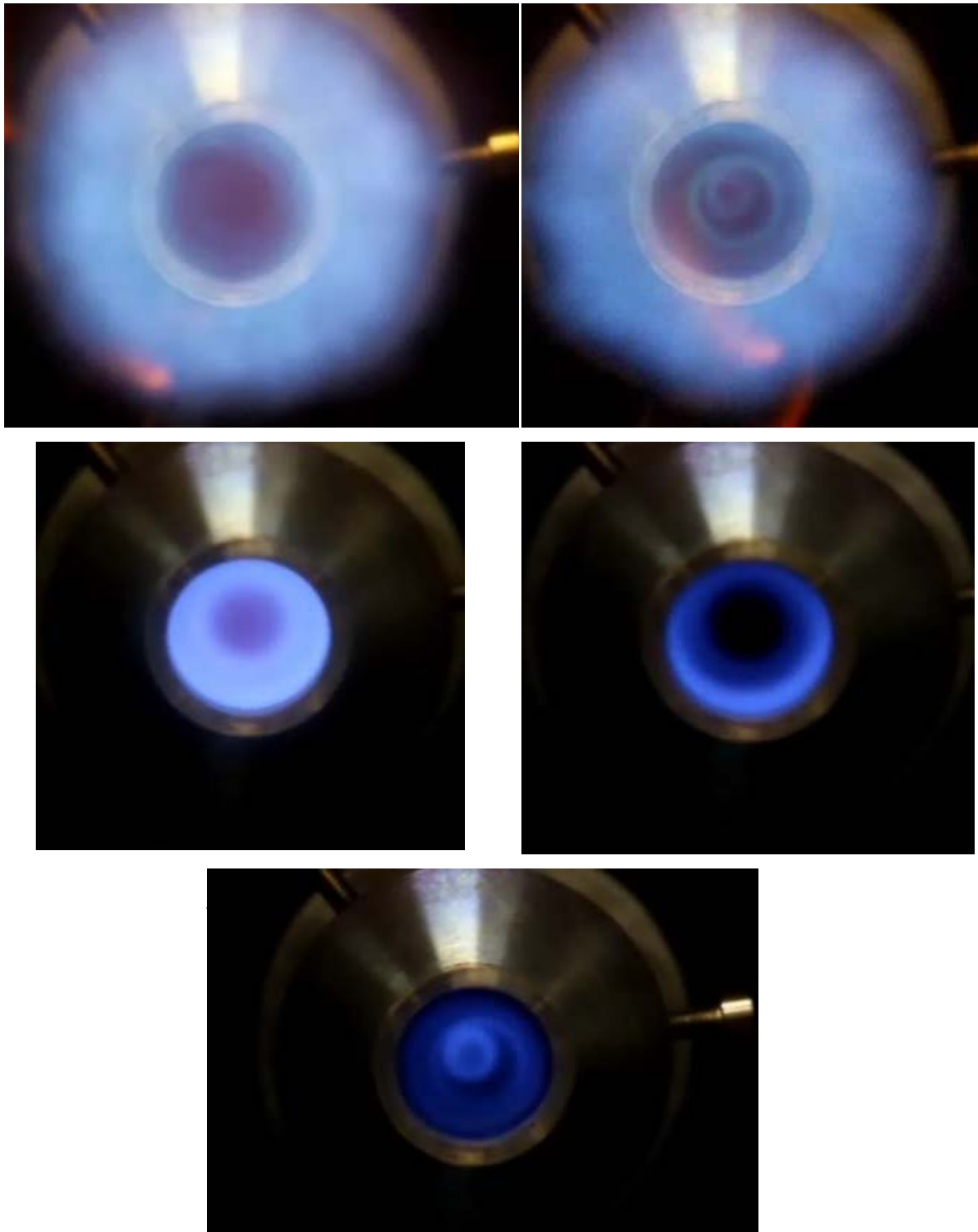


Figure 7.12: 30% H_2 +70% CH_4 Mixture blowoff flame stages for swirl burner number $S_C=0.8$ with cylindrical confinement and conical cup exhaust ($\dot{m}_f = 0.35g/s$).

A crucial factor with the case of 30% H_2 is the change in combustion behaviour when the fuel mass flowrate is increased from 0.35g/s to 0.6g/s. This is illustrated below:

Figure 7.13 shows a series of images, 1 to 4 of combustion with the open exhaust cylindrical confinement ($S_c=0.8$, 0.35g/s of fuel). These start from the fuel rich condition, image 1, and progress through $\phi = 1$ to the lean premixed condition and flame blowoff. Note how the flames are located generally, at least in part, in and past the exhaust of the confinement near until near the blowoff point, image 4. Blowoff was a smooth process with little noise.

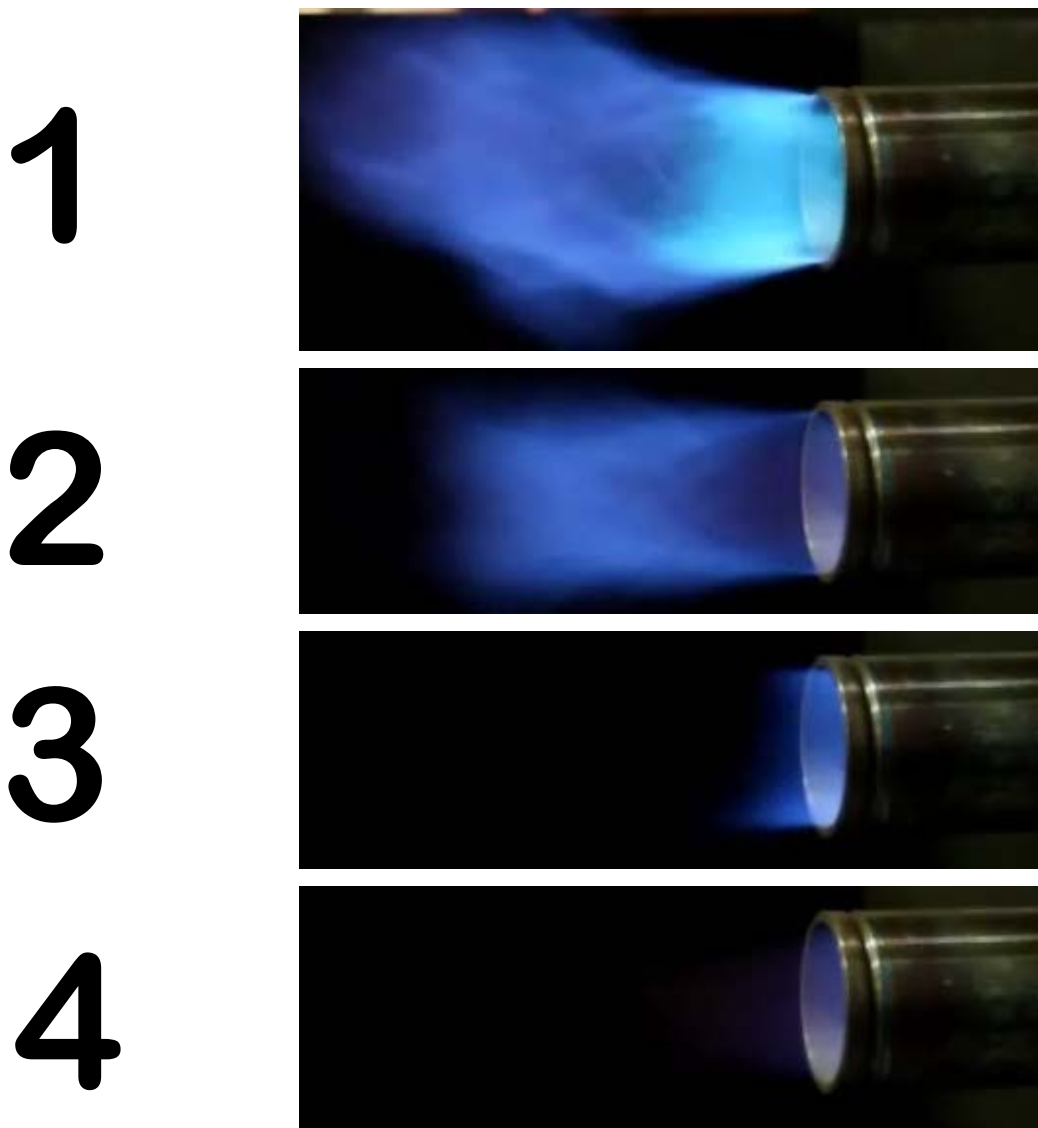
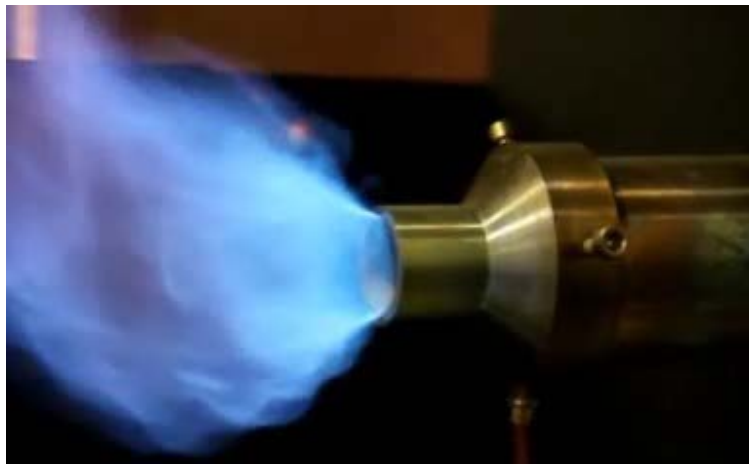


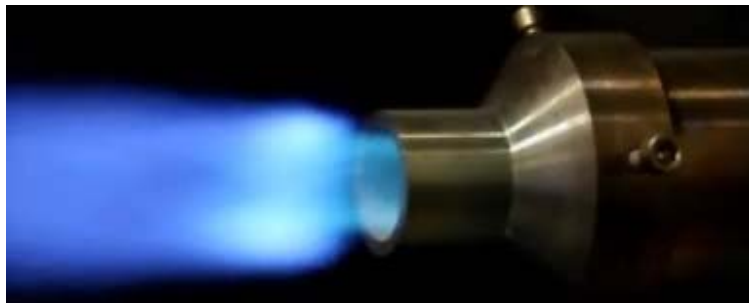
Figure 7.13: 30% H_2 +70% CH_4 Mixture blowoff flame stages for swirl burner number $S_c=0.8$ with Cylindrical Confinement ($\dot{m}_f = 0.35g/s$).

Similarly, in Figure 7.14 the images 1 to 4 show the same conditions as Figure 7.14, but with the conical cup exhaust. The conical cup exhaust is forcing more of the combustion process to occur in the open past the end of the conical cup exhaust. It is only in image 5, close to blowoff that the flame is largely located in the confinement. Blowoff is a gradual, smooth, process again.

1



2



3



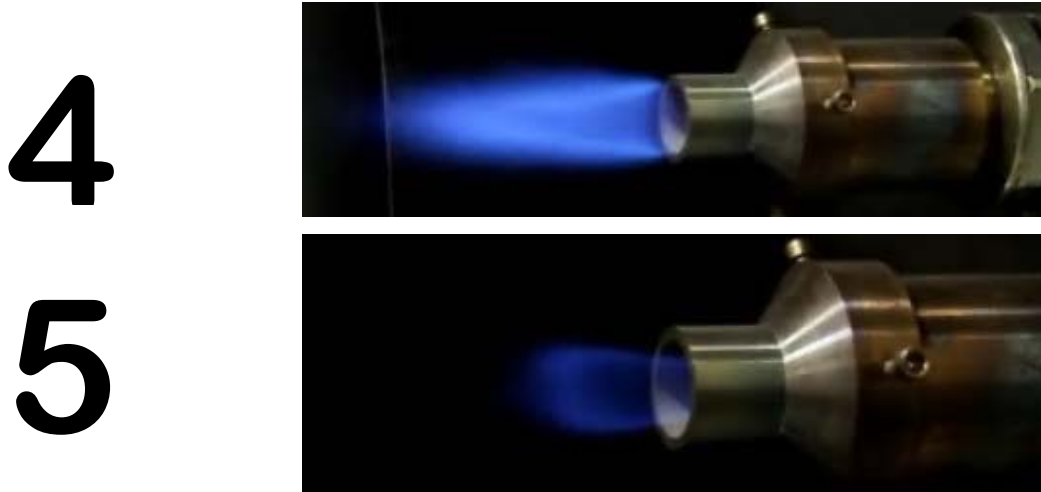


Figure 7.14: 30%H₂+70%CH₄ Mixture blowoff flame stages for swirl burner number $S_c=0.8$ with cylindrical confinement and conical cup ($\dot{m}_f = 0.35\text{g/s}$).

Significant changes occurred when the fuel mass flowrate was increased to 0.6 g/s, especially for lean combustion with the cylindrical confinement and conical cup exhaust, $S_c=0.8$. Figure 7.15 shows images of the combustion process moving from fuel rich to fuel lean and then blowoff. Images 1 to 3 show rich combustion with the flames extending beyond the confinement exhaust. Stoichiometric combustion occurs at image 4 when intense combustion occurs inside the confinement with no external flame. Image 5 shows very lean premixed combustion with a small external flame whilst, image 6 shows the flame just before blowoff. Blowoff itself is very gradual and smooth. At $\phi \sim 1$ the combustion process was intense and very noisy, indicating the presence probably of the precessing vortex core and /or acoustic coupling.

1



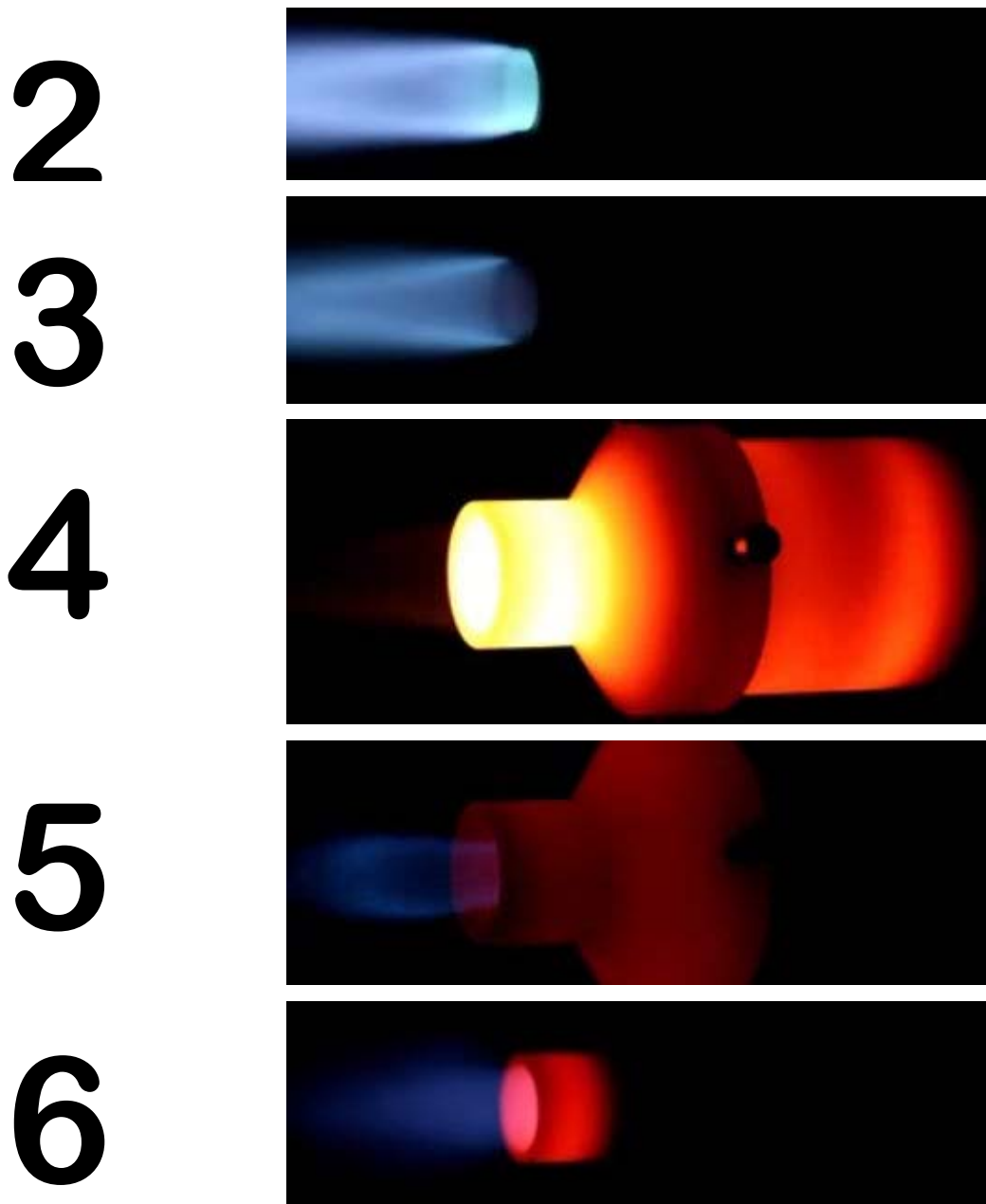


Figure 7.15: 30% H_2 +70% CH_4 Mixture blowoff flame stages for swirl burner number $S_c=0.8$ with cylindrical confinement and conical cup ($\dot{m}_f = 0.6 g/s$).

Coke oven gas was also investigated to obtain the blowoff limit map. Figures 7.16 and 7.17 show the blowoff map for the open flame case and the cylindrical confinements for swirl numbers $S_B=1.04$ and $S_c=0.8$. The flashback and blowoff limits were very close together for

the case of the cylindrical confinement and conical cup exhaust. The combustion process could be very violent here and restricted the range of measurements.

Nevertheless, coke oven gas still has the best blowoff limits with the open flames and the open exhaust cylindrical confinement compared to all the other fuel blends that have been tested in this PhD programme. The effect of the confinement has been useful, but not as significant as the effects occurring with other fuel blends.

For both swirl numbers the effect of the confinement has been an enhancement of blowoff limits by 15% to 20% at 5g/s total mass flowrate rising to 40% with maximum total mass flowrate of 27 g/s.

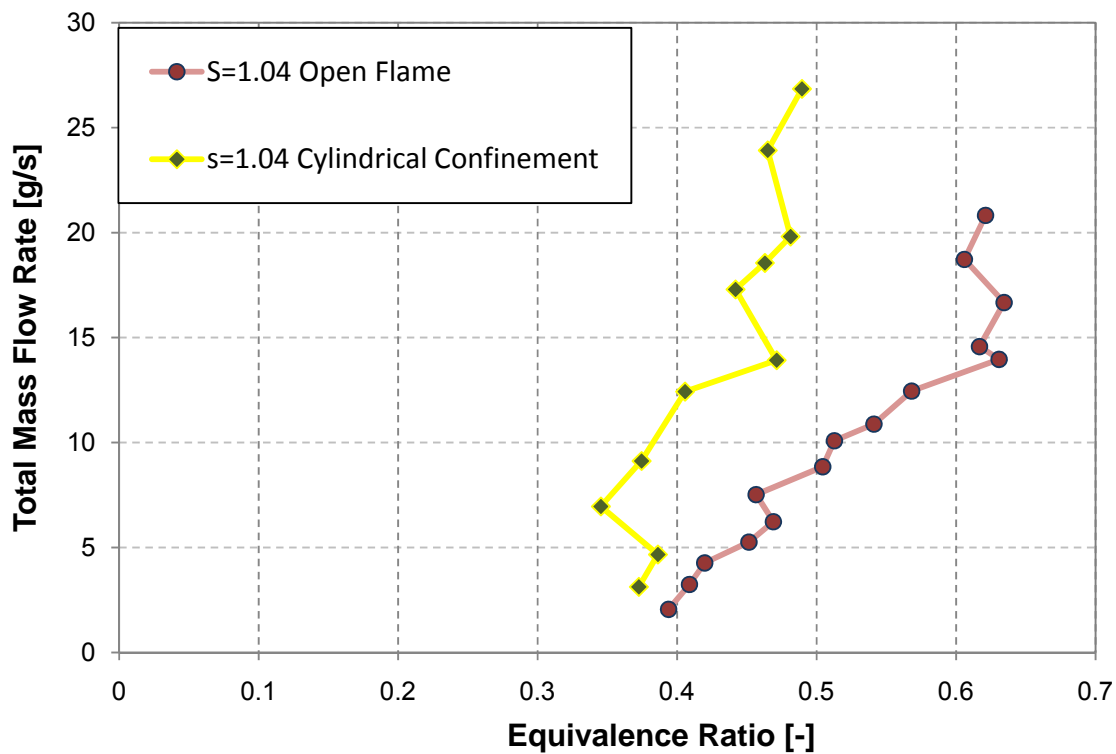


Figure 7.16: Blowoff comparison between two types of flame for swirl burner number $S_C=1.04$ for coke oven gas

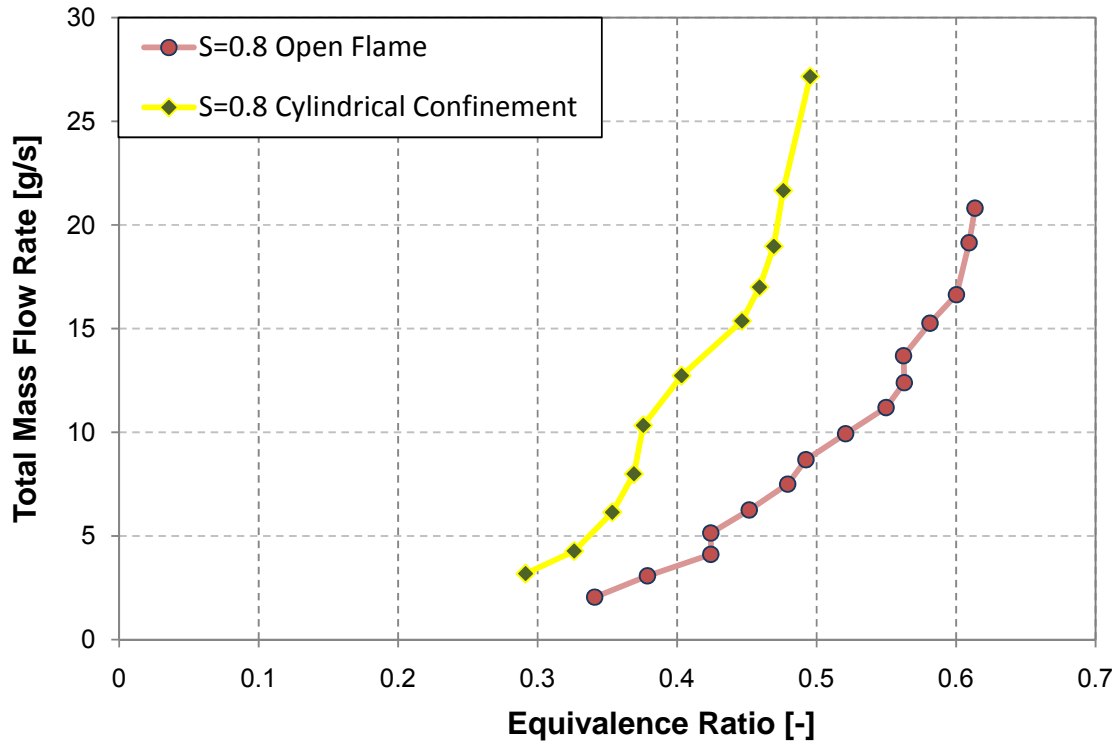


Figure 7.17: Blowoff Comparison between two types of flame for swirl burner number $S_C=0.8$ for coke oven gas

It is to be expected that blowoff will improve as the % of hydrogen in the fuel mix increases. Indeed one problem is that there do not appear to be measurements of the blowoff of hydrogen flames as assumptions are made that flashback is the crucial parameter with hydrogen. This work has shown that there is a problem of coalescence of the blowoff and flashback limits with hydrogen rich fuel mixes, as shown by this work with COG fuel gas blend.

The effect of the confinement is as to be expected, restricting heat loss from the flame root and preventing entrainment of cool gases into the flame, hence quenching. What is unexpected is the effect of the conical cup exhaust to the confinement and its effect on blowoff limits. This clearly needs further investigation and a range of different exhaust nozzles investigated that are appropriate for guiding the combustion gases into the turbine stage.

Chapter Eight

**COMPARISONS OF
FB/BF AND
DERIVATION OF
OPERATIONAL
REGIONS FOR
BURNER**

CHAPTER EIGHT

COMPARISONS OF FB/BO AND DERIVATION OF OPERATIONAL REGIONS FOR THE BURNER

"Intelligence is the ability to adapt to change."

Stephen Hawking

8.1 Introduction

A gas turbine, required to be dual fuelled, with given compressor and turbine systems has air mass flowrates at given thermal inputs which vary little as the fuel mass flow is relatively small and the exhaust gas composition, hence enthalpy, is still dominated by the 80% nitrogen content from the air. To produce this thermal input different quantities of fuel and thus equivalence ratio are needed for different fuels such as natural gas, coke oven gas and especially pure hydrogen. When dual fuelling/changeover is needed ideally the operational range of the system between flashback and blowoff for two different fuels (such as hydrogen and natural gas) should be such that there is sufficient overlap between the blowoff and flashback limits to enable easy fuel change over. Because of the different stoichiometry and heating value, hydrogen containing fuels will always have to be operated at weaker equivalence ratios compared to natural gas fired systems, typically 78% of the

natural gas equivalence ratio for pure hydrogen. This infers that the overlap region between the flashback limit and blowoff limit of given fuels is crucial in determining whether or not the system can be dual fuelled. In Chapter 5, Table 5.2 indicates that because of similar adiabatic flame temperature and lower heating values, fuel gases containing up to 65% hydrogen (as with coke oven gas) with a base fuel of natural gas can be best accommodated in existing or somewhat modified combustion systems.

Flashback and blowoff limits are both extremely important when fuel flexibility is desired as the different stoichiometry requirements and different turbulent flame speeds of different fuel blends means that for a given air flow (for instance in a gas turbine) different fuel flows and stoichiometry are needed. Moreover, for the same or similar combustor geometry the operating points for pure hydrogen and natural gas should lie in an operational regime between the blowoff and flashback limits of both fuels. In practice, this is extremely difficult but is achievable with certain fuel blends where the hydrogen content is not too high.

The above two mentioned phenomena are affected by many factors: the type of fuel blend mixture, the swirl number, air pressure, air temperature and flame speed. The first two parameters have been discussed during this research in Chapters 6 and 7.

8.2 FB/BF Operation Region Open Flame (Unconfined Burner)

Using the data of flashback and blowoff gathered from Chapter 6 and 7, respectively, FB/BF operational regions can be plotted for a specific value of swirl number and to include all fuel blends.

For open flame case at $S_A=1.47$ the data of flashback limits from Figure 6.1.a and blowoff limit (when available) from Figure 7.2, has been re-plotted in terms of heat input [116] to give Figure 8.1. Here total mass flow is plotted against thermal input, the important parameter for gas turbines. Only for methane has there been included weak and rich values of equivalence ratio, for the rest of the blends only lean combustion up to a maximum

equivalence ratio of 1.1 have been used. The four sets of curves compare four other fuel blends against methane to see what extent premixing can be accommodated, this judgement being based on there being areas of the plots where the combustor can operate without flashback or blowoff. The curves show the burner could be operated with premixed methane up to thermal limits of ~ 70 kW for a total mass flow of air and fuel of ~ 12 g/s. Flashback with methane could be avoided by operating at mass flows > 2 g/s and thermal inputs > 5 kW.

Figure 8.1.a compares pure methane and pure hydrogen. No blowoff limits could be obtained for hydrogen, only flashback. As the hydrogen flashback limit is far above the methane blowoff limit the option for alternative fuel firing is impossible, unless the hydrogen is burnt via diffusion flames. This is entirely possible but gives high NO_x.

Figure 8.1.b compares methane and Coke Oven gas (COG). Again, the flashback curve for the COG is above the blowoff limit for methane for the lean premixed side of COG. There is no option for alternative fuel firing in the lean premixed regime. As with pure hydrogen diffusion flames for the coke oven gas can be considered with a high NO_x penalty.

Figure 8.1.c compares methane and 15% H₂/CH₄. Here the flashback curve is also above the blowoff limit and again there is no possibility for premixed dual firing with this fuel. Again diffusion flames would have to be used.

Figure 8.1.d compares methane and 30% H₂/CH₄ fuel mix. Again, the flashback curve of 30% H₂ is above the blowoff limit of methane and there is no possibility for swapping fuel between methane and 30% H₂+70% CH₄ mixture.

Premixed fuelling for all these cases, swirl burner open flame $S_A=1.47$, is not possible because all types of fuel will encounter a flashback problem with hydrogen fuels if the designer wants to operate under lean premixed conditions, as the possible operational regimes do not overlap.

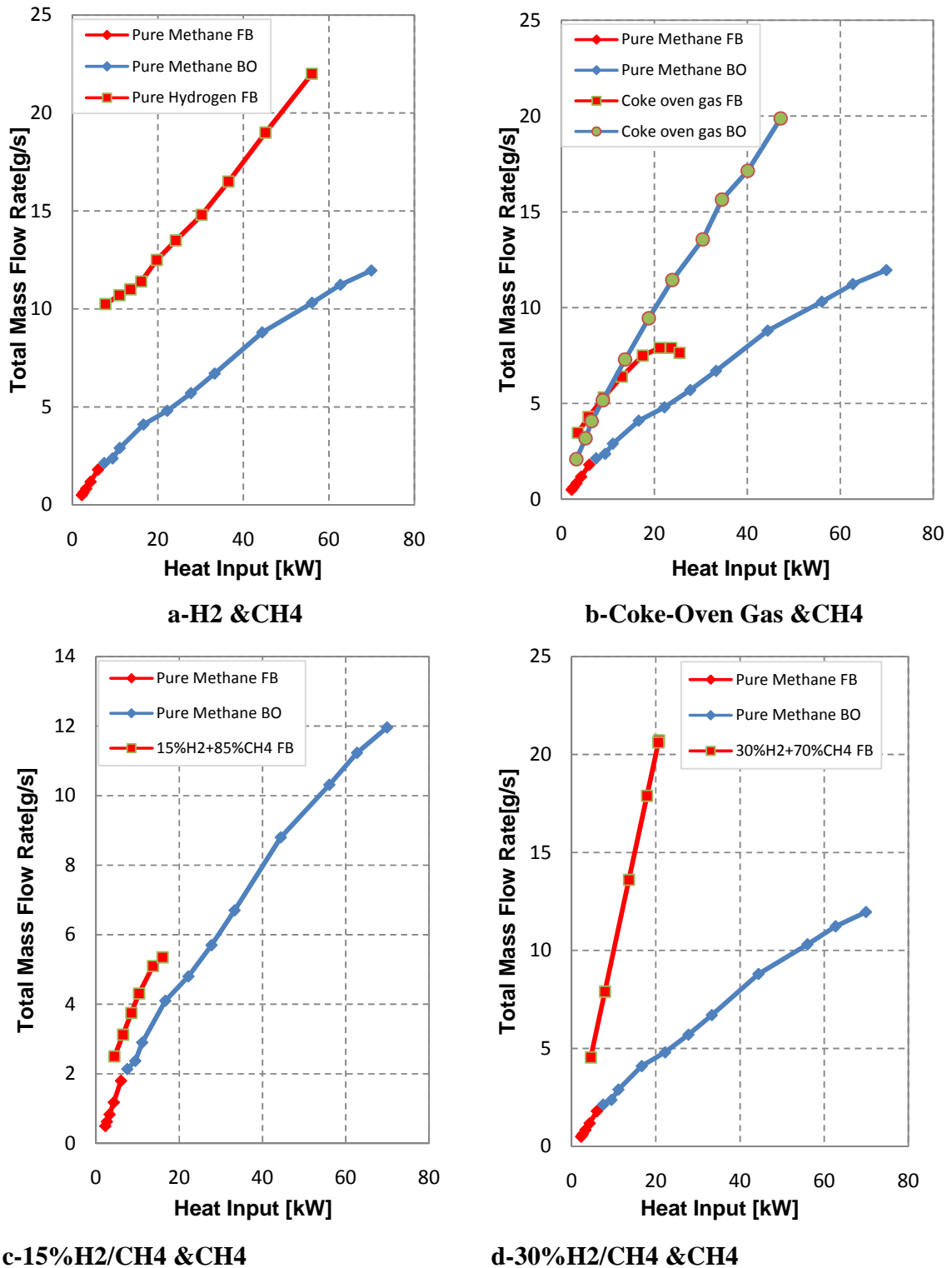


Figure 8.1: FB/BO limits as a function of total mass flow and heat input for combination of methane and other gas, open flame for swirl number $S_A=1.47$

In Figure 8.2 the data of Figure 6.1.b and 7.2 has been re-plotted in terms of heat input, solely for weak combustion up to an equivalence ratio of 1 ($S_B=1.04$, open flame). Blowoff limits have also been incorporated when available: The four sets of curves compare four other fuel blends against methane to see what extent premixing can be accommodated. The curves show the burner could be operated with premixed methane up to thermal limits of ~ 22 kW for a total mass flow of air and fuel of ~ 6.2 g/s. Flashback with methane could be avoided by operating at mass flows > 0.8 g/s and thermal inputs > 2.5 kW [42-43].

Figure 8.2.a compares pure methane and pure hydrogen. No blowoff limits could be obtained for hydrogen, only flashback. As the hydrogen flashback limit is far above the methane blowoff limit the option for alternative fuel firing is as follows: For a given thermal input, say 15 kW and 4 g/s total flowrate, only 4kW of heat could be provided by hydrogen premixed combustion if hydrogen flashback is to be avoided. The rest of the heat, 11kW, would have to be produced by diffusion combustion.

Figure 8.2.b compares methane and coke oven gas (COG). Again, the flashback curve for the COG is above the blowoff limit for methane. The options for alternative fuel firing are thus: For the same given thermal input, 15 kW and 4 g/s total flowrate, only ~ 7.5 kW of heat could be provided by COG premixed combustion if COG flashback is to be avoided. The rest of the heat, 7.5 kW, would have to be produced by diffusion combustion.

Figure 8.2.c compares methane and 15% H_2/CH_4 . Here the flashback curves for the two fuels are quite close together, only restricting the mass flow to above 1 g/s and a thermal input of ~ 4 kW. As blowoff limits are also close together, alternative premixed fuelling is quite possible with premixed combustion at the conditions of 15 kW and mass flow of 4 g/s; there are also numerous other possible operating conditions.

Figure 8.2.d compares methane and 30% H_2/CH_4 fuel mix. Again, the blowoff limits are quite close, whilst the worsening flashback limits for the 30% H_2/CH_4 fuel mix only restrict mass flow to above 2 g/s and thermal input to 5 kW. Alternative premixed fuelling is again quite possible with premixed combustion at 15 kW and 4 g/s and again with numerous other possible operating conditions.

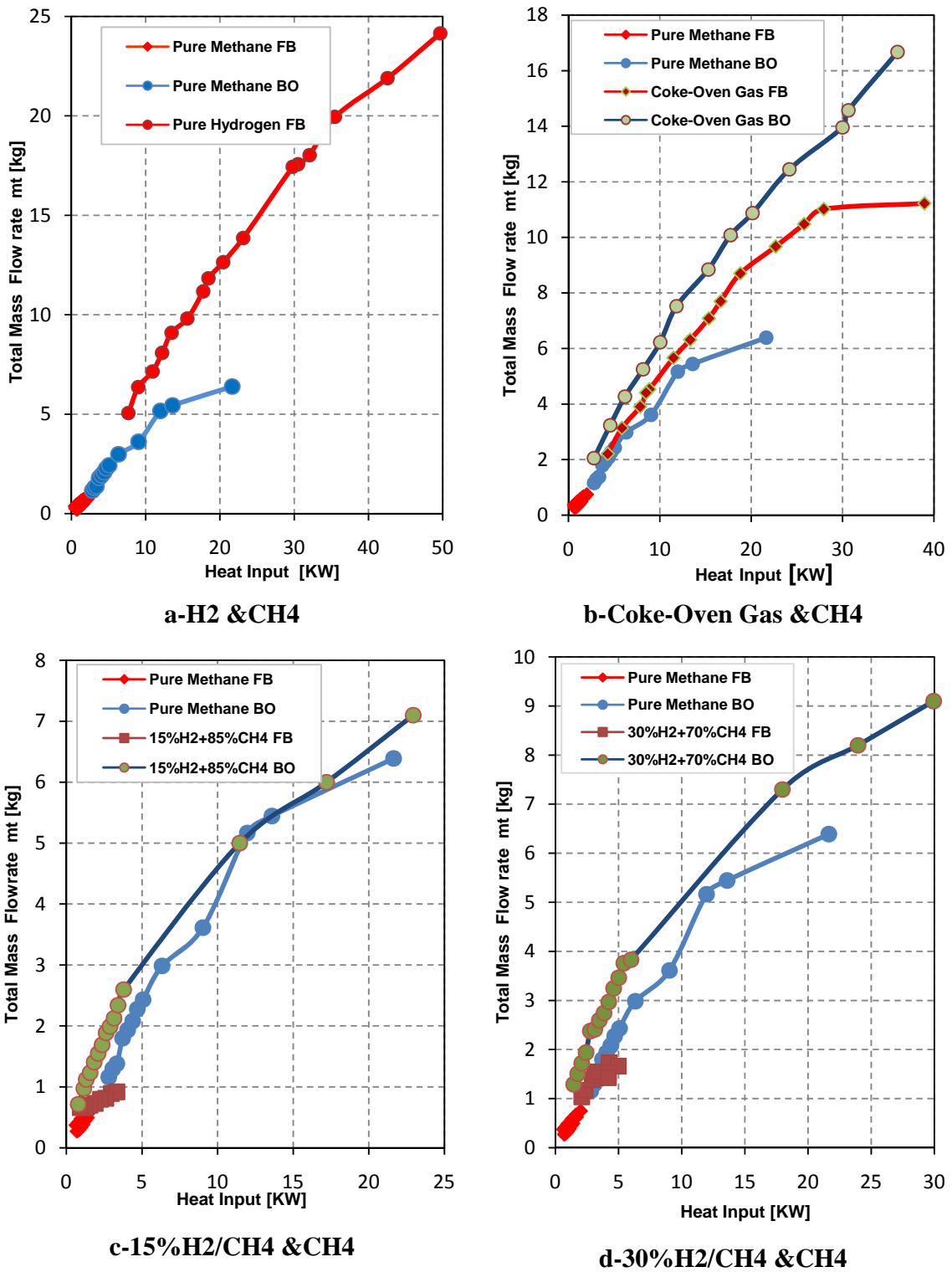


Figure 8.2: FB/BO limits as a function of total mass flow and heat input for combination of methane and other gas, open flame, for equivalence ratios up to 1 for swirl number $S_B=1.04$

Thus the swirl number of $S_B=1.04$ gives two possibilities for using alternative fuel mixture blends containing 15% and 30% hydrogen.

Pursuing this concept further, Figure 8.3 [118] shows four graphs that describe the capability of swapping fuel from methane to four other fuel blends for a swirl burner with $S_C=0.8$. Methane flashback limit curves have an equivalence ratio range from lean mixture $\Phi=0.6$ to rich mixture $\Phi=1.5$ but all the data that has been used for blowoff is for lean combustion.

Figure 8.3.a shows that a pure hydrogen flashback curve comes over the blowoff limit of methane and is similar to other previous cases. So, there is no way to swap the fuel from pure methane to pure hydrogen with premixed combustion.

Coke oven gas (COG) follows the same scenario in Figure 8.3.b. Flashback and blowoff curves are above the blowoff limit of pure methane, which means there is no possibility to change between them because either the system will encounter flashback or will operate under a rich fuel mixture, which is undesirable.

Figure 8.3.c compares pure methane and 15% H_2/CH_4 . Here the flashback curves are quite close for the two fuels, only limiting the mass flow to above 1.5 g/s and to above a thermal input of ~ 5 kW. As blowoff limits for the two fuels are close, alternative premixed fuelling is quite possible with premixed combustion at the conditions of 20 kW and mass flow of 5 g/s, for instance.

Figure 8.3.d compares methane and a 30% H_2/CH_4 fuel mixture. Again, the blowoff limits are quite close, whilst the worsening flashback limits for the 30% H_2/CH_4 fuel mixture only confine mass flow to being above 1.6 g/s and a thermal input of above 6.5 kW. Alternative premixed fuelling is again to a certain extent possible with premixed combustion at 20 kW and 5 g/s for instance. Again, there is a wide possible operational regime.

The swirl burner with $S_C=0.8$ therefore gives the widest range of premixed fuelling with the fuel blends tested, certainly up to 30% H_2 , 70% CH_4 fuel blends.

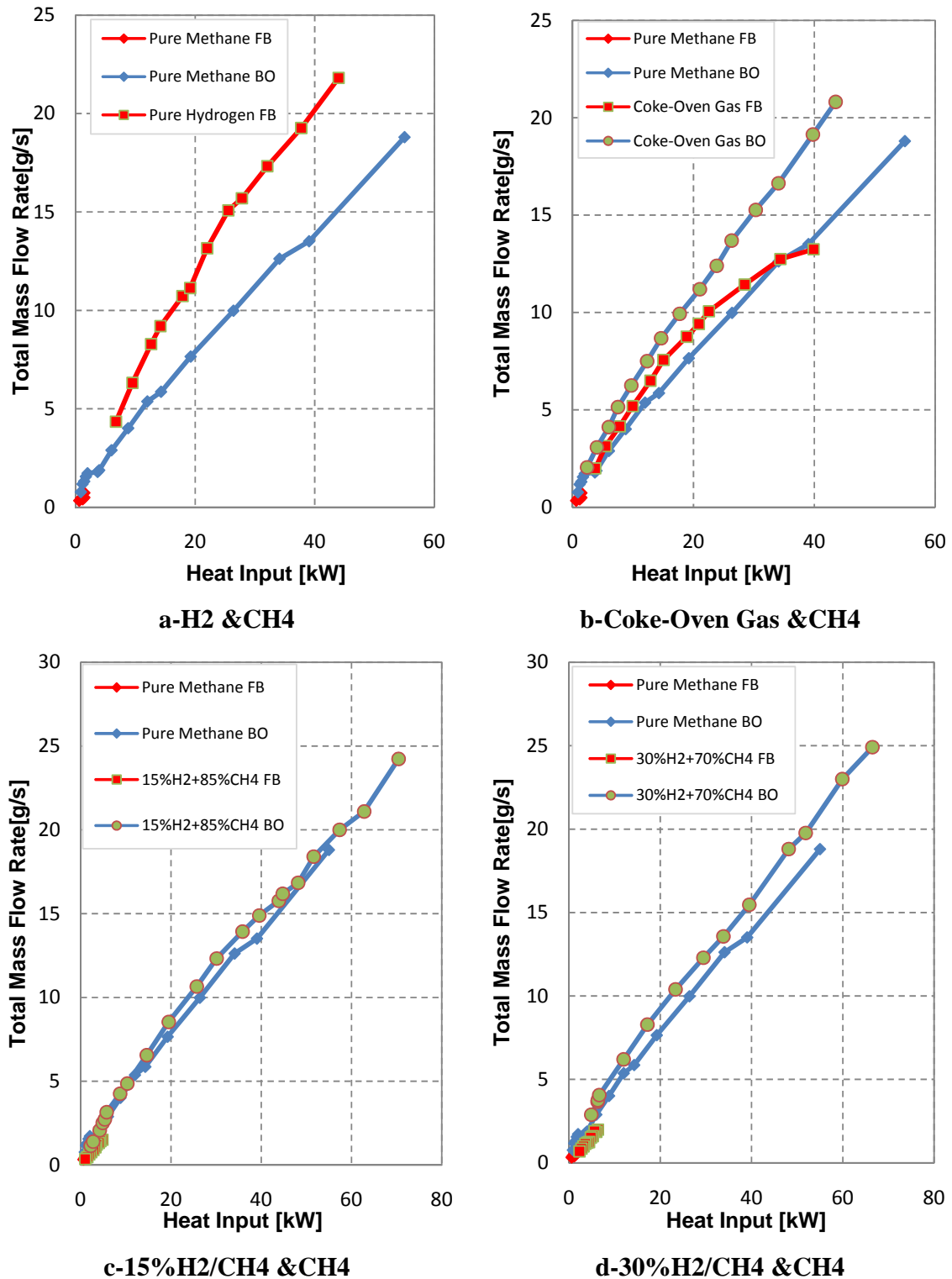


Figure 8.3: FB/BO limits as a function of total mass flow and heat input for combination of methane and other gas, open flame, for swirl number $S_C=0.8$

8.3 FB/BF Operation Region of the Burner with Confinements

It has been found in the analysis (Chapters 6 and 7) that adding confinements to the swirl burner have strongly improved blowoff limits and at least for one confined configuration kept flashback limits without any substantial degradation from the open flame condition.

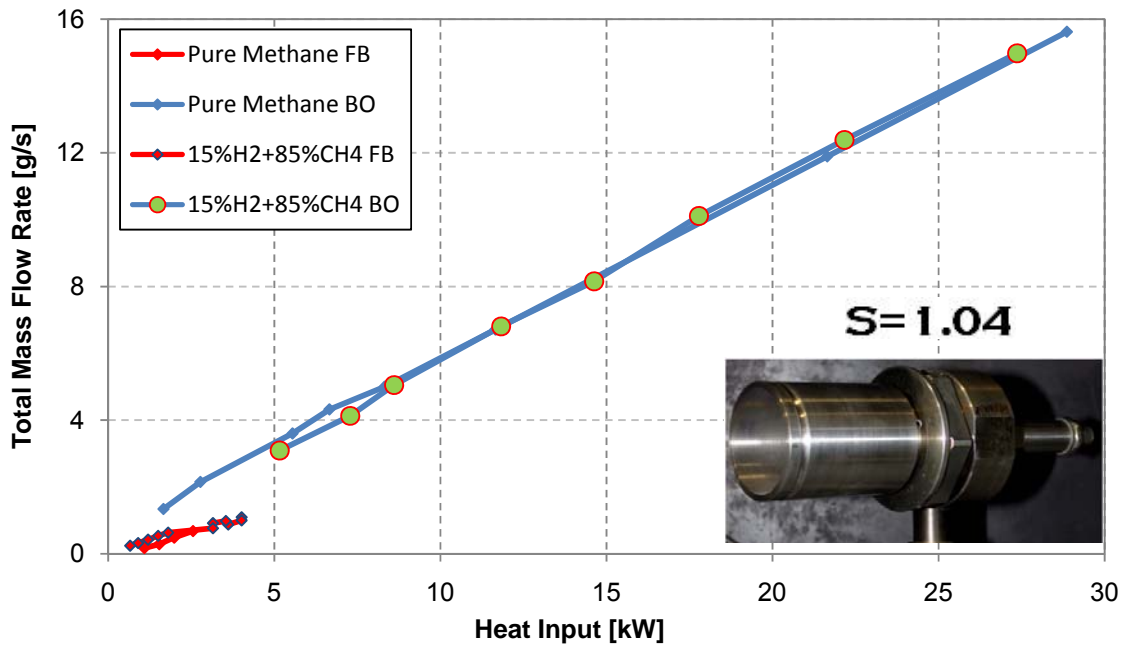
The FB/BO relationship has been determined and plotted for only two fuel blends (15% H_2/CH_4 and 30% H_2/CH_4) to compare with pure methane. This was not possible with pure H_2 and coke oven gas as flashback and blowoff limits were often very close and difficult to determine.

The following figures, numbered 8.4 to 8.7, have used the data of flashback limits and blowoff limits from Chapters 6 and 7 and include swirl burners with confinements (cylindrical confinements with and without the conical exhaust cup). These data have been re-plotted in terms of heat input.

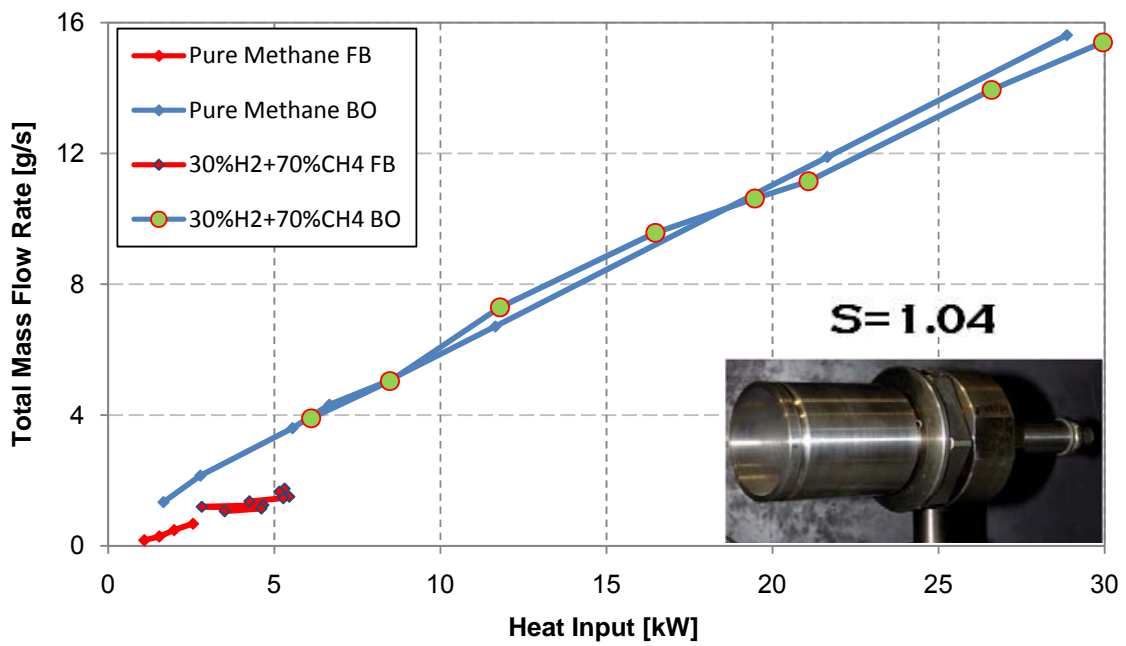
The two sets of curves in Figures 8.4.a and 8.4.b compare two fuel blends, 15% H_2 and 30% H_2 , against methane to see to what extent premixing can be accommodated in a swirl burner with $S_B = 1.04$. The curves show the burner could be operated typically with premixed methane up to a thermal limit of 30 kW for a total mass flow of air and fuel of ~ 16 g/s. Data ran out at this point due to rig limitations. Flashback with methane could be avoided by operating at mass flows > 1.5 g/s and thermal inputs > 4 kW.

Figure 8.4.a compares pure methane and 15% H_2/CH_4 . Here the flashback curves are quite close, only restricting the mass flow to above 1.5 g/s and a thermal input of ~ 4 kW. As blowoff limits are close, alternative premixed fuelling is quite possible with premixed combustion at the conditions of 15 kW and mass flow of 4 g/s for instance.

Figure 8.4.b compares side methane and 30% H_2/CH_4 fuel blend. Again, the blowoff limits are quite close, whilst the worsening flashback limits for the 30% H_2/CH_4 fuel mixture only confine mass flow to above 2 g/s and thermal input to 6 kW. Alternative premixed fuelling is again possible with premixed combustion at 15 kW and 4 g/s.



a- CH4 & 15%H2+85%CH4



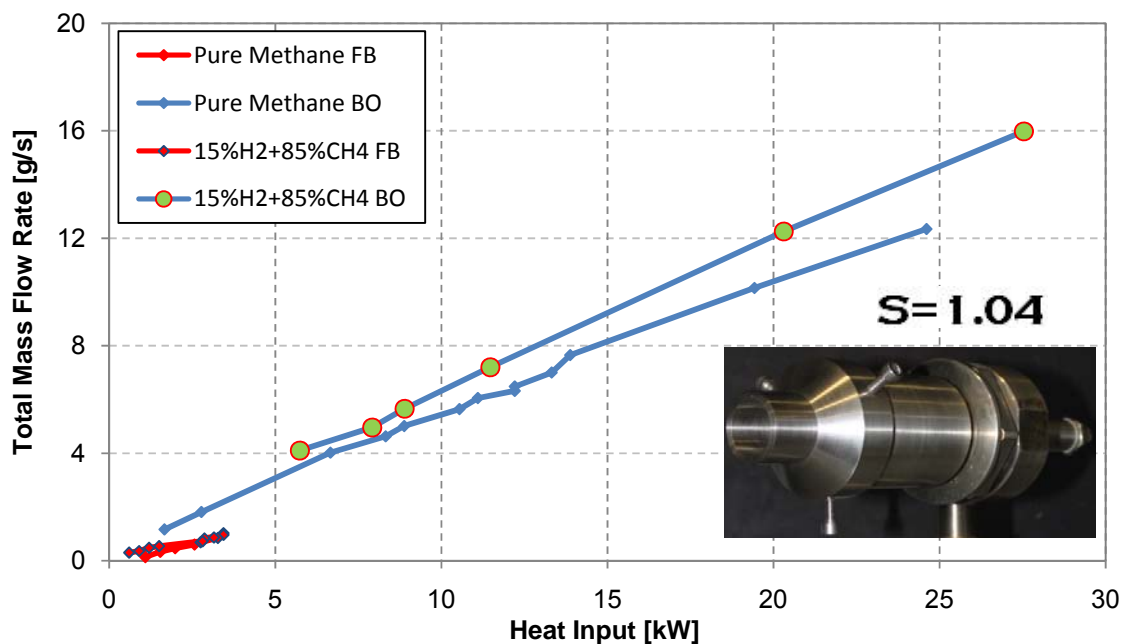
b- CH4 & 30%H2+70%CH4,

Figure 8.4 FB/BO limits as a function of total mass flow and heat input, $S=1.04$, confined flame (cylindrical confinement open exhaust)

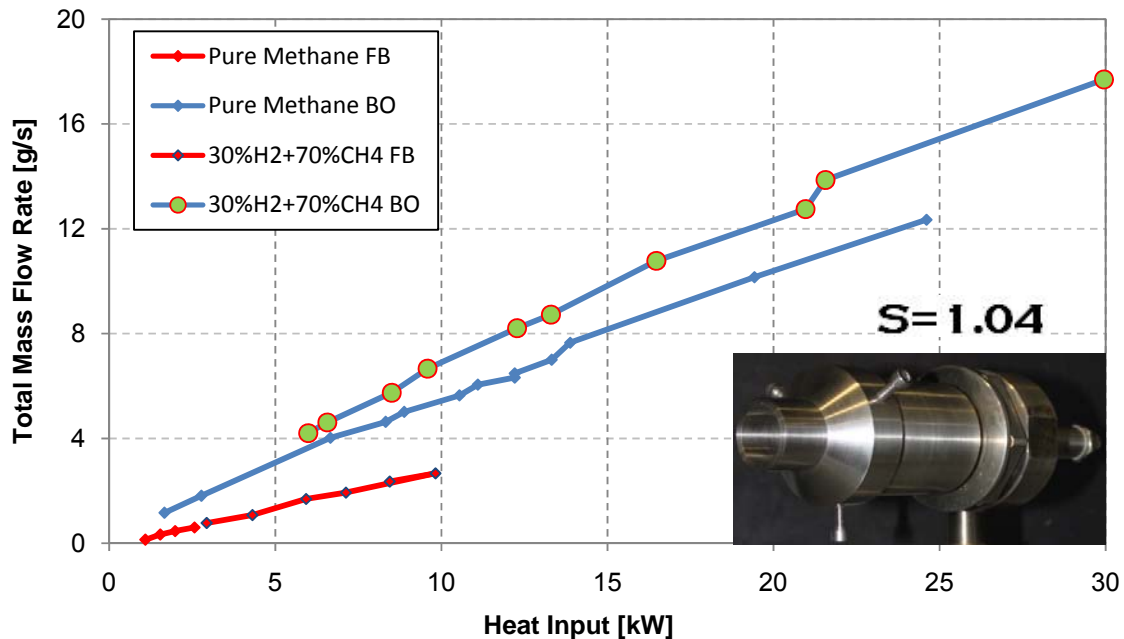
The cylindrical confinement with conical cup exhaust show quite similar results for 15% H_2 fuel blend but a worsened result for the 30% H_2 fuel blend compared to with the cylindrical confinement results on (without conical cup), as shown in Figure 8.5. The two sets of curves compare 15% and 30% hydrogen content fuel blends against methane to see what extent premixing with dual fuelling can be achieved.

The curves in Figure 8.5.a shows there is a wide operational range for dual fuelling with 15% H_2/CH_4 fuel blends with methane, the only limits being flashback below 1.5 g/s total mass flow and 4kW thermal input and the methane blowoff curve (the lowest).

Figure 8.5.b compares methane and 30% H_2/CH_4 fuel blends. Again, dual fuelling is entirely possible over a substantive range of heat inputs and mass flowrates, the operational range is determined by the flashback limit for the 30% H_2/CH_4 fuel blend and the methane blowoff curve. One possible operational point is 15 kW thermal input and 4 g/s total mass flow.



a- CH_4 & 15% H_2 +85% CH_4



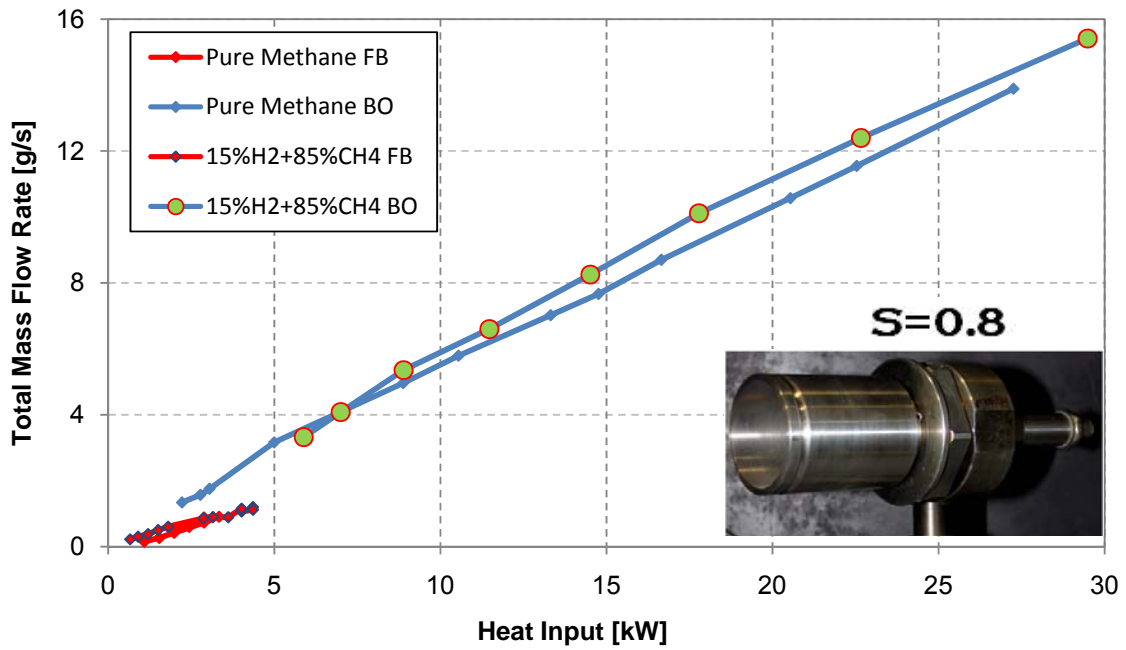
b- CH₄ & 30%H₂+70%CH₄

Figure 8.5: FB/BO limits as a function of total mass flow and heat input, $S=1.04$, confined flame (cylindrical confinement & conical cup exhaust)

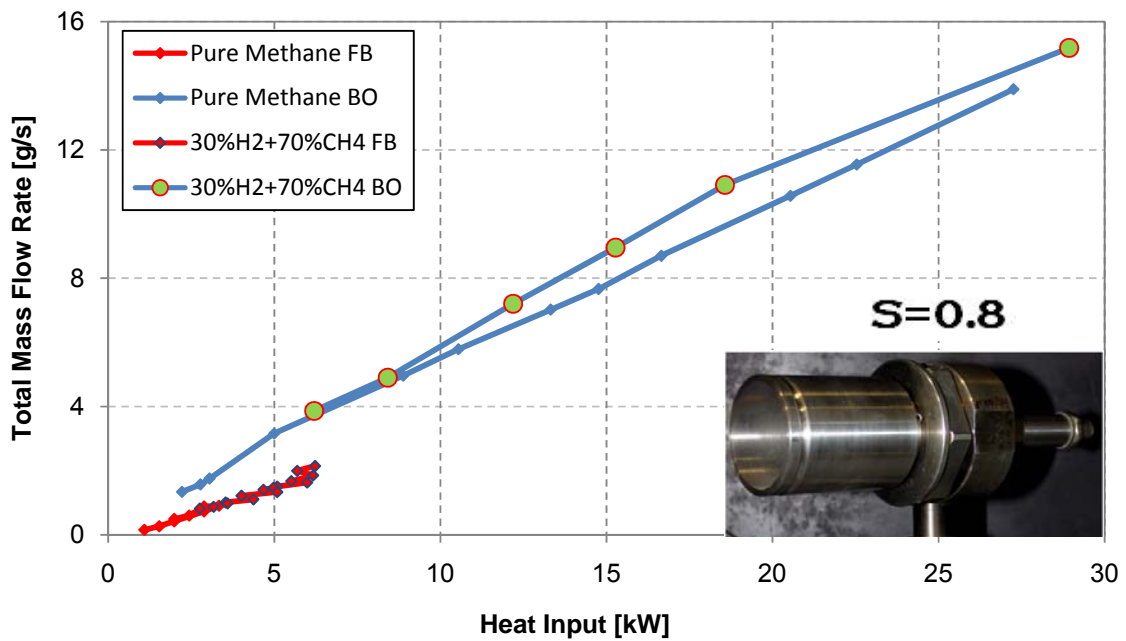
A similar set of results has also been derived for the $Sc=0.8$ case and the two different confinements, these results are shown in Figures 8.6.a and 8.6.b. They compare the two fuel blends, 15%H₂/85%CH₄ and 30%H₂/70%CH₄, against methane as well. The curves show the burner could be operated with premixed methane up to a thermal limit of before 30 kW for a total mass flow of air and fuel of ~ 16 g/s. Flashback with methane could be avoided by operating at mass flows > 1.5 g/s and thermal inputs > 4kW.

Figure 8.6.a compares pure methane and a 15%H₂/CH₄ fuel blend. Here the flashback curves are quite close, only restricting the mass flow to above 1.5 g/s and a thermal input of ~ 4kW. As blowoff limits are close, alternative premixed fuelling is quite possible with premixed combustion at the conditions of 15 kW and mass flow of 4 g/s, for example.

Figure 8.6.b compares methane and a 30%H₂/CH₄ fuel blends. Again, the blowoff limits are quite close, whilst the worsening flashback limits for the 30%H₂/CH₄ fuel mixture only confine mass flow to above 2 g/s and thermal input to 6 kW. Alternative premixed fuelling is again to a certain extent possible with premixed combustion at 15 kW and 4 g/s. The limits are again determined by the flashback limit of the 30%H₂/CH₄ fuel blend and the blowoff limit of the methane.



a- CH₄ & 15%H₂+85%CH₄



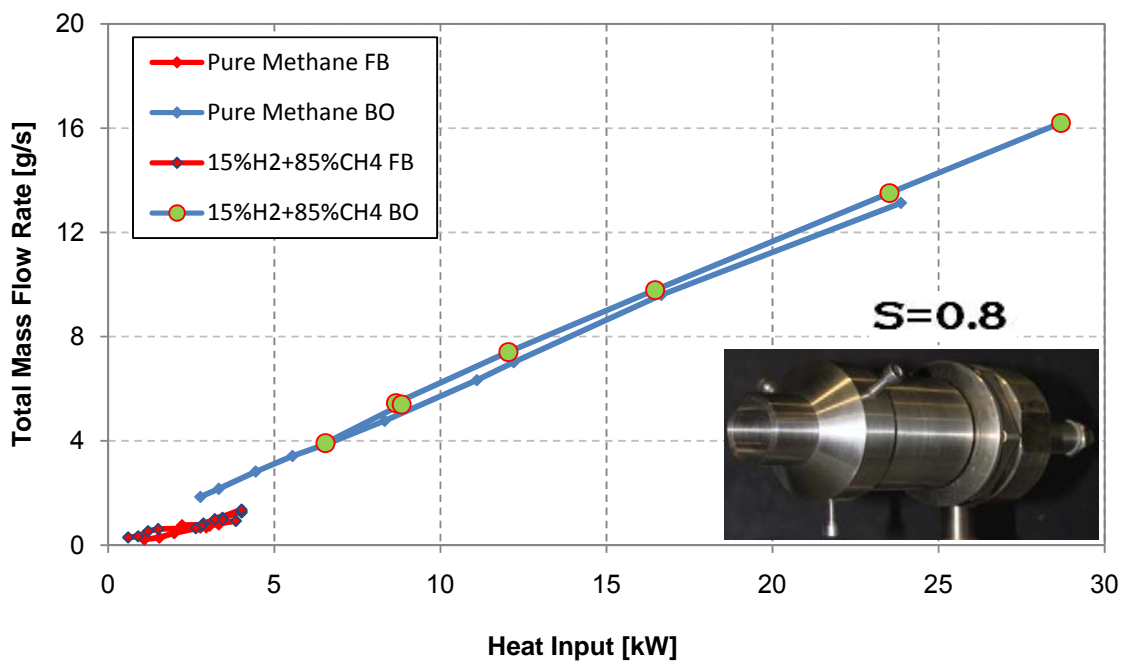
b- CH₄ & 30%H₂+70%CH₄

Figure 8.6: FB/BO limits as a function of total mass flow and heat input, $S=0.8$, confined flame (cylindrical confinement)

The addition of the conical cup exhaust to the cylindrical confinement gives very similar results for the 15% H_2 fuel blend compared to the cylindrical confinement without the conical cup. However significantly worsened results are obtained for the 30% H_2 /70% CH_4 fuel blend compared to the results for cylindrical confinement only (without conical cup), as shown in Figures 8.7. The two sets of curves compare 15% and 30% hydrogen content fuel blends against methane to see to what extent premixing can be exchanged.

The curve in Figure 8.7.a shows that the flashback for methane could be avoided by operating at mass flows > 1.5 g/s and thermal inputs > 4 kW and premixed fuelling can be changed from methane to 15% H_2 / CH_4 mixture after this value whilst avoiding reaching the blowoff limit, which is quite close for both fuel blends.

Figure 8.7.b compares methane and 30% H_2 / CH_4 fuel blend. Again, the blowoff limits are quite close, whilst the worsening flashback limits for the 30% H_2 / CH_4 fuel mixture only confine mass flow to above 3 g/s and thermal input to 10 kW. Alternative premixed fuelling is again to a certainly possible with premixed combustion at 15 kW and 4 g/s. The limitations are again the flashback curve for the 30% H_2 / CH_4 fuel blend and the methane blowoff curve.



a- CH_4 & 15% H_2 +85% CH_4

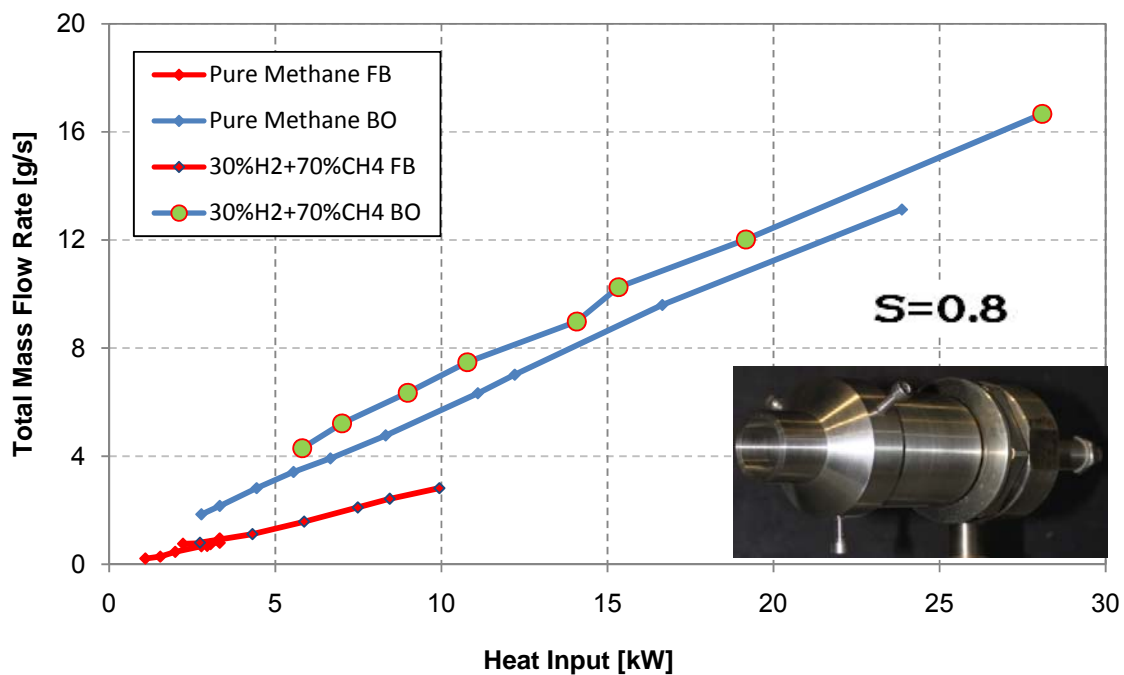
b- CH₄ & 30%H₂+70%CH₄

Figure 8.7: FB/BO limits as a function of total mass flow and heat input, $S=0.8$, confined flame (cylindrical confinement and conical cup)

8.4 Pure Hydrogen and Coke Oven Gas FB/BO Specialty

During this research, there were two gases that behaved differently to the other five alternative fuel blends used. These were pure hydrogen (100% H₂) and coke oven gas (65% H₂, 25% CH₄, 6% CO, and 4% N₂). Both gases give unstable performance in testing flashback and blowoff and it sometimes becomes impossible to identify a point of flashback and blowoff because of the violent reaction of both gases, especially with pure hydrogen. In the following section, I will explore these issues detail in more.

8.4.1 Pure Hydrogen

As discussed in the preceding chapters, the flashback and blowoff characteristics have been determined for different fuel blends. However, in some cases, a number of technical problems have been encountered during the experiments when estimating the flashback and the blowoff limits for pure hydrogen, for both unconfined and confined flames. Pure

hydrogen exhibits a different behaviour from other fuel blends during the burning process because its properties are highly dissimilar from pure methane. One problem was the size of the combustor: to fully explore the characteristics of pure hydrogen much higher mass flows were needed than were available on my rig. Unfortunately, this quantity of air is out of range of the Coriolis flow meter, which has been used in the tests. For all swirl numbers, there was no capability of completing the flashback limits or indeed determining any blowoff limits. Moreover, it is now realized that like the coke oven gas results the flashback and blowoff limits for pure H₂ are probably too close together to enable separate determination to be made in the swirl burner configuration used.

Figure 8.8 shows a pure hydrogen performance flashback map for three different swirl numbers: $S_A=1.47$, $S_B=1.04$, $S_C=0.8$. The curve covers lean and rich regions for the two latter swirl numbers and only the lean region is depicted for $S_A=1.47$. The graph shows unconnected data because of the technical difficulty mentioned above regarding air mass flowrate limitation. The flashback map is roughly the same for both $S_B=1.04$, $S_C=0.8$ and is slightly different for $S_A=1.47$. For the lower swirl numbers, $S_B=1.04$ and $S_C=0.8$ the total mass flow for stable combustion is around 5 g/s for $\phi \leq 0.4$. For $S_A=1.47$ it is about 10 g/s at $\phi \sim 0.2$. This means that the lower swirl numbers increase the region of operation for pure hydrogen. Clearly, there is a need for more work in this area to improve the pure H₂ flashback limits. A good starting point would appear to be a series of tests with fuel blends of say 50%, 60%, 70% H₂ with CH₄ to investigate flashback and blowoff. The advantage is that much lower fuel and air flowrates would be needed and progress could be slowly built up towards 100% H₂ tests.

Another difficulty with hydrogen previously mentioned is that the lean flame is invisible in normal light. Either thermocouples or other techniques need to be developed so as to be able to more easily detect flashback and blowoff with high hydrogen context fuel blends.

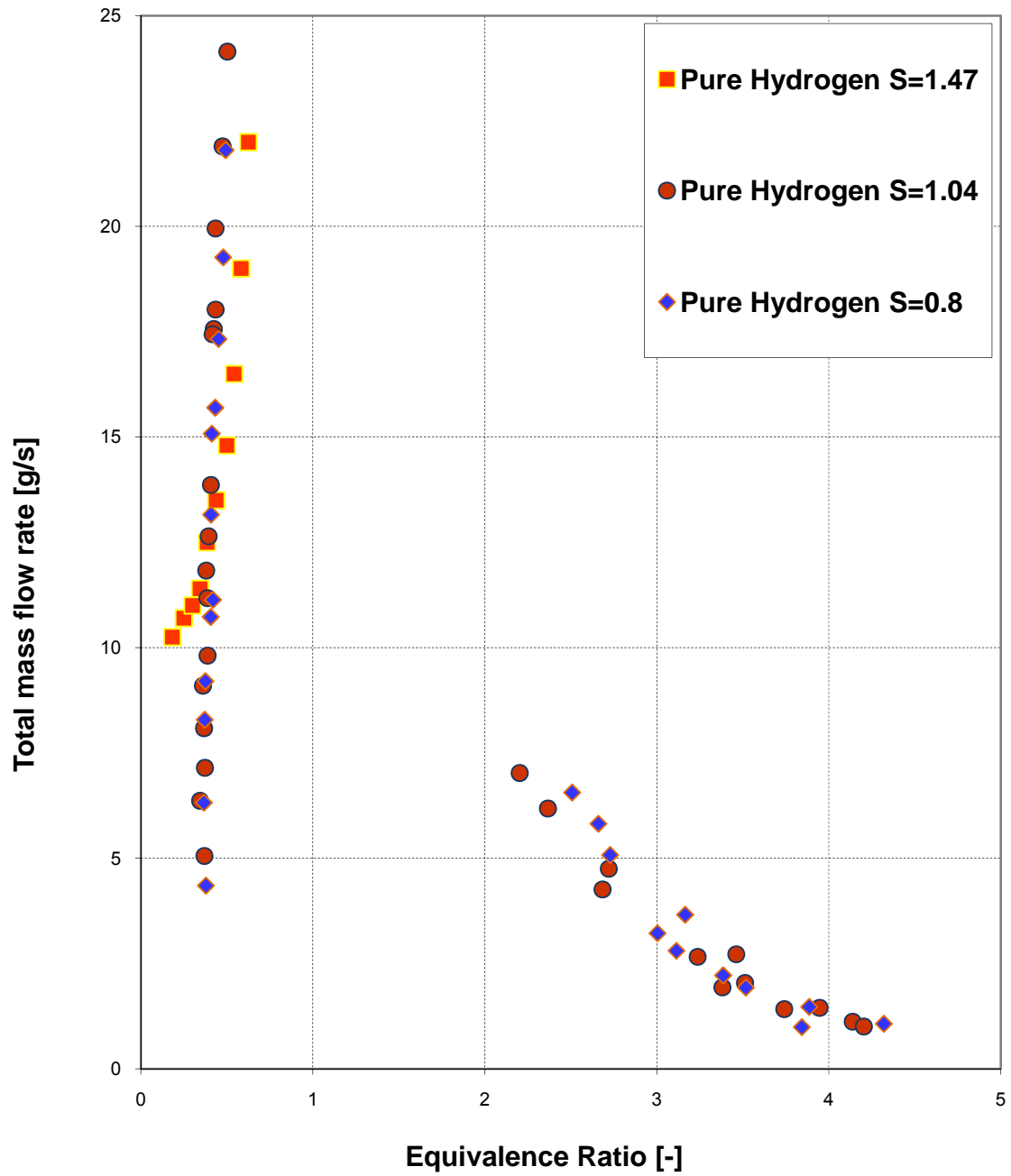


Figure 8.8: Flashback limits comparison as a function of total mass flow for pure hydrogen for different swirl numbers

8.4.1 Coke Oven Gas

Generally, coke oven gas is a complex mixture mainly containing hydrogen, methane, light oil, ammonia, pitch, tar, and other minerals released during coke oven production. The production of the gas is accomplished by the pyrolysis (heating in the absence of air) of suitable grades of coal. The process also includes the processes of remove tar, ammonia, phenol, naphthalene, light oil, and sulphur before the gas is used as fuel for heating the ovens.

Likewise, pure hydrogen has technical problems that have appeared and been encountered in the experimental measurement and prediction of flashback and blowoff limits. The problems here, coke oven gas FB/BF measurements are less than for pure hydrogen with some measurement capability on the GTRC rigs. Figure 8.9 shows flashback and blowoff limits of coke oven gas for the three swirl numbers, using the open flame data because of the difficulties of measuring these limits under confinement conditions. Figure 8.9 clearly shows that the blowoff limits for all swirl numbers are very similar, the one for $S_A=1.46$ being slightly worse than the other two. Flashback limits look similar for the burner with swirl numbers of 1.04 and 0.8 but for the high swirl number 1.47, the flashback limit peak is reduced by 50% at $\phi \sim 0.8$. However for $\phi \leq 0.5$ there is a widened flashback which makes flashback worse than for $S_B=1.04$ and $S_C=0.8$. Additionally, one important issue can be observed from Figure 8.9 below is that the flashback and the blowoff limits have become very close to each other at the fuel weak side of the graph and even, in some cases, intersect at some points. This behaviour makes it difficult in some cases to recognize flashback from the blowoff as the gas behaves violently. With the two confinements things became worse because the confinements make the flashback and blowoff limits move even closer together and they become difficult to measure. However, it would be perfectly possible to operate above the flashback limit and to the right of the blowoff curves with coke oven gases. The following summarises these limits:

$S_A=1.47$ -operation possible for total mass flowrates ≥ 8 g/s and $\phi \geq 0.5$ to 0.7 dependent upon mass flowrate;

$S_B=1.04$ and $S_C=0.8$ - operation possible for total flowrate ≥ 12 g/s and $\phi \geq 0.55$.

If sufficient airflow and fuel flow was available on the GTRC rig similar limits could probably be derived for 100% H₂ premixed combustion.

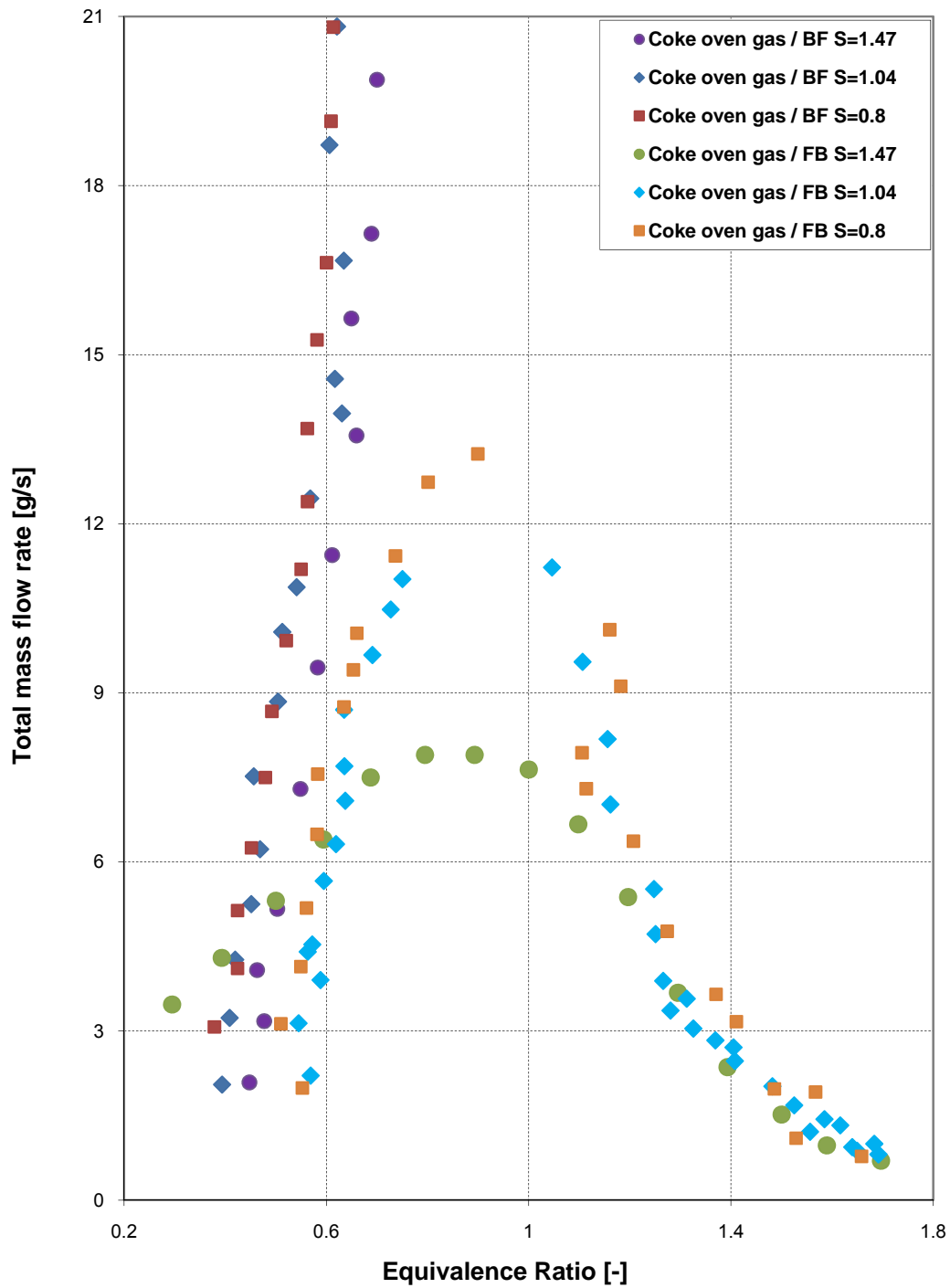


Figure 8.9: Flashback and blowoff limits comparison as a function of total mass flow for coke oven gas for different three swirl numbers.

8.5 Summary

Chapter 8 analyses further the results of Chapters 6 and 7 to try to determine the extent to which the generic swirl burner could be dual fuelled. The work has shown that the generic swirl burner can be dual fuelled with methane/hydrogen fuel mixes containing up to 30% H₂ by volume with no modifications. Best results are obtained with the open ended cylindrical confinement. With pure hydrogen and coke oven gases many difficulties were encountered; flashback and blowoff characteristics could be obtained for some, but not all conditions. Both exhaust confinements caused particular problems here as discussed above. It was shown that small levels of dual fuelling could be found with pure H₂ and coke oven gas using the open flame data. The coke oven results for flashback and blowoff with the open flame clearly showed there is a problem with the nearness of the blowoff and flashback limits for coke oven gas that has not been recognized before; this probably also applies to pure hydrogen flames.

Chapter Nine

**CONCLUSIONS
AND
RECOMMENDATIONS
FOR FUTURE
WORK**

CHAPTER NINE

CONCLUSIONS AND RECOMMENDATIONS FOR FUTURE WORK

"The saddest aspect of life right now is that science gathers knowledge faster than society gathers wisdom."

Isaac Asimov

9.1 Introduction

The importance of the various characteristics of Gas Turbine Swirl Combustors has been demonstrated throughout this work. These characteristics included stability, flashback, blowoff, swirl number, and fuel type. Therefore, their analysis requires extensive theoretical and experimental work in order to understand these characteristics, with the aim of being able to control some or all of them to reach the optimum burning condition; this gives the minimum design and operation costs as well as decreasing the amount of pollution produced through the operation of gas turbine combustors.

FLUENT software has been used in the present work and by past PhD students to analyse the tangential swirl burner and derive various characteristics for comparison with experiments.

Extensive experimental work at Cardiff over many years allowed the development, followed by the design and manufacture of a prototype generic swirl combustor with variable in the Cardiff University Gas Turbine Research Centre (GTRC). This burner has been used to investigate flashback and blowoff limits and match the results in order to discuss the possibility of dual fuelling in gas turbine combustors. The techniques, equipment and design processes so developed will be key factors in producing stable gas turbine swirl burners, whilst avoiding damaging effects such as flashback and blowoff at different values of flowrates or equivalence ratios.

The major conclusions that were found in this PhD research programme are summarised and classified into two groups: numerical simulations and experimental tests. The information below gives an outline of the final conclusions.

9.2 100 kW Tangential Swirl Burner

- Results of the FLUENT predictions and the interaction between experimental and simulation research have shown acceptable agreement in some cases (with fuel injector) and unacceptable agreement in others (without fuel injector). This could be due to many factors like mesh quality, the turbulence model and combustion model and 3-dimensional time dependent effects. Nevertheless, FLUENT could be a good pre-predictor for combustion and these results could be the starting point for large eddy simulations (LES) or time dependent CFD predictions.
- Time averaged FLUENT predictions gave a fair indication of the main characteristics of the isothermal swirl flow.
- The non-premixed combustion was stable both in experiments and simulations with no flashback.
- Premixed combustion advantages are the reduction of emissions during the operation, although the flow with premixed combustion can be unstable leading to either flashback or blowoff.
- Premixed combustion processes are generally unstable and need care whilst being used.
- Flashback for some cases is predictable by using CFD simulation.
- This work clearly shows there is a considerable interaction between a number of parameters in swirl burners that determine the final characteristics of the flame produced for a given fuel. Indeed, this flexibility and adaptability are one of the attractions of swirl burners.
- Swirl flow creates normally a CRZ to help flame stabilization at high Reynolds Numbers.
- The fuel injector can also act as bluff body stabilizer.
- CFD can be conducted via various commercial software packages. The new ANSY-12 consists of three programs: Geometry modelling (drawing the shape), Meshing and FLUENT (solver).

- FLUENT software uses one of the turbulent models to solve the flow inside the shape under study.
- The turbulent model has to be chosen according to many criteria. This is difficult for swirl flows as they are highly complex
- K-Omega method has been used as the turbulence model for simulation in FLUENT. It is considered to be acceptable in this instance because flashback occurs at low Reynolds Numbers before the formation of a CRZ or indeed vortex breakdown. Moreover the focus has been on the outer wall boundary layer and this turbulence model has special features for use in this area
- The mode of fuel injection is vital, whether premixed or diffusive or partially premixed.
- The combustion process is a chemical process represented in FLUENT by different kinds of combustion model. The selection of the combustion model has to be compatible with the combustion process under study.
- There is great complexity of the swirl phenomenon under the combustion conditions, making it extremely difficult to undertake the numerical study of such a type of flow, without considering alternative fuels, which in turn increase the level of difficulty.
- Geometry and Mesh have to be constructed accurately because they have considerable effect on solution divergence or convergence, especially the mesh.
- Premixed swirling flames usually tend to reduce blowoff limits compared to diffusive combustion and require some diffusive fuel to stabilize them and expand the blowoff limits. This appears to occur because the outer region of the initial flame stabilization occurs in the high-velocity shear layer. The quantities of diffusive fuel required are generally quite small to ease this phenomenon.
- Flashback is an unwanted phenomenon in the combustion process because it has many of unwanted consequences that could lead to the destruction of a part of the combustor.
- Flashback is affected by many parameters that can increase the tendency of occurrence, like swirl number, type of fuel, shape of the burner exit, velocity of incoming mixture, flame speed and flow turbulence. The latter factor plays the most important role in increasing the propensity of flame flashback.
- Confinement alters the combustion aerodynamics of the swirling flames compared to the case of open flames.

- Flashback is a very difficult phenomenon to predict and needs substantial experimental verification.
- Numerical simulation CFD was able to predict flashback for the swirl burner with natural gas and the central fuel injector only. However, the range of the experimental data was small.
- Flashback was only successfully predicted for the cases with the central fuel injector. Here flashback occurred through the outer boundary layer and FLUENT was able to simulate this. FLUENT failed to predict successfully flashback when the central fuel injector was removed. Using a low swirl number combined with a central fuel injector decreases the tendency to flashback because it increases the velocity gradient in the outer boundary layer.
- Partial premixing of fuel and air is shown to have significant advantages, as is well known industrially in reducing flashback. Certain rig nozzle configurations are shown to have advantages in reducing the flashback limits.
- CFD has been used to study conditions pertaining just upstream of the flame before flashback and to determine the critical boundary velocity gradient. This has been shown to be an order of magnitude higher than that originating from the Lewis and von Elbe formulae. The CFD indicates that the boundary layer extends up to 15 to 18% of the exit diameter and can be influenced by geometrical modifications to reduce flashback. The CFD also predicted quite well flashback limits with the fuel injector, albeit over a fairly narrow range of equivalence ratios for which experimental data existed.

9.3 Generic Swirl Burner

- As mentioned earlier, the advantages of using swirl flows in gas turbines and furnaces are significant. Much of this project is dedicated to looking at the characteristics of swirl burners in the context of using different swirl numbers and the next generation of fuels, which are hydrogen containing alternative fuels. However, these new fuels create some difficulties during the operation of the gas turbine. The main problems are related to stability, burning rate and heat capacity of the fuel of concern, which may cause flame speed changes, increased temperature in mechanical components, an increase of NO_x due to higher flame temperatures, increment of noise and stabilities, etc.

- The mechanism of flashback appeared to be different with a high swirl number as the CRZ extended back over the fuel injector to the baseplate and flashback occurred by radial movement of the flame front from the CRZ boundary to the tangential inlets. Conversely, at lower swirl numbers (and with a different exhaust nozzle) the mechanism of flashback appeared to be via the outer wall boundary layer and the critical boundary velocity gradients. Comparison of the various critical boundary velocity gradients using the analysis of Lewis and von Elbe showed that the low swirl burner produced values even lower than that from laminar flames, whilst the high swirl burner was substantially worse.
- As has been proved numerically, low swirl number gives fewer tendencies to flashback as it decreases the turbulence inside the mixing zone.
- Flashback and blowoff limits are decisively influenced by swirl number, exhaust configuration, fuel type and especially those containing significant quantities of up to 30% hydrogen with methane. With methane alone, the lowest swirl number gave the best flashback limits, when the low pressure drop is taken into account. Similar results were found with up to 30% CO₂/CH₄ fuel blends.
- Hydrogen increases flashback, as the hydrogen increases the turbulent flame speed.
- Conversely, carbon dioxide reduces the turbulent flame speed and as a result the propensity to flashback decreases. Furthermore, CO₂ dilution of methane fuels can reduce NO_x emissions as a result of reducing the flame temperature. The flashback decreases considerably with the CO₂ addition and low swirl number.
- Hydrogen enriched methane (up to 30% hydrogen) or natural gas flashback decreases when the swirl number decreases.
- The blowoff improves as the swirl number decreases because turbulence decreases.
- Hydrogen enriched fuels improves the blowoff limit because the hydrogen increases the turbulent flame speed allowing easier flame stabilization in regions of higher velocities. Also, exhaust confinements enhance blowoff limits because of the protection afforded to the flame root.
- The most important conclusion of this research is that it shows the ability of a gas turbine combustor to operate with more than one type of fuel and that it is possible to

switch between these fuels according to the requirements, the conditions of operation and the energy demand.

- It has been found in this research that dual fuels are possible for 30%, 15% hydrogen content and unlikely for COG (65%) and for pure hydrogen under the operational circumstances and swirl burner specifications of this project.

9.4 Suggestions for Further Work

The theoretical elements of this research have been achieved at **Cardiff University** whilst the experimentally elements were accomplished at the **Gas Turbine Research Centre** in Port Talbot. Many suggestions and ideas could be made for forthcoming research, and can be summarised as follows:

- The CFD work could be continuing by using Reynold's stress method to solve the turbulent flow regime. Zimont [121] has suggested a strategy of solution consisting of two steps: the first step is to use one FLUENT turbulence methods (k-epsilon, k-omega, etc....) and then these results could be a starting point for large eddy simulation (LES) or direct numerical method (DNS).
- Some designs have very complex geometry; this could result in bad meshing. Hence, geometry design and mesh creation have to be planned well together.
- This research could continue with the investigations on swirling flows with newly commissioned equipment in **Port Talbot**, at the **Gas Turbine Research Centre**.
- Moreover, the system needs to be run with a greater variety of fuels such as those with more hydrogen content, to see the effect of these fuels upon the flashback and blowoff limits.
- Partially premixed fuel could be used for future research to see the effect of the fuel upon all the characteristics that have been studied.
- More inserts could be developed to give a greater range of swirl numbers.
- Different shapes of confinement could be investigated, especially the configuration of the confinement exhaust as the conical cup exhaust was not very successful with hydrogen enriched fuels.
- The development of new fuel injectors in conjunction with appropriate rig nozzles, which can increase stability by anchoring the flame and reducing flashback.

- Moreover, different methods of generating swirl need to be investigated as this clearly has a substantial effect on the results. Vaned type swirlers are especially favoured in gas turbines owing to their compactness, and this is an area needing considerable study. Complete analysis for isothermal and combustion conditions is required, as demonstrated by this work.
- Another important issue to be considered is the usage of other methods of visualization, such as Planar Laser Induced Fluorescence (PLIF), which has been used successfully in the analysis of swirling flames and the propagation of CH* and OH* radicals, which according to the theory are related to the burning region and temperature intensity.
- The balance point between parameters during the flashback has to be analyzed in more depth. It is interesting to see that this balance occurs at the same equivalence ratio, probably a phenomenon caused by the geometry of the system.
- The flame speed of fuel mixtures is an important factor that needs to be included for future work.
- More attention needs to be paid to full calculation of combustion emission to estimate the pollutant reduction of using these methods.
- The effect of the levels of air preheating typically found in a gas turbine are likely to improve blowoff, but also increase flashback. Pressure effects are likely to alter flashback limits as well; some work indicates that the flashback will also increase. Further experiments are obviously needed. The unit has been designed for testing under simulated gas turbine conditions with air preheat and pressure up to 12 bar; this work should commence soon.
- The coalescing of the blowoff and flashback limits for COG at lower mass flowrates with confinement is of concern as this can seriously limit turndown and ways need to be found to improve this situation for practical combustors, as this trend is likely to continue for higher hydrogen content fuels. It must be noted that there is little information on blowoff for pure hydrogen swirl stabilized flames and how this interacts with flashback limits.

REFERENCES

REFERENCES

1. World Energy Council (WEC) <http://www.worldenergy.org>.
2. International Energy Agency (IEA); a 26-member-states policy-advice cooperative agency www.iea.org.
3. Herranz, M., lecture note Aeronáuticos Pz. Cardenal Cisneros 3 Spain UPM ETSI E 28040 Madrid.
4. <http://www.conserve-energy-future.com/EnergyConsumption.php>.
5. *Everything You Need To Know About America's Strategic Threats For The Next 25 Years* <http://www.businessinsider.com/everything-you-need-to-know-about-global-strategic-risks-for-the-next-25-years>. 2010.
6. European Union's Directorate-General for Energy and Transport http://europa.eu.int/comm/energy/index_en.html.
7. *BP is a global energy company* <http://www.bp.com/statisticalreview>.
8. H.I.H. Saravanamuttoo, G.F.C.R.a.H.C., *Gas Turbine Theory*. Fifth edition ed. 2001: Pearson Education Limited.
9. *Encyclopedia Britannica, I*, "Open-cycle constant-pressure gas turbine engine" <http://www.britannica.com/EBchecked/topic-art/187279/19424/Open-cycle-constantpressure-gas-turbine-engine>.
10. Lefebvre, A.H., *Gas Turbine Combustion*. 1999 LLC, Oxon, UK: Taylor & Francis Group
11. Peters, N., *Turbulent Combustion*, institute für Technische Mechanik, Rheinisch-Westfälische Technische, Hochschule Aachen. 2000, Germany: Cambridge University Press.
12. *ANSYS FLUNET 12.0, Theory Guide*. April 2009, USA.
13. Valera-Medina, A., *Coherent Structures and Their Effects on Process Occurring in Swirl Combustors*. April 2009, Cardiff University: Cardiff.
14. German, A.E. and T. Mahmud, *Modelling of non-premixed swirl burner flows using a Reynolds-stress turbulence closure*. *Fuel*, 2005. **84**(5): p. 583-594.
15. Burke, S.P. and T.E.W. Schumann, *Diffusion flames*. *Proceedings of the Symposium on Combustion*, 1948. **1-2**(0): p. 2-11.
16. Sadanandan, R., M. Stöhr, and W. Meier, *Simultaneous OH-PLIF and PIV measurements in a gas turbine model combustor*. *Applied Physics B: Lasers and Optics*, 2008. **90**(3): p. 609-618.
17. Nicholas, S., *A review of oscillation mechanisms and the role of the precessing vortex core (PVC) in swirl combustion systems*. *Progress in Energy and Combustion Science*, 2006. **32**(2): p. 93-161.
18. Lieuwen, T. and V. Yang, *Combustion Instabilities in Gas Turbine Engines*. AIAA, Progress in Astronautics and Aeronautics, USA, 2005. **210**.
19. Valera-Medina, A., et al., *Flame Stabilization and Flashback Avoidance using Passive Nozzle Constrictions*, in *IFRF International Meeting*. June 8th-10th, 2009: Boston, USA.

References

20. Lacarelle, A., J. Moeck, and C.O. Paschereit, *Dynamic Mixing Model of a Premixed Combustor and Validation with Flame Transfer Function Measurement*, in *47th AIAA Aerospace Sciences Meeting*. 2009: Orlando, USA.
21. Huang, Y. and V. Yang, *Bifurcation of flame structure in a lean-premixed swirl-stabilized combustor: transition from stable to unstable flame*. *Combustion and Flame*, 2004. **136**(3): p. 383-389.
22. Plee, S.L. and A.M. Mellor, *Review of flashback reported in prevaporizing/premixing combustors*. *Combustion and Flame*, 1978. **32**(0): p. 193-203.
23. Syred, N., A.K. Gupta, and D.J. Lilley, *Swirl Flows* 1984, Tunbridge Wells, United Kingdom.: Abacus Press.
24. Huang, Y. and V. Yang, *Effect of swirl on combustion dynamics in a lean-premixed swirl-stabilized combustor*. *Proceedings of the Combustion Institute*, 2005. **30**(2): p. 1775-1782.
25. Coghe, A., G. Solero, and G. Scribano, *Recirculation phenomena in a natural gas swirl combustor*. *Experimental Thermal and Fluid Science*, 2004. **28**(7): p. 709-714.
26. Fick, W., *Characterisation and Effects of the Precessing Vortex Core*. 1998, Cardiff University: Wales, UK.
27. Khalatov, A. and N. Syred. *Generation and alleviation of combustion instabilities in Swirling Flow*. *Advanced Combustion and Aerothermal Technologies*. in *Proceedings of the NATO*, pp. 3-20. 2006.
28. Claypole, T. and N. Syred. *Integration of swirl burners with furnaces for the combustion of Low Calorific Value gases*. in *IMEchE Conference publications, International Conference on Combustion in Engineering 2*. 1981. 19th-20th May, Birmingham, UK, pp. 139-145.
29. Mongia, H., et al. *Experimental Study on coherent structures of a counter-rotating multi-swirler cup*. in *Collection of technical papers 43rd AIAA/ASME/SAE/ASEE 7*, pp. 6594-6604. 2007.
30. Shtork, S.I., N.F. Vieira, and E.C. Fernandes, *On the identification of helical instabilities in a reacting swirling flow*. *Fuel*, 2008. **87**(10-11): p. 2314-2321.
31. Chen, Z., et al., *Gas/particle flow characteristics of a centrally fuel rich swirl coal combustion burner*. *Fuel*, 2008. **87**(10-11): p. 2102-2110.
32. O'Doherty, T. and R. Gardner. *Turbulent Length Scales in an Isothermal Swirling Flow*. in *The 8th Symposium on Fluid Control, Measurement and Visualization*. 2005. 22nd-25th August, Chengdu, China, pp. 6.
33. Jester-Zurker, R., S. Jakirlić, and C. Tropea, *Computational Modeling of Turbulent Mixing in Confined Swirling Environment Under Constant and Variable Density Conditions*. *Turbulence and Combustion*, @Springer 2005. **75**: p. 217-244.
34. Galpin, J., et al., *Large-eddy simulation of a fuel-lean premixed turbulent swirl-burner*. *Combustion and Flame*, 2008. **155**(1-2): p. 247-266.
35. Syred, N. and J.M. Beér, *Combustion in swirling flows: A review*. *Combustion and Flame*, 1974. **23**(2): p. 143-201.
36. Beer, J. and N.A. Chigier, *Combustion Aerodynamics*. 1972, London. : Applied Science, LTD.
37. D.G., L., *Swirl flows in combustion*. *AIAA Journal*, 1977. **15**(8).

References

38. Lefebvre, A.H., *Gas Turbine Combustion*. 2 ed. 1999, New York: Taylor & Francis Group.
39. Goy, C.J., S.R. James, and S. Rea, *Monitoring combustion instabilities: E.ON UK's experience*, *Combustion instabilities in gas turbine engines: operational experience, fundamental mechanisms, and modeling*, T. Lieuwen, and V. Yang, eds. Progress in Astronautics and Aeronautics, pp. 163-175, 2005.
40. Nauert, A., et al., *Experimental analysis of flashback in lean premixed swirling flames: conditions close to flashback*. Experiments in Fluids, 2007. **43**(1): p. 89-100.
41. Syred, N., *Generation and Alleviation of Combustion Instabilities in Swirling Flow*, in *Advanced Combustion and Aerothermal Technologies*, N. Syred, and A. Khalatov. 2007, Springer. p. 3–20.
42. Abdulsada, M., et al., *Effect of swirl number and fuel type upon the flashback in swirl combustors*, in *AIAA conference paper*. 4-7 January 2011: Orlando, Florida.
43. Abdulsada, M., et al., *Effect of swirl number and fuel type upon the combustion limits in swirl combustors*, GT2011- 45544, in *ASME Turbo Expo*. 6-10 June 2011: Canada, Vancouver.
44. Fritz, J., M. Kroner, and T. Sattelmayer, *Flashback in a Swirl Burner with Cylindrical Premixing Zone*. Journal of Engineering for Gas Turbines and Power, 2004. **126**(2): p. 276-283.
45. Lewis, B. and G. von Elbe, *Combustion, Flames and Explosions of Gases*. 3 ed. 1987, London: Academic press.
46. Gummer, J., M.E. Harris, and H. Schultz. *Flame Stabilization on Burners with Short Ports or Noncircular Ports*. in *Proc. 4th Int. Symposium of Combustion*. 1953.
47. Wohl, K., N.M. Kapp, and C. Gazley, *The stability of open flames*. Symposium on Combustion and Flame, and Explosion Phenomena, 1949. **3**(1): p. 3-21.
48. Dobbeling, K., Erglu, A., Winkler, D., Sattelmayer, T., and Keppel, W., 1997, "Low Nox Premixed Combustion of MBTu Fuels in a research Burner," ASME J. Eng. Gas Turbine Power, 119, pp. 553-558.
49. Subramanya, M. and A. Choudhuri, *Investigation of Combustion Instability Effects on the Flame Characteristics of Fuel Blends*, in *5th International Energy Conversion Engineering Conference and Exhibit (IECEC) AIAA*. 2007: St. Louis, Missouri.
50. Kroner, M., J. Fritz, and T. Sattelmayer, *Flashback Limits for Combustion Induced Vortex Breakdown in a Swirl Burner*. Journal of Engineering for Gas Turbines and Power, 2003. **125**(3): p. 693-700.
51. Kiesewetter, F., M. Konle, and T. Sattelmayer, *Analysis of Combustion Induced Vortex Breakdown Driven Flame Flashback in a Premix Burner With Cylindrical Mixing Zone*. Journal of Engineering for Gas Turbines and Power, 2007. **129**(4): p. 929-936.
52. Brown, G.L., *Axisymmetric Vortex Breakdown Part 2: Physical MEchanisms*. Journal of Fluid Mechanics, 1990. **221**: p. 553- 576.
53. Dhanuka, S.K., et al., *Vortex-shedding and mixing layer effects on periodic flashback in a lean premixed prevaporized gas turbine combustor*. Proceedings of the Combustion Institute, 2009. **32**(2): p. 2901-2908.

References

54. Lamnaouer, M., *Flashback Analysis for ULN Hydrogen Enriched Natural Gas Mixtures* Department of Mechanical Engineering University of Central Florida, Orlando, FL 32826.
55. Chaparro, A.A. and B.M. Cetegen, *Blowoff characteristics of bluff-body stabilized conical premixed flames under upstream velocity modulation*. *Combustion and Flame*, 2006. **144**(1-2): p. 318-335.
56. Williams, G.C., H.C. Hottel, and A.C. Scurlock, *Flame stabilization and propagation in high velocity gas streams*. Symposium on Combustion and Flame, and Explosion Phenomena, 1949. **3**(1): p. 21-40.
57. J.P. L., *Flame stabilization by bluff bodies and turbulent flames in ducts*. Symposium (International) on Combustion, 1953. **4**(1): p. 90-97.
58. Zukoski, E.E. and F.E. Marble. in *Proceedings of the Gas Dynamics Symposium on Aerothermochemistry*, Northwest University Press. 1955.
59. Zukoski, E.E. and F.E. Marble. *Combustion Researchers and Reviews AGARD*. 1955.
60. Lieuwen, T., *Chapter 3.1.1: Static and Dynamic Combustion Stability.*, in *Gas Turbine Handbook*. 2006, U.S. Department of energy, office of fossil energy, national energy technology: U.S.A.
61. Lieuwen, T., et al., *A Mechanism of Combustion Instability in Lean Premixed Gas Turbine Combustors*. *Journal of Engineering for Gas Turbines and Power*, 2001. **123**(1): p. 182-189.
62. Noble, D.R., et al., *Syngas Mixture Composition Effects Upon Flashback and Blowout*. ASME Conference Proceedings, 2006. **2006**(42363): p. 357-368.
63. Nair, S. and T. Lieuwen, *Acoustic Characterization of Premixed Flames under Near Blowout Conditions*, in *AIAA Paper 2002-4011, 38th AIAA Joint Propulsion Conference*. July 2002.
64. Nair, S. and T. Lieuwen, *Acoustic Detection of Imminent Blowout in Pilot and Swirl Stabilized Combustors*. ASME Conference Proceedings, 2003. **2003**(36851): p. 55-65.
65. Nair, S. and T. Lieuwen, *Acoustic Emissions of Premixed Flames In Swirl And Bluff Body Stabilized Combustors Near Flameout*, in *AIAA Paper 2003-5084, 39th AIAA Joint Propulsion Conference*. July 2003.
66. Tuttle, S.G., et al., *Transitional Blowoff Behavior of Wake-Stabilized Flames in Vitiated Flow*, in *48th AIAA Aerospace Sciences Meeting Including the New Horizons Forum and Aerospace 4 - 7 January 2010*: Orlando, Florida AIAA 2010-220.
67. Muruganandam, T.M., et al., *Optical And Acoustic Sensing Of Lean Blowout Precursors*, in *38th AIAA Joint Propulsion Conference, AIAA Paper 2002-3732*. July 2002.
68. *GE Energy report, Addressing Gas Turbine Fuel Flexibility, GER4601 (05/11) revB*, Robert Jones, Manager of Syngas Power Island Products, Jeffrey Goldmeer, Product Marketing Manager, Bruno Monetti, Product Marketing Manager.
69. Kobayashi, H., et al., *Effects of CO₂ dilution on turbulent premixed flames at high pressure and high temperature*. *Proceedings of the Combustion Institute*, 2007. **31**(1): p. 1451-1458.

References

70. Cohé, C., et al., *CO₂ addition and pressure effects on laminar and turbulent lean premixed CH₄ air flames*. Proceedings of the Combustion Institute, 2009. **32**(2): p. 1803-1810.
71. Gelfand, B.E., V.P. Kapov, and E. Popov, *Turbulent flames in lean H₂-air-CO₂ mixtures*, in *Mediterranean combustion symposium*. 1999: Antalya , Turquie.
72. Kobayashi, H., et al., *Burning velocity of turbulent premixed flames in a high-pressure environment*. Symposium (International) on Combustion, 1996. **26**(1): p. 389-396.
73. Schefer, R.W., C.M. White, and J. Keller, *Lean Hydrogen Combustion in Lean Combustion Technology and Control*, A.P.-. Derek Dunn-Rankin, Editor. 2007.
74. Chiesa, P., G. Lozza, and L. Mazzocchi, *Using hydrogen as gas turbine fuel*. Journal of Engineering for Gas Turbines and Power, 2005. **127**(1): p. 73-80.
75. Shy, S.S., et al., *Effects of H₂ or CO₂ addition, equivalence ratio, and turbulent straining on turbulent burning velocities for lean premixed methane combustion*. Combustion and Flame, 2008. **153**(4): p. 510-524.
76. Di Sarli, V. and A. Di Benedetto, *Laminar burning velocity of hydrogen-methane/air premixed flames*. International Journal of Hydrogen Energy, 2007. **32**(5): p. 637-646.
77. Badin, J.S. and S. Tagore, *Energy pathway analysis - A hydrogen fuel cycle framework for system studies*. International Journal of Hydrogen Energy, 1997. **22**(4): p. 389-395.
78. Ogden, J.M., *Developing an infrastructure for hydrogen vehicles: A Southern California case study*. International Journal of Hydrogen Energy, 1999. **24**(8): p. 709-730.
79. Thomas, C.E., B.D. James, and F.D. Lomax Jr, *Market penetration scenarios for fuel cell vehicles*. International Journal of Hydrogen Energy, 1998. **23**(10): p. 949-966.
80. Verhelst, S. and R. Sierens, *Aspects concerning the optimisation of a hydrogen fueled engine*. International Journal of Hydrogen Energy, 2001. **26**(9): p. 981-985.
81. Law, C.K. and O.C. Kwon, *Effects of hydrocarbon substitution on atmospheric hydrogen-air flame propagation*. International Journal of Hydrogen Energy, 2004. **29**(8): p. 867-879.
82. Schefer, R. and J. Oefelein, *Reduced Turbine Emissions Using Hydrogen- Enriched Fuels*. 2003, Sandia National Laboratories, Livermore CA.
83. Schefer, R.W., D.M. Wicksall, and A.K. Agrawal. *Combustion of hydrogen-enriched methane in a lean premixed swirl-stabilized burner*. 2002.
84. Wicksall, D.M., et al. *Fuel composition effects on the velocity field in a lean premixed swirl-stabilized combustor*. 2003.
85. Jackson, G.S., et al., *Erratum: Influence of H₂ on the response of lean premixed CH₄ flames to high strained flows (Combustion and Flame (2003) 132:3 (503-511) PII: S0010218002004960)*. Combustion and Flame, 2003. **135**(3): p. 363.
86. Kido, H., et al., *Improving the combustion performance of lean hydrocarbon mixtures by hydrogen addition*. JSAE Review, 1994. **15**(2): p. 165-170.
87. Patankar, S.V., *Numerical Heat Transfer and Fluid Flow*. 1980, New York: Hemisphere Publishing Corporation, Taylor & Francis Group.

References

88. Versteeg, H.K. and W. Malalasekera, *An Introduction to computational Fluid Dynamics – The Finite Volume Method*. 1995: Longman Group Ltd.
89. Douglas, J.F., et al., *Fluid Mechanics*. 4 ed. 1979, UK: Pitman International Text.
90. Fraser, T., *Numerical Modelling of an Inverted Cyclone Gasifier*. 2033, Cardiff Cardiff.
91. R., L., *Applied CFD Techniques, An introduction based on finite element methods*. 2001, West Sussex, UK: John Willey & Sons Ltd.
92. Date, A.W., *Introduction to Computational Fluid Dynamics*. 2005: Cambridge University Press.
93. Baukal, C.E., V.G. Jr., and X. Li, *Computational Fluid Dynamics in Industrial Combustion*. 2001: CRC Press.
94. turbulence., h.w.c.-o.c.W.I.t.t.N.o.
95. Gleick, J., *Chaos: Making a New Science*. 2001, New York: Viking Press.
96. Tennekes, H., J.L. Lumley, and A.f.c.i. turbulence, *The MIT Press*. 1972, Cambridge, Massachusetts, London
97. George, P.W.K., *Lectures in Turbulence for the 21st Century, Professor of Turbulence* Chalmers University of Technology: Gothenburg, Sweden.
98. Hinze, J.O., *Turbulence* 2ed. 1975: McGraw-Hill, Inc.
99. Launder, B.E. and D.B. Spalding, *The numerical computation of turbulent flows*. *Computer Methods in Applied Mechanics and Engineering*, 1974. **3**(2): p. 269-289.
100. Chika, A. and A. Kulkarni. *Modeling Turbulent Flows in FLUENT*
101. Shelil, N., *Flashback Studies With Premixed Swirl Combustion*. 2009, Cardiff: Wales, UK.
102. Wilcox, D.C., *Turbulence Modeling for CFD*. 1998, La Canada, California: DCW Industries, Inc.
103. Menter, F.R., *Two-Equation Eddy-Viscosity Turbulence Models for Engineering Applications*. *AIAA Journal*, August , 1994. **32**(8): p. 1598–1605.
104. Zimont, V.L. and A.N. Lipatnikov., *A Numerical Model of Premixed Turbulent Combustion of Gases*. 1995, *Chemical Physics Report*. p. 993-1025.
105. Zimont, V., et al., *An Efficient Computational Model for Premixed Turbulent Combustion at High Reynolds Numbers Based on a Turbulent Flame Speed Closure*. *Journal of Engineering for Gas Turbines and Power*, 1998. **120**(3): p. 526-532.
106. V.L, Z., *Gas premixed combustion at high turbulence. Turbulent flame closure combustion model*. *Experimental Thermal and Fluid Science*, 2000. **21**(1-3): p. 179-186.
107. Zimont, V.L., F. Biagioli, and K.J. Syed, *Modelling Turbulent Premixed Combustion in the Intermediate Steady Propagation Regime*. *Progress in Computational Fluid Dynamics*, 2001. **1**(1): p. 14-28.
108. Patrick, M.K., *Remarks on Mesh Quality*, *Sandia National Laboratories, P. O. Box 5800 Albuquerque, NM 87185*, in *45th AIAA Aerospace Sciences Meeting and Exhibit*. 7-10 January, 2007, Reno, NV.
109. Fraser, T., *Numerical Modelling of an Inverted Cyclone Gasifier*. 2003, Cardiff: Cardiff.
110. Valera-Medina, A., *Precessing Vortex Core and its impacts on NOx reduction*. 2006, Cardiff University: Wales, UK.

References

111. Thornton, J.D., et al., *Flashback Detection Sensor for Hydrogen Augmented Natural Gas Combustion*. ASME Conference Proceedings, 2007. **2007**(4790X): p. 739-746.
112. Lieuwen, T., et al., *Burner development and operability issues associated with steady flowing syngas fired combustors*. Combustion, Science and Technology, 2008. **180**(6): p. 1169-1192.
113. Shelil, N., et al., *Investigations of Gaseous Alternative Fuels at Atmospheric and Elevated Temperature and Pressure Conditions*, in *ASME Turbo Expo*. 2010.
114. Lucca-Negro, O. and T. O'Doherty, *Vortex breakdown: A review*. Progress in Energy and Combustion Science, 2001. **27**(4): p. 431-481.
115. Stappert, K., *Coriolis mass flow meters for natural gas measurement* Global Business Development Manager-Natural Gas Emerson Process Management-Micro Motion, Inc.: 9906A 43rd St. Tulsa, Oklahoma 74146.
116. Syred, N., et al., *The effect of hydrogen containing fuel blends upon flashback in swirl burners*. Applied Energy, 2012. **89**(1): p. 106-110.
117. Abdulsada, M., et al., *Effect of Swirl Number and Fuel Type upon the Blow off Limits in Swirl Combustors* in *The Fifth European Combustion Meeting*. 28th June - 1st July 2011: Cardiff University, Cardiff, UK.
118. Abdulsada, M., et al., *Effect of Swirl Number and Fuel Type upon the Blowoff Limits in Unconfined and Confined Swirl Combustors*, in *TATA Conference Meeting*. 25th-26th October, 2011: Newcastle, UK.
119. Valera-Medina, A., N. Syred, and A. Griffiths, *Visualisation of isothermal large coherent structures in a swirl burner*. Combustion and Flame, 2009. **156**(9): p. 1723-1734.
120. Shelil, N., et al., *Premixed Swirl Combustion and Flashback Analysis with Hydrogen /Methane Mixture* in *48th AIAA Aerospace Sciences Meeting*. Orlando, USA, ref. AIAA-2010-1169, 2010.
121. Zimont, V.L., *Gas Turbine Lean Premixed Combustion: Principle of Modelling*, in *TOTeM34*. 20th-21th October 2010.: Cardiff University, Cardiff, Wales, UK. .

APPENDIX I:

AWARD

CERTIFICATE AND

SELECTED

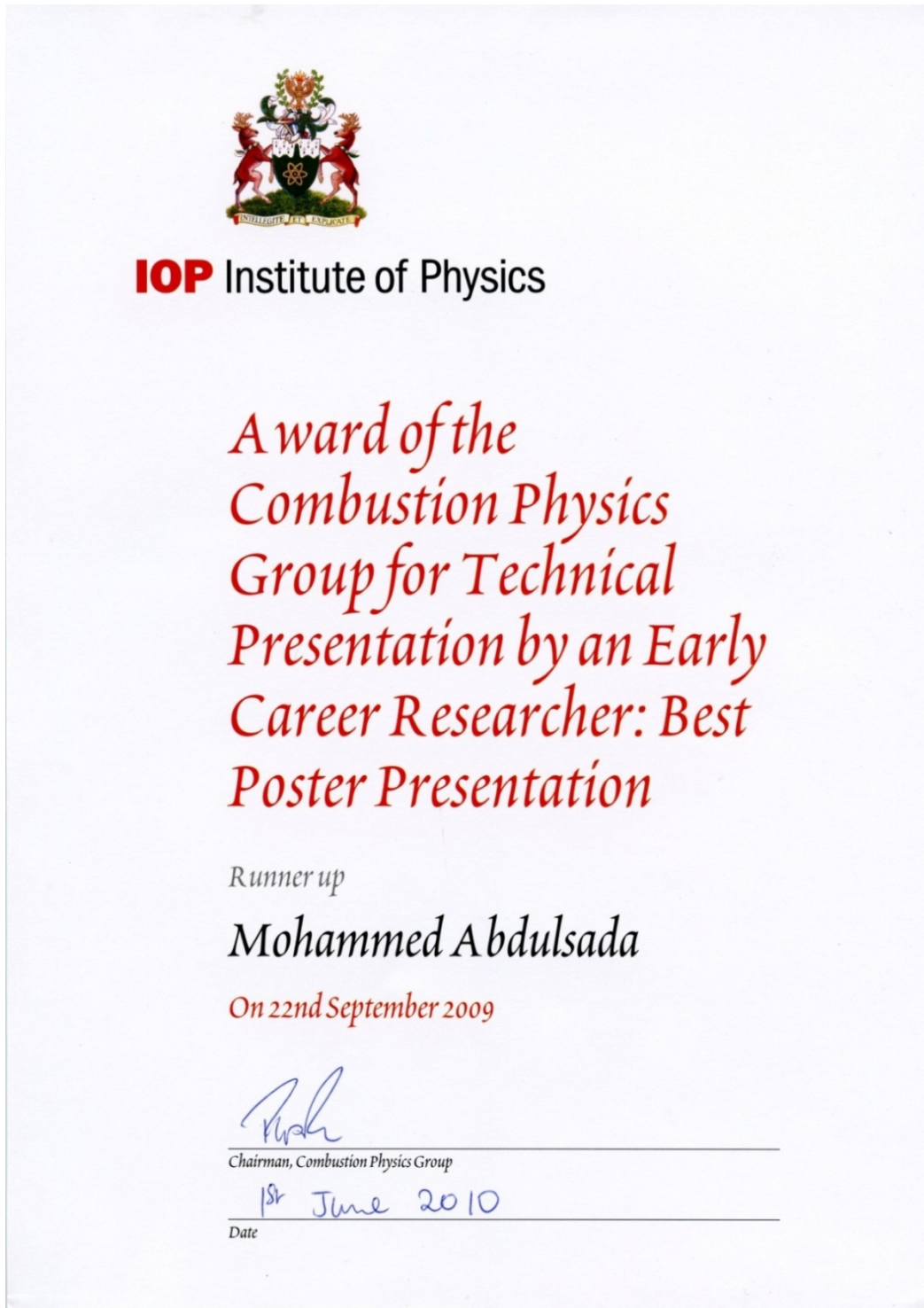
PAPERS

Appendix I

Award Certificates and Selected Papers

AI.1 Certificates:

Flashback Avoidance Analysis using Geometrical Constrictions in a Tangential Swirl Burner (Second Poster Prize)



Studies of Large Coherent Structures and their Effects on Swirl Combustion (Best Conference Paper Prize)



CERTIFICATE OF MERIT

*For the purpose of promoting
technical and scientific excellence*

presented to

**Agustin Valera-Medina,
Mohammed Hamza Abdulsada,
Nicholas Syred, and Anthony Griffiths**

for the Best Paper titled

*“Studies of Large Coherent Structures and Their
Effects on Swirl Combustion”*

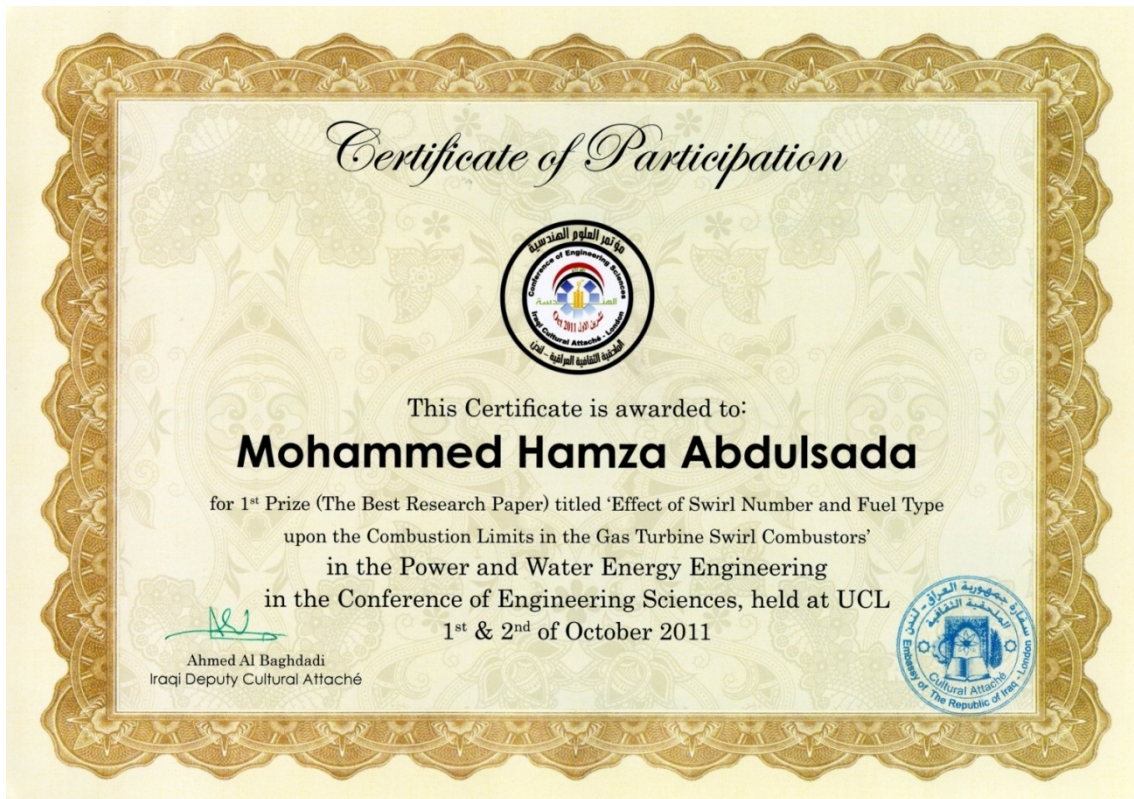
**AIAA Aerospace Sciences Meeting
January 2010**



A handwritten signature in black ink, reading 'Laura J. McGill'.

Laura J. McGill
VP Technical Activities

Effect of Swirl Number and Fuel Type upon the Combustion Limits in Gas Turbine Swirl Combustors (Best Paper and Presentation Prize)



AI.2 Selected Papers:

- Agustin Valera-Medina, Mohammed Abdulsada, Nicholas Syred and Anthony Griffiths, Studies of Large Coherent Structures and their Effects on Swirl Combustion, 48th AIAA Aerospace Sciences Meeting Including the New Horizons Forum and Aerospace Exposition 4th -7th January 2010, Orlando, Florida, **AIAA 2010-1168**.
- Nicholas Syred, Mohammed Abdulsada, Anthony Griffiths, Tim O'Doherty, and Philip Bowen, The effect of hydrogen containing fuel blends upon flashback in swirl burners, Applied Energy, vol 89, p106-110, 2012.

Studies of Large Coherent Structures and their Effects on Swirl Combustion

Agustin Valera-Medina^{*}, Mohammed Abdulsada[®], Nicholas Syred[†] and Anthony Griffiths[‡]
Gas Turbine Research Centre, Cardiff University, CF24 3AA, United Kingdom

Lean fuel premixing is considered as one of the most reliable and promising technologies for emission reduction in Gas Turbine combustion systems. However, there are some inner structures that appear in the field barely understood. Therefore, this study shows experimental results obtained to characterize the Central Recirculation Zone formed during combustion at different equivalence ratios and flow rates. The results are then compared to different numerical models in order to specify which one works better for the correct prediction of the structures observed. It was found that the Recirculation Zone passes through a process of evolution based on the equivalence ratio and flowrate used, with the increment of coherence caused at lean equivalence ratios whose injection is attained via diffusive-premixed method. Numerical simulations show traces of asymmetry in the structure as those noticed experimentally. Although the structures are not entirely equal, the simulation compares satisfactorily to the experiments.

The experiments are then extended to the study of flashback inside of the swirl chamber, a phenomenon that has attracted current research for the use of alternative fuels. Using a centered diffusive injector, it was demonstrated that the phenomenon was reduced and the resistance limit to flashback increased considerably. Aided by numerical simulations, it was confirmed that the increment was caused by the increase of axial velocity and the disappearance of the Combustion Induced Vortex Breakdown in the system by the diffusive injector.

Nomenclature

CRZ	= Central Recirculation Zone	Γk	= Effective dissipation rate of k (J/kg)
G _x	= turbulence kinetic energy due to mean velocity gradients (J/kg)	$\Gamma \omega$	= Effective dissipation rate of ω (J/kg)
G ω	= generation of dissipation rate (J/kg)	k	= turbulence kinetic energy (J/kg)
PVC	= Precessing Vortex core	Φ	= Equivalence Ratio (-)
Re	= Reynolds number (-)	ω	= Specific dissipation rate (J/kg)
S	= Swirl Number, (-)		
Sk - S ω	= Source Terms, user-defined (J/kg)		
U _l	= laminar flame speed (m/s)		
U _t	= turbulent flame speed (m/s)		
W _o	= Wobbe Number (-)		
Y _k	= dissipation of k due to turbulence (J/kg)		
Y ω	= dissipation of ω due to turbulence (J/kg)		

I. Introduction

Amongst the most promising technologies used to reduce the impact and production of NO_x, lean premixing and swirl stabilized combustion are regarded as very good options. However, premixing is not perfect because usually fuel and air are mixed shortly before entering the combustion chamber leading to a significant degree of unmixedness¹. On the other hand, it has been found that the levels of swirl used in some combustors, coupled with the mode of fuel injection can induce the appearance of unwanted and undesirable regular fluid dynamic instabilities. Swirl stabilized combustion creates coherent structures that may produce low-frequency modes capable

^{*}Research Student, valeramedinaa@cardiff.ac.uk. Student member.

[®]Research Student, scema13@groupwise.cf.ac.uk. Non-member.

[†]Professor, nsyred@cf.ac.uk. Member.

[‡]Professor, aj2griffiths@cf.ac.uk. Non-member.

of coping with natural frequencies of the equipment², exciting oscillations that can damage the system. Therefore, there is vast room for improvement for both technologies. Recent research³⁻⁵ has focused on the use of both technologies for the improvement of the combustion process, adding passive and active mechanisms of suppression for the reduction of combustion related instabilities.

Swirling flows are defined as a flow with undergoing simultaneous axial-tangential and vortex motions. This results from the application of a spiraling motion, a swirl velocity component (tangential velocity component) being imparted to the flow by the use of swirl vanes, axial-plus-tangential entry swirl generators or by direct tangential entry into the chamber. Swirling flows have been studied extensively with special emphasis on their three dimensional characteristics and methodology for flame holding^{2,5-6}. These flows are designed to create coherent recirculation zones capable of recycling hot chemically active reactants to enable excellent flame stability.

Different Laser, direct and indirect techniques have been used for the analysis of such flows⁵⁻⁹. However, it was been found that good spatial resolution is found when the system is phased locked using the highest velocity peaks of the swirling flow^{2,6}. Qualitative agreement between experimental data and theoretical analysis of the observed flame motion is obtained, interpreted as originating primarily from variation of the burning velocity. However, some structures recently discovered in the system¹⁰⁻¹¹ have caused some debate amongst the researchers involved in the topic. Secondary recirculation zones, the appearance of anchored and weaker vortices inside of the field that merge to create stronger structures and the helicity of the Precessing Vortex Core (PVC) are all themes of further analysis numerically and experimentally.

New combustion systems based on ultra-lean premixed combustion have the potential for dramatically reducing pollutant emissions in transportation systems, heat, and stationary power generation¹². However, lean premixed flames are highly susceptible to fluid dynamical combustion instabilities, making robust and reliable systems difficult to design. It has been shown that flames in high swirled flows undergoing vortex breakdown are characterized by complex stabilization properties¹³. It is shown that the narrowing of the Central Recirculation Zone (CRZ) inside the burner is responsible for bi-stable behavior of the flame, very likely driven by flame-velocity flow field interaction. Close to the critical conditions separating the two stable positions of the flame (inside and outside the burner), the flame anchoring location is strongly sensitive to flow and equivalence ratio perturbation. Fractal analysis of the flame has been also numerically applied to the study of swirling flows⁹. Fractal dimension (FD) of the boundary is examined and found to change from 1.10 to 1.40 with swirling intensities of a primary and secondary air injection. When FD is small, the complex level of the interface is low, and mixture between the primary and secondary air is weak near the exit of the burner at the initial phase of combustion. When FD is big, the mixture becomes strong near the exit. It has been proposed when FD ranges from 1.10 to 1.20 this favors the reduction of NO_x, whilst being from 1.25 to 1.40 produces significant amount of NO_x. All this confirms some of the complex mechanisms that these flows present.

The complexity becomes even greater when alternative fuels are used. Biomass and coal gasification pilot and prototype plants have been operating for many years. They, in association with other plant, can be operated to produce hydrogen rich fuel gases for testing as gas turbine fuels¹⁴⁻¹⁵. Many of the current models of swirl combustion leave much to be desired when considering hydrogen rich fuels due to the variety of parameters to be considered in highly turbulent flows¹⁶. Flashback is one of the major problems related to the use of alternative fuels in premixed lean technologies. Flame flashback from the combustion chamber into the mixing zone limits the reliability of swirl stabilized lean premixed combustion in gas turbines. In a former study, the Combustion Induced Vortex Breakdown (CIVB) has been identified as a prevailing flashback mechanism of swirl burners¹⁷⁻¹⁸. It was found that the quenching of the chemical reaction is the governing factor for the flashback limit. A Peclet number model was successfully applied to correlate the flashback limits as a function of the mixing tube diameter, the flow rate and the laminar burning velocity, showing that the position of the vortex and equivalence ratios as mechanisms of heat release are vital to the predisposition of the system to flashback. Although it was shown earlier that the sudden change of the macroscopic character of the vortex flow leading to flashback can be qualitatively computed with three-dimensional as well as axisymmetric two-dimensional URANS-codes, the proper prediction of the flashback limits could not be achieved with this approach.

Numerical simulations have been also applied for the study of these flows, since various structures inner in the field are barely understood. High-intensity swirling flows subjected to large density variations have been examined computationally⁷. The focus of the simulation is on the Favre-averaged Navier–Stokes computations of the

momentum and scalar transport employing turbulence models based on the differential second moment closure (SMC) strategy. The computed axial and circumferential velocities agree fairly well with the reference experiment, reproducing important features of such a weakly supercritical flow configuration. Large-eddy simulations (LES) of fuel-lean premixed turbulent swirling flame have also been performed successfully¹⁹⁻²⁰. Most of the turbulent flame features are reproduced, and observed discrepancies are analyzed to seek out possible improvements of the sub-grid-scale modeling. However, despite the successes, the results obtained for more intricate cases with high flow rates, high swirl involving combustion and alternative fuels leave much to be desired²¹⁻²³. Therefore, systems that use high swirl numbers require extensive and expensive experimentation for optimization. A relatively simple swirl burner design is thus used to characterize a whole family of coherent structures which arise from complex combustive flows.

In this paper, experiments on a tangential swirl burner are analyzed for the definition and understanding of the formation of the CRZ at different conditions, extending the analysis for the study of flashback under different geometries. Simulations of this burner using detailed chemistry and transport without incorporating explicit models for turbulence or turbulence/chemistry interaction are presented.

II. Experimental and Numerical Study

II.a. Experimental Approach

Experiments were performed in a 100 kW Steel versions of a 2 MW Swirl burner under combustion conditions. Two tangential inlets were used together with a 25% blockage insert each in order to change the swirl number to the most stable configuration observed in previous experiments^{8, 10}. The system was fed by a centrifugal fan providing air flow via flexible hoses and two banks of rotameters for flow rate control and a further bank for the injection of natural gas. Two different modes of natural gas injection were utilized for the prototype; a diffusive mode with fuel injected along the central axis from the burner bottom and a premixed mode with entry in one or both tangential inlets, located before the inserts used for varying the swirl number. Premixed gas injectors, extending across the inlet ducts, were located just before the inlets. Overall equivalence ratio ϕ is reported as well as the fuel proportion injected diffusively by the fuel injectors mounted along the axis followed by that injected as premixed in the tangential inlets. The format (25-80) here refers to 25 l/min diffusive natural gas injection, the 80 l/min to that injected as premixed. Due to the high temperature variation, the Reynolds number (Re) is defined from the nozzle diameter and isothermal conditions. Coherent structures were framed in a spatial frame, phase locking the measuring system with the pressure signal from a swirling high momentum region previously observed in these burners. The Pressure fluctuation was measured with a EM-1 Yoga Electret Condenser Microphone, with a frequency response of 20 Hz-16 kHz and sensitivity of -64 ± 3 dB positioned 30 mm upstream the nozzle. When the flow crossed the same position the system was triggered, allowing a spatial representation of the same phenomenon every cycle. The signal was analyzed using the Tektronic DS2024B Oscilloscope at 2 Gsamples/s, 200 MHz and four channels.

Different equivalence ratios were investigated, from very lean conditions at 0.108 to rich values at 1.666. A wide variation in the airflow and gas flow rates was also made to visualize the progressive development of the coherent structures.

A diffusive fuel injector was used, extended from the burner baseplate to near to the burner nozzle. This study is carried out as a consequence of the problems related to the injection system²⁴. High momentum injection within the swirler shows less sensitivity to pressure variations than those observed in air. Fluctuations in air supply can thus produce significant variation of equivalence ratio, creating gas pockets of varying equivalence ratio inside of the system. The geometry of the injector is 23.4 mm diameter positioned 47.5 mm upstream of the burner exhaust.

Experiments were made using a Phase Locked PIV system. This technique has proved to be consistent with the results of different experiments under a variety of conditions¹⁰.

The Microphone condenser signal was redirected to a BNC Model 500 Pulse Generator, whose TTL signal was sent to a Dantec PIV system. The latter consists of a Nd: YAG Litron Laser of 532 nm at 5 Hz and a Hi Sense MkII Camera model C8484-52-05CP, with 1.3 MPixel resolution at 8 bits. A 60mm Nikon lens was used for resolution purposes, with a depth of view of 1.5 mm. The inlet air was seeded with aluminium oxide Al₂O₃ by a Venturi

system positioned 2.0 m upstream of the burner inlets. 250 l/min of air were used to fluidize the seeding material; this was accounted for the determination of the final flowrate. The entire system was triggered at 90% of the highest peak observed after 5 minutes of free run.

For the flashback analysis, Coherent structures were framed using a High Speed Photography system. No Phase Locked measurements were tried so free runs were allowed for the recording of the entire phenomenon. A Fastcam High Speed Camera model Apx RS of 250,000 frames/s maximum speed was used with a 105mm, 1:2.8 Nikon Lens. The camera was setup at only 4,000 frames/s to avoid resolution problems and increase the visual field, since the frequency of the large coherent structures has been observed to lay on the range of 100-200 Hz^{2,10}. The resulting images were analyzed using the PFV ver 2.4.1.1 software. The entire setup is shown in figure 1.

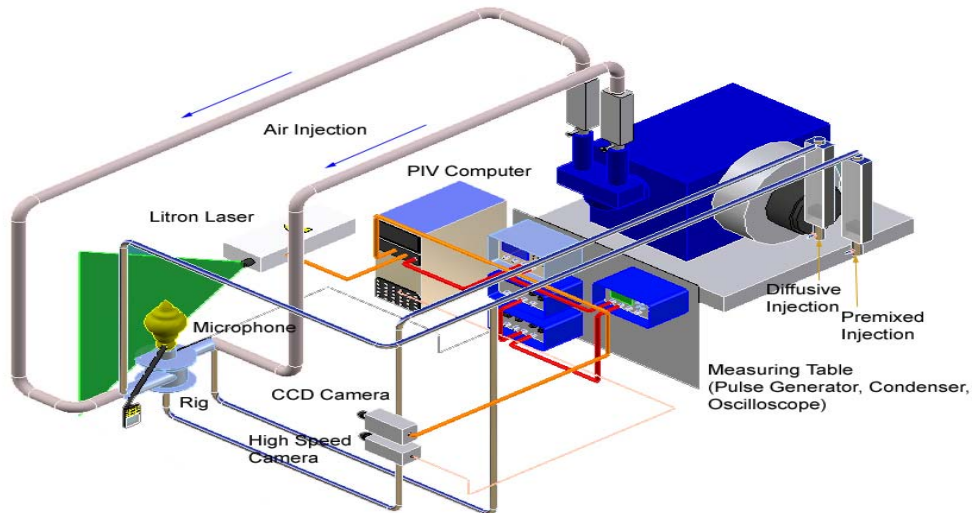


Figure 1. Experimental Setup

The inclusion of two stainless steel mirrors at the outlet and bottom of the rig (and rotated by 45°) allowed the radial-tangential visualization of the flashback. A quartz crystal was used at the bottom to maintain similar confined conditions, enabling the internal visualization without risk. The experiments were performed using confined conditions, with a cylindrical confinement made of quartz in order to allow the axial visualization using the PIV system. No nozzle constriction was used. Figures 2 and 3 show a diagram of the burner and the configuration analyzed, respectively.

The objective was to recognize the position of zero velocities where and CRZ existed so as to define the boundaries of the structure. After acquisition, a frame-to-frame correlation technique was then carried out at 32 x 32 pixels, with an overlap of 50% between frames to reduce noise. 150 frames per plane were used to create an average velocity map. A vector substitution of 2.8% was observed. The velocity maps were developed in the range of -3.0 to 6.00 m/s.

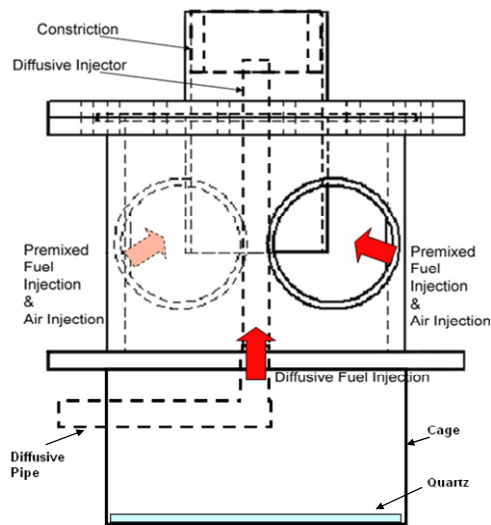


Figure 2. Diagram of the system.



Figure 3. Analyzed configuration.

II.a. Numerical Approach

Partially premixed combustion systems are premixed flames with non-uniform fuel-oxidizer mixtures (equivalence ratios). Such flames include premixed jets discharging into a quiescent atmosphere, lean premixed combustors with diffusion pilot flames and/or cooling air jets, and imperfectly mixed inlets. The partially premixed model is a simple combination of non-premixed model and premixed model.

In non-premixed combustion, fuel and oxidizer enter the reaction zone in distinct streams. This is in contrast to premixed systems, in which reactants are mixed at the molecular level before burning. Under certain assumptions, the thermo chemistry can be reduced to a single parameter: the mixture fraction. The mixture fraction, denoted by f , is the mass fraction that originated from the fuel stream.

In turn, the mixture fraction is a conserved scalar quantity, and therefore its governing transport equation does not have a source term. Combustion is simplified to a mixing problem, and the difficulties associated with closing non-linear mean reaction rates are avoided. Once mixed, the chemistry can be modeled as being in chemical equilibrium with the Equilibrium model, being near chemical equilibrium with the steady laminar flamelet model, or significantly departing from chemical equilibrium with the unsteady laminar flamelet model.

In premixed combustion, fuel and oxidizer are mixed at the molecular level prior to ignition. Combustion occurs as a flame front propagating into the unburnt reactants. Premixed combustion is much more difficult to model than non-premixed combustion. The reason for this is that premixed combustion usually occurs as a thin, propagating flame that is stretched and contorted by turbulence. For subsonic flows, the overall rate of propagation of the flame is determined by both the laminar flame speed and the turbulent eddies. The essence of premixed combustion modeling lies in capturing the turbulent flame speed, which is influenced by both parameters.

Partially premixed flames exhibit the properties of both premixed and diffusion flames. They occur when an additional oxidizer or fuel stream enters a premixed system, or when a diffusion flame becomes lifted off the burner so that some premixing takes place prior to combustion.

The turbulence model used was the standard $k-\omega$ model, a method based on the Wilcox $k-\omega$ model²⁵, which incorporates modifications for low-Reynolds-number effects, compressibility, and shear flow spreading. The Wilcox model predicts free shear flow spreading rates that are in close agreement with measurements for far wakes, mixing layers, and plane, round, and radial jets, and is thus applicable to wall-bounded flows and free shear flows. The standard $k-\omega$ model is an empirical model based on transport equations for the turbulence kinetic energy (k) and the specific dissipation rate (ω). As the $k-\omega$ model has been modified over the years, production terms have been

added to both the k and ω equations, which have improved the accuracy of the model for predicting free shear flows. The transport equations for the model can be defined by,

The transport equations for the model can be defined by,

$$\frac{\partial}{\partial t}(\rho k) + \frac{\partial}{\partial x_i}(\rho k u_i) = \frac{\partial}{\partial x_j} \left(\Gamma_k \frac{\partial k}{\partial x_j} \right) + G_k - Y_k + S_k \quad (1)$$

$$\frac{\partial}{\partial t}(\rho \omega) + \frac{\partial}{\partial x_i}(\rho \omega u_i) = \frac{\partial}{\partial x_j} \left(\Gamma_\omega \frac{\partial \omega}{\partial x_j} \right) + G_\omega - Y_\omega + S_\omega \quad (2)$$

The model used is the same as the one used during the experiments. Two different modes of natural gas injection were utilized for the prototype; a diffusive mode (non-premixed) with fuel injected along the central axis from the burner bottom and a premixed mode with entry in one or both tangential inlets, located before the inserts used for varying the swirl number. The simulation was performed utilizing FLUENT as solver. A three dimensional model is used for the analysis, which can be seen in figure 4.

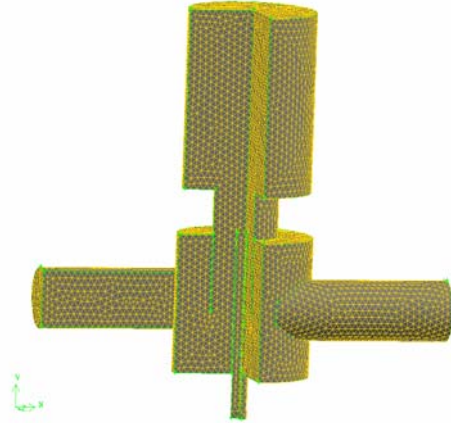


Figure 4. Tangential Swirl Burner Model.

III. Results

III.a. Coherent Structures

Experiments were performed in order to obtain more insights into the system at different fuel ratios and regimes. Figure 5 shows a diffusive weak flame at different air flowrates. It is observed that the condition creates a coherent stable recirculation zone even at low air flowrates. This appears to be a consequence of the weak equivalence ratios. Only the fastest flows show what seems to be a harmonic related to the PVC/High Momentum Region (HM), but it is not as clear as under isothermal conditions, confirming the suppression of the PVC amplitude. The strength of the CRZ has increased with the flowrate and reduction of ϕ . Moreover, the shape of the Recirculation Zone maintains an irregular, lobbed pattern, as observed by Syred² and Dawson²⁶.

The addition of 40 l/min premixed natural gas for a diffusive-premixed case followed. These conditions showed stronger flames with weaker inner structures, figure 6. This is to be expected as the overall equivalence ratios are higher with more heat release, increased axial flux of axial momentum and more reduction of swirl number.

A coherent stable Recirculation Zone developed at moderate-high air flowrates, with a wobbling unattached Vortex Breakdown at low air flowrates. Clear harmonics of the high momentum shear flow region were observed at moderate and high Re in the range of 0-100 Hz for a first harmonic, followed by another one at 200-250 Hz, the latter being characteristic of hot flows^{2,25}.

At 600 l/min airflow, figure 6.A. $\phi=1.030$, heat release is near its maximum, axial flux of axial momentum is near its maximum and the swirl number has been reduced to being close to the point of vortex breakdown. At $\phi=0.620$, figure 6.B. reduction of swirl number is not so high and a stronger CRZ has re-established itself, the effect continuing as the airflow is increased and equivalence ratio decreases to figure 6.D. where $\phi=0.281$.

Thus, swirling combustion is highly dependant on the Re, equivalence ratio and injection mechanism. The use of diffusive injection creates a recirculation zone that remains moderate even at high equivalence ratios. However, when the premixed gas is added, the energy in the system and consequent reduction of density make more difficult the appearance of the structure at low Re. Nevertheless, the CRZ forms faster at high equivalence ratios, and at high Re its strength overcomes those observed with purely diffusive injection, suggesting that the mechanism of appearance under those circumstances is due to the higher pressure inside of the system and augmented energy of the reacting particles, which due to a higher recirculation are more prompt to react and contribute to the negative movement inside of the structure.

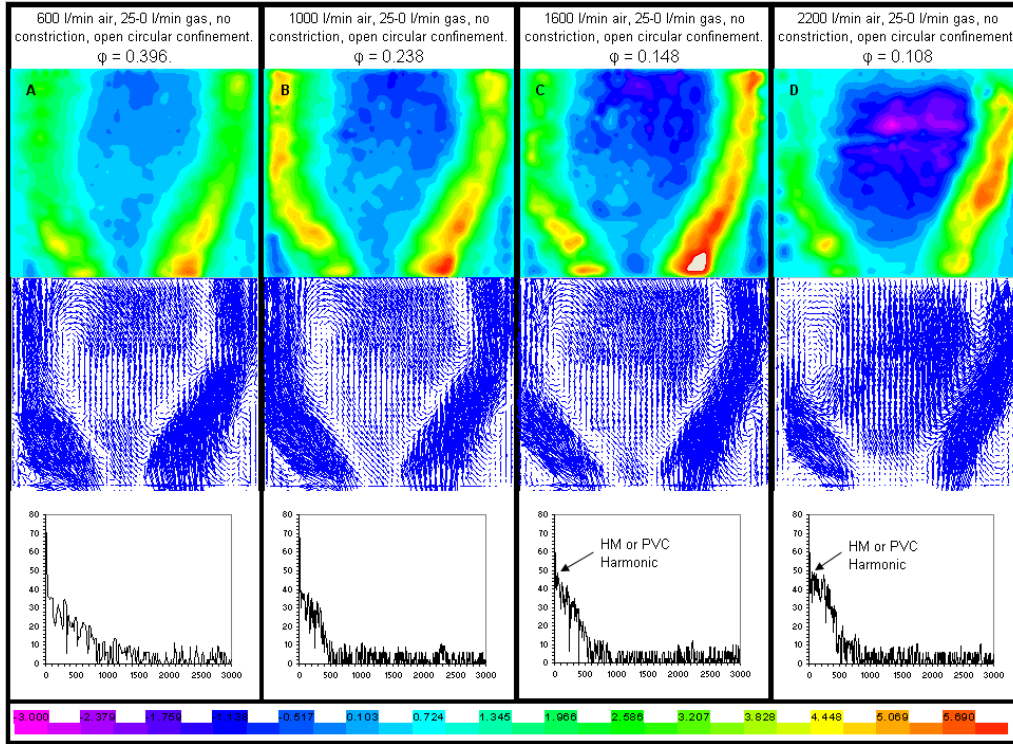


Figure 5. Confined flame analysis at low diffusive gas injection at different flowrates and equivalence ratios with their vectorial map and frequency analysis. Color scale in [m/s]. The CRZ is defined by the dark-blue central region with velocities lower than 0.273 m/s.

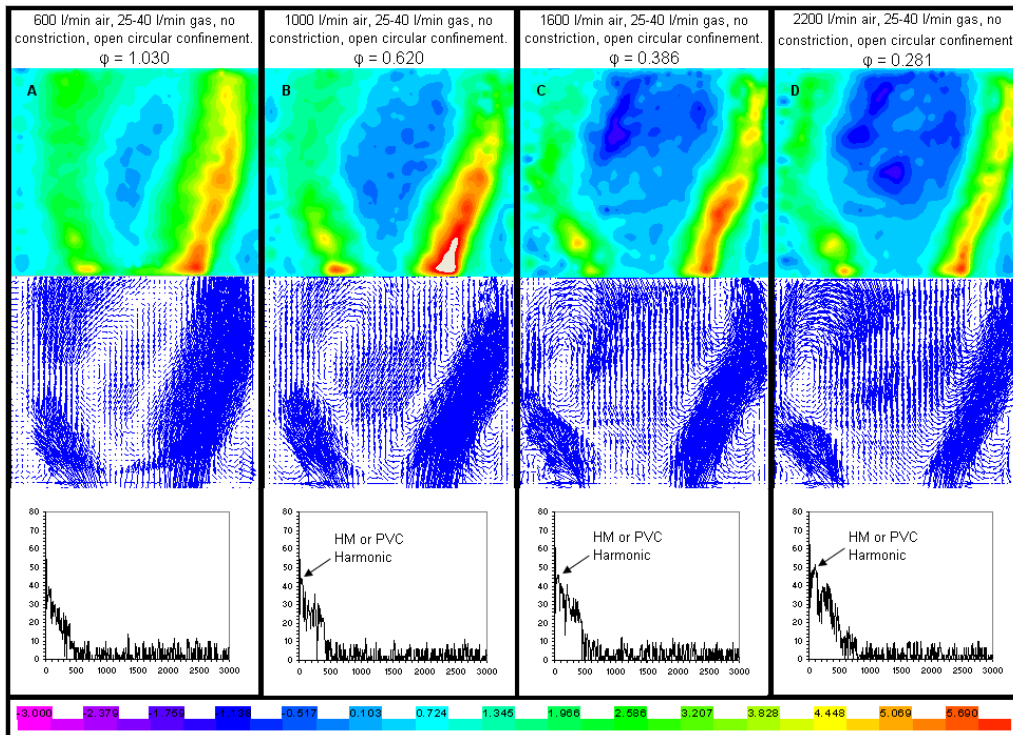


Figure 6. Confined flame analysis at low diffusive-premixed gas injection at different flowrates and equivalence ratios with their vectorial map and frequency analysis. Color scale in [m/s]. The CRZ is defined by the dark-blue central region with velocities lower than 0.273 m/s.

Various models were tested prior to the selection of the one that would be used for the analysis of the entire system. Large Eddy Simulations (LES) and Reynolds Stress Model (RSM) were used first for the resolution of the problem. However, the shapes, strength and location of the CRZ did not match the ones observed with the PIV system. The $k-\omega$ model was then used for the validation of the numerical code. When the latter was applied under different conditions, it was confirmed that the velocity profile between experiments and simulations were the closest observed. Thus, it was defined that this model would give the best results under the imposed conditions. Although it is a simpler model and some of the terms are defined by the user, the aid of experimental trials has allowed a better representation of the system via modeling with less computer memory.

Numerical simulations revealed a similar shape to the observed during the experimental trials. However, the results did not show the concave asymmetric form previously spotted in the experimental results, figure 5 and 6. This has been related to the fact that the numerical simulation still need refining but it is accurate enough to give close results to the experimental model. Figure 7 shows one of the results at 25-40 l/min gas and 1,600 l/min air.

Different conditions were used just to verify that the flame and the coherent structures in the system were as closed as those observed in the experimental trial. Another simulation using 2,200 l/min air and 25-80 l/min gas was run, figure 8. The results show how the coherent structure has evolved into a stronger entity, which is in accordance to the experiments that show how the increase of premixed gas and Re create stronger structures. Although the asymmetrical shape was not obtained, the relative position of the shear flow and the CRZ are in accordance to those obtained experimentally.

The temperature profile is also in accordance with the theory², which specifies that the swirling flows can reduce the temperature of the core and thus mitigate the production of NO_x. Figure 9 shows how the system is creating a region of colder products that not only improves the efficiency by exchange of energy with the reactants, but also reduces the temperature of the core with its inherent reduction of emissions. These results proved that the numerical simulation can be used for a close prediction of the system under swirl combustion conditions. This will aid in the analysis and validation of the model for the analysis of the flashback phenomenon in the swirl chamber.

III.b. Flashback

Previous experiments⁴ have proved that the use of the quarl and the diffusive injector under entirely premixed conditions improved up to 25% the resistance to flashback. The experiments were expanded to the analysis of the system with diffusive-premixed injection using the quarl constriction, this in order to characterize the real effect produced by this passive mechanism.

In order to observe the flashback phenomenon occurring inside of the rig, the steel baseplate was replaced by a quartz crystal. The phenomenon was successfully visualized.

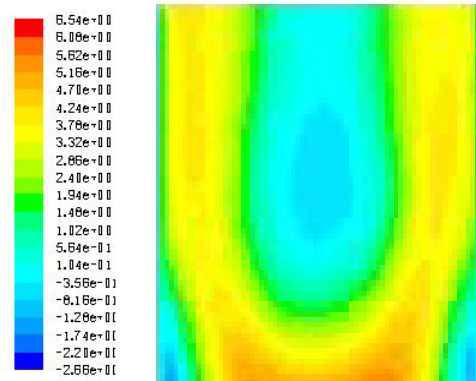


Figure 7. Numerical results. The position and strength observed in comparison to the experimental case is very close. Scale in m/s.

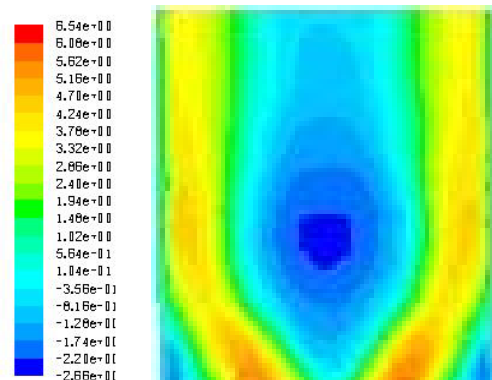


Figure 8. Numerical results, $\phi = 0.345$, 25-80 l/min. The position and strength of the CRZ is as expected. Scale in m/s.

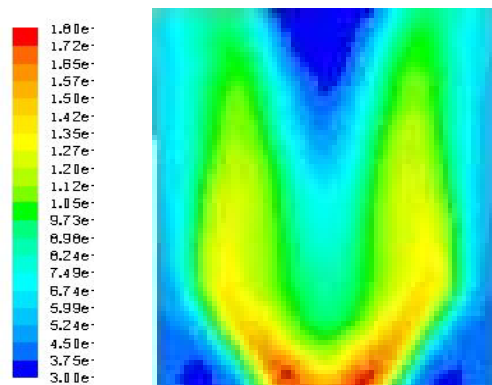


Figure 9. Numerical results, $\phi = 0.345$, 25-80 l/min. The position and strength of the CRZ is as expected. Scale in m/s.

First experiments were performed using a No Injector configuration, with entirely premixed injection. The results showed an extremely low resistance to flashback. The velocity used was obtained from the velocity of the flow through the transversal area formed by the sleeve of the rig and the baseplate. However, when the injector was re-placed the system regained a considerable resistance to the flashback effect, with a smaller slope trend, as observed in figure 10. A reattachment effect to the nozzle was also observed using the injector, a phenomenon already associated with the incoming air-gas flow rate and the weakened CRZ.

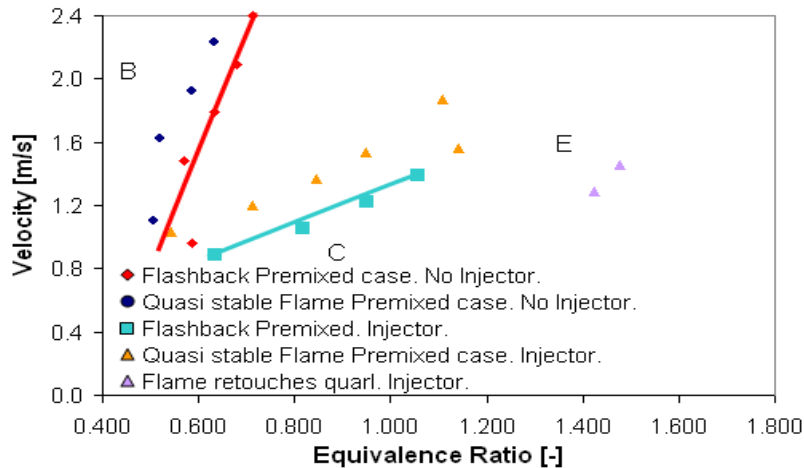


Figure 10. Comparison between the case with No injector (red trendline) and with injector (blue trendline). The case with injector is increasing considerably the flashback resistance. No diffusive injection attained. Confined conditions.

When the phenomenon was analyzed using the High Speed Camera, the case with No Injector showed a flame that moves along the sleeve, and tangentially-radially flashes into the swirl chamber. The primary flame collapses and propagates into the entire volume, igniting a couple of seconds later both tangential inlet jets. The time of ignition of the jets is longer with flames that are weaker and pulsating. This phenomenon is doubtless related to the turbulent flame speed. However, the flashback is not violent. Figure 11 shows the results.

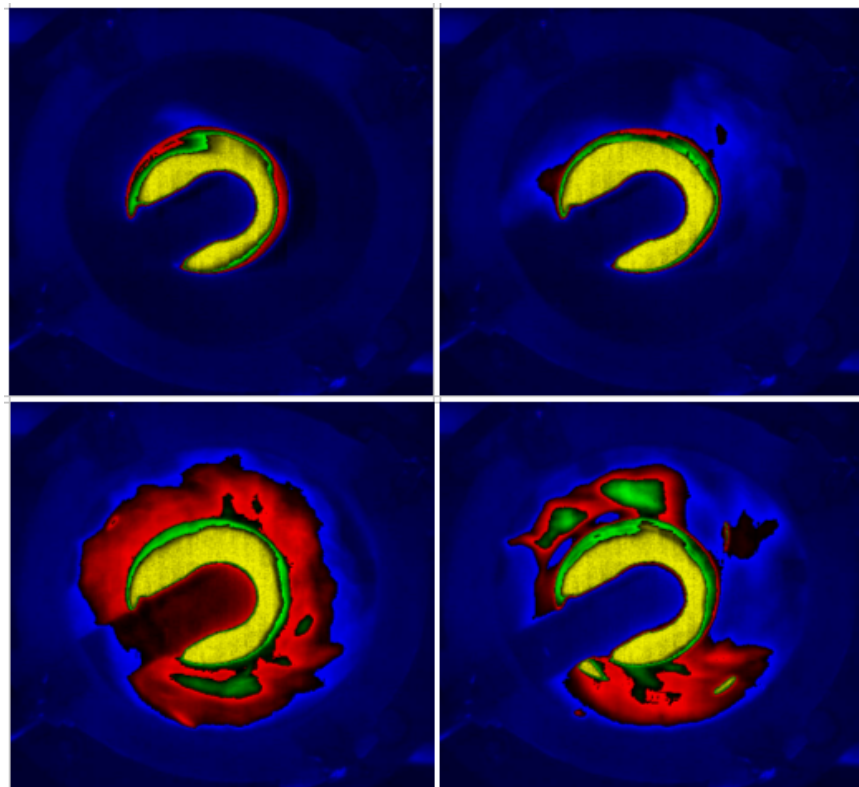


Figure 11. Flashback under Confined Open Exhaust. No Nozzle Constriction and No Injector. Quartz positioned at baseplate. 100% premixed, $\phi \sim 0.74$. The time measured from the first sign of flashback. Flowrate 1800 l/min.

When the injector was re-placed, apart from the higher resistance to flashback, an increase in equivalence ratio caused a more damaging explosion in the swirl chamber, figure 12. This is related to the increased equivalence ratio, the reduce relief vent area and altered flow dynamics produced by this geometry.

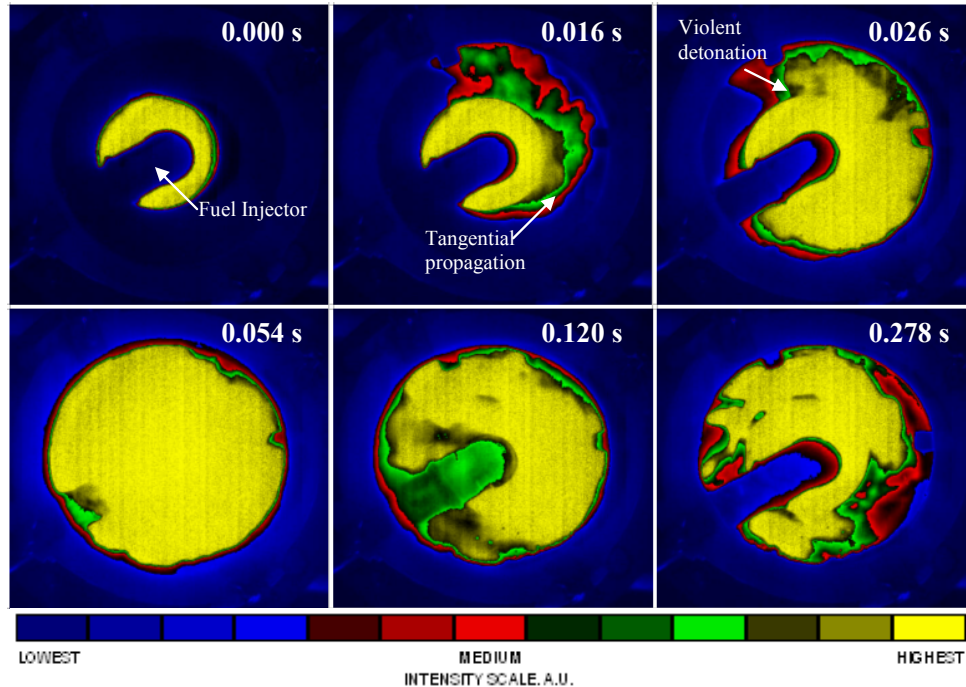


Figure 12. Flashback with injector. Flow injection of 900 l/min, 0-100 l/min gas (100% Premixed injection, $\phi \sim 1.06$). The explosion is very intense and noisy.

When the simulation was run, it was found that the system lacked the presence of the CIVB for those cases with injector, figure 13. Moreover, it was found that the system developed an asymmetric propagation, something observed during the experimental trials.

Therefore, the model validated the suppression of the CIVB, with a close correlation to the experimental results in terms of the behavior of the flashback. It is thus proved via experimental and numerical simulation that the system has completely suppressed the CIVB in the sleeve of the rig, increasing the resistance to flashback considerably. Yazbadani²⁷ demonstrated that the precession of several structures could be reduced or suppressed by means of using bluff bodies in cyclones. The same principle seems to apply to the appearance of the CIVB, which has been mitigated by the inclusion of a bluff body (injector), hence leaving a flashback phenomenon dependent only on boundary layer and turbulent speed propagations.

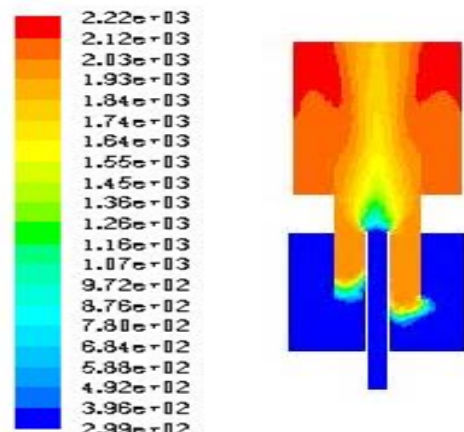


Figure 13. Asymmetric entrance of the flame via boundary layer propagation. No CIVB observed during the phenomenon. Similar results observed experimentally. m/s.

These results corroborate that the system resistance to flashback can be considerably increased by the use of bluff bodies/injectors in the sleeve passage of the rig. This can be extended to bladed swirl combustors, with the addition of alternative fuels, reducing flashback by passive means economically viable and simple to implement. The avoidance of the CIVB leaves a phenomenon that is basically composed by low velocity boundaries and strong turbulent speed propagation at the center line of the flame.

IV. Conclusion

This paper has described the characteristics of a swirl burner in terms of the size and shape of the CRZs formed in the burner exhaust as a function of geometry, equivalence ratio and burner loading. Premixing or partial premixing has the greatest effect on the CRZ as the early heat release causes substantial increase in axial flux of axial momentum and thus drop in swirl number to such an extent that the CRZ can be virtually eliminated at equivalence ratios near to 1. This means that the whole flame stabilization process is susceptible to perturbations in mixture strength and loading, far more so than systems with diffusive fuel entry.

Other work concentrated on Type 2 Flashback, whereby the flame could propagate radially outwards to the tangential inlets. It was shown that the presence of a fuel injector could substantially increase the flashback resistance by eliminating coherent structures near to the central axis, especially when used with a quarl outlet to the swirl burner. However with this configuration the flashback phenomenon was more violent, probably due to the reduced vent area. Numerical simulations proved to be useful in describing the phenomena found including the effects of flashback.

Acknowledgments

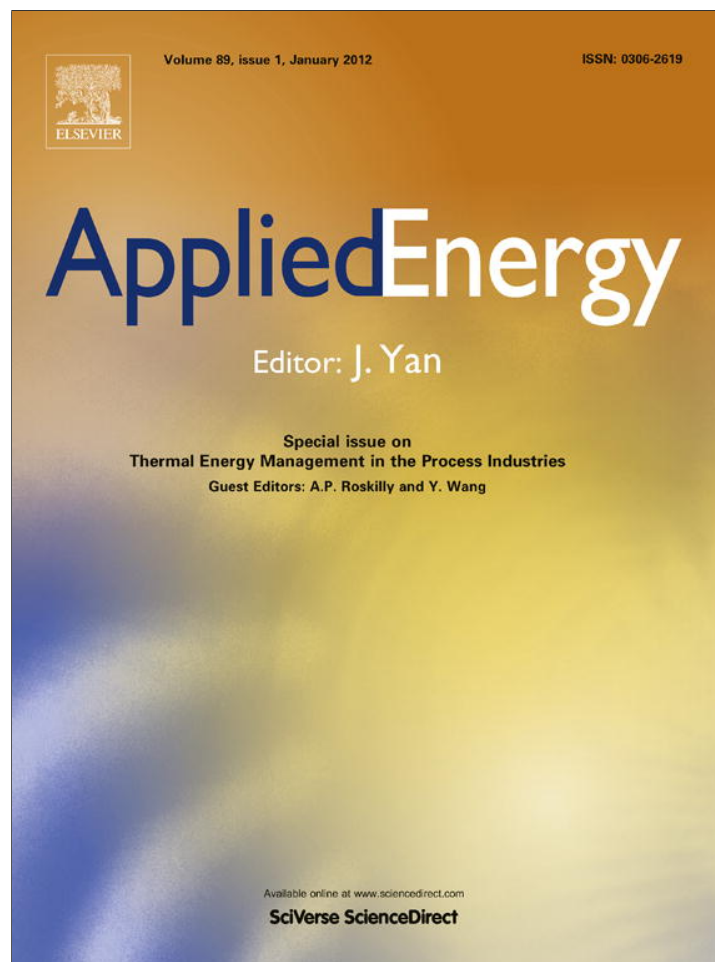
Agustin Valera-Medina gratefully acknowledges the receipt of a scholarship from the Mexican Government (CONACYT) and for the assistance of Malcom Seaborne during the setup of the experiments. Mohammed Abdulsada gratefully acknowledges the sponsorship of the Government of Iraq.

References

- ¹Sadanandan R., Stohr M., Meier W., “Simultaneous OH-PLIF and PIV measurements in a gas Turbine model Combustor”, *Applied Physics B*, vol. 90, pp. 609-618, 2008.
- ²Syred N., “A Review of Oscillation Mechanisms and the role of the Precessing Vortex Core (PVC) in Swirl Combustion Systems”, *Progress in Energy and Combustion Systems*, vol. 32, issue 2, pp. 93-161, 2006.
- ³Lieuwen T. and Yang V., “Combustion Instabilities in Gas Turbine Engines”, AIAA, Progress in Astronautics and Aeronautics, vol. 210, U.S.A., 2005.
- ⁴Valera-Medina A., Shelil N., Abdulsada M., Syred N., Griffiths A., “Flame Stabilization and Flashback Avoidance using Passive Nozzle Constrictions”, *IFRF International Meeting*, Boston, June 8th-10th, USA, 2009.
- ⁵Lacarelle A., Moeck J., Paschereit C.O., “Dynamic Mixing Model of a Premixed Combustor and Validation with Flame Transfer Function Measurement”, *47th AIAA Aerospace Sciences Meeting*, Orlando, USA, ref. AIAA-2009-0986, 2009.
- ⁶Valera-Medina A., Syred N., Griffiths A., “Characterisation of Large Coherent Structures in a Swirl Burner under Combustion Conditions”, *47th AIAA Aerospace Sciences Meeting*, Orlando, USA, ref. AIAA 2009-646, 2009.
- ⁷Jester-Zurker R., Jakirlic S., Tropea C., “Computational Modelling of Turbulent Mixing in Confined Swirling Environment Under Constant and Variable Density Conditions Flow”, *Turbulence and Combustion*, vol. 75, pp. 217-244, 2005.
- ⁸Fick W., Griffiths A. and O’Doherty T., “Visualization of the Precessing Vortex Core in an Unconfined Swirling Flow”, *Optical Diagnostics in Engineering*, vol. 2, issue 1, pp. 19-31, 1997.
- ⁹Wu J., Zhang M., Fan H., Fan W., Zhou Y., “A study on fractal characteristics of aerodynamic field in low-NOx coaxial swirling burner”, *Chemical Engineering Science*, vol. 59, pp. 1473 – 1479, 2004.
- ¹⁰Valera-Medina A., Syred N., Griffiths A., “Large Coherent Structures Visualization in a Swirl Burner”, *Proceedings 14th International Symposium on Applications of Laser Techniques to Fluid Mechanics*, Lisbon, Portugal, 2008.
- ¹¹Cala E., Fernandes C., Heitor M., Shtork S., “Coherent Structures in unsteady swirling jet flow”, *Experiments in Fluids*, vol. 40, pp. 267-276, 2006.
- ¹²Bell J.B., Cheng R., Day M., Beckner V., Lijewski M., “Interaction of turbulence and chemistry in a low-swirl Burner”, *Journal of Physics: Conference Series 125*, 012027 doi:10.1088/1742-6596/125/1/012027, 2008.
- ¹³Biagioli F., Guthe F., Schuermans B., “Combustion dynamics linked to flame behavior in a partially premixed swirled industrial burner”, *Experimental Thermal and Fluid Science*, vol. 32, pp. 1344-1353, 2008.
- ¹⁴Bagdanavicius A., Bowen P., Syred N., Kay P., Crayford A., Wood J., “Burning Velocities of Alternative Gaseous Fuels at Elevated Temperature and Pressure”, *47th AIAA Aerospace Sciences Meeting*, Orlando, USA, ref. AIAA-2009-0229, 2009.
- ¹⁵Arias B., Feroso J., Plaza M., Pevida C., Rubiera F., Pis J., Garcia-Pena F., Casero P., “Production of H₂ by Co-gasification of Coal with biomass and petroleum coke”, *Proceedings of 7th European Conference on Coal Research and Its Applications*, Wales, UK, 2008.
- ¹⁶Jakirlic S., Hanjalic K., Tropea C., “Modelling Rotating and Swirling Turbulent Flows, A Perpetual Challenge”, *AIAA Journal*, vol. 40, no. 10, pp. 1984-1997, 2002.
- ¹⁷Kroner M., Fritz J., Sattelmayer T., “Flashback Limits for Combustion Induced Vortex Breakdown in a Swirl Burner”, *Journal of Engineering for Gas Turbines and Power*, vol. 125, pp. 693-700, 2003.
- ¹⁸Kiesewetter F., Konle M., Sattelmayer T., “Analysis of Combustion Induced Vortex Breakdown Driven Flame Flashback in a Premix Burner with Cylindrical Mixing Zone”, *Journal of Engineering for Gas Turbines and Power*, vol. 129, pp. 929-236, 2007.

- ¹⁹Galpin J., Naudin A., Vervisch L., Angelberger C., Colin O., Domingo P., “Large-eddy simulation of a fuel-lean premixed turbulent swirl-burner”, *Combustion and Flame*, vol. 155, pp. 247–266, 2008.
- ²⁰Sadiki A., Maltsev A., Wegner B., Fleming F., Kempf A., Janicka J., “Unsteady Methods (URANS and LES) for simulation of combustion systems”, *International Journal of Thermal Sciences*, vol. 45, issue 8, pp. 760-773, 2006.
- ²¹Davidson P., *Turbulence: an introduction for Scientists and Engineers*, Oxford University Press, United Kingdom, 2004.
- ²²Pope S., *Turbulent Flows*, Cambridge University Press, United Kingdom, 2000.
- ²³**Strohle, J. and Myhrvold, T. “An evaluation of detailed reaction mechanisms for hydrogen combustion under gas turbine conditions”, *Hydrogen Energy*, Vol. 32, pp. 127 – 135, 2007.**
- ²⁴Brundish K., Miller M., Morgan L., Wheatley A., “Variable Fuel Placement Injector Development”, *Advanced Combustion and Aerothermal Technologies, NATO Science for Peace and Security Series*, Springer, PP. 425-444, 2007.
- ²⁵Wilcox D.C., *Turbulence Modeling for CFD*. DCW Industries, Inc., La Canada, California, 1998.
- ²⁶Dawson J., Rodriguez-Martinez V., Syred N., O’Doherty T., “The Effect of Combustion Instability on the Structure of Recirculation Zones in Confined Swirling Flames”, *Combustion Science and Technology Journal*, vol. 177, issue 12, pp. 2341-2371, 2005.
- ²⁷Yazdabadi P.. A study of the Precessing Vortex Core in Cyclone dust separators and a method of Prevention. PhD thesis, Cardiff University, Wales, UK, 1996.

Provided for non-commercial research and education use.
Not for reproduction, distribution or commercial use.



This article appeared in a journal published by Elsevier. The attached copy is furnished to the author for internal non-commercial research and education use, including for instruction at the authors institution and sharing with colleagues.

Other uses, including reproduction and distribution, or selling or licensing copies, or posting to personal, institutional or third party websites are prohibited.

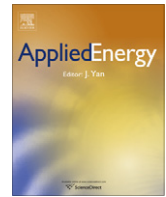
In most cases authors are permitted to post their version of the article (e.g. in Word or Tex form) to their personal website or institutional repository. Authors requiring further information regarding Elsevier's archiving and manuscript policies are encouraged to visit:

<http://www.elsevier.com/copyright>



Contents lists available at ScienceDirect

Applied Energy

journal homepage: www.elsevier.com/locate/apenergy

The effect of hydrogen containing fuel blends upon flashback in swirl burners

Nicholas Syred*, Mohammed Abdulsada, Anthony Griffiths, Tim O'Doherty, Phil Bowen

Gas Turbine Research Centre, Cardiff University, CF24 3AA, United Kingdom

ARTICLE INFO

Article history:

Received 14 July 2010

Received in revised form 21 January 2011

Accepted 25 January 2011

Available online 25 February 2011

Keywords:

Flashback
Swirl burner
Lean premixed
Hydrogen

ABSTRACT

Lean premixed swirl combustion is widely used in gas turbines and many other combustion processes due to the benefits of good flame stability and blow off limits coupled with low NO_x emissions. Although flashback is not generally a problem with natural gas combustion, there are some reports of flashback damage with existing gas turbines, whilst hydrogen enriched fuel blends, especially those derived from gasification of coal and/or biomass/industrial processes such as steel making, cause concerns in this area. Thus, this paper describes a practical experimental approach to study and reduce the effect of flashback in a compact design of generic swirl burner representative of many systems. A range of different fuel blends are investigated for flashback and blow off limits; these fuel mixes include methane, methane/hydrogen blends, pure hydrogen and coke oven gas. Swirl number effects are investigated by varying the number of inlets or the configuration of the inlets. The well known Lewis and von Elbe critical boundary velocity gradient expression is used to characterise flashback and enable comparison to be made with other available data.

Two flashback phenomena are encountered here. The first one at lower swirl numbers involves flashback through the outer wall boundary layer where the crucial parameter is the critical boundary velocity gradient, G_f . Values of G_f are of similar magnitude to those reported by Lewis and von Elbe for laminar flow conditions, and it is recognised that under the turbulent flow conditions pertaining here actual gradients in the thin swirl flow boundary layer are much higher than occur under laminar flow conditions. At higher swirl numbers the central recirculation zone (CRZ) becomes enlarged and extends backwards over the fuel injector to the burner baseplate and causes flashback to occur earlier at higher velocities. This extension of the CRZ is complex, being governed by swirl number, equivalence ratio and Reynolds Number. Under these conditions flashback occurs when the cylindrical flame front surrounding the CRZ rapidly accelerates outwards to the tangential inlets and beyond, especially with hydrogen containing fuel mixes. Conversely at lower swirl numbers with a modified exhaust geometry, hence restricted CRZ, flashback occurs through the outer thin boundary layer at much lower flow rates when the hydrogen content of the fuel mix does not exceed 30%. The work demonstrates that it is possible to run premixed swirl burners with a wide range of hydrogen fuel blends so as to substantially minimise flashback behaviour, thus permitting wider use of the technology to reduce NO_x emissions.

© 2011 Elsevier Ltd. All rights reserved.

1. Introduction

Lean premixed (LP) combustion is a widely used strategy to decrease undesirable emissions in gas turbines. In LP systems, fuel and air are mixed prior to the combustion chamber to promote mixing, combustion efficiency, uniform temperatures and low NO_x . Swirl combustors are almost universally used in some form or other in gas turbine [1–3] and numerous other systems. Especially when operated in a LP mode many problems can be encountered including blow off and flashback [2–4].

Using alternative fuels has become another option to reduce emissions of CO_2 . Hydrogen, hydrogen and other fuel blends can

cause major issues with many swirl combustors, because of the considerable variation in flame speed with such fuel blends compared to natural gas. Similar comments apply to process gases such as coke oven gas (COG) widely produced in the steel industry. Biomass and coal gasification prototype power plants have performed well, but have not proved to be competitive against conventional boiler technology for power production [5–7], primarily because gas turbine manufacturers have had full order books for conventional units. Demand for systems capable of economically and efficiently producing power and CO_2 for sequestration may well change this. There are many other problems associated with the use of alternative fuels as discussed in [8].

Basically, swirling flows are defined as a flow undergoing simultaneous axial-tangential vortex motion. This flow motion can be generated using swirl vanes or many other methods [9,10]. The

* Corresponding author. Tel.: +44 (0) 2920874318.

E-mail address: syredn@cf.ac.uk (N. Syred).

main desirable characteristic of swirl combustors is the formation of unattached reverse flow zones (RFZ) and central recirculation zones (CRZ) capable of recycling hot chemically active reactants to substantially enhance flame stability [4]. The swirl number (S) is one of the main parameters used to characterise swirling flow. It is defined as the ratio of axial flux of swirl momentum divided by axial flux of axial momentum, divided by the equivalent nozzle radius [3]. Commonly owing to flow complexities a geometric swirl number (S_g) is used which depends entirely on the geometry of the burner.

Flashback is a problem which has arisen when using LP combustors especially with hydrogen based fuel mixtures. Flashback occurs when the gas velocity becomes lower than the burning velocity due to flame propagation within boundary layer, core flow or because of combustion instabilities [2, 11–13]. One important manifestation of the flashback phenomenon is that due to flame propagation in the low velocity region of the wall boundary layer. Flame propagation is thus limited by quenching in the very near wall region [13]; for turbulent flow this will be the laminar sub layer. Lewis and von Elbe [14] have suggested use of the critical boundary velocity gradient, based on considerations of the velocity gradient G_f at the wall, the laminar flame speed S_L and the quenching distance d_q .

$$G_f = \left[\frac{\partial u}{\partial r} \right]_{wall} \leq \frac{S_L}{d_q} \quad (1)$$

Flashback can also occur because of turbulent flame propagation in the core flow. Combustion instabilities have a very considerable effect on system dynamics and can cause flashback due to non-linear interaction of pressure fluctuations, hence periodic heat release and non linear flame propagation [15]. Finally flashback in swirl burners can be caused by a phenomena termed combustion induced vortex breakdown (CIVB) due to rapid expansion at the burner exit creating a recirculation zone which acts as a flame holder: the breakdown of this structure can occur due to flow perturbations and chemical reaction effects causing the CRZ and hence flame to propagate upstream into the premixing zone [16,17].

2. Experimental setup

The generic swirl burner was used to examine flame stability limits at atmospheric conditions (1 bar, 293 K). The was designed and assembled at Cardiff University's Gas Turbine Research Centre (GTRC). A single tangential inlet feeds an outer plenum chamber which uniformly distributes premixed air/fuel to the inserts, eventually into the burner body. A central fuel injector extended through the whole body of plenum and the insert burner. Principally, the fuel injector is used to produce both non-premixed and partially premixed flames; its position is shown in Figs. 1 and 2. This simulates many industrial applications where liquid fuels are sprayed through a central fuel injector.

Three swirl numbers have been used in the experiments, with the only change in the system being in the exhaust insert with tangential inlets which force flow into the swirl chamber, then exhaust. Three inserts are used with different swirl numbers, achieved by changing the number, length and width of the tangential inlets. The three swirl burners have swirl numbers of: $S_I = 1.47$, $S_{II} = 1.04$, $S_{III} = 0.8$. Based on other work [9,21] an exhaust nozzle extension $0.5D_e$ long was added to the exhaust of two of the inserts. The fuel injector was left in the same position Swirl insert III is very similar to II the only differences lying in the width of the tangential inlets, 5 as opposed to 4 mm (nine inlets used). Swirl insert I only has four inlets, but operated at a significantly higher swirl number of 1.47, Fig. 2.



Fig. 1. Exploded view of swirl burner.

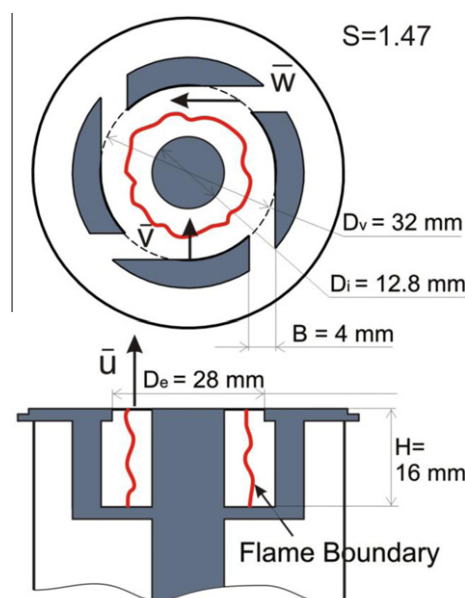


Fig. 2. Schematic diagram of Internals of swirl burner.

Coriolis flow metres have been used simultaneously to measure the mass flow rate of both fuel and air separately.

3. Results and discussion

Three swirl burners plus five different fuels has been used to obtain results, these are summarised in Tables 1 and 2:

Typically the pressure loss coefficient at $S_{II} = 1.04$ is nearly half that at $S_I = 1.47$ and again is about 20% lower again at $S_{III} = 0.8$. Lower pressure drop is a major advantage to designers and operators of gas turbines and other large burners and thus there is a drive to use lower swirl numbers, providing the flame stability advantages of the CRZ are not lost. coke oven gas has been used as a representative process industry fuel gas, which is widely

Table 1
Swirl burners and their specifications.

Swirl Burner name	I	II	III
Geometrical swirl number	1.47	1.04	0.8
Exhaust sleeve $0.5 D_e$ long	No	Yes	Yes

Table 2
Fuels Blends and their composition.

Fuel name	CH ₄ (%)	H ₂ (%)	CO (%)	N ₂ (%)	LHV (MJ/kg)	T _{max} adiabatic (K)
Pure methane	100	0	0	0	50.1	2237
Pure hydrogen	0	100	0	0	126.1	2406
15%H ₂	85	15	0	0	51.6	2245
30%H ₂	70	30	0	0	53.7	2253
Coke oven gas	25	65	6	4	54.2	2300

available at steelworks and has the potential to be widely used in power generation in process industry, providing appropriate efficient reliable technology can be developed to utilise it. The system has been tested on a wide range of fuel blends as shown below, Table 2. Up to 15 combinations of swirl burner and fuel gases have been used to investigate their effects on the flashback and blow-off characteristics. Fuel characteristics are interesting as they show similar lower heating values and adiabatic flame temperatures. The

exception is pure hydrogen with much higher lower heating value, but adiabatic flame temperature about ~100 K higher than coke oven gas.

Three families of flashback curves are shown in Fig. 3 below, one for a swirl number of $S_{II} = 1.47$, Fig. 3a, the other at a swirl number $S_{II} = 1.04$, Fig. 3b and 3c for $S_{III} = 0.8$.

Associated flame photographs at conditions just before flashback for pure methane are shown in Fig. 4a ($S_I = 1.46$) and Fig. 4b ($S_{II} = 1.04$).

The comparison is extremely interesting whilst other analysis has revealed two different flashback mechanisms for the different swirl numbers [10,18–21]. With $S_I = 1.47$ the central recirculation zone (CRZ) extends over the central fuel injector to the base plate for all fuels, with an associated flame front on the CRZ boundary. This is illustrated in Fig. 2 (and does not happen with $S_{II} = 1.04$ and $S_{III} = 0.8$). Flashback occurs when the radial velocity in the swirl level drops to such a level that the near radial flame front can flashback to the inlets and often into the plenum chamber [10]. Conversely with $S_{II} = 1.04$ and $S_{III} = 0.8$ flashback occurs by a

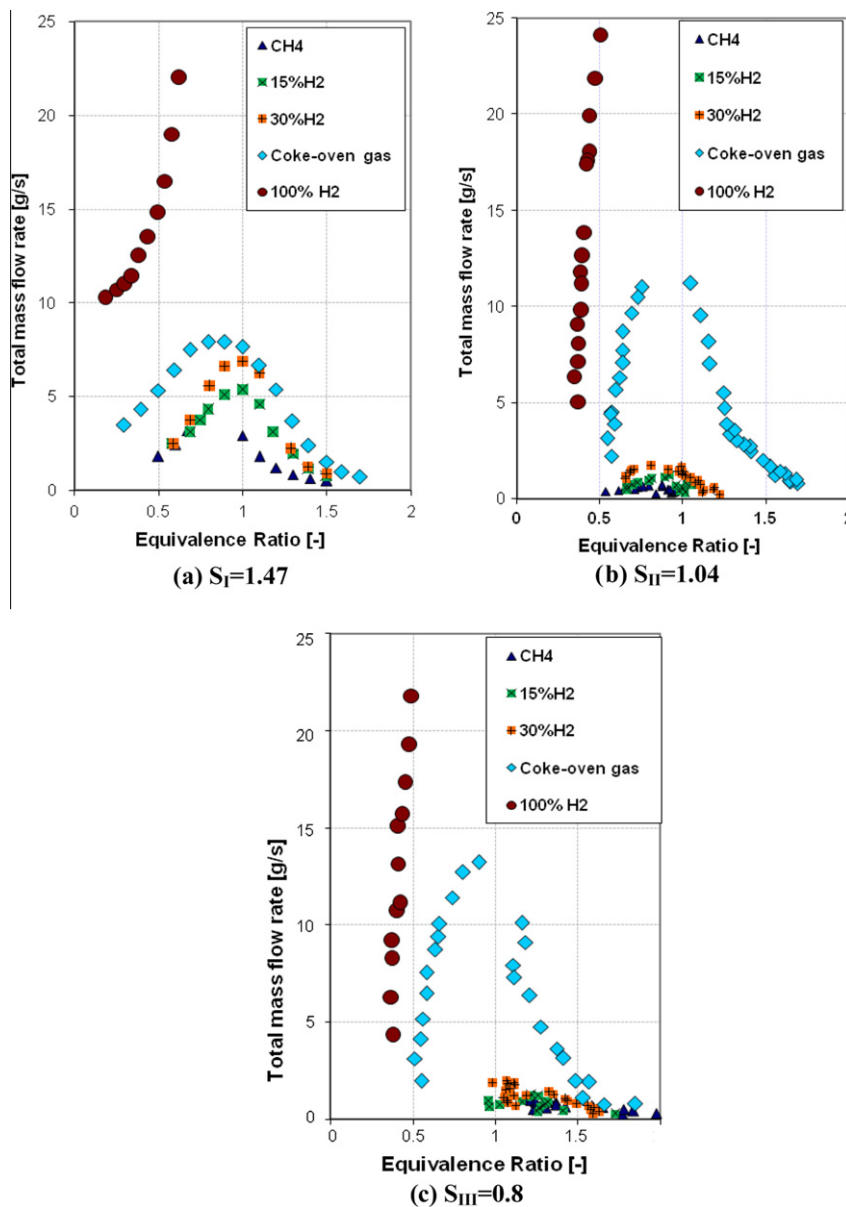


Fig. 3. Flashback limits of the generic swirl burners with three different swirl numbers for five different fuels.

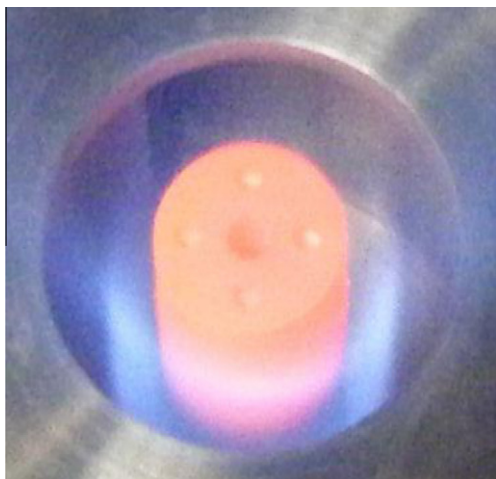


Fig. 4a. Photo of flame surrounding central fuel injector at $S_I = 1.47$, just before radial flashback.



Fig. 4b. Photo of flame just before flashback through outer wall boundary layer, $S_{II} = 1.04$.

different mechanism via flashback in the outer wall boundary layer of the exhaust nozzle, then being controlled by the critical boundary velocity gradient [21] as defined by Lewis and von Elbe [14]. This can be readily derived from geometrical and simple flow considerations and enables comparison with the large quantities of data available in past literature as summarised in [14]. Other work using CFD analysis of the boundary layer region close to flashback has shown that under the turbulent flow conditions of the swirl burner, critical boundary velocity gradients are an order of magnitude higher than those predicted by the Lewis and von Elbe formula [21].

In terms of flashback limits for methane and methane containing up to 30% hydrogen a value of $S_{II} = 1.04$ and $S_{III} = 0.8$ produces flashback which occurs at a mass flow (and hence velocity levels) up to 1/3 of those found for $S_I = 1.47$ for a wide range of equivalence ratios. However with coke oven gas (COG) different effects start to appear as the hydrogen content of the fuel increase beyond

50%. For Swirl Numbers of 0.8 and 1.04 flashback performance is better than $S = 1.47$ for values of equivalence ratio up to 0.6 to 0.65 and mass flows of ~ 7 g/s. Beyond this point for equivalence ratios > 0.65 and < 1.2 a swirl number of 1.47 is better by up to 50%. However for LP combustors the aim is to operate around an equivalence ratio of ~ 0.7 or less and thus this is not a disadvantage. Comparison of the three Swirl Number cases, Fig. 3, shows that there is a significant change in flashback behaviour moving between a fuel with 30% hydrogen content to one with 65% hydrogen content as with COG. Moving onto the pure hydrogen results similar trends were evident, although the range of equivalence ratios tested was restricted to being below 0.5 and above 2 due to the very large hydrogen and air flow rates required. Here the higher mass flow, hence velocity levels, associated with hydrogen flashback, produce higher levels of turbulent kinetic energy, thus augmenting the turbulent flame speed and thus worsen the hydrogen flashback limits beyond that expected from considerations of laminar flame speed data [14,21].

More detailed inspection of the results for $S_{II} = 1.04$ and $S_{III} = 0.8$, showed generally both swirlers have very similar characteristics with differences being within experimental limits. $S_{III} = 0.8$ is preferred as it gives lower pressure drop.

Another interesting result was that the peaks of the flashback curves tended to occur at weak equivalence ratios as opposed to the expected just on the rich side of stoichiometric [14]. This effect is thought to be due to changes in the recirculation zone occurring as the equivalence ratio approaches 1. This is also illustrated by Fig. 5 where all the methane data has been plotted as a function of critical boundary layer gradient at flashback, G_f ; also included is laminar data on natural gas. The swirl burners at $S_{II} = 1.04$ and $S_{III} = 0.8$ are flashing back at lower values of G_f than the laminar results (albeit at a higher pressure drop), whilst for $S_I = 1.47$ values of G_f are significantly higher.

Overall $S_{III} = 0.8$ gives the best flashback limits for methane based fuels with hydrogen content up to 30% and for hydrogen based fuels with hydrogen content $\geq 65\%$ for equivalence ratios ≤ 0.65 . However for fuels with hydrogen content in the range $30\% \leq H_2 \text{ content} \leq 65\%$ a more complex picture emerges. The Critical Boundary Velocity Gradient for flashback is higher at lower swirl numbers and equivalence ratios ~ 1 when compared to $S_I = 1.47$. Separate tests on blow off limits show that the Swirl Number $S = 0.8$ produces the best results.

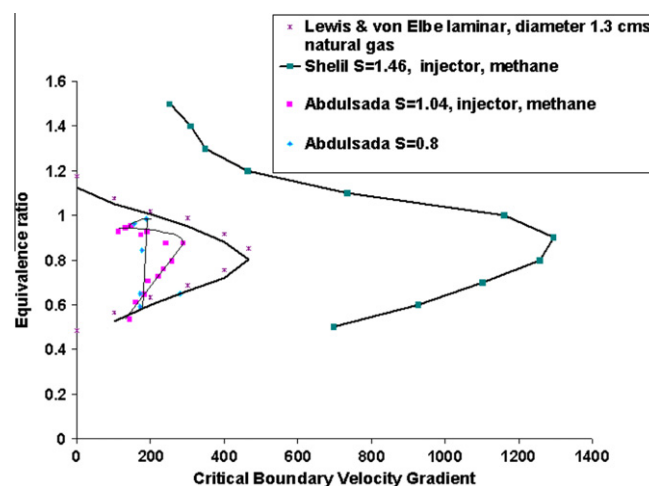


Fig. 5. Lewis and von Elbe Critical boundary velocity gradient comparison for three swirl numbers and laminar data [14].

A gas turbine, required to be dual fuelled, with given compressor and turbine system has air mass flow rates at given thermal inputs which vary little as the fuel mass flow is relatively small and the exhaust gas composition, hence enthalpy, is still dominated by the 80% nitrogen content from the air. To produce this thermal input different quantities of fuel and thus equivalence ratio are needed for different fuels such as natural gas, coke oven gas and especially pure hydrogen. When dual fuelling/changeover is needed ideally the operational range of the system between flashback and blow off for two different fuels (such as hydrogen and natural gas) should be such that there is sufficient overlap between the blow off and flashback limits to enable easy fuel change over. Because of the different stoichiometry and heating value, hydrogen containing fuels will always have to be operated at weaker equivalence ratios than natural gas fired systems, typically 78% of the natural gas equivalence ratio for pure hydrogen. This infers that the overlap region between the flashback limit and blow off limit of given fuels is crucial in determining whether or not the system can be dual fuelled. Table 2 indicates that because of similar adiabatic flame temperature and lower heating values fuel gases containing up to 65% hydrogen (as with coke oven gas) with a base fuel of natural gas can be best accommodated in existing or somewhat modified combustion systems.

4. Conclusion

This paper has discussed the flashback limits of three different swirl burners and shown that considerable differences exist. Preference is given to the system with low swirl number as it gives lowest pressure drop. The behaviour of methane based fuels with hydrogen content up to 30% has been shown to follow that of methane as the hydrogen content is increased. However coke oven gas shows distinctly different behavioural patterns, as does pure hydrogen which needs to be investigated further.

Acknowledgments

Mohammed Abdulsada gratefully acknowledges the receipt of a scholarship from the Iraqi Government and for the assistance of Steve Morris, Malcolm Seaborne, Terry Pole during the setup of the experiments. The financial support of the RCUK Energy Programme is gratefully acknowledged. The Energy programme is an RCUK cross-council initiative, led by EPSRC and contributed to by EPSRC, NERC, BBSRC and STFC.

References

- [1] Huang Y, Yang V. Effect of swirl on combustion dynamics in a leanpremixed swirl-stabilized combustor. *Proc Combust Inst* 2005;30(2):1775–82.
- [2] Sankaran R, Hawkes ER, Chen JH, Lu T, Law CK. Direct numerical simulations of turbulent lean premixed combustion. *J Phys* 2006;46:38–42.
- [3] Lefebvre AH. *Gas Turbine Combustion*. LLC, Oxon, UK: Taylor & Francis Group; 1999.
- [4] Gupta AK, Lilley DJ, Syred N. *Swirl Flows*. Tunbridge Wells, United Kingdom: Abacus Press; 1984.
- [5] Goy CJ, James SR, Rea S. 2005. Monitoring combustion instabilities: E.ON UK's experience. In: Lieuwen T, Yang V. editors. *Combustion instabilities in gas turbine engines: operational experience, fundamental mechanisms, and modeling*, Progress in Astronautics and Aeronautics. p. 163–75.
- [6] Bagdanavicius A, Bowen P, Syred N, Kay P, Crayford A, Wood J. Burning velocities of alternative gaseous fuels at elevated temperature and pressure. In: 47th AIAA Aerospace Sciences Meeting, Orlando, USA, ref. AIAA-2009-0229; 2009.
- [7] Arias B, Feroso J, Plaza M, Pevida C, Rubiera F, Pis J, Garcia-Pena F, Casero P. Production of H₂ by Co-gasification of Coal with biomass and petroleum coke. In: *Proceedings of 7th European conference on coal research and its applications*. Wales, UK; 2008.
- [8] Chiesa P, Lozza G, Mazzocchi L. Using hydrogen as gas turbine fuel. *J Eng Gas Turb Power* 2005;127:73–80.
- [9] Valera-Medina A, Syred N, Griffiths A. Visualisation of isothermal large coherent structures in a swirl burner. *Combust Flame* 2009;156:1723–34.
- [10] Shelil N, Bagdanavicius A, Syred N, Griffiths A, Bowen P. Premixed swirl combustion and flash back analysis with hydrogen/methane mixture. In: 48th AIAA Aerospace Sciences Meeting, Orlando, USA, ref. AIAA-2010-1169; 2010.
- [11] Syred N. A review of oscillation mechanisms and the role of the Precessing Vortex Core (PVC) in swirl combustion systems. *Progr Energy Combust Syst* 2006;32(2):93–161.
- [12] Syred N. Generation and alleviation of combustion instabilities in swirling flow. In: Syred N, Khalatov A, editors. *Advanced combustion and aerothermal technologies*. Springer; 2007. p. 3–20.
- [13] Plee SL, Mellor AM. Review of flashback reported in prevaporizing/premixing combustors. *Combust Flame* 1978;32:193–203.
- [14] Lewis B, Elbe G. *Combustion, flames and explosions of gases*. New York: Academic Press; 1987.
- [15] Subramanya M, Choudhuri A. investigation of combustion instability effects on the flame characteristics of fuel blends. In: 5th International Energy Conversion Engineering Conference and Exhibit (IECEC) AIAA, St. Louis, Missouri; 2007.
- [16] Fritz J, Kroner M, Sattelmayer T. Flashback in a swirl burner with cylindrical premixing zone. *J Eng Gas Turb Power* 2004;126(2):276–83.
- [17] Kroner M, Fritz J, Sattelmayer T. Flashback limits for combustion induced vortex breakdown in a swirl burner. *J Eng Gas Turb Power* 2003;125(3):693–700.
- [18] *Fluent 6.2 Users Guides*. ed. F. Incorporated. Lebanon, USA; 2005.
- [19] Zimont V et al. An efficient computational model for premixed turbulent combustion at high reynolds numbers based on a turbulent flame speed closure. *J Gas Turb Power* 1998;120:526–32 (July).
- [20] Valera-Medina A, Abdulsada M, Shelil N, Syred N, Griffiths A. Flame stabilization and flashback avoidance using passive nozzle constrictions. In: IFRF International Meeting, Boston, 8th–10th, USA; 2009.
- [21] Bagdanavicius A, Shelil N, Syred N, Griffiths A. Premixed swirl combustion and flashback analysis with hydrogen/methane mixtures. In: AIAA 47th Aerospace Sciences Meeting, Orlando, Florida, ref. AIAA-2010-1169; 2010. p. 4–7.